METHODS IN MOLECULAR BIOLOGY™ 385

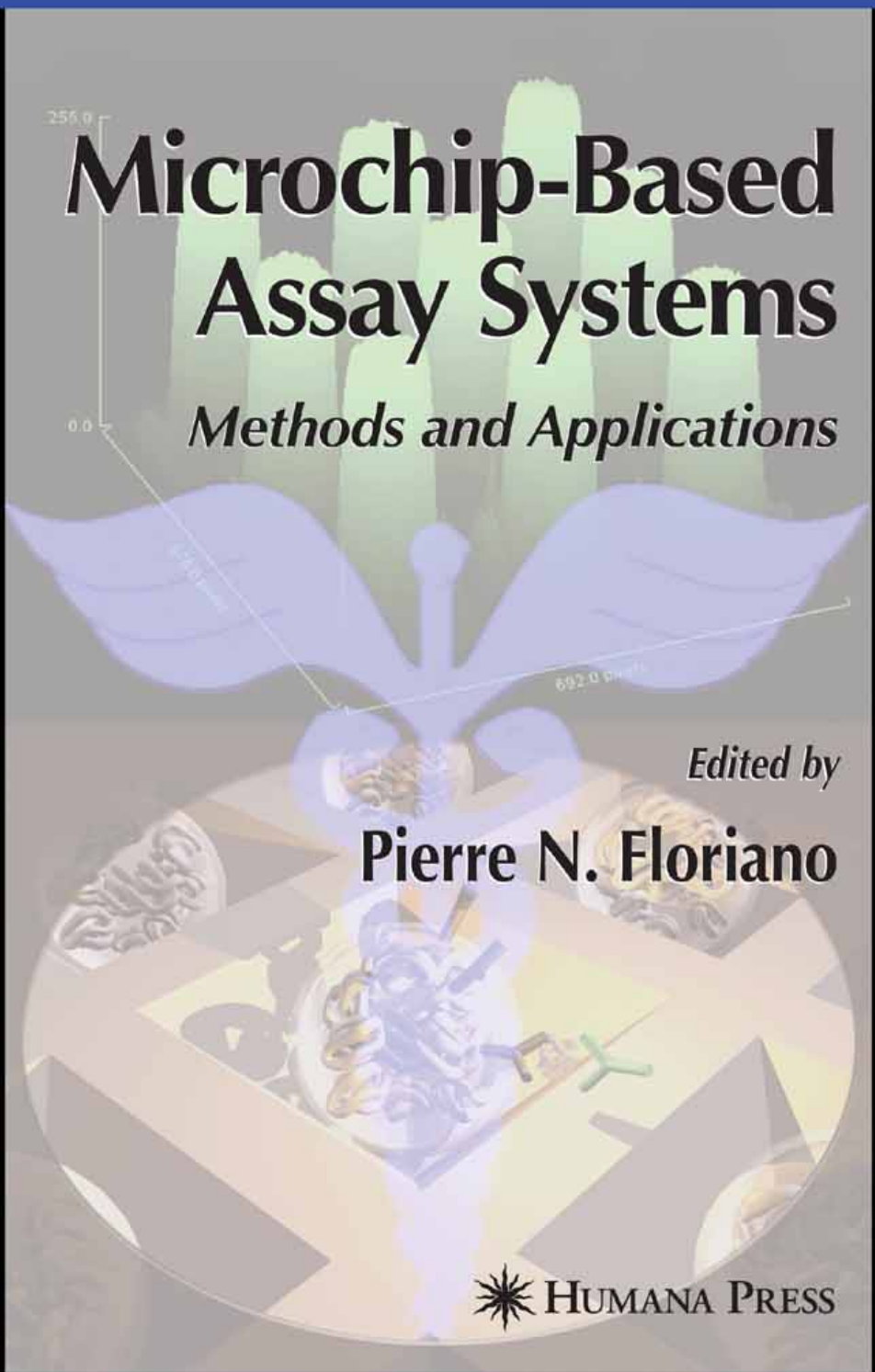

Microchip-Based Assay Systems

Methods and Applications

Edited by

Pierre N. Floriano

HUMANA PRESS

Microchip-Based Assay Systems

METHODS IN MOLECULAR BIOLOGY™

John M. Walker, SERIES EDITOR

386. Peptide Characterization and Application Protocols, edited by *Gregg B. Fields, 2007*

385. Microchip-Based Assay Systems: *Methods and Applications,* edited by *Pierre N. Floriano, 2007*

384. Capillary Electrophoresis: *Methods and Protocols,* edited by *Philippe Schmitt-Kopplin, 2007*

383. Cancer Genomics and Proteomics: *Methods and Protocols,* edited by *Paul B. Fisher, 2007*

382. Microarrays, Second Edition: *Volume 2, Applications and Data Analysis,* edited by *Jang B. Rampal, 2007*

381. Microarrays, Second Edition: *Volume 1, Synthesis Methods,* edited by *Jang B. Rampal, 2007*

380. Immunological Tolerance: *Methods and Protocols,* edited by *Paul J. Fairchild, 2007*

379. Glycovirology Protocols, edited by *Richard J. Sugrue, 2007*

378. Monoclonal Antibodies: *Methods and Protocols,* edited by *Maher Albitar, 2007*

377. Microarray Data Analysis: *Methods and Applications,* edited by *Michael J. Korenberg, 2007*

376. Linkage Disequilibrium and Association Mapping: *Analysis and Application,* edited by *Andrew R. Collins, 2007*

375. In Vitro Transcription and Translation Protocols: *Second Edition,* edited by *Guido Grandi, 2007*

374. Quantum Dots: *Methods and Protocols,* edited by *Charles Z. Hotz and Marcel Bruchez, 2007*

373. Pyrosequencing® Protocols, edited by *Sharon Marsh, 2007*

372. Mitochondrial Genomics and Proteomics Protocols, edited by *Dario Leister and Johannes Herrmann, 2007*

371. Biological Aging: *Methods and Protocols,* edited by *Trygve O. Tollefsbol, 2007*

370. Adhesion Protein Protocols, *Second Edition,* edited by *Amanda S. Coutts, 2007*

369. Electron Microscopy*: Methods and Protocols, Second Edition,* edited by *John Kuo, 2007*

368. Cryopreservation and Freeze-Drying Protocols, *Second Edition,* edited by *John G. Day and Glyn Stacey, 2007*

367. Mass Spectrometry Data Analysis in Proteomics, edited by *Rune Matthiesen, 2007*

366. Cardiac Gene Expression: *Methods and Protocols,* edited by *Jun Zhang and Gregg Rokosh, 2007*

365. Protein Phosphatase Protocols: edited by *Greg Moorhead, 2007*

364. Macromolecular Crystallography Protocols: *Volume 2, Structure Determination,* edited by *Sylvie Doublié, 2007*

363. Macromolecular Crystallography Protocols: *Volume 1, Preparation and Crystallization of Macromolecules,* edited by *Sylvie Doublié, 2007*

362. Circadian Rhythms: *Methods and Protocols,* edited by *Ezio Rosato, 2007*

361. Target Discovery and Validation Reviews and Protocols: *Emerging Molecular Targets and Treatment Options, Volume 2,* edited by *Mouldy Sioud, 2007*

360. Target Discovery and Validation Reviews and Protocols: *Emerging Strategies for Targets and Biomarker Discovery, Volume 1,* edited by *Mouldy Sioud, 2007*

359. Quantitative Proteomics by Mass Spectrometry, edited by *Salvatore Sechi, 2007*

358. Metabolomics: *Methods and Protocols,* edited by *Wolfram Weckwerth, 2007*

357. Cardiovascular Proteomics: *Methods and Protocols,* edited by *Fernando Vivanco, 2006*

356. High-Content Screening: *A Powerful Approach to Systems Cell Biology and Drug Discovery,* edited by *D. Lansing Taylor, Jeffrey Haskins, and Ken Guiliano, and 2007*

355. Plant Proteomics: *Methods and Protocols,* edited by *Hervé Thiellement, Michel Zivy, Catherine Damerval, and Valerie Mechin, 2006*

354. Plant–Pathogen Interactions: *Methods and Protocols,* edited by *Pamela C. Ronald, 2006*

353. Protocols for Nucleic Acid Analysis by Nonradioactive Probes, *Second Edition,* edited by *Elena Hilario and John Mackay, 2006*

352. Protein Engineering Protocols, edited by *Kristian Müller and Katja Arndt, 2006*

351. *C. elegans:* *Methods and Applications,* edited by *Kevin Strange, 2006*

350. Protein Folding Protocols, edited by *Yawen Bai and Ruth Nussinov 2007*

349. YAC Protocols, *Second Edition,* edited by *Alasdair MacKenzie, 2006*

348. Nuclear Transfer Protocols: *Cell Reprogramming and Transgenesis,* edited by *Paul J. Verma and Alan Trounson, 2006*

347. Glycobiology Protocols, edited by *Inka Brockhausen, 2006*

346. *Dictyostelium discoideum* Protocols, edited by *Ludwig Eichinger and Francisco Rivero, 2006*

345. Diagnostic Bacteriology Protocols, *Second Edition,* edited by *Louise O'Connor, 2006*

344. Agrobacterium Protocols, *Second Edition: Volume 2,* edited by *Kan Wang, 2006*

343. Agrobacterium Protocols, *Second Edition: Volume 1,* edited by *Kan Wang, 2006*

342. MicroRNA Protocols, edited by *Shao-Yao Ying, 2006*

341. Cell–Cell Interactions: *Methods and Protocols,* edited by *Sean P. Colgan, 2006*

340. Protein Design: *Methods and Applications,* edited by *Raphael Guerois and Manuela López de la Paz, 2006*

339. Microchip Capillary Electrophoresis: *Methods and Protocols,* edited by *Charles S. Henry, 2006*

METHODS IN MOLECULAR BIOLOGY™

Microchip-Based Assay Systems

Methods and Applications

Edited by

Pierre N. Floriano

University of Texas at Austin
Austin, TX

HUMANA PRESS TOTOWA, NEW JERSEY

999 Riverview Drive, Suite 208
Totowa, New Jersey 07512

www.humanapress.com

This publication is printed on acid-free paper. ∞
ANSI Z39.48-1984 (American Standards Institute)
Permanence of Paper for Printed Library Materials.

Production Editor: Christina M. Thomas

Cover illustration: From Pierre N. Floriano and the University of Texas Faculty Innovation Center. The bottom panel represents a silicon microchip hosting polymeric beads, onto which capturing antibodies are covalently attached. A sandwich-type immunoassay is represented here with a bead-captured antigen, detected with a fluorescently-labeled antibody. The detecting antibody is shown in green to symbolize the detection scheme upon excitation of a green fluorophore with a light source. The top panel is a surface plot of the signal developed on C-Reactive Protein (CRP)-sensitized beads loaded on a 3 x 3 array, as acquired with a charge-coupled device camera. Overlayed is the Caduceus, symbol of Medicine, an insignia modeled after Hermes' staff, as most of the microchip-based assays presented in this book have clinical utility.

For additional copies, pricing for bulk purchases, and/or information about other Humana titles, contact Humana at the above address or at any of the following numbers: Tel.: 973-256-1699; Fax: 973-256-8341; E-mail: orders@humanapr.com; or visit our Website: www.humanapress.com

Printed in the United States of America. 10 9 8 7 6 5 4 3 2 1

eISBN 978-1-59745-426-1

Library of Congress Cataloging-in-Publication Data

Microchip-based assay systems : methods and applications / edited by Pierre N. Floriano.

p. ; cm. -- (Methods in molecular biology ; 385)

Includes bibliographical references and index.

ISBN 978-1-58829-588-0 (alk. paper)

1. Biochips--Laboratory manuals. 2. DNA microarrays--Laboratory manuals. 3. Protein microarrays--Laboratory manuals. I. Floriano, Pierre N. II. Series: Methods in molecular biology (Clifton, N.J.); v. 385

[DNLM: 1. Microchip Analytical Procedures--methods--Laboratory Manuals. W1 ME9616J v.385 2007 / QY 25 M6255 2007]

R857.B5M535 2007

610.28--dc22

2006022683

Preface

Over the past five decades, the microelectronics industry has sustained tremendous growth and has become what is arguably the most dominant industrial sector for our society. The electronics industry has spawned annual growth of more than 30% over this extended time period and has touched almost every aspect of our modern lives through the development of personal computers, portable communication devices, various consumer electronics, navigation tools, and imaging devices. The availability of a powerful microfabrication tool set that can be used to process these devices in a highly parallel manner has led to this explosive growth. Recently, it has become clear that the electronics industry will face new and significant challenges as component device feature sizes shrink into the nanometer size regime. However, with the challenge here has come the opportunity to develop a number of fascinating new sensors and devices using nanometer-sized building blocks. Challenges with spiraling health care costs, the global HIV crisis, environmental, and homeland defense areas all provide strong motivation for the creation of a bridge between microelectronics, nanoscience engineering, and the health sciences. The ultimate applications to be derived from such interdisciplinary efforts are likely to occur for the sectors of environmental, life sciences, and health industries.

Indeed, remarkable advances have been made recently in the development of miniaturized sensing and analytical components for use in a variety of chemical, biological, biomedical, and clinical applications. These efforts have led to the development of microcomponents, such as microchambers, microfilters, microchannels, microarrays, micropumps, and microvalves, whose presence in analytical systems earns them the denomination of "microchip." However, the ability to assemble and interface individual components in order to achieve a high level of functionality in complete working devices continues to pose a daunting challenge for the scientific community as a whole. Lessons learned from the microelectronics and computer software industries provide inspiration for what may be gained from the marriage of microelectronics and sensing areas, through the development of micro-total analysis systems (μ-TAS), and integrated lab-on-a-chip (LOC) approaches. Although chemical and medical tests have traditionally been completed in central laboratories that are filled with specialized equipment and trained technicians, there is currently a trend to complete more tests using portable instrumentation.

Tremendous advances have been made recently in the area of LOC devices exploiting the advantages of miniaturization mediated by the small reagent and sample volumes required. Smaller sample and reagent volumes translate to rapid analysis times and less waste volumes, and result in more cost-effective assays that can be operated with less technological constraints making them amenable to point-of-care or field testing. Most importantly, these characteristics when fully developed into a functional system have the potential to lead to a significant reduction in the time that is needed for an accurate diagnosis or analysis, and subsequent treatment or action (i.e., "turn-around time"). Although there are still only a few commercially available microchips for use as environmental, chemical, military, or medical sensor devices, the area has attracted significant attention as research teams strive to develop new miniaturized sensor devices.

We wish to express our immense gratitude to all the authors for their dedication and expert contributions. Most of the exciting work presented here has greatly benefited from ground-breaking research in the fields of sensing, nanotechnology, and microfluidics, across multidisciplinary collaborative work in chemistry, biology, immunology, physics, and engineering. Therefore, we would also like to extend our appreciation to such pioneers who were not able to contribute to this book but kindly responded with helpful suggestions. Although the presentation of a specific technique alone would require at least an entire volume for appropriate coverage, presented here are examples of DNA-, cellular-, chemical-, protein-based assays conducted on microchips utilizing various aspects of microchip fabrication for application in specific disease diagnostic, and chemical or biological sensing. The overall purpose of this volume is to provide a "taste" of what can be envisioned and realized with microchip approaches. Moreover, the protocols here detailed will help foster interest in microchip-based assays by providing readers with all the tools necessary to create their own microchip-based assays targeted to new applications. It is hoped that this compilation of methods and protocols will help to expand the scope and accelerate the transition of microchip-based assays from academic and industrial research and development centers to real-world use.

I would like to join Satie Siewah and her colleagues in remembrance of Dr. Kenneth Anil Deisingh who tragically passed away during the editing phase of this book.

Pierre N. Floriano

John T. McDevitt

Contents

Contributors

Shelley Acosta • Department of Chemistry and Biochemistry, University of Texas at Austin, Austin, TX
Joanna S. Albala • Department of Otolaryngology, University of California at Davis, Sacramento, CA
Padmapriya P. Banada • Molecular Food Microbiology Laboratory, Purdue University, West Lafayette, IN
Peter T. Beernink • Biosciences Division, Lawrence Livermore National Laboratory, Livermore, CA
Arun Bhunia • Molecular Food Microbiology Laboratory, Purdue University, West Lafayette, IN
Julio A. Camarero • Chemical and Materials Sciences Division, Lawrence Livermore National Laboratory, Livermore, CA
Madhu Prakash Chatrathi • Chemistry Division, Naval Research Laboratory, Washington DC
Shu-Hui Chen • Department of Chemistry, National Cheng Kung University, Taiwan
Nicolaos Christodoulides • Department of Chemistry and Biochemistry, University of Texas at Austin, Austin, TX
Tony K. H. Chung • Department of Obstetrics & Gynaecology, The Chinese University of Hong Kong, Hong Kong
Matthew A. Coleman • Biosciences Division, Lawrence Livermore National Laboratory, Livermore, CA
Greg Collins • Chemistry Division, Naval Research Laboratory,Washington DC
Anil Deisingh • Caribbean Industrial Research Institute, University of the West Indies, St. Augustine, Trinidad and Tobago
Priya Dharshan • Department of Chemistry and Biochemistry, University of Texas at Austin, Austin, TX
Pierre N. Floriano • Department of Chemistry and Biochemistry, University of Texas at Austin, Austin, TX
Ludivine Grosjean • CEA Grenoble, Département de Recherche Fondamentale sur la matière condensée, Grenoble, France
Anthony Guiseppi-Elie • Chemical and Biomolecular Engineering, Clemson University, Clemson, SC
Anja Gulliksen • Norchip AS, Klokkarstua, Norway
Christian Harwanegg • VBC Genomics Bioscience Research GmbH, Rennweg, Vienna, Austria

Reinhard Hiller • Cape Biotech Trust, Capetown, South Africa
Tani Hirofumi • Division of Biotechnology and Macromolecular Chemistry, Graduate School of Engineering, Hokkaido University, Sapporo, Japan
Sabine Hutter • VBC Genomics Bioscience Research GmbH, Rennweg, Vienna, Austria
Tamio Kamidate • Division of Biotechnology and Macromolecular Chemistry, Graduate School of Engineering, Hokkaido University, Sapporo, Japan
James Karlinsey • Department of Chemistry, University of Virginia, Charlottesville, VA
Frank Karlsen • Norchip AS, Klokkarstua, Norway
James P. Landers • Department of Chemistry, University of Virginia, Charlottesville, VA
Louise Lingerfelt • Center for Bioelectronics, Biosensors, and Biochips, School of Engineering, Virginia Commonwealth University, Richmond, VA
Thierry Livache • CEA Grenoble, Département de Recherche Fondamentale sur la matière condensée, Grenoble, France
Chang Lu • Department of Agricultural and Biological Engineering, Purdue University, West Lafayette, IN
Koji Maehana • Division of Biotechnology and Macromolecular Chemistry, Graduate School of Engineering, Hokkaido University, Sapporo, Japan
Lara K. Mahal • Department of Chemistry and Biochemistry, University of Texas at Austin, Austin, TX
John T. McDevitt • Department of Chemistry and Biochemistry, University of Texas at Austin, Austin, TX
Emilie Mercey • CEA Grenoble, Département de Recherche Fondamentale sur la matière condensée, Grenoble, France
Dean Neikirk • Department of Chemistry and Biochemistry, University of Texas at Austin, Austin, TX
Kanoelani Pilobello • Department of Chemistry and Biochemistry, University of Texas at Austin, Austin, TX
Andre Roget • CEA Grenoble, Département de Recherche Fondamentale sur la matière condensée, Grenoble, France
Brent C. Satterfield • Department of Chemistry, Arizona State University, Tucson, AZ
Satie Siewah • Department of Chemistry, University of the West Indies, St. Augustine, Trinidad and Tobago
D. I. Smith • Department of Experimental Pathology, Mayo Foundation School of Medicine, Rochester, MN
Nardos Tassew • Department of Molecular Biology, The Scripps Research Institute, La Jolla, CA

Michael Thompson • Department of Chemistry, University of Toronto, Toronto, Ontario, Canada
Cheng C. Wang • Qiagen, Pudong, Shanghai, China
Hsiang-Yu Wang • Department of Agricultural and Biological Engineering, Purdue University, West Lafayette, IN
Joseph Wang • Departments of Chemical and Materials Engineering and Chemistry and Biochemistry, Arizona State University, Tempe, AZ
Vivian W. Wang • Department of Obstetrics, Gynecology and Reproductive Medicine, Brigham and Women's Hospital, Harvard Medical School, Boston, MA
Shannon Weigum • Department of Chemistry and Biochemistry, University of Texas at Austin, Austin, TX
Jay A. A. West • Arcxis Biotechnologies, Castro Valley, CA
Jorge Wong • Department of Chemistry and Biochemistry, University of Texas at Austin, Austin, TX
Yick-Fu Wong • Department of Obstetrics & Gynaecology, The Chinese University of Hong Kong, Hong Kong

1

Microchip Electrophoresis for DNA Separation by Wire-Imprinted Microchannels on PMMA Substrates

Shu-Hui Chen

Summary

Microchip electrophoresis has become a mature separation technique in recent years. Compared to agarose gel electrophoresis, which is commonly used for DNA separation, microchip electrophoresis has several advantages such as automation, fast analysis speed and minimum sample requirement. For the fabrication of electrophoretic microchips, silica-based and polymer-based materials are two commonly used substrates. Among the polymer-based materials, poly(methyl methacrylate) (PMMA) substrate can be wire-imprinted in a common laboratory to form microfluidic channels without expensive fabrication facilities. Moreover, the neutral hydrophilic surface chemistry of PMMA allows direct DNA separation to be performed on bare microchips without the tedious surface modifications that are normally required for silica-based materials. This chapter presents an imprinting method for fabricating PMMA microchips as well as the on-chip assay for performing electrophoretic DNA separation on the fabricated microchip.

Key Words: Microchip electrophoresis; DNA; poly(methyl methacrylate); wire imprinting.

1. Introduction

Capillary electrophoresis (CE) on microchips ***(1–8)*** is an electrically driven separation technique that allows the separation speed to reach a new milestone because of its compact device configuration. Applications of microchip electrophoresis are very diverse, including DNA, proteins, and many organic compounds. Among these applications, DNA assays have an enormous scope of uses in biotechnology and medicine, ranging from agriculture and farming to the detection of pathogens in foods to drug discovery and genetic diagnostics on human subjects. Such a broad-based application may prove to be the ultimate technology driver of all time. The performance and costs of genetic

From: *Methods in Molecular Biology, Vol. 385: Microchip-Based Assay Systems: Methods and Applications*
Edited by: Pierre N. Floriano © Humana Press Inc., Totowa, NJ

assays can be improved in the microscale because of the reduced analysis time and reagent consumption as well as the automation and control provided by miniature electronic devices.

While most of the reports on microfabricated electrophoretic devices have utilized glass or silica as substrates, polymer substrates are viewed as promising alternatives for the production of microfluidic systems because these materials are less expensive and easier to manipulate than silica-based substrates. Moreover, the inherent neutral hydrophilic nature of the polymer substrate allows direct use of the channel for the analysis of biomolecules without the need for surface modifications to reduce the wall adsorption and contamination ***(6–8)***. Wire-imprinting methods have been demonstrated for the fabrication of simple cross microchannels on PMMA substrate without expensive clean room facilities ***(6–8)***, and the fabrication method will likely be used by research laboratories to explore microchip techniques. Results also indicate that the performance of the resulting microchips for DNA separation is comparable to those fabricated by other professional means.

2. Materials

2.1. Wire-Imprinting Microchips

1. Two Chromel wires (79 μm i.d., 6 and 15 cm in length, respectively) from McMaster, Los Angeles, CA.
2. PMMA Plexiglas pieces (2 cm wide × 10 cm long × 2.0 mm thick) from local suppliers.
3. Glass slides (2 cm in width × 10 cm in length and 5.0 mm thickness) from local suppliers.
4. T-Handle Clampers from McMaster, Los Angeles, CA.
5. Drill (1.6 mm i.d.) from local suppliers.
6. High temperature oven with the applicable operation temperature up to 120°C.

2.2. On-Chip DNA Separation Assay

1. DNA fragment standard ϕX-174-RF DNA digested by *Hae*III; is from Amersham-Pharmacia Biotech (Buckinghamshire, England), and the total concentration is 5 μg/mL as purchased.
2. The intercalating dyes, YOPRO-1, are from Molecular Probes (Eugene, OR) (*see* **Note 1**).
3. Hydroxypropyl methyl cellulose (HPMC) with a viscosity range of 80–120 cps (2 wt% in H_2O) is from Aldrich (St. Louis, MO)
4. TBE buffer: 100 m*M* Tris, 100 m*M* boric acid, and 5 m*M* ethylene diamine tetraacetic acid (EDTA), pH 8.2. Store buffer at 4°C.
5. Separation buffer: 1.5% (w/w) HPMC in TBE buffer with 1% (v/v) of YOPRO-1. Store at 4°C and sonicate the buffer for 10 min before use (*see* **Note 2**).

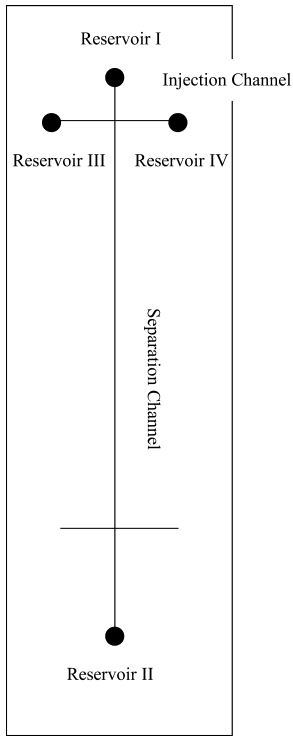

Fig. 1. Microchip configuration.

6. Microchip electrophoresis system equipped with a mercury lamp or other light sources for laser-induced fluorescence: Basically, any systems ***(1–8)*** can be used as long as the microchip can be read by the instrument. The injection and separation conditions described in this chapter are based on a home-made system described in **refs. *7*** and ***8*** except that a mercury lamp was used instead of He-Ne laser. This system was modified from a commercial reflection microscope (Model BX40, Olympus, Tokyo, Japan) using a photomultiplier tube. The operation parameters such as the separation/injection voltages shown here may be changed to fit the optimum condition for different instruments.

3. Methods

3.1. Wire-Imprinting Microchips

The configuration of the cross microchannels and the imprinting procedures are depicted in **Fig. 1** and **Fig. 2**, respectively. Detailed steps are described in the following.

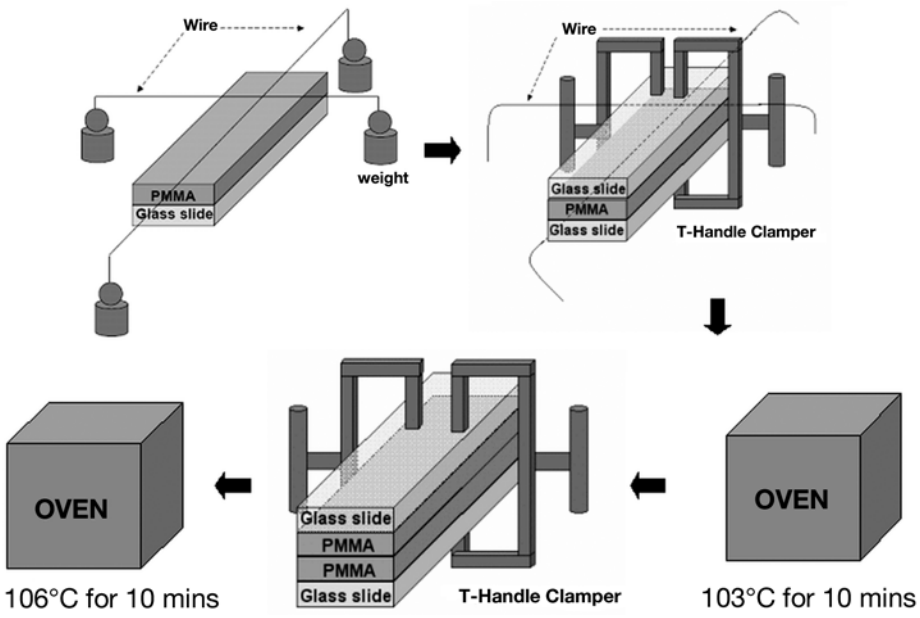

Fig. 2. Wire-imprinting procedures.

To form a simple cross-microchannel (**Fig. 1**) on PMMA substrate, prepare two pieces of PMMA Plexiglas plates: one for base plate and one for cover plate. Wash the surface of the plates thoroughly with deionized water to remove dust and contaminants and then use air compressor to clean and dry the surface.

1. Two Chromel wires (6 cm for the injection channel and 15 cm for the separation channel) are used as the template to imprint the microchannels. The wires are stretched tightly by two weights that are connected to both ends and then crossed over on the top of the base plate (**Fig. 2**).
2. The base plate and the wires are placed between two clean glass slides, and the assembly is clamped tightly by eight T-handle clampers. The clamping pressure was estimated to be around 8 kg/cm^2. Both ends of the Chromel wires are cut out to separate the weights.
3. The clamped assembly is placed into the oven, and PMMA channels are formed by heating at 103°C for 10 min. This temperature is called the softening temperature. After 10 min, the temperature is lowered to 50°C and left for cooling. The assembly is subsequently removed from the oven and allowed to cool to room temperature completely.
4. The clampers and the Chromel wires are removed to release the imprinted PMMA base plate.

5. Prior to bonding, four through holes (1.6 mm in diameter) are drilled on the cover plate to form the buffer reservoirs. These holes are aligned with the ends of the channels imprinted on the base plate to create the buffer and sample reservoirs.
6. The imprinted base plate is covered by the cover plate, and the assembly is clamped again with two glass slides and heated at 106°C for 10 min to make sure the two pieces are completely bonded. After 10 min the temperature is lowered to 50°C for cooling, and then the assembly is removed from the oven to cool to room temperature completely. The resulting length of the injection channel (between reservoirs III and IV) is 2 cm, and the length of the separation channel (between reservoirs I and II) is 5 cm.

3.2. On-Chip DNA Separation Assay

The capability of the fabricated chip for electrophoretic injection and separation is demonstrated via the analysis of DNA fragments ϕX174-RF digested by *Hae*III. Detailed experimental procedures are described here.

1. Before performing separation assay, the microchannels need to be cleaned thoroughly. Pipet 7 μL of 1 *N* NaOH into reservoirs I, II, and IV and then flush the solution through the microchannels for 10 min by applying vacuum through reservoir III. DI (*see* **Note 3**). Water is subsequently flushed through the microchannels following the same procedure (*see* **Note 4**).
2. Seven μL of the separation buffer are pipetted into reservoirs I, II, and IV, and the channels are filled with the separation buffer by applying vacuum through reservoir III (*see* **Note 5**).
3. Five μL of the DNA fragments solution are pipetted into reservoir III for separation and then the microchip is placed into the instrument. The detection light is focused at a distance of 3 cm from the channel cross, which gives a 3-cm separation length (*see* **Note 6**).
4. For sample injection, a voltage of –300 V (–150 V/cm) is applied to the injection channel between reservoir III (–300 V) and reservoir IV (grounded) for 0.15 min while keeping the separation channel (between reservoirs I and II) floating. For sample separation, a voltage of –1.5 kV (–300 V/cm) is applied to the separation channel between reservoir I (–1.5 kV) and reservoir II (grounded) while keeping the injection channel floating.
5. Under normal conditions, the voltage-switching scheme described in **step 4** may be repeated up to 7–10 times to give consecutive electropherograms for the same sample *(7)*. This information is useful for deducing the relative standard deviation of the migration time and peak area. Consecutive voltage switching may also be required when the first injection does not give satisfactory signals (*see* **Note 7**).
6. A typical electropherogram obtained is shown in **Fig. 3**. As indicated, all 11 DNA fragments of the ϕX174-RF size marker could be separated and identified in less than 2–3 min. The performance of the current assay can be checked from the resolution between the fragment pair of 271 and 281 bp. Under the current sepa-

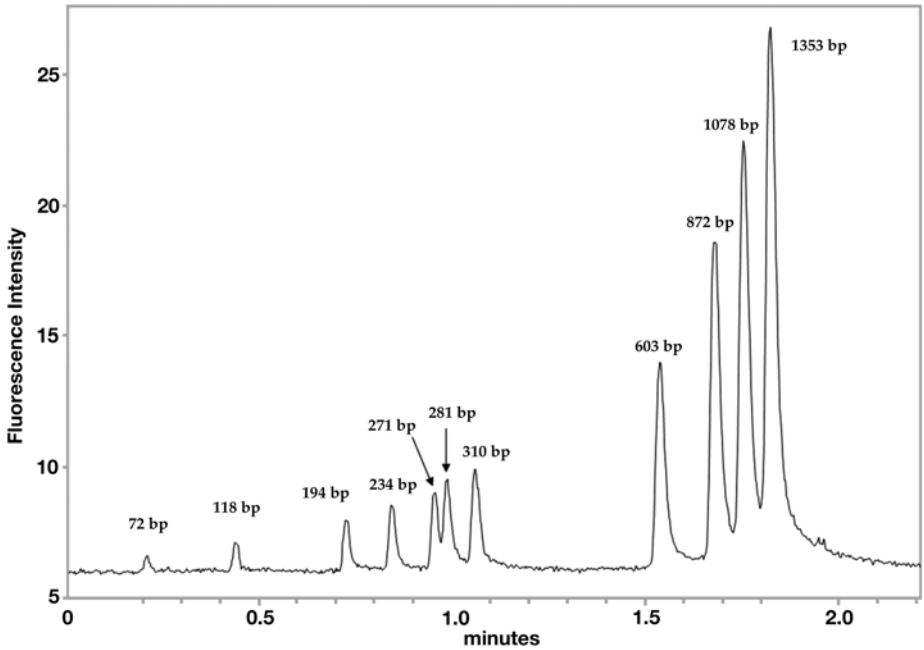

Fig. 3. Chip electropherogram of DNA fragment standard ϕX-174-RF DNA digested by *Hae*III.

ration condition, 300 V/cm electric field, 3-cm separation length, and 1.5% HPMC separation buffer, the resolution for the 271/281 pair should be as displayed in **Fig. 3** (*see* **Note 8**) with an R value of around 0.8. However, the resolution for longer fragments ({GT}800 bp) is worse than that for the shorter fragments under the current separation conditions (*see* **Note 9**). The detection limit for the current assay was estimated at around 0.1 µg/mL (signal-to-noise ratio approx 3) for the total DNA concentration *(7)*.

7. The imprinted microchip may be reused if no clear damage or channel blocking is noticed (*see* **Note 10**).

4. Notes

1. Other intercalating dyes such as TOPRO-3 may also be used for different detection wavelengths.
2. Since the separation buffer includes intercalating dyes, it must be kept in darkness.
3. CE water is deionized distilled water that is filtered through a Barnstead E-pure system. The resistance of the water is more than 18.0 MΩ/cm^3. Both the buffer and the sample solutions are filtered through a 0.22-µm membrane before chip electrophoresis.

4. During the microchip fabrication, dusts and particles should be thoroughly removed by air compressor to prevent the channel blocking.
5. Prior to performing separation, microchannels need to be inspected under the microscope for air bubbles. Air bubbles need to be removed completely by vacuum before the separation.
6. The length of the separation channel does not mean the length of the separation. The distance between the detection point and the channel cross determines the separation length, and it can be varied by focusing the light source at different points along the separation channel. A longer separation length normally gives a slightly better resolution.
7. The first injection may sometimes fail for unknown reasons. If this happens, try to perform the injection and separation again; the signal will normally come out in the second or the third injection under these circumstances.
8. The resolution for the 271/281 pair of digested fragments may be further improved to reach baseline resolution either by increasing the HPMC concentration or by increasing the electric field strength. However, the separation buffer becomes rather viscous under higher polymer concentrations and the baseline becomes rather unstable under higher electric fields.
9. Other polymers may be tried to develop separation assays with higher resolving powers, especially for longer DNA fragments. The current assay is more suitable for detecting and identifying DNA fragments shorter than 800 bp.
10. If the microchip is to be reused, the microchannels need to be rinsed with deionized water for 10 min after the assay and then dried.

Acknowledgments

The author would like to thank Chun-Che Lin, Bi-Kai Hsu, and Dr. Wang-Chou Sung for their help in preparing this chapter.

References

1. Harrison, D. J., Fluri, K., Seiler, Z. Fan, Effenhauser, C. S., and Manz, A. (1993) Micromachining a miniaturized capillary electrophoresis-based chemical analysis system on a chip. *Science* **261,** 895–897.
2. Harrison, D. J., Manz, A., Fan, Z., Ludi, H., and Widmer, H. M. (1992) Capillary electrophoresis and sample injection systems integrated on a planar glass chip. *Anal. Chem.* **64,** 1926–1932.
3. Raymond, D. E., Manz, A., and Widmer, H. M. (1994) Continuous sample pretreatment using a free-flow electrophoresis device integrated onto a silicon chip. *Anal. Chem.* **66,** 2858–2865.
4. Regnier, F. E., He, B., Lin, S., and Busse, J. (1999) Chromatography and electrophoresis on chips: critical elements of future integrated, microfluidic analytical systems for life science. *Trends Biotechnol.* **17,** 101–106.
5. Effenhauser, C. S., Paulus, A., Manz, A., and Widmer, H. M. (1994) High-speed separation of antisense oligonucleotides on a micromachined capillary electrophoresis device. *Anal. Chem.* **66,** 2949–2953.

6. Martynova, L., Locascio, L. E., Gaitan, M., Kramer, G.. W., Christensen, R. G., and MacCrehan, W. A. (1997) Fabrication of plastic microfluid channels by imprinting methods. *Anal. Chem.* **69,** 4783–4789.
7. Chen, Y.-H. and Chen, S.-H. (2000) Analysis of DNA fragments by microchip electrophoresis fabricated on poly(methyl methacrylate) substrates using wire-imprinting method. *Electrophoresis* **21,** 165–170.
8. Chen, Y.-H., Wang, W.-C., Young, K.-C., Chang, T.-T., and Chen, S.-H. (1999) Plastic microchip electrophoresis for analysis of PCR products of serum hepatitis C virus. *Clin. Chem.* **45,** 1938–1943.

2

Fabrication of Porous Polymer Monoliths in Microfluidic Chips for Selective Nucleic Acid Concentration and Purification

Jay A. A. West and Brent C. Satterfield

Summary

Efficient and rapid isolation of nucleic acids is of significant importance in the field of genomics for a variety of applications. Current techniques for the isolation of specific nucleic acids or genes typically involve multiple rounds of amplification of the target sequence using polymerase chain reaction. Described here is a recent development in the fabrication and modification of porous polymer monoliths for the selective concentration and extraction of nucleic acids sequences. The rigid monoliths are cast to shape and are tunable for functionalization using a variety of amine-terminated molecules including oligonucleotide capture probes. Efficient and rapid isolation of nucleic acids can be performed using polymer monoliths in microchannels in a time frame as short as 2 s. The described materials and methods offer the ability to perform concentration of nucleic acids in solution and elute purified samples in volumes as low as 3 μL without the requirement of altering salt concentration in the wash and elution buffers.

Key Words: Sample preparation; nucleic acids; DNA; RNA; mRNA; monolith; microfluidics.

1. Introduction

Microfluidics is playing an increasingly central role in diagnostics as it represents faster, cheaper, and more sensitive portable technologies ***(1,2)***. However, for the majority of microfluidic applications, real world samples present a major challenge in device functionality. As a result, the increased benefits of microfluidic analysis apply only to highly purified and highly concentrated samples ***(3,4)***. Thus, there is a need for more efficient and equally portable sample preparation technologies in order to fully automate the process.

From: *Methods in Molecular Biology, Vol. 385: Microchip-Based Assay Systems: Methods and Applications*
Edited by: Pierre N. Floriano © Humana Press Inc., Totowa, NJ

Sample preparation can be divided into four major steps: (1) separation of sample from matrix through cell lysis and filtration, (2) sample preconcentration, (3) derivatization, and (4) biochemical pretreatment. The actual methodologies in implementing these steps vary according to the sample type and end analysis ***(5)*** **.** Eukaryotic mRNA as a polynucleotide analyte has particular appeal as it represents the active portion of DNA or the part of DNA that is actively engaged in phenotypic expression in an organism. It is readily extracted from the eukaryotic cellular matrix via the presence of a polyadenaline tail using a variety of techniques ***(6–8)***.

Recently, functionalized photo-polymerized monoliths have been used as an alternative to traditional sample preparation and analysis methods for chemicals ***(9)***, polypeptides ***(10,11)***, and, polynucleotides ***(12)***, most of these being used in conjunction with capillary electrochromatography or high-performance liquid chromatography. These technologies, and other solid supports, have been reviewed extensively by Peterson and Svec ***(13,14)***. They provide high surface area for adsorption of the analyte of interest ***(15)***, variable pore size and porosity based on concentration and type of porogenic solvent ***(9)***, and are easily and cost-effectively created inside of microfluidic channels through ultraviolet (UV) light exposure. They also exhibit good surface adhesion and make even contact with channel walls ***(16)***.

Despite these advances, to date there are few examples of sample preparation devices that truly take advantage of current technology and trends for preconcentration and purification of nucleic acids. Described here is a nucleic acid sample preconcentration method that allows for facile incorporation into a microfluidic detection unit and furthermore allows for constant flow through binding kinetics with the use of a single solvent. Using a photoinitiated monolith that is polymerized and functionalized *in situ*, it is possible to take advantage of the large surface area and controllable pore size inherent to monoliths. High efficiencies and fast hybridization times dictate that oligonucleotide functionalized porous polymer monoliths (PPMs) will be an ideal material for nucleic acid sample preparation using microfluidic devices.

2. Materials

2.1. Porous Polymer Monoliths

1. PPMs can be fabricated in a variety of microchannel devices including custom microfluidic chips. For ease of experimentation, we describe a technique to fabricate the PPM material in fused silica capillary. The described methods here are appropriate for the PPM fabrication in capillaries ranging in size from 30 to 500 μm internal diameter, which can be purchased from Polymicro Sciences (Phoenix, AZ).
2. Pretreatment solution: 50% v/v distilled deionized water, 30% glacial acetic acid, and 20% Z-6030 (Dow Corning, Midland, MI).

3. Sodium phosphate buffer: 10 m*M* NaH_2PO_4 buffer, pH 7.0.
4. Monomer solution: 12.5% v/v 10 m*M* NaH_2PO_4, pH 7.0, 12.5% ethyl acetate, 40% methanol, 10.5% 3-glycidylpropyldimethoxymethylsilane (GMA), 24.5% ethyleneglycoldimethacrylate (EGDMA) (Sigma, St. Louis, MO), also containing either 2.5 mg Irgacure (Ciba Specialty Chemicals, McIntosh, AL) or 5.0 mg azobisisobutyronitrile (AIBN) (Sigma-Aldrich, St. Louis, MO) per 1 mL of monomer solution.

2.2. Functionalization of PPM

1. Amine-linked oligonucleotides: amine terminated oligonucleotides 30–40 nucleotides in length contain a terminal amine moiety attached to the nucleotide via a C6-linker. In some cases we commonly used oligonucleotides that contained either 6-carboxyfluorescein or Cy5 label to optimize the attachment chemistry.
2. Functionalization buffer: 3X standard sodium citrate (SSC) and 0.05–0.1% sodium dodecyl sulfate (SDS) (Sigma-Aldrich, St. Louis, MO).
3. Sodium phosphate buffer: 10 m*M* NaH_2PO_4 (Sigma-Aldrich, St. Louis, MO) buffer, pH 7.0.

2.3. Nucleic Acid Labeling and Hybridization

1. Ulysis DNA labeling kits were purchased from Molecular Probes (Eugene, OR) and used to label mRNA as suggested by the manufacturer.
2. PCR clean-up kits were purchased from Qiagen (Valencia, CA) and used as suggested by the manufacturer.
3. Blocking buffer: 10 m*M* Tris-HCl buffer pH 9.0, 0.05–0.1% SDS, 0.1 m*M* bovine serum albumin (BSA), and 5 m*M* ethanol amine.
4. Sample buffer: 1X SSC in 5 m*M* TE buffer, pH 7.5.
5. Wash and elution buffer: 1X SSC in 5 m*M* TE buffer, pH 7.5.

2.4. Hardware and Thermocontrol

1. The microfluidic components can be constructed on site using Ultem (polyetherimide, GE Plastics, Southfield, MI). Microfluidic fittings made with PEEK were supplied by Sandia National Laboratories or purchased from Upchurch Scientific (Oak Harbor, WA).
2. Temperature control: a thermoelectric cooler (Model no. XLT2386) from Marlow industries (Dallas, TX) capable of temperature ranges between 4 and 120°C was used to control the temperature of the microchannel containing devices (both capillary and microfluidic chips).
3. Thermoelectric control board: an integrated circuit board to perform active temperature control of the thermoelectric heating/cooling device (TEC) was purchased from Marlow Industries.
4. Thermocouple: temperature at the surface of the PPM device was monitored at the exterior of the device. Unless otherwise stated, the temperature is assumed to be uniform from the surface of the device to the active area within the trapping column. This assumption is valid as a result of the rapid heat transfer in

microfluidic devices. Temperature was monitored using a K-type thermocouple purchased from Omega Engineering (Stamford, CT), which was connected to either a Fluke 712 RTD Process Calibrator (Everett, WA) or a data acquisition card for active temperature control of the PPM-containing device.

5. Control software: control software for the thermoelectric cooler was programmed using National Instruments (Austin, TX) LabView program. The control software can be arranged to both measure the temperature at the thermocouple interface and adjust where necessary to control the voltage output to the thermoelectric cooler to control the temperature of the PPM device.

2.5. Imaging

1. Microscope: an inverted Olympus (Melville, NY) fluorescent microscope was used to image microchannel devices containing the PPM material for both brightfield and fluorescence imaging of the PPM devices. A back-cooled color MicroFire CCD camera (Optronics Inc., Goleta, CA) connected to the microscope was used to capture images of the functionalized PPM.
2. Scanner: a GenePix 4000B (Molecular Devices, Sunnyvale, CA) microarray scanner was used to acquire confocal images of the functionalized PPM devices. Image processing: images were acquired using GenePix software to optimize the background and gain levels of the images. Microsoft picture viewer was then used to reformat the acquired image from a 12-bit image to an 8-bit image. Further image processing using Adobe Photoshop was used to produce high-quality publication images.

3. Methods

Nucleic acids, especially mRNA, are inherently unstable molecules. With respect to RNA, this instability results mainly from the ubiquitous presence of RNases present on our bodies (skin, hair, etc.). Standard techniques to isolate and purify nucleic acids usually include a series of labor-intensive steps to exchange buffers, isolate the target nucleic acids on a stationary phase, wash away contaminants, and, finally, elute purified nucleic acids. Described in this procedure is a technique to rapidly isolate and purify nucleic acids using a simplified microfluidic platform. While the technique in this procedure is optimized for microfluidics, there is no technical limitation in scaling the process up to larger devices for mass isolation and purification of nucleic acids. In the described arrangement, the only critical step is creating the porous polymer monolithic material and maintaining the intact glycidyl chemistry prior to functionalization of PPM with the desired macromolecular structure.

3.1. Porous Polymer Monoliths

1. Trapping and purification of target oligonucleotides was accomplished using a UV cured porous polymer monolith, which was fabricated in a fused silica capillary.

2. To begin the procedure, capillaries or microchannels roughly from 75 to 500 µm id (inner diameter) (Polymicro Technology, Phoenix, AZ) are pretreated with a mixture consisting of 50% v/v distilled deionized water, 30% glacial acetic acid, and 20% Z-6030 (Dow Corning, Midland, MI). The capillary should be extensively flushed with the solution, then allowed to stand for 1 h.
3. The microchannels are then flushed with filtered 10 m*M* NaH_2PO_4 buffer, pH 7.0, and dried.
4. Monoliths are readily created by choosing a crosslinker, a functional monomer, a porogenic diluent, and a photoinitiator. An optimized solution contains 12.5% v/v 10 m*M* NaH_2PO_4, pH 7.0, 12.5% ethyl acetate, 40% methanol, 10.5% GMA, 24.5% EGDMA, also containing 2.5 mg Irgacure (Ciba Specialty Chemicals, McIntosh, AL) per 1 mL monomer solution. The solution is first vortexed until the initiator is solubilized. The solution is then passed through a hydrophobic filter to remove any insoluble particles. (*see* **Notes 1** and **2**).
5. Immediately prior to polymerization the microchannel is flushed with 30 vol of the sodium phosphate buffer.
6. The capillaries are then filled and photoinitiated at 365 nm using either a UV crosslinking oven (Spectronics Corporation, Westbury, NY) for 30 min or an Optilux™ 501 UV dental curing gun for 6–7 min. Devices and capillaries should be masked where appropriate to avoid polymerization of the monolith in undesired regions of the microfluidic device. Masking of microfluidic chips can be easily accomplished using black electricians tape.
7. After polymerization the polymerized monolith is immediately flushed again with the sodium phosphate buffer, and then passively dried in the presence of N_2.
8. The devices can then be stored until postmodification with amine-terminated macromolecules in a dessicator under vacuum with N_2 (**Fig. 1**).

3.2. Functionalizing PPM

1. Typical functionalization chemistry (**Fig. 2**), such as primary amine-terminated molecules was employed to perform nucleophilic attack on the existing epoxide chemistry intact on the PPM material (*see* **Note 3**). For hydrophobic molecules, such as fluorescent dyes, the reactions were carried out in solutions based in an organic solvent such as acetonitrile or methanol (*see* **Note 4**). For hydrophilic molecules such as amine-terminated nucleic acids or proteins, reactions were carried out in a water-based buffer containing 3X SSC and 0.05–0.1% SDS (*see* **Note 5**).
2. To covalently attach an oligonucleotide to the PPM, a 5'NH_3-C6 linked nucleotide typically 30 or 40 bases in length is dissolved (10–20 µg/µL) in the 3X SSC 0.05% SDS buffer.
3. This solution is then denatured at 95°C for 5–10 min prior to introduction onto the PPM-filled channel (*see* **Note 6**).
4. The solution is then introduced to the PPM at modest pressure (75–200 psi) using a standard plastic syringe.
5. The PPM containing the oligonucleotide solution is then heated at 120°C for a period of 30 min to facilitate irreversible covalent attachment of the macromolecule to the PPM (*see* **Note 7**).

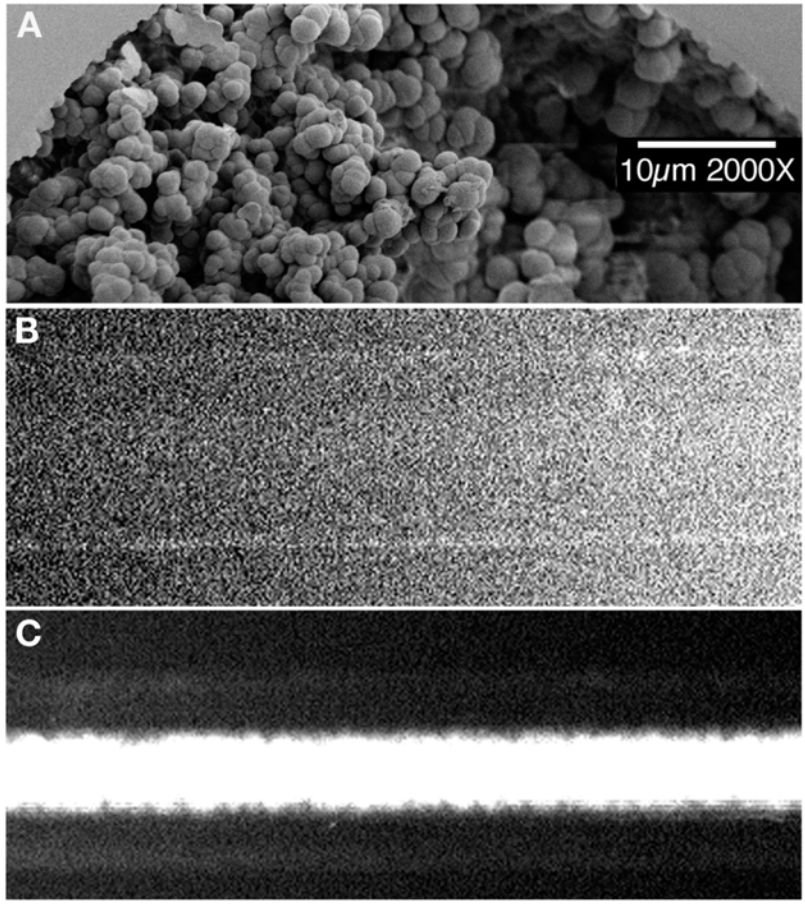

Fig. 1. Porous polymer monolith (PPM): using GMA, EGDMA, and the Irgacure initiator, PPM materials can be easily fabricated in microchannels. The PPM **(A)** has a nodular, high-surface-area structure. PPMs form a covalent bond with the microchannel wall, negating the use of frits to contain the polymer in a discrete location. In addition, the PPM material is functionalization ready. Here the polymer was functionalized with an amine-terminated fluorescent dye **(C)**. In contrast to control **(B)**, an intense fluorescent signal is apparent in the capillary after functionalization. **B** and **C** were imaged using a fluorescent microscope with a filter set to capture images using 488-nm excitation and 525-nm emission wavelengths.

6. After the columns are functionalized, the excess solution containing the unbound amine terminated oligonucleotide is flushed off using a 30X channel volume of the 3X SSC 0.05% SDS buffer.

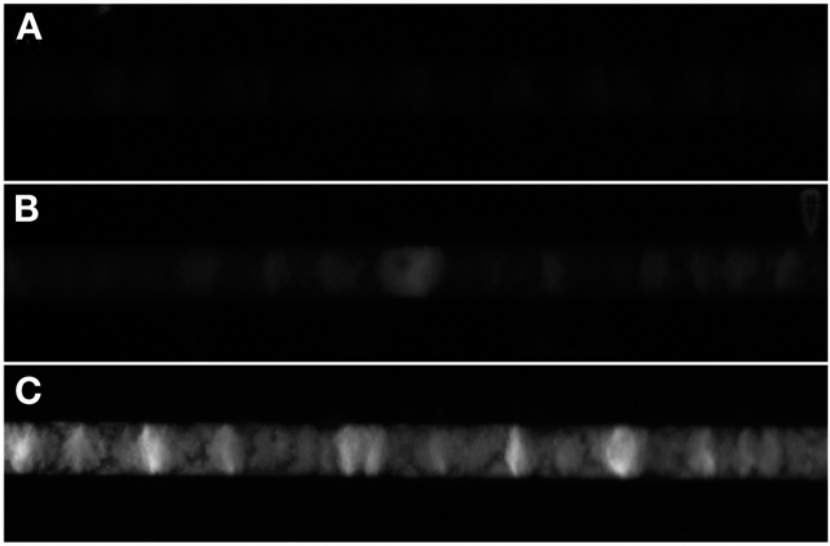

Fig. 2. Functionalization of porous polymer monolith (PPM) with oligonucleotides. PPM material was covalently modified using a 6-carboxyfluorescein containing 30-mer Oligo dT. The reaction was temperature dependent. When the PPM was incubated at 60°C for 30 min **(A)**, no apparent attachment of the Oligo dT occurred. When the temperature was raised to 90°C **(B)**, there was an increased the fluorescent intensity on the column after 30 min, indicating increased binding of the Oligo dT. The intensity was maximal when the temperature was increased further to 120°C for 30 min **(C)**. We found that higher temperature or longer incubation times did not increase fluorescent intensity further.

7. Functionalized PPM columns can be stored dry or containing solution for extended periods of time, up to 6 mo (*see* **Note 8**).

3.3. Hybridization of mRNA to Oligo dT Monolith

The isolation of nucleic acids can be performed under either stopped flow conditions or under active flow. Typically when small volumes <10 µL) are employed, stopped flow conditions are more desirable.

1. One of the most critical steps in the process of performing hybridizations using the microchannel-based PPM material is the blocking of the unbound active epoxide sites that are not occupied during the functionalization. The blocking of nonspecific binding can be easily achieved by introducing a 0.1-m*M* solution of BSA dissolved in the hybridization buffer prior to active hybridization using target nucleic acids. Once introduced the blocking buffer should be allowed to

stand for a period of 30–60 s at 95°C. The hybridization can then be performed immediately after this blocking step. Alternatively, the capillary can be flushed with the hybridization prior to isolation and purification of nucleic acids (*see* **Note 9**).

2. After blocking is complete, small volumes as low as 0.5–1.0 µL of nucleic-acid-containing sample can be introduced to the column (*see* **Note 10**).
3. Prior to introduction of the sample to the column, it must be denatured at 95°C for 1 min. This can be simply achieved by heating the sample contained in a syringe or extended length of capillary on a heating block.
4. Quickly after the denaturation step, the sample should be loaded into the capillary containing the functionalized PPM. When the column is loaded it is important to maintain a temperature above the theoretical melting temperature (Tm) of the target-probe complement to avoid nonspecific oligonucleotide hybridizations. As an example, for mRNA purification the column is maintained at approx 75°C during the introduction of the sample. When the sample is loaded, the PPM-containing device should be cooled to approx 5–10° below the *Tm* of the hybrid pair.
5. During this period of cooling, the target analyte will have annealed to the probe specifically. The column can then be flushed to remove nonhybridized nucleic acids. Typically this can be carried out using a fresh volume of 1x SSC in 5 m*M* TE buffer at the same temperature used to perform the isolation of the target nucleic acids.
6. Elution of the purified nucleic acids can be carried out by increasing the temperature to 95°C. This is accomplished by placing the capillary on a heating block or alternatively raising the temperature of the device using a TEC device. While heating, volumes as low as 3.0 µL are adequate to elute all bound nucleic acids.
7. The presence of pure nucleic acids can then be confirmed by using a variety of techniques. We routinely verify the 260/280 ratio of the nucleic acids using a standard spectrophotometer. Most commonly we use the columns to purify mRNA from a mixture of nucleic acids. Typical ratios for the highest quality RNA are about 2.2. Appropriate 260/280 ratios for DNA are typically between 1.7 and 1.8.

3.4. Continuous Flow mRNA Hybridizations

It is often desirable to hybridize nucleic acids in a dilute solution. In these cases, the volume in which the sample is contained is typically fairly large (up to 1.0 mL), whereas the concentration of the target analytes is typically low (fM). We have optimized the ability to concentrate rarified sequences of nucleic acids, such as RNA, from low-concentration solutions. In order to perform this technique, alterations to the experimental apparatus are required.

1. In order to perform continuous flow hybridizations, controlling the folding state of the nucleic acid becomes critical. We have determined the optimal arrangement to accomplish thermocontrol of the actively flowing fluid. Appropriate thermocontrol is achieved by dividing the heating device into two zones, the first

for denaturing the nucleotides and the second for maintaining an adequate hybridization temperature. The two zones are located sufficiently close to each other so that the fluid temperature is not permitted to fall below the optimal hybridization temperature following denaturing. This precludes the reformation of nucleic acid secondary structure.

2. To perform constant flow hybridizations, the segment of the capillary where the solution enters is heated to 95°C, while the PPM column is maintained at 42°C.
3. Once the arranged system is assembled and steady-state temperatures are reached, a sample is prepared in the standard hybridization buffer consisting of 1X SSC in 5 m*M* TE buffer. The sample is contained in a syringe and placed on to a syringe pump to meter the appropriate flow onto the PPM column.
4. The flow rate was set at 0.5 µL/min, providing an average fluid velocity of 3 mm/s, or approx 10 s for the mRNA to hybridize with the oligonucleotide capture probes.
5. Immediately after the sample is dispensed, a volume of wash buffer is introduced to the polymer column.
6. Once unbound nucleic acids are removed from the column, the bound sample analytes are eluted from the column by raising the temperature of the PPM column to 95°C and pumping a minute volume of elution buffer through the column (**Fig. 3**).
7. This process of hybridization, washing, and elution can be accomplished because of the rapid kinetics associated with the target probe interaction on the PPM column. Because PPM have a high surface area, the number of binding sites is extremely high. In addition, the tightly packed porous structure decreases diffusion distances to enable a high number of interactions between the target analyte and the covalently bound capture probes attached to the PPM material on the column (*see* **Note 11**).

4. Notes

1. The pore size can be optimized within the monolithic structure to allow µL/min flow at pressures ranging from 0 to more than 2000 psi simply by varying the constituents in the porogenic solvent. For ease of use, we created monolithic structures that allowed flow at pressures under 200 psi, which was accomplished by selecting methanol as the porogenic solvent. The monolith mix was photopolymerized inside a 75-µm i.d. silica capillary. We estimate 65% porosity in a polymer of 75 µm id and 3 cm in length. Thus the total porous volume (porosity × capillary volume) is approx 84 nL. This assumed that full polymerization of all constituents occurred and that the density of the constituents did not change significantly during polymerization.
2. An advantage of the PPM is that the nodules in these materials are bound to the channel wall (**Fig. 1A**). These functionalized polymerized monoliths were rigid and similar to previous studies ***(11,16)***, mitigating the use of frits to contain the polymer in the capillary channel and allowing the deposition of the polymer in a discrete location, such as in a microfluidic device.
3. Following the optimization of the monolith material, we then optimized the

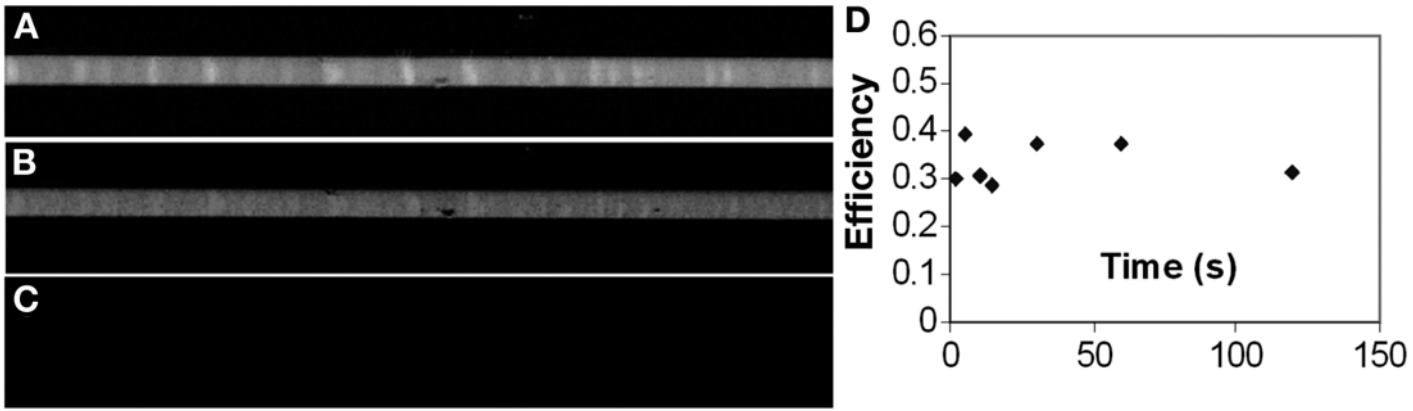

Fig. 3. Development of porous polymer monolithic (PPM) material for the selective isolation of nucleic acids sequences. In this figure, a mixture of DNA and RNA are introduced to the column **(A)**, which appears as an orange fluorescent image. The PPM is then washed to remove unbound material (in this case the green-labeled DNA), leaving RNA (B), which is labeled with a red fluorescent dye. Finally, the column is eluted (at 95°C) to remove the selectively bound RNA **(C)**. The reaction is rapid **(D)**, reaching maximal intensity within 2 s. This demonstrates the ability to selectively concentrate nucleic acid sequences as only 200 ng of Poly A RNA was diluted in 1 μg of DNA.

ability to postfunctionalize the materials. The gylcidyl methacrylate monomers selected for these studies allowed the attachment of a variety of biological entities, provided the molecule could perform a nucleophilic attack of the intact epoxide ring on the synthesized PPM, including proteins (antibodies, enzymes, etc.) nucleic acids (DNA, RNA, PNA, etc.), and chemicals (for modifying charge or hydrophobicity).

4. To optimize the conditions for functionalization, we initially made use of a Cadaverine fluorescent dye (**Fig. 1**). Oregon green cadaverine was employed because of its high fluorescent intensity and the presence of a terminal amine on the dye molecule, enabling direct covalent reactivity with the GMA. In order to functionalize the PPM, the column was filled with Oregon Green cadaverine and allowed to stand overnight at room temperature. After this overnight incubation the columns were extensively flushed, typically for 3 h, to remove unbound species.
5. Irreversible attachment of the nucleic acids was usually confirmed by imaging the PPM using a fluorescent microscope or microarray scanner. In this arrangement, the oligonucleotide used to functionalize the PPM typically contained a fluorescent dye molecule. We commonly used either 6-carboxyfluorescein or Cy5-labeled Oligo dT to optimize the attachment chemistry.
6. Prior to functionalization, the oligonucleotides were denatured before introducing them to the naïve PPM. The oligonucleotide can then be introduced on to the column and incubated appropriately to functionalize the PPM. The attachment of the oligo dT was confirmed by imaging the fluorescently derivatized column.
7. Functionalization of the PPM was carefully studied. We noted a significant temperature dependence of the attachment of oligonucleotides. For example, attempts to functionalize the polymers at low temperature (60°C) yield poor attachment (**Fig. 2A**). In contrast, raising the temperature demonstrated a dramatic effect on functionalization of the PPM. When the temperature of the functionalization reaction was increased to 90°C with an incubation time of 30 min, the amount of fluorescent signal was double (**Fig. 2B**) the maximum intensity seen at 60°C (**Fig. 2A**). The minimum incubation time to reach maximal binding was found when the temperature of the functionalization was raised to 120°C, equaling the maximum fluorescent intensity of the 90°C incubation after only 25 min (**Fig. 2C**). However, when the time increment for incubation was increased to 60 min at the same temperature, no further increase in fluorescent intensity was observed. The observed plateau in fluorescent intensity was assumed to indicate maximum binding.
8. Functionalized monoliths also maintained fluorescence for more than 6 mo, demonstrating the robustness of the polymer once functionalized, which is ideal for the rugged requirements of field tests.
9. An experimental configuration was set up using a microfluidic junction and syringe pumps to allow repeatable experimental conditions. The T-junction had two points of entry and one exit. In this arrangement one connection was used to load the mRNA samples, while the other, which contained the sample buffer only, was used to wash and elute the loaded sample. To the third connection a

capillary functionalized with Oligo dT was inserted. This allowed precise control over the amount of time between load, wash, and elution steps.

10. Although the trapping and elution of mRNA from the monolith may seem self-explanatory, there are some precautions. Failure to properly block the column can potentially preclude mRNA elution. Further, denaturing the mRNA is absolutely essential to successful hybridization. Finally, selecting a proper salt concentration can facilitate finding a single binding/washing/elution buffer, thereby solving one of the many problems of automated microfluidic analysis in determining how and where to store the multitude of reagents ***(17)***.
11. We found through our experimentation with mRNA isolation that longer oligonucleotides (40 mer) had improved efficiencies over shorter oligonucleotides (30 mer) while maintaining similar hybridization kinetics. There is likely an upper limit with respect to oligonucleotide length for optimal trapping, especially when the desire is to purify sequence specific nucleic acids. Regardless, since both the 30- and 40-mer functionalized polymers demonstrated linear binding characteristics with a nonsignificant slope, it can be concluded that hybridization is already complete by the time the monoliths are washed, regardless of nucleotide probe length.

Acknowledgments

The authors would like to acknowledge Kyle Hukari, Gary Hux, and Dr. Timothy Shepodd for their technical assistance in the development of the porous polymer monoliths and supporting hardware. This research was supported by a Laboratory Directed Research and Development Grant from Sandia National Laboratories. We further acknowledge the Department of Homeland Security Scholars and Fellows Program for their support of Brent Satterfield while conductiong this research.

References

1. Mouradian, S. (2002) Lab-on-a-chip: applications in proteomics. *Curr. Opin. Chem. Biol.* **6(1),** 51–46.
2. Bilitewski, U., Genrich, M., Kadow, S., and Mersal, G. (2003) Biochemical analysis with microfluidic systems. *Anal. Bioanal. Chem.* **377(3),** 556–469.
3. Verpoorte, E. (2002) Microfluidic chips for clinical and forensic analysis. *Electrophoresis* **23(5),** 677–712.
4. de Mello, A. J. and Beard, N. (2003) Dealing with real samples: sample pre-treatment in microfluidic systems. *Lab. Chip.* **3(1),** 11N–19N.
5. Selvaganapathy, P. R., Carlen, E. T., and Mastrangelo, C. H. (2003) Recent progress in microfluidic devices for nucleic acid and antibody assays. *Proc. IEEE* **91(6),** 954–975.
6. Jacobsen, N., Nielsen, P. S., Jeffares, D. C., et al. (2004) Direct isolation of poly(A)+ RNA from 4 M guanidine thiocyanate-lysed cell extracts using locked nucleic acid-oligo(T) capture. *Nucleic Acids Res.* **32(7),** e64.

7. Burgener, M., Candrian, U., and Gilgen, M. (2003) Comparative evaluation of four large-volume RNA extraction kits in the isolation of viral RNA from water samples. *J. Virol. Methods* **108(2),** 165–170.
8. Aviv, H. and Leder, P. (1972) Purification of biologically active globin messenger RNA by chromatography on oligothymidylic acid-cellulose. *Proc. Natl. Acad. Sci. USA* **69(6),** 1408–1412.
9. Yu, C., Davey, M. H., Svec, F., and Frechet, J. M. (2001) Monolithic porous polymer for on-chip solid-phase extraction and preconcentration prepared by photoinitiated in situ polymerization within a microfluidic device. *Anal. Chem.* **73(21),** 5088–5096.
10. Throckmorton, D. J., Shepodd, T. J., and Singh, A. K. (2002) Electrochromatography in microchips: reversed-phase separation of peptides and amino acids using photopatterned rigid polymer monoliths. *Anal. Chem.* **74(4),** 784–789.
11. Shediac, R., et al. (2001) Reversed-phase electrochromatography of amino acids and peptides using porous polymer monoliths. *J. Chromatogr. A* **925(1–2),** 251–263.
12. West, J. A. A., Hukari, K. W., Hux, G., and Shepodd, T. J. (2004) Microfluidic gene arrays for rapid genomic profiling, in *Proceedings of the Society of Photo-Optical Instrumentation Engineers (spie) Conference on Lab-on-a-Chip: Platforms, Devices, and Applications,* October 26–28, 2004, Philadelphia, pp. 167–173.
13. Yu, C., Svec, F. and Frechet, J. M. (2000) Towards stationary phases for chromatography on a microchip: molded porous polymer monoliths prepared in capillaries by photoinitiated in situ polymerization as separation media for electrochromatography. *Electrophoresis* **21(1),** 120–127.
14. Peterson, D. S., Rohr, T., Svec, F., and Frechet, J. M. (2003) Dual-function microanalytical device by in situ photolithographic grafting of porous polymer monolith: integrating solid-phase extraction and enzymatic digestion for peptide mass mapping. *Anal. Chem.* **75(20),** 5328–5335.
15. Yu, C., Xu, M. C., Svec, F., and Frechet, J. M. (2002) Preparation of monolithic polymers with controlled porous properties for microfluidic chip applications using photoinitiated free-radical polymerization. *J. Polymer Sci. Part A Polymer Chem* **40(6),** 755–769.
16. Ngola, S. M., Fintschenko, Y., Choi, W. Y., and Shepodd, T. J. (2001) Conduct-as-cast polymer monoliths as separation media for capillary electrochromatography. *Anal. Chem.* **73(5),** 849–856.
17. Lichtenberg, J., de Rooij, N. F. and Verpoorte, E. (2002) Sample pretreatment on microfabricated devices. *Talanta* **56(2),** 233–266.

3

Rapid Electrical Lysis of Bacterial Cells in a Microfluidic Device

Hsiang-Yu Wang, Padmapriya P. Banada, Arun K. Bhunia, and Chang Lu

Summary

Electrical lysis of biological cells on a microfluidic platform has evoked significant interest because of its applications in rapid recovery of intracellular contents such as nucleic acids or proteins without introducing lytic agents. Applying a direct current (DC) field for cell lysis typically requires field strength of 1–10 kV/cm, which is dependent on the cell type: prokaryotes or eukaryotes. Bubble generation and Joule heating can often be induced under such high field strengths. In this study we fabricated a simple microfluidic device using low-cost soft lithography with channel widths considerably larger than the cell size to avoid clogging and ensure stable performance, which was able to lyse green fluorescent protein (GFP)-expressing *Escherichia coli* cells under continuous DC voltage while cells were flowing through the channels. The cell lysis only happened in a defined section of a microfluidic channel because of local field amplification by geometric modification. The geometric modification also effectively decreased the required voltage for lysis severalfold. The cell lysis was verified by plate count on nutrient agar plates and by fluorescence spectroscopy.

Key Words: Cell lysis; *Escherichia coli*; microfluidics; electric field; polydimethylsiloxane; fluorescence microscopy; soft lithography.

1. Introduction

Microfluidic devices allow chemical analysis and biological assays to be performed based on a small number of single biological cells with unprecedented precision and throughput ***(1)***. Moreover, microfluidic devices are portable and enable biological assays such as pathogen detection to be carried out on-site. Most bacterial detection methods are antibody (immunoassay)- and nucleic-acid-based. As an essential step to obtain the intracellular contents, cell lysis based on microfluidics has been studied in recent years. The methods employed to achieve cell lysis on microfluidic devices reported so far can be

From: *Methods in Molecular Biology, Vol. 385: Microchip-Based Assay Systems: Methods and Applications*
Edited by: Pierre N. Floriano

roughly grouped into four categories: thermal lysis, mechanical lysis, chemical lysis, and electrical lysis. Thermal lysis was achieved by elevating the temperature to 94°C ***(2)***. Mechanical lysis was done either by microscale sonication or by nanobarb filtration ***(3–5)***. These methods are useful in the analysis of DNA but impractical in the assays based on protein or enzymes because the generated heat usually denatures proteins. Additionally, these methods are relatively slow and may be problematic when rapid results are intended. In chemical lysis method, lytic agents such as sodium dodecyl sulfate (SDS) or hydroxides are applied to cause lysis by dissolving or reacting with membrane lipids ***(6–8)***. Although these lytic agents are common in prevailing protocols, they interfere with certain biological analyses and thus are not omnipotent.

Electrical lysis has gained a lot of attention because it doesn't require lytic agents and lysis happens rapidly (<33 ms) ***(9–15)***. During electrical lysis, electrical pulses with defined voltages and widths cause the formation of small holes in the cell membrane and the reorientation of lipid molecules. The localized Joule heating on the membrane also contributes to the disruption of the membrane structure. If the electrical pulses are moderate in strength and short in duration, the membrane can regenerate itself upon removal of the field and the cell remains alive ***(16)***. Increasing the strength and the duration of the electric field leads to cell lysis and burst of intracellular materials. Cell lysis under DC electric field has been demonstrated, and the demanding field strength was reported to be 1–10 kV/cm ***(12)***. To accomplish such high field strength, an extremely high voltage is normally required. Bubble generation and adverse conditions because of severe Joule heating and electrolysis of solution are common under these conditions. Because of this difficulty, most of the studies in electrical lysis focused on using alternating current (AC) electric field or a microscale electrode to avoid these problems. In this study we designed a simple microfluidic device for continuous-flow bacterial cell lysis under relatively low DC voltage ***(17)***. We used geometric modification to locally amplify the electrical field in a predetermined section of a microfluidic channel. The overall voltage needed for the operation was substantially lower than that needed by a channel without the special geometry. The microfluidic devices were made by standard soft lithography ***(18)***. GFP-expressing *E. coli* was used as a model cell line in our research. The fluorescence offers an effective way to observe the movement and lysis of cells. The GFP-expressing *E. coli* was electrically lysed rapidly while flowing through the geometrically defined section. The viability of the cell after the treatment was determined by their ability to grow on the nutrient agar plates. We found that a threshold of 1500 V/cm inside the lysis section was required to lyse nearly 100% of the *E. coli*. The value of field strength is much lower than that reported in the literature, probably because of the longer duration of the field.

2. Materials

2.1. Fabrication of Si/SU-8 Masters

1. Mask for photolithography: high-resolution (5080 dpi) printed transparency with micropatterns designed by computer-aided-design (CAD) software (FreeHand, Macromedia, San Francisco, CA).
2. Silicon wafer: 3 in. in diameter (Silicon Quest International Inc., Santa Clara, CA). Wafers with micropatterns serve as the masters for molding the poly(dimethylsiloxane) (PDMS) replica.
3. Negative tone photoresist: NANO SU-8 2000, formulations 2–15 (MicroChem Corp., Newton, MA).
4. Acetone (Mallinckrodt Laboratory Chemicals, Phillipsburg, NJ); isopropyl alcohol (IPA) (Mallinckrodt Laboratory Chemicals, Phillipsburg, NJ).
5. SU-8 developer: organic solvent used to resolve the micropattern on the wafer (MicroChem Corp., Newton, MA).
6. Optical contact aligner: Karl Suss MJB3 Mask Aligner (Suss Microtech Inc.). The UV light is tuned for 365-nm wavelength. The power was 275 W when these experiments were conducted.

2.2. Treatment of Slides

1. 27% (w/w) Ammonium hydroxide (NH_4OH) (Mallinckrodt Laboratory Chemicals).
2. 30% Hydrogen peroxide (H_2O_2) (Mallinckrodt Laboratory Chemicals).
3. Coverslip Mini-Rack (Molecular Probes, Eugene, OR).

2.3. Fabrication of Microfluidic Device

1. PDMS: RTV615 silicone potting kit (GE Silicones, Waterford, NY). It includes two parts: A contains prepolymers and B serves as the curing agent.
2. Silanization agent: tridecafluoro-1,1,2,2,-tetrahydrooctyl-1-trichlorosilane (United Chemical Technologies, Bristol, PA). Silanization of the wafers facilitates the peeling of PDMS replica after molding.
3. Post: Teflon PFA tubing with 1/8-in. outer diameter and 0.062-in. inner diameter (Upchurch Scientific Inc., Oak Harbor, WA). The tubing is cut into 1 cm long post to form the reservoirs of the device.
4. Petri dish: polystyrene, sterile, 100 mm in diameter and 15 mm in depth (VWR International Inc., West Chester, PA). Petri dishes are used as containers for PDMS molding.
5. Microscope slide: Fisherfinest Premium Plain Glass Microscope Slides with a dimension of 75 × 25 mm and 0.97–1.07 mm thick (Fisher Scientific International Inc., Hampton, NH).
6. Vacuum desiccators: 150 mm in diameter (Bel-Art Products, Pequannock, NJ).
7. 0.0074% HCl solution: add 1 mL of 37% HCl reagent (Mallinckrodt Laboratory Chemicals, Phillipsburg, NJ) into 499 mL of distillated water to result in a stock acid solution of 0.074% HCl. Dilute the stock solution 10 times using distillated water to obtain the working solution of 0.0074% HCl.

2.4. Bacterial Culture

1. GFP-expressing *E. coli*: transformed *E. coli* with GFP plasmid pQBI-T7 (Qbiogene, Irvine, CA).
2. Culture medium: the culture medium is made by adding 25 capsules of Luria-Bertani (LB) broth (BIO 101 Systems, Irvine, CA) into 1 L of distillated water. The mixture is heated for 30 s in a microwave oven and mixed thoroughly at approx 80*g* for 10 min using a stirrer. Sterilize the medium by autoclaving at 120°C for 15 min and cool to room temperature (25°C). Add 50 mg/mL ampicillin (Amresco Inc., Solon, OH) to the desired amount of LB (LB-amp$^+$) prior to culture inoculation.
3. 15-mL Sterile centrifuge tube (Greiner Bio-One International Inc., Longwood, FL).
4. 1.5-mL Microcentrifuge tube (GENEMate; ISC BioExpress, Kaysville, UT): sterilize by autoclaving at 120°C for 30 min.
5. Incubator: Controlled environment incubator shaker (New Brunswick Scientific Co. Inc., Edison, NJ).
6. Centrifuge: Eppendorf centrifuge 5415D (Eppendorf North America, Westbury, NY).

2.5. Electrical Lysis and Fluorescence Microscopy

1. High-voltage power supply (PS350; Stanford Research Systems, Sunnyvale, CA).
2. Phosphate buffer: 1.35 m*M* KH_2PO_4, 2.00 m*M* Na_2HPO_4, and 0.05% Tween-20, pH 7.0. KH_2PO_4 and Na_2HPO_4 are purchased from Mallinckrodt Laboratory Chemicals. Tween-20 is purchased from Amresco Inc. (Solon, OH).
3. Fluorescence microscopy: the microfluidic device was mounted on an inverted fluorescence microscope (IX-71; Olympus, Melville, NY) with a 20× dry objective (NA = 0.40). The epifluorescence excitation was provided by a 100 W mercury lamp, together with brightfield illumination. The excitation and emission were filtered by a fluorescence filter cube (Exciter HQ480/40, emitter HQ535/50, and beam splitter Q505lp; Chroma technology, Rockingham, VT). The images of the cells were taken with a CCD camera (ORCA-285; Hamamatsu, Bridgewater, NJ) at a frame rate of 10 Hz.

2.6. Plate Count

Preparation of LB-agar plates is as follows:

1. Add 4 g of the LB–agar powder (Bio101 Systems, Irvine, CA) into 100 mL of distilled water and the resulting solution is enough to make four or five agar plates.
2. Stir the solution at approx 80*g* for 10 min or until the powder is completely dissolved. Sterilize the medium by autoclaving (120°C for 15 min) and cool to 55°C by partially immersing the container in a water bath to prevent agar from congealing.
3. Add ampicillin (Amresco Inc.) to the solution to a final concentration of 50 µg/mL, mix thoroughly, and pour about 25 mL per Petri dish.
4. Once the agar is solidified, the plates are inverted to prevent the condensed vapor from dripping onto the agar surfaces and stored at 4°C until use.
5. Plates should be brought back to room temperature before use.

3. Methods

The extent of electroporation of the cells depends on both the strength and the duration of the electric field experienced by the cells. The field strength is defined as potential drop per unit length. To electrically lyse cells, a device should be designed to provide large field strength within a short duration. Based on Ohm's law, in a DC circuit with a fixed overall voltage the potential drop within each segment is proportional to its resistance. For a microfluidic channel of uniform depth and filled with buffer, the voltage drops in different sections as determined by the width and the length of the section. In our device, we had three sections with equal lengths and different widths in one channel. Accordingly, the field strength E (V/cm) inside the lysis section of our device (*see* **Fig. 1**) could be obtained by the following equation:

$$E = \frac{V}{L\left[1 + 2\left(\frac{W_2}{W_1}\right)\right]}$$

The variables length (L), width 1 (W_1), and width 2 (W_2) (the unit for these variables is cm in this equation) are depicted in **Fig. 1**, and V is the total voltage employed on the device. A device based on this configuration provides lysis field strength of 3 V/cm per volt applied. The field strengths in sections other than lysis section are too low to contribute to the cell lysis; thus the lysis is confined in the lysis section.

To fabricate a device with designed microchannels, several steps were followed. First, silicon wafers were coated with photoresist and exposed to UV light to form photoresist patterns on it. These wafers served as masters in the subsequent molding of PDMS. The PDMS (ratio between A and B parts is 10:1) was poured onto the master and baked at 80°C to yield a replica. Finally, the replica was mounted to a precleaned slide to form a device with desired channels.

E. coli cells are straight rods approx 0.5 µm wide and less than 2 µm long. Culturing the GFP-expressing *E. coli* in LB medium containing ampicillin ensures the presence of GFP plasmid. To determine the performance of the device, GFP-expressing *E. coli* cells were loaded into the cell reservoir at the cathode region and treated with a DC electric field. Solutions from both reservoirs were diluted using phosphate buffer and surface plated onto LB-amp$^+$ agar plates and incubated at 37°C overnight to determine the viability of the cells. We found that lysis strength of 1500 V/cm was required to cause lyses of nearly 100% of GFP-expressing *E. coli* cells after flowing through the lysis section. The total voltage required to achieve this field strength could be decreased to 500 V because of the geometric modification.

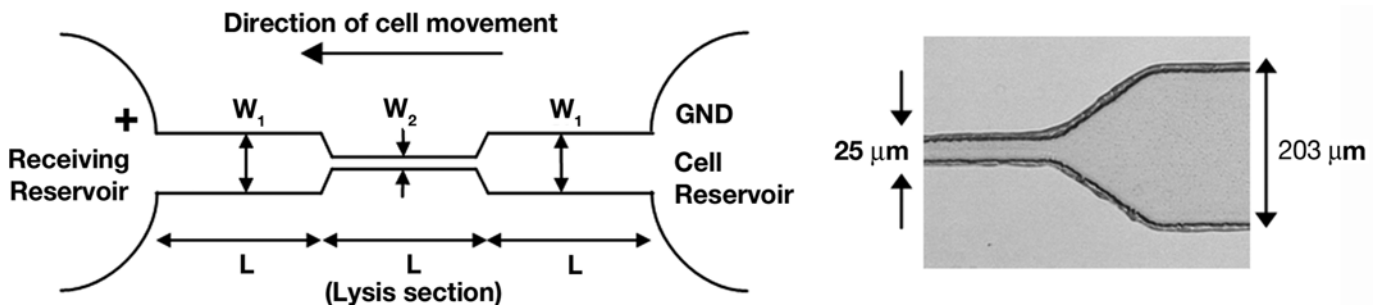

Fig. 1. The design of the microfluidic device for cell lysis. **(A)** The layout of the device. Cells were loaded in the cell reservoir and transported to the receiving reservoir by a DC electric field. Cell lysis occurred in the lysis section when the field strength was sufficiently high. **(B)** A typical microscope image showing a part of one of the devices. The wide and narrow sections have widths of 203 and 25 μm, respectively. (From **ref. *17***.)

3.1. Fabrication of SU-8/Si Masters

1. The microfluidic channels are designed using CAD software (FreeHand, Macromedia) and printed out by a high-resolution (5080 dpi) printer on a transparency with the channels transparent and the rest of the surface black.
2. The photoresist is stored at 4°C and brought back to room temperature before use. Split the photoresist into aliquots to prevent denaturing because of the repeated freezing and warming.
3. Place the wafer on the chuck of a spinner and apply vacuum to hold it. Clean the wafer by spinning it at 800*g* and rinsing with acetone and isopropyl alcohol sequentially (*see* **Note 1**).
4. Use a dropper to load the proper amount of photoresist on the wafer. Usually 3 mL of the photoresist is enough to cover a 3-in. wager. Attention should be paid to avoid bubbles in the photoresist layer.
5. A 13-mm-thick film of photoresist can be formed on the wafer by spinning at 400*g* for 30 s.
6. The coated wafer is prebaked at 65°C for 1 min and 95°C for 2 min on a hot plate.
7. Align the wafer with the mask on a contact aligner and expose it at 275 W for 11 s.
8. After the exposure, the wafer is baked at 65°C for 1 min and 95°C for 3 min on a hot plate.
9. The wafer is developed in the SU-8 developer in the developer for 3 min to resolve the patterns. The solution is agitated gently to facilitate the process.
10. Blow the wafer dry using nitrogen. The SU-8 pattern is observed under a microscope. The pattern should be well resolved and have good adhesion to the wafer. The wafer with SU-8 features will serve as the master for making the PDMS replica.

3.2. Treatment of Slides

We used glass slides as substrates to form close channels. Impurities on the glass surface could easily contribute to bubble formation. We found that thorough cleaning of slides was crucial in avoiding bubbles generation during the lysis experiments

1. Place the mini-rack in a 500-mL beaker and lean mini-rack to the beaker wall to prevent it from tipping over. Fit slides into the slots of the rack.
2. A basic solution was used to remove the organic residue from the slides. The composition of the solution was deionized (DI) H_2O:NH_4OH:H_2O_2=5:1:1 (*see* **Note 2**).
3. Add 300 mL of DI H_2O to the beaker, followed by 60 mL of NH_4OH and then 60 mL of H_2O_2.
4. Stir the solution at approx 80*g* and heat it up to 75°C on a hot stirring plate for 40 min.
5. Remove the slides from the solution using a tweezers and rinse them with DI water immediately.
6. Blow the slides dry with nitrogen and store them in a clean box.

3.3. Fabrication of the Microfluidic Device

1. Blow the masters with nitrogen to remove dust or other impurities.
2. Add a couple of drops of the silanization agent in a vial.
3. Together with the vial, a Petri dish (the container for molding), the master, and the posts for forming reservoirs are placed in a desiccator. The surfaces of the items are exposed to the vapor of silanization agent for 70 min with the pressure pumped down to 20 psi. The silane coating facilitates the separation of PDMS replica from the master.
4. Measure the desired amount of RTV 615. The weight ratio of A and B parts is 10:1. Around 22 g (i.e., 20 g of A and 2 g of B) of the total mixture are enough for resulting in a 0.5-cm-thick PDMS replica in a 4-in. Petri dish.
5. Mix the solutions thoroughly using a glass rod for 3 min to ensure complete and even cure.
6. Apply vacuum to the mixed PDMS prepolymer solution in a desiccator to remove the gas from the mixture. The vacuum level needs to be gradually increased to prevent overflowing of the mixture.
7. Let the degassing run for 70 min and then stop pumping.
8. Put the master in the Petri dish and place the posts on the master to serve as the template for reservoirs.
9. Pour the degassed PDMS prepolymer mixture into the Petri dish. Be careful not to introduce bubbles. If bubbles appear, remove them using a pipet.
10. The Petri dish containing the PDMS prepolymer mixture is placed in an oven at 80°C for 2 h.
11. Peel the solid PDMS sheet off the master and remove the posts.
12. Immerse the PDMS replica in the 0.0074% HCl solution. Stir at approx 80*g* and heat up the solution to 70°C on a heating/stirring plate for 40 min (*see* **Notes 3** and **4**).
13. Rinse the replica using distilled water for 1 min to remove the acid solution.
14. Blow the replica dry using nitrogen and immediately mount it onto a clean slide to form microfluidic channels (*see* **Note 5**).

3.4. Preparation of Bacterial Culture

1. Inoculate GFP-expressing *E. coli* by adding 1% (v/v) of suspension culture or a single colony from the agar plate to 5 mL of the freshly prepared LB-amp$^+$ broth.
2. Incubate the culture for 16 h at 37°C in a shaking incubator; generally the concentration of the culture is around 10^8–10^9 colony-forming units (CFU)/mL when harvested.
3. Transfer 1 mL of the culture to a microcentrifuge tube and centrifuge the solution at 9300*g* for 5 min. The resulting pellet appears fluorescent green.
4. Decant the supernatant and add 1 mL of phosphate buffered saline (PBS, pH 7.6) and vortex for 30 s to resuspend the cells.
5. Wash the cells by repeating **steps 3** and **4** in order to remove the media components.
6. Dilute the cells serially in PBS to achieve a cell concentration of about 10^6–10^7 CFU/mL.

3.5. Electrical Lysis and Fluorescence Microscopy

1. Add 30 µL of PBS into one of the reservoirs. The buffer fills the channel spontaneously because of the hydrophilic surface.
2. The phosphate buffer is used to condition the channel for 5 min by applying vacuum to the other reservoir that does not have buffer in it. In case of trapped bubbles, a higher flow rate usually helps to flush them out.
3. The channel is observed under the microscope to make sure no gas bubbles are trapped inside.
4. Remove buffer in both reservoirs using a pipet.
5. Add 30 µL of buffer to the receiving reservoir and 30 µL of cell suspension to the cell reservoir (**Fig. 1A**).
6. Put the anode in the receiving reservoir and the cathode in the cell reservoir to generate a DC electric field with a direction toward the cell reservoir.
7. Observe GFP-expressing *E. coli* cell movement under the fluorescence microscope. The GFP-expressing *E. coli* cells respond immediately to the electric field and move toward the receiving reservoir because of their negatively charged surface (**Fig. 2**). The movement is against the direction of electro-osmotic flow.
8. The lysis of cells is confirmed by the absence of cells at the outlet of lysis section (**Fig. 2**; *see* **Note 6**) or the slow decay of the fluorescence intensity from cells (**Fig. 3**). The quantification of lysis is performed using plate count method (*see* **Subheading 3.6.**)
9. The duration of the electric field is 20 min.
10. Transfer solutions from both reservoirs to fresh 1.5-mL micocentrifuge tubes containing 270 µL of PBS.

3.6. Plate Count to Determine Bacterial Viability

1. Dilute the sample **(Subheading 3.5., step 10)** obtained from the cell reservoir 1000 times using PBS. The samples from the receiving reservoir typically need not be diluted.
2. Spread 100 µL of the sample from either the cell reservoir or the receiving reservoir onto LB-amp$^+$ agar plates in triplicate and incubate the plates at 37°C for 16 h.
3. The resulting number of colonies on a single plate needs to be in the range of 30–300 CFUs. Adjust the times of dilution if the colony number is not in this range. Then the numbers of cells originally from both reservoirs can be obtained by multiplying the number of dilutions with the average plate count. A typical curve between the field strength inside the lysis section and the number of viable cells in the receiving reservoir is shown in **Fig. 4.**

4. Notes

1. Acetone is used first because of its high volatility. Residue can be left if isopropyl alcohol is not used after the acetone. This step needs to be done in the chemical hood.

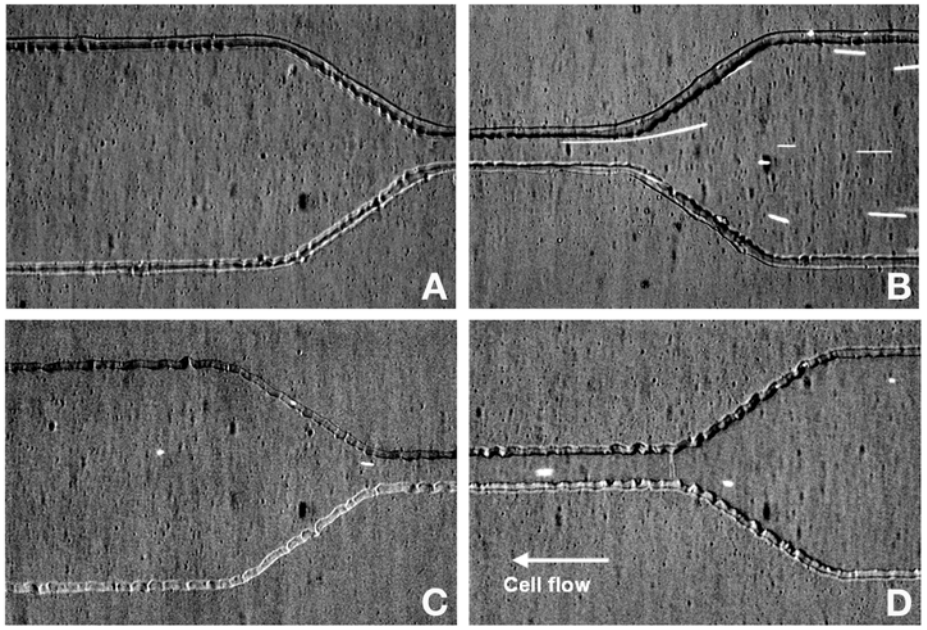

Fig. 2. GFP-expressing *E. coli* cell lysis or transportation observed using fluorescence spectroscopy. Images **A** and **B** were taken with a total voltage of 1500 V (2400 V/cm in the narrow section), and images **C** and **D** were taken with a total voltage of 350 V (560 V/cm in the narrow section). There are fewer cells in images **C** and **D** than in image **B** because of the lower electrical field. In every image, the direction of cell flow was from the right to the left. The exposure time in every image was 11.25 ms at a frame rate of 10 Hz. **(A)** At the exit of the lysis section (2400 V/cm): cells were lysed exclusively in the narrow section so they were not observed here. **(B)** At the entrance of the lysis section (2400 V/cm): the cells flowed into the narrow section. **(C)** At the exit of lysis section (560 V/cm). **(D)** At the entrance of the lysis section (560 V/cm).

2. We found that excess NH_4OH could result in deposition of residues on the glass slide.
3. The time for the replica to be immersed in the acid solution needs to be limited to an hour. The PDMS can absorb water and become opaque. This would interfere with the fluorescence microscopy.
4. Treating the replica and slide with an ozone cleaner is also an effective way to make the surface hydrophilic. The PDMS replica will seal the slide irreversibly after being treated by the ozone cleaner.
5. The channel surface will regain hydrophobicity quickly when exposed to the air. After the PDMS replica is taken out of HCl solution and blown dry, the PDMS replica is immediately sealed to a clean glass slide and phosphate buffer is filled in.

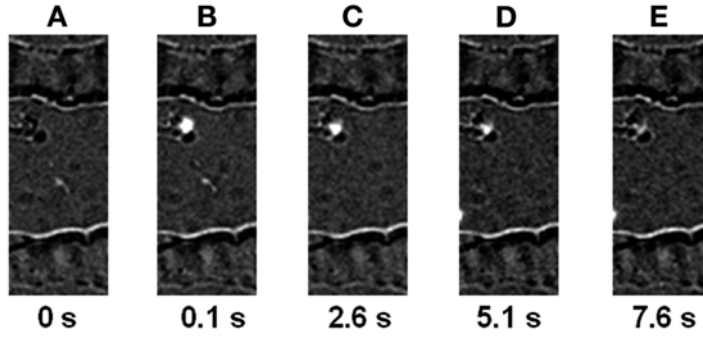

Fig. 3. Release of cellular contents from a single GFP-expressing *E. coli* cell observed by fluorescence microscopy. These pictures were taken in the lysis section with local field strength of 1500 V/cm. The exposure time was 5 ms and the frame rate was 10 Hz.

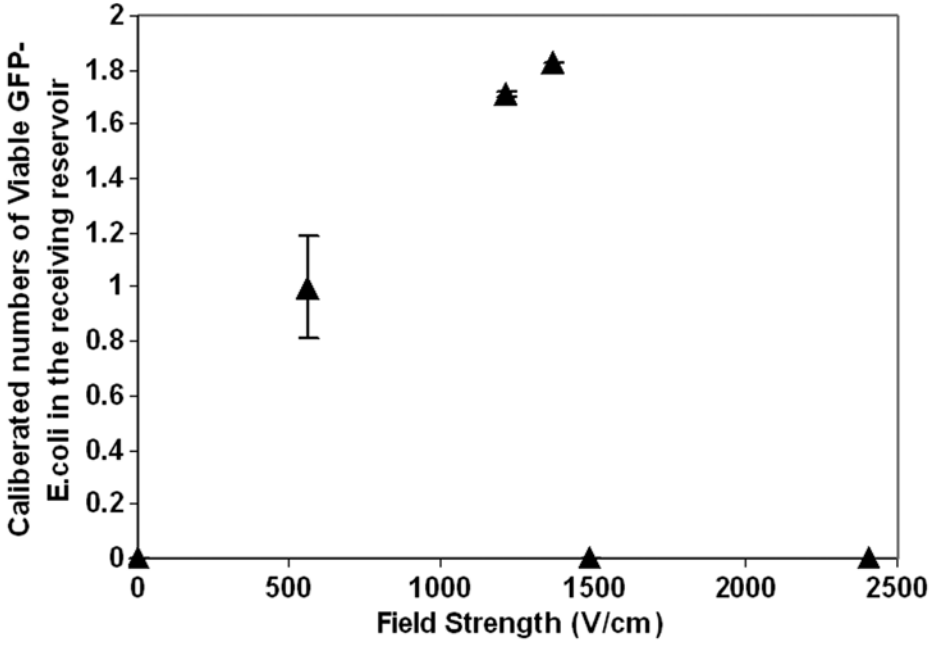

Fig. 4. The relationship between the field strength inside the lysis section and the number of viable cells in the receiving reservoir. The numbers of viable cells in the receiving reservoir were calibrated by designating the number of viable cells at the lowest field strength to be 1. (From **ref. *17***.)

6. Cells disappear at the outlet of the lysis section only when the lysis field strength is higher than 2000 V/cm. Even when the cells are nearly 100% dead after the lysis, based on results from the plate count, they still remain fluorescent at the exit because the quenching rate of fluorescent protein is slow compared to the velocity of cell movement when the lysis filed strength is 1500–2000 V/cm.

Acknowledgments

The microfabrication was carried out at Birck Nanotechnology Center at Purdue University. The authors acknowledge financial support through a cooperative agreement with the Agricultural Research Service of the US Department of Agriculture project number 1935–42000–035 and the Center for Food Safety and Engineering at Purdue University.

References

1. Andersson, H. and van den Berg. A. (2003) Microfluidic devices for cellomics: a review. *Sens. Actuators B*. **92,** 315–325.
2. Waters, L. C., Jacobson, S. C., Kroutchinina, N., Khandurina, J., Foote, R. S., and Ramsey, J. M. (1998) Microchip device for cell lysis, multiplex PCR amplification, and electrophoretic sizing. *Anal. Chem.* **70,** 158–162.
3. Belgrader, P., D. Hansford, G. A., Kovacs, K., et al. (1999) A minisonicator to rapidly disrupt bacterial spores. *Anal. Chem.* **71,** 4232–4236.
4. Taylor, M. T., Belgrader, P., Furman B. J., Pourahmadi, F., Kovacs, G. T. A., and Northrup, M. A. (2001) Lysing Bacterial Spores by Sonication Through a Flexible Interface in a Microfluidic System. *Anal. Chem.* **73,** 492–496.
5. Di Carlo, D., Jeong, K. H., and Lee, L. P. (2003) Reagentless mechanical cell lysis by nanoscale barbs in microchannels for sample preparation. *Lab Chip* **3,** 287–291.
6. Li, P. C. H. and Harrison, D. J. (1997) Transport, manipulation, and reaction of biological cells on-chip using electrokinetic effects. *Anal. Chem.* **69,** 1564–1568.
7. Wu, H. K., Wheeler, A., and Zare, R. N. (2004) Chemical cytometry on a picoliter-scale integrated microfluidic chip. *Proc. Nat. Acad. Sci. USA* **101,** 12,809–12,813.
8. Hong, J. W., Studer, V., Hang, G., Anderson, W. F., and Quake, S. R. (2004) A nanoliter-scale nucleic acid processor with parallel architecture. *Nat. Biotechnol.* **22,** 435–439.
9. Cheng, J., Sheldon, E. L., Wu, L., et al. (1998) Electric field controlled preparation and hybridization analysis of DNA/RNA from *E. coli* on microfabricated bioelectronic chips. *Nat. Biotechnol.* **16,** 541–546.
10. Lee, S. W. and Tai, Y. C. (1999) A micro cell lysis device. *Sens. Actuators, A*. **73,** 74–79.
11. McClain, M. A., Culbertson, C. T., Jacobson, S. C., Allbritton, N. L., Sims, C. E., and Ramsey, J. M. (2003) Microfluidic devices for the high-throughput chemical analysis of cells. *Anal. Chem.* **75**, 5646–5655.

12. Gao, J., Yin, X. F., and Fang. Z. L. (2004) Integration of single cell injection, cell lysis, separation and detection of intracellular constituents on a microfluidic chip. *Lab Chip* **4,** 47–52.
13. Lu, H., Schmidt, M. A., and Jensenm, K. F. (2005) A microfluidic electroporation device for cell lysis. *Lab Chip* **5,** 23–29.
14. Munce, N. R., Li, J., Herman, P. R., and Lilge. L. (2004) Microfabricated system for parallel single-cell capillary electrophoresis. *Anal. Chem.* **76,** 4983–4989.
15. Khine, M., Lau, A., Ionescu-Zanetti, C., Seo, J., and Lee, L. P. (2005) A single cell electroporation chip. *Lab Chip* **5,** 38–43.
16. Tien, H. T. and Ottova, A. (2003) The bilayer lipid membrane (BLM) under electrical fields. *IEEE Trans. Dielectr. Electr. Insul.* **10,** 717–727.
17. Wang, H. Y., Bhunia, A. K., and Lu, C. (2006) A microfluidic flow-through device for high throughput electrical lysis of bacterial cells based on continuous dc voltage. *Biosens. Bioelectron.* **22,** 582–588.
18. Duffy, D. C., McDonald, J. C., Schueller, O. J. A., and Whitesidesm G. M. (1998) Rapid prototyping of microfluidic systems in poly (dimethylsiloxane). *Anal. Chem.* **70,** 4974–4984.

4

On-Chip Bioassay Using Immobilized Sensing Bacteria in Three-Dimensional Microfluidic Network

Hirofumi Tani, Koji Maehana, and Tamio Kamidate

Summary

An on-chip whole-cell bioassay has been carried out using *Escherichia coli* tester strains for genotoxicity. In this assay format, the mutagen-responsive bioluminescence (BL) strains are immobilized in a chip assembly in which a silicon chip is placed between two poly(dimethylsiloxane) (PDMS) chips. In the chip assembly, microchannels fabricated on the two separate PDMS layers are connected via perforated microwells on the Si chip, and thus a three-dimensional microfluidic network is constructed. The strains mixed with agarose are loaded from the channels on one of the two PDMS layers into the wells on Si chip, followed by gelation. Induction of the expression of firefly luciferase in the tester strains and BL reaction are successively carried out by filling the channels on another PDMS layer with samples containing inducer (genotoxic substance) and then adenosine triphosphate/luciferin mixture, respectively. BL emission from each of the wells can be monitored by using a charge-coupled device camera to obtain an overall picture of the chip. The on-chip format based on a three-dimensional microfluidic network provides a combinatorial bioassay for multiple samples with multiple tester strains in a simple chip assembly. Thus, the presented method could be applied not only to various microbial sensing applications but also to other (bio)chemical analyses.

Key Words: On-chip bioassay; three-dimensional microfluidic network; sensing bacteria; reporter assay; bioluminescence; luciferase; genotoxicity.

1. Introduction

Whole-cell bioassays using sensing bacteria such as the Ames test ***(1)*** for assessing genotoxicity are becoming essential analytical methods for the quantitative estimation of the effects of substances on organisms and biological systems. A whole-cell bioassay has important advantages over bioassays using living organisms with regards to speed and efficiency of the assay and ethical

From: *Methods in Molecular Biology, Vol. 385: Microchip-Based Assay Systems: Methods and Applications*
Edited by: Pierre N. Floriano © Humana Press Inc., Totowa, NJ

concerns in the case of animal experiments. Thus, various principles for bacteria-based assay have been proposed and widely exploited for primary screening of new chemicals, such as drugs, food additives, and pesticides, and for monitoring of environmental pollution *(2,3)*. With the recent increase in the diversity of chemical substances in the environment, there is a growing need for high-throughput rapid assays. The formats of the traditional bioassay using Petri dishes, test tubes, and microtiter plates are still important for various fields, but new formats are required for responding to above situations in the manner of DNA microarrays for genomic analysis *(4)*. There is no difference in chemical processes between the chip and the traditional assays from the hybridization perspective, but the array format has become widely accepted as a key tool in genomic research because of its high-throughput performance. Microfluidic-based analysis systems, such as micro total analysis systems (μTAS) or Lab-on-a-Chip (LOC), are also promising in performing chemical and biochemical assays *(5)*. Currently, for example, on-chip capillary electrophoresis (CE) systems are commercially available from several manufacturers. Such microchip-based approaches could become a successful methodology for rapid and high-throughput biological assays.

Recently we have developed a microfluidic-based on-chip bioassay *(6)* inspired by the micromosaic immunoassay format proposed by Bernard et al. *(7)*. In the micromosaic assay format, a series of antibodies is immobilized on a planar substrate as narrow stripes using a multichannel chip. A series of samples (antigen) is then brought from a second multichannel chip as the lines of antibody and sample make a grid pattern. The specific binding between immobilized antibodies and antigen molecules takes places at each intersection of the two lines in a combinatorial fashion. The overall mosaic pattern of the chip has been expanded to a three-dimensional (3D) format suitable for stable immobilization of tester strains. For this purpose, the assay format presented here is exploiting the 3D microfluidic network, which consists of the assembly of two multichannel and one perforated microwell chips. The tester strains are immobilized in one of the channel chips and in the well chip using agarose. Sample solutions are then brought into the remaining channel chip.

This format has been used to carry out SOS-based genotoxicity assays *(8,9)*. The assay is based on activation of the bacterial SOS system. The SOS regulon is strongly induced by DNA damage under chemical and/or physical genotoxic stresses and is controlled by the RecA and the LexA proteins *(10)*. In the uninduced state, LexA protein represses SOS genes by binding to the SOS boxes upstream of each gene. Following DNA damage, RecA protein becomes activated. The activated RecA promotes self-cleavage of LexA repressor, activating transcription of SOS genes. We have constructed the reporter plasmid carrying *luc* under transcriptional control of *umuDC* (SOS gene) promoter.

Escherichia coli tester strains, KT1008 wild type (wt), *tolC*$^-$, and *lexA*$^-$, and XL1-Blue (as *recA*$^-$), all bearing the above plasmid, have been made for the genotoxicity assay. The TolC protein constitutes an efflux pump system in *E. coli* ***(11)***, and thus, its defective strain lacks the ability to pump out undesired molecules that intrude into the strain. The TolC defective strain shows higher sensitivity for genotoxic substances than wild-type because of an accumulation of substances in the strain.

Here we describe the method for this genotoxicity assay as an example of a bacteria-based bioassay in the on-chip format as well as the standard method for fabrication of chips required for this assay. Standard molecular biological protocols, such as the construction of plasmids and tester strains, are not covered within the scope of this chapter.

2. Materials

All solutions should be prepared with water that is over 18 MΩ-cm resistivity. In this section, this standard is referred to as "water."

2.1. Fabrication of Si Microwell Array Chip

1. A Silicon wafer with both sides polished (p-type, 6-in. diameter, 625-mm thickness, [100] surface; Osaka Tokusyu-gokin Co., Ltd, Osaka, Japan) is diced into 35 × 30 mm chips with a dicing saw.
2. RCA 1 cleaning solution: combine 100 mL of water, 20 mL of 30% (w/w) H_2O_2, and 20 mL of 25% (w/w) aqueous NH_4OH. Prepare RCA 1 freshly for each use (*see* **Note 1**).
3. RCA 2 cleaning solution: combine 120 mL of water, 20 mL of 30% (w/w) H_2O_2, and 20 mL of hydrochloric acid. Prepare RCA 2 freshly for each use (*see* **Note 1**).
4. RCA cleaning solution: combine 100 mL of water, 20 mL of 30% (w/w) H_2O_2, and 20 mL of sulfuric acid. Prepare RCA freshly for each use (*see* **Note 1**).
5. Hexamethyldisilazane (HMDS), positive photoresist OFPR-800, and NMD-3 developer are all from Tokyo Ohka Kogyo Co., Ltd (Kawasaki, Japan) and used in photolithography process.
6. The photomask for the microwell array chip is made by printing negative well array pattern desired on a transparency sheet with a high-resolution (multipurpose) printer (*see* **Note 2**). The negative pattern used is shown in **Fig. 1A**.
7. Buffered hydrofluoric acid (BHF) etchant for SiO_2 layer: combine 20 mL of 46% (v/v) aqueous HF and 140 mL of 40% (w/w) aqueous NH_4F in a screw-capped Teflon bottle. BHF can be used for up to about 10 etchings within a year under 4°C storage (*see* **Note 3**).
8. KOH/2-propanol etchant for anisotropic etching of Si chip: combine 300 mL of 25% (w/v) KOH and 50 mL of 2-propanol (*see* **Note 4**).
9. Quartz chip holder: laboratory made.

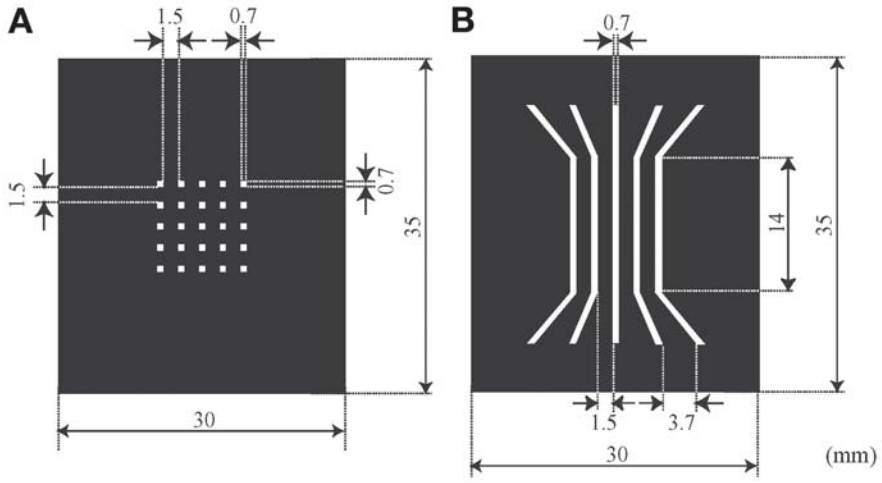

Fig. 1. Photomask designs as negative for microwell array **(A)** and microchannel **(B)**.

2.2. Fabrication of Poly(dimethylsiloxane) Microchannel Chip

1. PDMS prepolymer and curing agent: Sylgard 184 Silicone Elastomer Kit (Dow Corning).
2. Epoxy-based negative photoresist SU-8 no. 2075 and NANO XP SU-8 developer (MicroChem Corp.) are used for make a template.
3. Piranha solution: carefully combine 45 mL of 30% (w/w) H_2O_2 and 105 mL of sulfuric acid. Prepare the solution freshly for each use (*see* **Note 5**).
4. The Photomask for the channel chip is made by the same way as that for the fabrication of well array chip. The negative pattern used is shown in **Fig. 1B**.
5. 2-Propanol from Wako Pure Chemical, Osaka, Japan.
6. Plastic Petri dish from BD Falcon, Franklin Lakes, NJ.

2.3. Immobilization of Sensing Bacteria in the Chip

1. Tester strains used for genotoxicity assay are *E. coli* strains KT1008 wild type, KT1008 *tolC*$^-$, KT1008 *lexA*$^-$, and XL1-Blue (as *recA* defective), all containing the plasmid pRSSL, which carries a reporter *luc* gene under transcriptional control of an SOS promoter (*umuD*). They are made by standard molecular biological techniques ***(8)***.
2. Luria-Bertani (LB) medium: dissolve 10 g of Bacto Tryptone (Difco), 5 g of Bacto Yeast Extract (Difco), and 5 g of NaCl in 950 mL of water. Adjust pH to 7.0 with NaOH solution, and then adjust volume of the solution to 1000 mL with water. Sterilize the medium by autoclaving for 20 min at 120°C.
3. Ampicillin (Wako Pure Chemical, Osaka, Japan) is dissolved at 100 mg/mL in water as a stock. Sterilize the stock solution by filtration through a 0.22-μm filter and store in single use aliquots at –20°C until use.

4. Tris-buffered saline (TBS): 10 m*M* Tris-HCl, pH 7.4, 137 m*M* NaCl, 2.7 m*M* KCl. Sterilize the buffer by autoclaving for 20 min at 120°C and store at room temperature.
5. Agarose type VII (low gelling temperature; Sigma, St.Louis, MO) is used as a support for immobilization of strains in the chip (*see* **Note 6**). Agarose solution is prepared just before each use by dissolving agarose in hot water at 3% (w/v), followed by cooling down to room temperature.
6. Polytetrafluoroethylene (PTFE) membrane filter (1.0-µm pore size; Advantec, Tokyo, Japan).

2.4. Induction of Luciferase Expression and Detection of Bioluminescence

1. Mitomycin C (MMC, Wako Pure Chemical) is dissolved at 2 mg/mL in sterilized water containing 10 mg/mL NaCl (*see* **Note 7**). Dilute the solution to required concentrations with sterilized water. The solutions are preferably prepared just before use, but can be stored at 4°C within 3 d (*see* **Note 8**).
2. Luciferin solution: dissolve luciferin, potassium salt (Promega, Madison, WI) in water at 10 m*M*. Store the solution in small aliquots at –80°C, and use each aliquot only once and then discard.
3. ATP solution: dissolve ATP, disodium salt (Sigma) in water at 50 m*M*. Store the solution at 4°C in the dark, and make a fresh solution every month.
4. Substrate mixture for luciferase: 1 m*M* luciferin, 2 m*M* ATP, 20 m*M* $MgSO_4$, 40 m*M* Tris-HCl, pH 8.0. Prepare the mixture by using above luciferin and ATP solutions just before use.

3. Methods

3.1. Fabrication of Si Microwell Array Chip

The Si microwell array chip is made according to standard photolithography protocols, wet etching of SiO_2 layer, and anisotropic etching of Si wafer. Briefly, a SiO_2 layer is first formed by thermal oxidation of the Si chip. A photoresist is then coated on the chip, and a photolithography follows. The exposed SiO_2 layer is etched in BHF, while the remaining photoresist protects the unexposed part of the chip. Finally, the exposed Si area is etched by aqueous KOH with the remaining SiO_2 layer acting as a protective layer. A flow diagram of this protocol is shown in **Fig. 2**.

3.1.1. Formation of SiO_2 Layer on the Si Chip

1. Silicon chips with size of 35 × 30 mm are washed by soaking in RCA 1 solution at 80°C for 10 min, and then in RCA 2 solution at the same condition. Rinse the chips in water and dry them by a spin dryer.
2. Mount the chips on a quartz chip holder. The mounted chip holder is inserted into a thermal oxidizer, and heat at 1100°C for 10 h under stream of steam and nitrogen gas at flow rates of 11 mol/h and 70 mL/s, respectively (*see* **Note 9**). After cooling to room temperature, bring out the holder. A schematic of the equipment build in our laboratory is shown in **Fig. 3**.

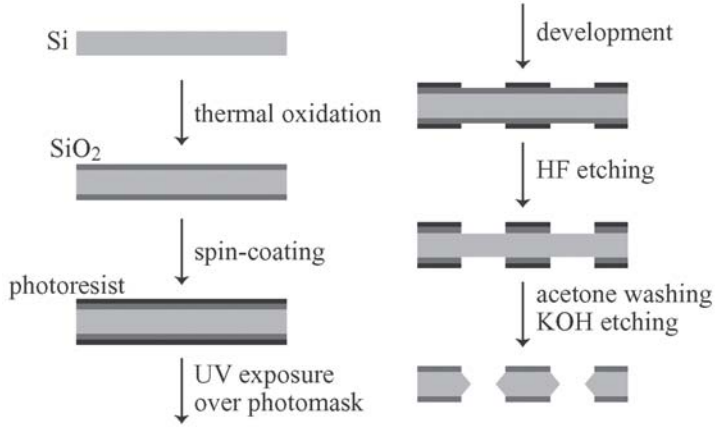

Fig. 2. Schematic diagram for fabrication of Si microwell array chip.

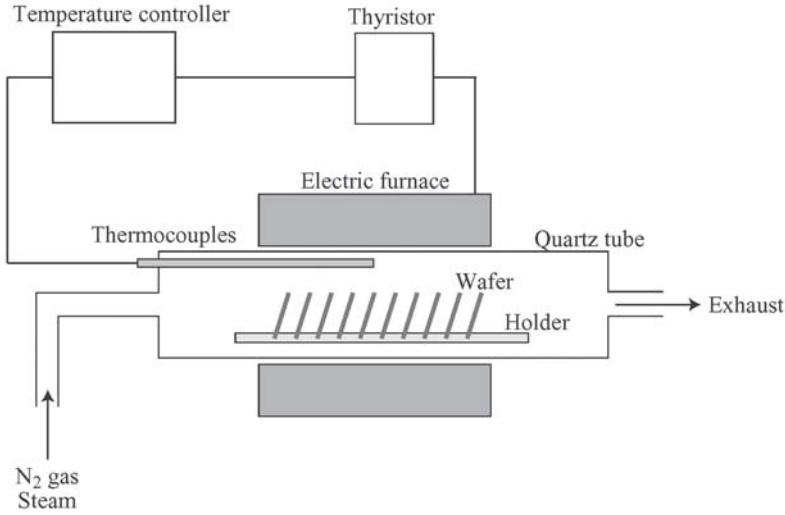

Fig. 3. Schematic of the equipment for thermal oxidation of Si chip.

3.1.2. Photolithography of the Si Chip

1. All procedures must be carried out in a yellow-lighted room to prevent exposure of photoresist-coated chips.
2. The Si chip with oxidized layer is washed by soaking in RCA solution at 80°C for 20 min, and then rinsed with water.

3. After spin-drying, the chip is mounted in a spin coater. A few drops of HMDS are deposited on one side of the chip, and then the spin coater is activated under programmed speed of rotation; start at 300 rpm for 10 s, accelerate up to 3000 rpm for 10 s (270 rpm/s), keep at 3000 rpm for 20 s, and decelerate to stop for 10 s (–300 rpm/s) (*see* **Notes 10** and **11**).
4. Coat photoresist OFPR-800 on the HMDS-coated chip in the same way as for HMDS coating. Bake the chip at 85°C for 15 min on a hot plate (Prebake).
5. Another side of the chip is also coated with HMDS and then OFPR-800 and prebaked.
6. Expose one side of the chip to ultraviolet (UV) light through the photomask for 10 s (*see* **Note 12**). Repeat the UV exposure for the opposite side of the chip using the same photomask. The photomask must be placed on the chip as patterns on both sides of the chip are aligned (*see* **Note 13**).
7. Immerse the chip in the developer NMD-3 in a glass beaker for 90 s at room temperature, and then in another NMD-3 for 90 s. Rinse the chip by immersing in water for 2 min, and then spin-dry.
8. Bake the chip at 130°C for 5 min (Postbake) (*see* **Note 14**).
9. The photoresist should remain in the area that is *not* to be etched out in the following process (*see* **Note 15**).

3.1.3. Etching to Make Perforated Wells on the Chip

1. Mount the chip on the quartz chip holder. Immerse the loaded chip holder into the etchant, BHF, in a Teflon bottle at room temperature for 45 min with gentle agitation using a Teflon-coated magnetic stirring bar (*see* **Note 16**).
2. Rinse the chip with water and then with acetone to remove the photoresist. At this moment, Si areas should be exposed with each size of 700 × 700 μm on the chip, which are to be etched by KOH/2-propanol.
3. After rinsing the chip again with water, immerse it on the holder into the KOH/2-propanol etchant preheated at 70°C in a flask (*see* **Note 17**). Etching is carried out at 70°C with gentle agitation by using a magnetic stirring bar under reflux to prevent condensation of KOH. Anisotropic etching of the Si chip should proceed at the both sides on the chip until passing through it. This process will take about 7 h for a 625-μm Si chip (etching rate ~45 μm/h) (*see* **Note 18**).
4. After that, immediately rinse the chip with water, ethanol, and water again. An example of etched Si chip is shown in **Fig. 4A**. The volume of each perforated well should be about 150 nL.

3.2. Fabrication of PDMS Microchannel Chip

PDMS chip is made by molding using microstructure of thick photoresist SU-8 as a template. This so-called soft lithography process is very simple, and thus widely used for making microfluidic devices ***(12)***. In this protocol, SU-8 is first coated on a flat substrate, followed by photolithography to make a master plate. PDMS prepolymer mixed with curing agent is then poured over the SU-8 coated master plate. After curing, PDMS is peeled off from the master.

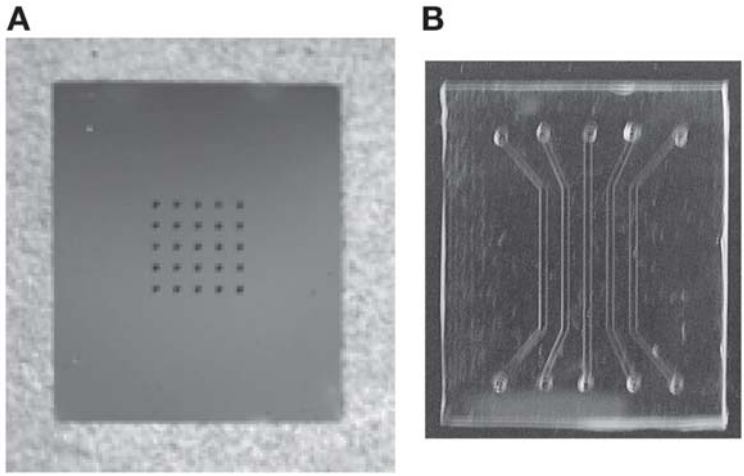

Fig. 4. Si microwell array chip **(A)** and PDMS microchannel chip **(B)**.

A flow diagram of this protocol is shown in **Fig. 5**. Two channel chips with identical structure are required for the presented on-chip bioassay.

3.2.1. Photolithography Using Photoresist SU-8

1. A silicon chip with size 35 × 30 mm is washed by soaking in piranha solution at 100°C for 20 min, and then rinsed with water, followed by spin-drying (*see* **Note 19**).
2. The chip is mounted in a spin coater. About 1 mL of SU-8 no. 2075 is poured on one side of the chip. The spin coater is then activated under programmed speed of rotation; start at 500 rpm for 5 s, acceleration up to 1000 rpm for 5 s (100 rpm/s), keeping at 1000 rpm for 30 s, and deceleration to stop for 10 s (–100 rpm/s) (*see* **Note 20**).
3. The SU-8 coated chip is baked at 65°C for 5 min and then at 95°C for 45 min on a hot plate (Softbake) (*see* **Note 21**).
4. The baked chip is exposed to UV light for 30 s through the photomask (*see* **Note 12**). The exposed chip is baked again at 65°C for 1 min, and then at 95°C for 15 min on a hotplate (post-exposure bake).
5. The chip is immersed in the SU-8 developer for 6 min with strong agitation at room temperature, and again in another SU-8 developer for 6 min. The developing time should be changed by the look of dissolving unexposed area.
6. The chip is rinsed with 2-propanol, followed by spin-drying. The resist SU-8 should remain as a convex structure at about 200-μm thickness with nearly vertical sidewalls on the chip, making the inverted pattern of the channel chip desired.
7. Finally, the chip is baked once again at 150–200°C for 10 min on a hot plate. After cooling to room temperature, the chip can be used as a template for PDMS channel chip.

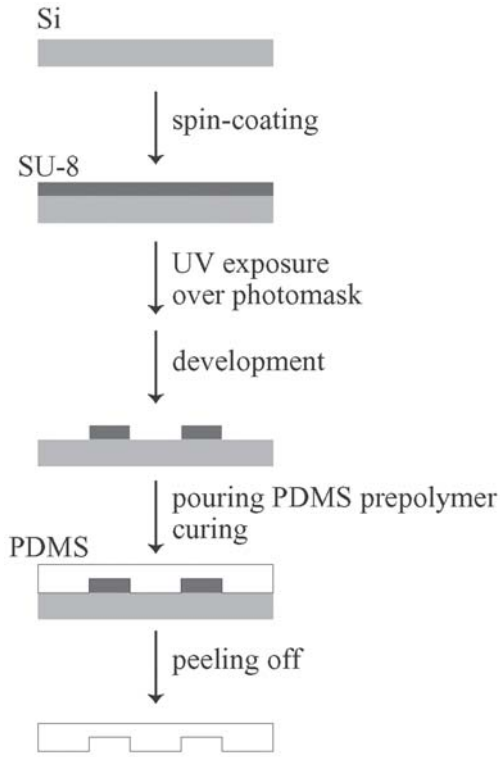

Fig. 5. Schematic diagram for fabrication of PDMS microchannel chip.

3.2.2. Fabrication of PDMS Microchannel Chip by Molding

1. Sylgard 184 Silicone Elastomer Kit is supplied in two parts as base (prepolymer) and curing agent. They are mixed in a ratio of 10 parts base to 1 part curing agent, by weight.
2. The SU-8-coated chip as a template is placed on a Petri dish, into which the above mixture of Sylgard 184 (PDMS) is poured. The amount of the mixture pouring should be about 5–10 mm depth in the dish.
3. The dish is set in a vacuum desiccator, followed by deairation to remove bubbles and dissolving gases in the PDMS mixture until bubbling subsides. This will take about 10 min.
4. After the dish is covered, it is allowed to stand at 4°C for 1 h in a refrigerator, and then at 60°C in a convection oven. PDMS should be cured within 4 h at this temperature.
5. The PDMS cured is peeled off from the dish and the SU-8 coated chip, and then cut to the appropriate size. The channel should be molded as a concave structure at about 200 μm depth on the PDMS chip.

6. For open access holes to the channels, the chip is pierced at both ends of each channel at about 1 mm diameter using a Pasteur pipet. An example of the PDMS chip is shown in **Fig. 4B**. The volume of each channel should be about 2 µL.

3.3. Immobilization of Sensing Strains in the Chip

Briefly, in this procedure, the PDMS microchannel chip is first sealed on the Si microwell chip. Each of the tester strains mixed with agarose is then loaded from each channel into the wells and immobilized by gelation. A schematic of this procedure is shown in **Fig. 6A**. Proper immobilization of the strains in all of the wells is very important in order to obtain good results.

3.3.1. Setup of the Chip

1. One of the PDMS channel chips is sealed on one side of the Si microwell chip as each of the five channels is aligned with each of the five well lines as shown in **Fig. 6A**.
2. The PDMS sealed Si chip is placed on the PTFE membrane filter laid on a Petri dish. It is vitally important to ensure the contact of the PDMS chip and the filter to the Si chip, or the mixture of the strain and agarose will leak from the gap before gelation of the mixture (*see* **Note 22**).

3.3.2. Preparation of the Sensing Strains

1. The tester strains are grown in LB medium containing 100 µg/mL ampicillin with shaking at 37°C until the OD_{600} is about 0.4.
2. The strains are collected by centrifugation at 3000*g* for 5 min and suspended in TBS at the concentration of approx 4×10^{10} cells/mL (*see* **Note 23**).
3. The suspensions are then mixed with the same volume of 3% (w/v) agarose at 37°C. It is advisable to prepare several types (up to five in this chip) of the mixture according to each purpose.

3.3.3. Immobilization of the Sensing Strains

1. Using a micropipet, the mixtures of the strain and agarose are loaded from the access holes into the chip on the dish until the channels and the wells are filled up with the mixtures.
2. The dish is covered and then placed in a refrigerator at 4°C. The mixture in the chip should gel in about 10 min.
3. After gelation, the chip is ready for the assay and can be treated at room temperature and even at 37°C without melting of the gel (*see* **Note 24**).

3.4. Induction of Luciferase Expression and Detection of Bioluminescence

Finally, the second PDMS chip is sealed on the Si chip, followed by filling of the channels with samples for the induction of the luciferase expression. For detection of luciferase, the substrate solutions are then filled in the channels as shown in **Fig. 6B**. The assembled chip constitutes the 3D microfluidic network (**Fig. 6C**), which enables the assay to be performed in a combinatorial fashion (*see* **Note 25**).

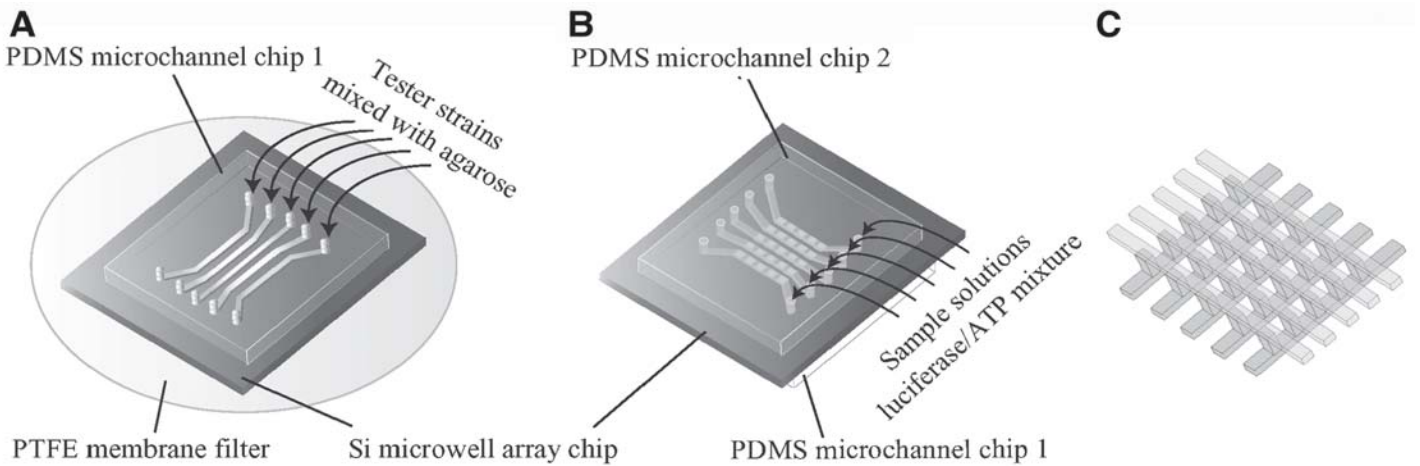

Fig. 6. Schematics of the method for on-chip bioassay using three-dimensional microfluidic network. **(A)** The mixtures of tester strain and agarose are filled and immobilized in the channels on the PDMS chip 1 and in the wells on the Si chip. **(B)** After turnover a set of the PDMS and Si chips, sample solutions are filled in the channels on the PDMS chip 2, followed by replacing sample with luciferin/ATP solution for BL measurement. **(C)** In the chip assembly, three-dimensional microfluidic network is constructed, in which sample and cell lines are connected via each well.

3.4.1. Setup of the Chip

1. The filter is peeled off from the PDMS sealed Si chip. Visually ensure that the mixture is filled in all of the wells. If voids or air bubbles are found in the wells, refilling with the mixture left over is recommended.
2. Another PDMS channel chip is then sealed on the Si side, just unsheltered, of the PDMS sealed Si chip. The channel lines on this PDMS chip are aligned with the well lines as with the previously sealed PDMS chip, but the lines on the two PDMS chips must be oriented 90° each other.
3. In the chip assembly prepared, the channels are due in overhead crossing with connections at each of the wells.

3.4.2. Mitomycin C and Substrate Loading and BL Detection

1. The solutions of mitomycin C (MMC) at various concentrations (up to five) are loaded from the access holes into the chip by using a micropipet until the channels are filled up.
2. The chip is placed in an incubator at 37°C for 1 h.
3. After the MMC solutions are removed from the chip by a pipet, the substrate mixture is loaded into each channel on the chip as with MMC loading.
4. The chip is then placed under a charge-coupled device (CCD) camera in a light-shielded housing, and BL emitted from the chip is measured for 15–30 min (*see* **Note 26**). Typical results are shown in **Fig. 7**. When the single strain, *E. coli* KT1008/pRSSL, was immobilized in each vertical well line (**Fig. 7A**), BL emissions from five wells on each sample (horizontal) line were almost identical, indicating that the immobilization of the strain and the introduction of sample and substrate were uniformly made. On the other hand, those on each vertical line showed the dose–response relationship. By using various types of strain, overall imaging of the chip will be a characteristic BL emission pattern according to the strains as shown in **Fig. 7B**. In the *tolC* strain, the concentration range of the dose–response was one order of magnitude lower than that in the wild type. The *recA*$^-$ XL1-Blue showed no emission at any concentration of MMC, while the *lexA*$^-$ strain did strong BL emission without dose dependence. Additionally, the results were in good agreement with those by using test tubes ***(6,9)***, indicating that the on-chip format can be used for this genotoxicity assay.

4. Notes

1. To obtain an accurate photolithographic pattern on the chip, contaminants present on the silicon surface have to be removed. The RCA clean is the industry standard for this purpose. RCA 1 and unnumbered RCA are used for removal of insoluble organic contaminants from the surface. RCA 2 is for ionic and heavy metal atomic contaminants. The chemicals used for RCA clean are all dangerous in case of contact. Handle with care.
2. In general, purpose-made, emulsion-coated glass plates are used to make the photomask for ultra-high-resolution photolithography. However, our patterns in this method are so simple and large that we have used transparency sheets in

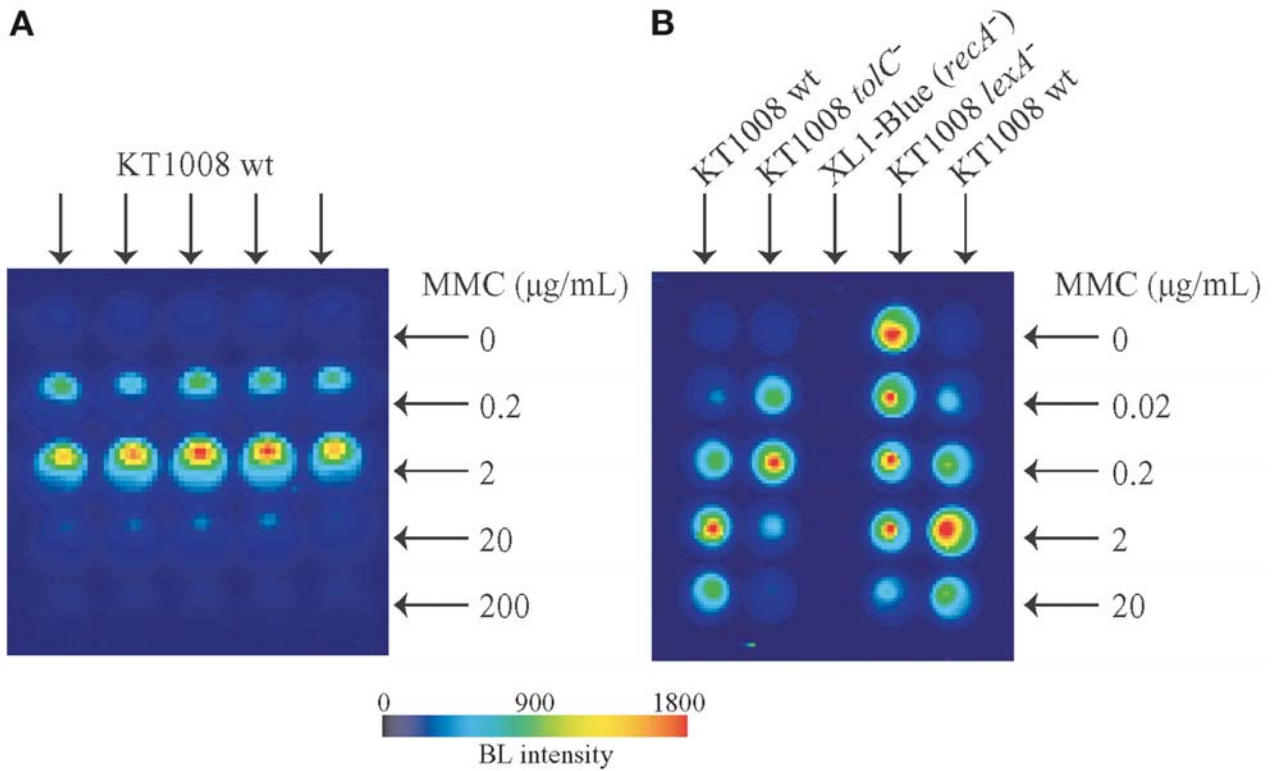

Fig. 7. Bioluminescence imaging in the on-chip genotoxicity assay using 5 × 5 well array. **(A)** Single strain, *E.coli* KT1008 wt/pRSSL, was immobilized in each well (vertical) line, and various concentrations of genotoxic substance, mitomycin C (MMC), were filled in each of the channels. **(B)** Various strains and concentrations of MMC were used in the single chip assembly. (Reproduced from **ref. *6*** with permission from American Chemical Society)

place of the glass plate and used a laser printer with resolution of 2400 dpi for printing patterns.

3. HF acid is very dangerous, and HF burns are extremely hazardous, so it must be also handled wearing acid-protecting gears.
4. Addition of 2-propanol prevents a corner undercut, which causes deviation from desired pattern. Aqueous KOH and 2-propanol are immiscible, but allow using as they are.
5. Piranha is a vigorous oxidant and potentially explosive. It should be handled with extreme caution.
6. Agarose with low-gelling temperature has several advantages in this method. Agarose solutions should not gelate readily at room temperature, making pouring them into the chip easy. Additionally, the solutions show hysteresis in the liquid-to-gel transition, that is, the gel point is not the same as the melting point. This indicates that agarose once gelate at low temperature should not melt readily at room temperature, even at 37°C. Thus, the chip immobilizing the tester strain with the agarose gel can be used under these temperatures.
7. Addition of NaCl helps solubilization of MMC in water.
8. Dissolved MMC is not stable. We have found the titer of MMC decreases about 80–90% under storage at 4°C for 4 d. If necessary, stable MMC solution is commercially available from several manufacturers.
9. In our experimental conditions and equipment, about 2 μm thickness of oxidized layer should be formed on the silicon chip. However, the thickness is largely dependent upon the conditions and the equipment for oxidization. Preliminary experiments are recommended to clarify the relationship between the thickness and the condition. Silicon wafers with oxidized layer at a desired thickness are also commercially available, but they are rather expensive.
10. HMDS promotes adhesion of photoresist to oxidized silicon layer.
11. Rotation number and spin time in the coating process are essential for controlling thickness of coated photoresist. Follow the instructions from the manufacturer.
12. UV wavelength, intensity, and exposure time are available from the instructions that come with the photoresist, but we have optimized these parameters under the process of trial and error using our UV lamp system.
13. Aligning patterns on both side of the chip should be carried out using a photomask aligner commercially available. However, manual aligning using a ruler is also possible for large patterns as in this method.
14. Temperature and time for pre- and postbake are different from those provided in the manufacturer's instructions. We have optimized these parameters under the process of trial and error in our laboratory.
15. If there are scratches on the baked photoresist, the oxidized layer and thus the Si surface will be etched at undesired areas through the described processes. Manicure of cosmetic is useful to repair the scratches.

16. The time for HF etching of the oxidized silicon layer is largely dependent not only on the thickness, but also on temperature and agitation. Thus, the time should be changed according to the progression of etching for each experiment. Completion of the etching process can be checked by spraying with water using a wash bottle. Si surface exposed by etching of oxidized layer should repel water, while remaining layers should not.
17. We have used three-necked separation flasks for this purpose. The center neck is used for reflux condenser, and the remaining two necks are for fixing a temperature indicator and the handle of the chip holder.
18. Time for KOH etching of silicon is also dependent on experimental conditions. We have checked occasionally by holding up to the light whether all of the wells are perforated.
19. For cost-saving purposes, in place of the Si chip, glass or Pyrex glass plates can be used. In our experience, however, glass plates show limited adhesion with SU-8.
20. Rotation number and time are set for 225μm thickness according to the manufacturer's instructions.
21. SU-8 is very viscous, but its layer can slant on the chip at the beginning of the softbake process, causing failure. To prevent this, it is important to keep the chip horizontal. We, therefore, have kept the hot plate horizontal and turned around the chip on the plate occasionally.
22. We have used PTFE filters with 1-μm pore size to prevent leakage of the strain/agarose mixture from the wells and to ensure the wells are filled with the mixture. Other materials with air permeability may be available.
23. As the cell concentration could influence the assay results, it should be optimized under each bioassay system.
24. At this time, the strain-loaded chip cannot be stored for a long time. We have confirmed that BL emission from the immobilized strain decreases about 20% for 1–wk storage at 4°C in our experimental conditions. The storage period would be improved by varying the conditions and the support for immobilization.
25. In this microfluidic network, all of the cell and sample lines are continuously connected to each other. This indicates that the sample in a channel line can diffuse via the wells and the cell lines into the wells on the neighbor sample lines and can induce the cell in the neighbor wells. This is a serious problem with the assay. We have checked the effect of the sample migration between the wells on the BL emission from each well. We have found no significant migration that affects the BL emission from the neighbor wells at the induction time for 1 h ***(6)***. However, this must be dependent on the induction time (standing time in each channel), distance between the wells, and depth of the channel and the well. Thus, if altering these parameters, the effect of sample migration should be checked.
26. After the assay, the chip can be recycled for the next use. Peel off the PDMS chips from the Si chip and immerse them in hot water for melting the gel away. Then, immerse them in detergent and rinse with water.

Acknowledgments

This work was supported in part by a Grant-in-Aid for Scientific Research (No. 17750063) from the Ministry of Education, Culture, Sports, Science and Technology of Japan.

References

1. Ames, B. N., McCann, J., and Yamasaki, E. (1975) Methods for detecting carcinogens and mutagens with the Salmonella/mammalian-microsome mutagenicity test. *Mutat. Res.* **31,** 347–364.
2. Wegrzyn, G. and Czyz, A. (2003) Detection of mutagenic pollution of natural environment using microbiological assays. *J. Appl. Microbiol.* **95,** 1175–1178.
3. Aryal, P., Terashita, T., Guengerich, F. P., Shimada, T., and Oda, Y. (2000) Use of genetically engineered Salmonella typhimurium OY1002/1A2 strain coexpressing human cytochrome P450 1A2 and NADPH-cytochrome P450 reductase and bacterial O-acetyltransferase in SOS/umu assay. *Environ. Mol. Mutagen.* **36,** 121–126.
4. Baldi, P. and Hatfield, G. W. (2002) *DNA Microarrays and Gene Expression: From Experiments to Data Analysis and Modeling*, Cambridge University Press, Cambridge, UK.
5. Baba, Y., Shoji, S., and van der Berg, A. (eds.) (2003) *Micro Total Analysis Systems 2002,* Volume 1 and 2; *Proceedings of the* μ *TAS 2002 Symposium*, Kluwer, Norwell, MA.
6. Tani, H., Maehana, K., and Kamidate, T. (2004) Chip-based bioassay using bacterial sensor strains immobilized in three-dimensional microfluidic network. *Anal. Chem.* **76,** 6693–6697.
7. Bernard, A., Michel, B., and Delamarche, E. (2001) Micromosaic immunoassays. *Anal. Chem.* **73,** 8–12.
8. Maehana, K., Tani, H., Shiba, T., and Kamidate, T. (2004) Effects of using a low-copy plasmid and controlling membrane permeability in SOS-based genotoxic bioassay. *Anal. Chim. Acta* **522,** 189–195.
9. Maehana, K., Tani, H., and Kamidate, T. (2006) On-chip genotoxic bioassay based on bioluminescence reporter system using three-dimensional microfluidic network. *Anal. Chim. Acta* **560,** 24–29.
10. Friedberg, E. C., Walker, G. C., and Siede, W. (1995) SOS response and DNA damage tolerance in prokaryotes, in *DNA Repair and Mutagenesis,* ASM Press, Washington, DC.
11. Fralick, J. A. (1996) Evidence that TolC is required for functioning of the Mar/AcrAB efflux pump of Escherichia coli. *J. Bacteriol.* **178,** 5803–5805.
12. McDonald, J. C. and Whitesides, G. M. (2002) Poly(dimethylsiloxane) as a material for fabricating microfluidic devices. *Acc. Chem. Res.* **35,** 491–499.

5

Microchip-Based Enumeration of Human White Blood Cells

Pierre N. Floriano, Shelley Acosta, Nicolaos Christodoulides, Shannon Weigum, and John T. McDevitt

Summary

The advent of flow cytometry has considerably changed the ways in which medical testing is conducted. However, the cost of flow cytometers, their large size, and their maintenance needs make them scarce in resource-poor settings and available almost only in clinical pathology laboratories in developed countries. Because cell enumeration is a basic and crucial support of diagnosis, prognosis, and treatment, an alternative cell-counting method that would potentially be cost-effective, portable, and suitable for use in resource-poor settings is warranted. We describe here a protocol for conducting cell-counting experiments in a simple microfluidic structure. This protocol describes how to build a simple microfluidic cell and perform a total white blood cell (WBC) count through capture and immunolabeling of the WBCs with an anti-CD45 antibody.

Key Words: White blood cells; flow cytometry; microchip; CD45; microfluidic sensor.

1. Introduction

The complete blood count (CBC) is one of the most commonly administered health tests worldwide. It includes the enumeration and analysis of red blood cells, platelets, and white blood cells (WBCs) and thus offers to physicians a tremendous amount of information that is often the basis for diagnosis or the administration of additional more specific tests. As WBCs help the body fight infections, an abnormal total WBC count can be associated with bacterial or viral infection, inflammation, or stress. The WBC differential count consists of the enumeration of three or all five of the WBC types: neutrophils, lymphocytes, monocytes, eosinophils, and basophils. Each subtype has a unique role in the immune system, and variations in these subpopulations have significant

From: *Methods in Molecular Biology, Vol. 385: Microchip-Based Assay Systems: Methods and Applications*
Edited by: Pierre N. Floriano © Humana Press Inc., Totowa, NJ

diagnostic and prognostic values. Although WBC differential counts are traditionally obtained with a hematology analyzer *(1)*, the use of flow cytometry (FC) as a means to count WBCs and WBC subtypes has substantially increased in the past decades *(2,3)*, as have the scope and number of FC-based applications *(4)*. Despite notable efforts in the past few years, the size, cost, and technological complexity of such instrumentation have limited its use for point-of-care (POC) testing. One particular example of such limitation is in the context of the fight against AIDS *(5)*. Values for the absolute counts for T-helper (CD4-positive) lymphocyte counts as well as viral load levels are crucial elements of AIDS monitoring and treatment *(6–8)*. Despite the advent of cheaper antiretroviral drugs, the cost of CD4 blood counts remains prohibitive in resource-poor countries, as it is mainly obtained from single platform FC and even hematology analyzer /FC dual platforms in some instances *(9)*. Efforts targeted toward the development of cheaper and more portable instrumentation capable of cell enumeration have been consistent with the miniaturization of FC components and methods *(9,10)*, or the development of new technologies fostered by tremendous advances in the field of microfluidics in recent years *(11–29)*.

We have recently demonstrated the development of a microchip-based approach to cell counting that was applied to the monitoring of CD4 cells from HIV-infected patients *(30)*. There are multiple microchip strategies and configurations of materials suitable for the capture and detection of WBCs on a membrane. We have chosen here to describe a simple microfluidic assembly composed of commercially available components that can be easily fabricated without any specialized components. This microchip structure is composed of a bottom plastic part machined to accommodate a plastic support grid with micrometer-scale holes, a stack featuring a 3-μm-pore membrane, various laminate adhesive layers, with embedded microchannels, and a glass cover slip. The microfluidic device features an inlet and a drain to allow fluid flow through the central membrane, which serves to retain WBCs, while allowing the red blood cells to deform and pass through the 3-μm-pore membrane.

We also present here a simple methodology that can be used to obtain in a reproducible manner total WBC counts from human blood. This method could easily be adapted and expanded to a three- or even a five-part differential that could be administered at the POC, including battlefield, emergency crews, and doctors' offices.

2. Materials

2.1. Fabrication of a Microfluidic Device

1. A sheet of polymethylmethacrylate (PMMA) at least 3/8 in. thick (*see* **Note 1**).
2. 22 × 30 mm glass cover slips.

3. Celcon acrylic 13-mm plastic grid from Pall Gelman Swinney holder (VWR, #4317).
4. 13-mm-Diameter, 3-µm Nuclepore® track-etched polycarbonate membranes. (Whatman, Florham Park, NJ), or 2.5-µm-pore Aquamarijn microsieve®.
5. 1-in.-cut, 0.039-in.-diameter stainless steel tubing.
6. 5-min Epoxy fast-setting adhesive.
7. A Summa Cut (model: D60/U) plotter cutter is used to cut the required designs for the double-sided adhesive and vinyl layers of material.
8. Summa Winplot software.
9. Double-sided adhesive 9500 (3M) or equivalent.
10. Single-sided adhesive MACal 9800 or equivalent.
11. Isopropanol (IPA).
12. Silicon tubing.

2.2. Instrumentation

1. BX2 Olympus compound microscope equipped with a 10X objective lens and a high-pressure 100 W mercury burner arc lamp as a light source.
2. Fluoroisothiocyanate (FITC) filter cube (480 nm excitation, 505 nm long pass beam splitter dichroic mirror, and 535 ± 25 nm emission) to image the Alexa Fluor® 488-stained WBC (Chroma 41003).
3. 12-bit CCD digital camera (DVC, Austin, TX) mounted on the microscope.
4. Computer controlled image acquisition software such as Image Pro Plus (Media-Cybernetics, Silver Springs, MD) or ImageJ (National Institutes of Health, Bethesda, MD) shareware.
5. Syringe pump. For these studies, we have used a New Era Pump Systems, model NE-1000 (New Era Pump Systems, Wantagh, NY). The experimental setup is shown in **Fig. 1**.

2.3. Sample and Reagents

1. Venous blood is collected fresh (less than 24 h) in a vacutainer with ethylene diamine tetraacetic acid (EDTA) anticoagulant. Blood is stored at 4°C.
2. BupH™ modified Dulbecco's phosphate-buffered saline pack (PBS, Pierce, Rockford, IL). PBS is prepared fresh for each experiment (*see* **Note 2**).
3. Mouse anti-human CD45: Alexa Fluor®488 (Serotec, Oxford, UK). The antibody is centrifuged for 1 min at 10,000*g* and 50-µL aliquots stored at –20°C in a non-frost-free freezer, protected from the light.
4. Cytofix/Cytoperm 4% paraformaldehyde (BD).
5. 1-cc syringes (Fisher Scientific).

3. Methods

3.1. Preparation of the Flow Cell

3.1.1. Preparation of the Machined Flow Cell Parts

1. Machine bottom a PMMA plastic part with dimensions corresponding to the chosen filtering strategy (*see* **Notes 3** and **4**). An example of such a part is shown in

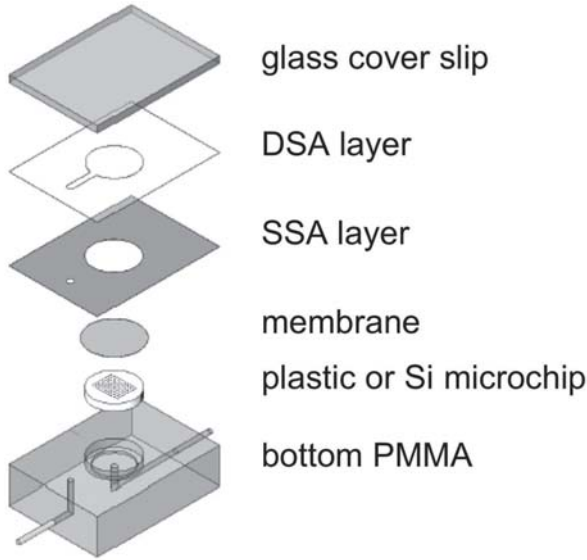

Fig. 1. Example of a simple stack that can be created for the membrane flow cell. DSA, double-sided adhesive; SSA, single-sided adhesive; PMMA, polymethylmethacrylate.

Fig. 2. There is great flexibility with regards to the choice of dimensions for this part. The only critical aspects are the flatness and smoothness of the top surface and the respect of the dimensions of the capturing components.

2. Drill 0.039-in. holes that will allow interfacing of the bottom part with tubing.
3. Clean by soaking in IPA, rinse with dI H_2O, and dry under nitrogen stream.
4. Epoxy tubes inside both the inlet and the outlet of the bottom PMMA part (*see* **Note 5**).

3.1.2. Preparation of the Laminate Layers

1. Draw in Solidworks® or other computer-aided drawing program the various layers constituting the stacks. Save the file as an ".isi" file. Such a stack is shown in **Fig. 2**. (*see* **Notes 6** and **7**).
2. Insert the single-sided adhesive (SSA) or double-sided adhesive (DSA) layer and align the edge so that it is approx 2 cm below the felt blade guard.
3. Position the rollers over the outer edges of the material.
4. Lower the camrollers and the machine will measure the material and proceed to the standby position.
5. Select the knife pressure. The knife pressure varies based upon the thickness of the material as well as the sharpness of the blade (*see* **Note 8**).

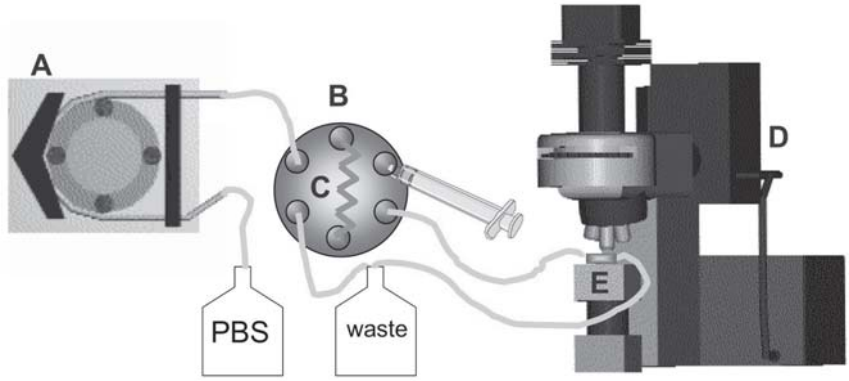

Fig. 2. **(A)** Peristaltic (or syringe) pump. **(B)** Injection valve. **(C)** Sample loop. **(D)** Modified compound microscope. **(E)** Microchip. PBS, phosphate-buffered saline.

6. In Winplot, select the tab "open new file" then look in "Designs." The file type is ISI Design file [*.isi].
7. Open the necessary file then select "Output."
8. Select "send to cutter." The Summa Cut plotter has measured the material. If the medium is not large enough for the design selected, it will not proceed.
9. Once the machine finishes the cut, lift the camrollers, remove the material, and leave the camrollers up.

3.1.3. Flow Cell Assembly

1. Peel the SSA and place it top side down on a clean, dust-free benchtop.
2. Carefully position the membrane top-side-down onto the SSA (*see* **Note 9**).
3. Carefully apply the membrane/SSA assembly onto the bottom part (*see* **Note 10**).
4. Peel off one side of the DSA layer, and gently apply onto the SSA layer(*see* **Note 11**).
5. Peel off the other side of the DSA layer and gently deposit the glass cover slip (*see* **Notes 12** and **13**). The flow cell is now ready for use.

3.2. CD45 Assay

Note: Use universal precautions when working with human blood and disposing waste.

1. Bring whole venous EDTA anticoagulated blood to room temperature, gently invert several times, and aliquot 30 µL into a 1.5 µL tube.
2. Fix the blood sample with 5 µL of 4% paraformaldehyde. Tap gently to mix.
3. Immediately add 5 µL of mouse anti-human CD45-Alexa Fluor® 488. Tap gently to mix and incubate 5 min at room temperature.
4. Dilute the sample with 700 µL of PBS and mix gently by pipetting.

5. Carefully transfer the diluted sample to a 1-cc syringe, while avoiding the introduction of bubbles into the syringe.
6. Remove any bubbles from syringe by gentle tapping.

3.3. Loading the Sample Onto the Flow Cell

1. Prime the pump lines and injection loop with PBS.
2. After confirming there are no bubbles in the system, turn the pump off.
3. Connect flow cell tubing to pump lines and turn pump on. Ensure there are no bubbles in the flow cell prior to adding sample.
4. Secure the flow cell onto the stage of the microscope and adjust the focus on membrane.
5. Deliver the fixed cells onto the flow cell via a calibrated injection loop at a flow rate of 2 mL/min.
6. Wash away excess antibody from the sample with PBS for approx 1 min at a flow rate of 2 mL/min.
7. Acquire images at various fields of view. A typical image acquired on our system is shown in **Fig. 3**.

3.4. Image Capture and Analysis

1. For each study subject, images are obtained randomly from a chosen number of nonoverlapping regions of the capture area in the flow cell (*see* **Note 14**).
2. Convert the images to RGB 24-bit pictures, and name them consistently to allow the use of an automated counting macro (*see* **Note 15**).
3. Install Image J Software on your computer according to instructions provided by the National Institutes of Health on the ImageJ website (http://rsb.info.nih.gov/ij/) ***(31)***.
4. Retrieve and download the FFT filter plugins from Joachim Walter (Walter at biz.uni-muenchen.de) on the ImageJ website. This plugin can be found under "plugins," under "filter," under "FFT filter" section.
5. Install the ImageJ plugins and restart Image J. The Image J environment is now ready to analyze captured images.
6. Copy and paste the macro code text given in **Note 15** and save it as a *.txt* file in the "ImageJ" folder in the "macros" folder (*see* **Note 16**) using any word-processing software (Wordpad, Notepad, Word, etc.).
7. Open ImageJ and, under the Plugins tab, select "Macros" and "Record." This will allow you to visualize the lines of code for every action taken in the Recorder window.
8. Open an image to be analyzed. Make sure that the "Open" command in the macro features the correct root listed in the "Recorder" window.
9. Modify loop variables in lines 11 and 14, depending on the number of measurements you are performing. Loop "i' is dedicated to the number of flow cells, whereas loop "j" corresponds to the number of fields of view within one flow cell. For example, if there are three flow cells per experiment and five fields of view per flow cell, line 11 would be: for (i=1;i<4;i++) { and line 14 would be: for (j=1;j<6;j++) {.

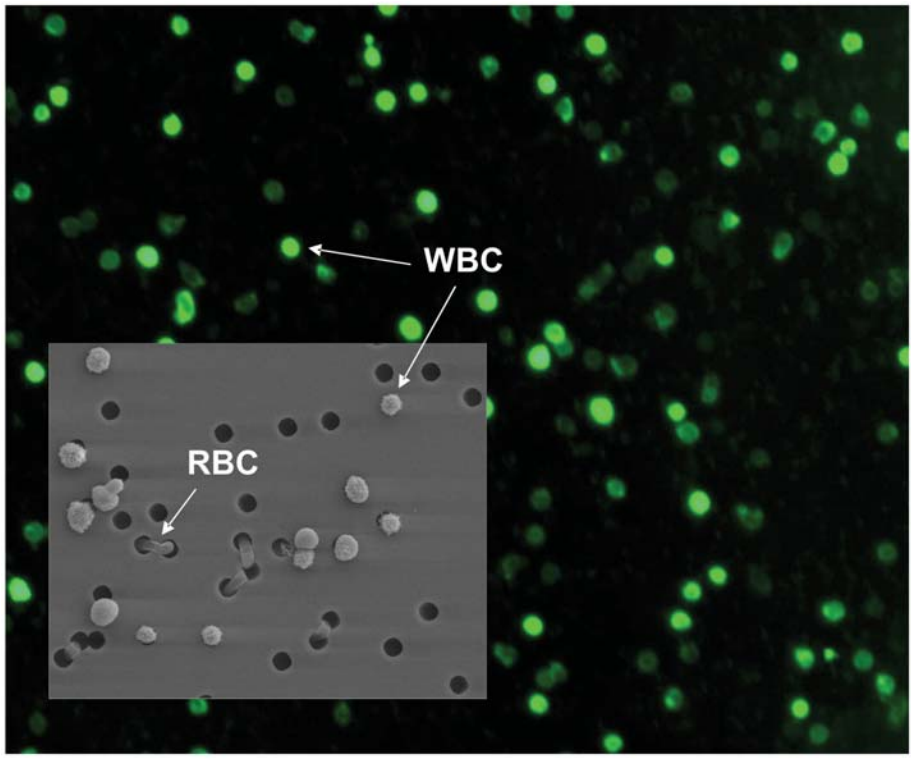

Fig. 3. Cropped section of a typical micrograph of anti-CD45-labeled white blood cells (WBC) on membrane within the microchip. The inset is a scanning electron micrograph of the membrane where WBC can be seen captured at the surface and red blood cells (RBC) are seen making their way through.

10. Save images at various exposures. Implement a corresponding loop in the macro, or state the correct exposure in the filename in line 16. The macro is now ready to count the cells in each image.
11. To run the macro to analyze the data, open tab "Plugins," open "macros" then "run…" Click on your saved macro.
12. Data can be imported in most spreadsheet software such as Excel® or SigmaPlot®.
13. Determine the total capture area (A1), as defined from the flow cell patterns, the area (A2) of a field of view (from the camera manufacturer and optical setup). The number of fields of view (fov) is calculated as fov = A1/A2.
14. Determine the total volume of blood introduced to the flow cell (v), making sure to take into account all dilutions. Absolute counts/μL (CD45 ABS) are calculated as CD45 ABS = average × fov/v.

4. Notes

1. Other materials can be used here for the bottom of the device. Some examples include polycarbonate (PC), cyclic olefin copolymer (COC), and Delrin, to name a few. The only requirement for choosing a material is that a solid bond can be established between the chosen material and adhesive layer *(32)*.
2. For long-term storage of PBS, add 0.05% sodium azide.
3. For ease of assembly and for safety reasons, we have chosen the overall dimensions of the whole assembly to be that of the glass cover slip. As the cover slips are available in a variety of sizes, there is great flexibility in terms of the overall dimensions of the flow cell you can choose based on your particular application and setup.
4. The main feature of this bottom part is a drain that is placed under the microchip. The bottom part is machined to accommodate a Pall screen, Aquamarijn, or other microchip. For use with Aquamarijn microchips, make sure to order the support ABS mounting ring.
5. When gluing the tubing inside the inlet and outlet holes, great care must be taken to not introduce epoxy into the channels. This is easily achieved by first introducing the tube inside the inlet or outlet and then applying a small bead of glue around the tube, slowly twisting while sliding it in.
6. Depending on the chosen strategy for capture, SSA must efficiently bond to the filtering medium.
7. Depending on the chosen strategy for capture, ensure that the opening in the SSA spans the entire porous area of the microchip.
8. The knife pressure varies based upon the thickness of the material as well as the sharpness of the blade. A blade with a moderate amount of wear can have a knife pressure that varies between 130 and 115 g when used to cut a layer of vinyl and approx 180+ g for DSA. To determine what pressure setting to use, it is best to start at a lower setting and perform a test cut of the material. Perform a test cut for each pressure setting to ensure that the material is adequately cut, but not deep enough to penetrate the paper backing the adhesive. Cutting through the paper backing can result in dulling of and possible damagie to the blade of the cutter.
9. To avoid wrinkling the membrane and facilitate handling, use an antielectrostatic gun. Avoid letting the membrane rest exposed to air because particulate matter and dust will accumulate and cause imaging problems such as increased background fluorescence.
10. For best success in alignment, present the bottom part top side down.
11. It is generally helpful to keep one side of the adhesive unpeeled. While gently grabbing the edge of the DSA with tweezers, use a piece of tubing positioned in the inlet hole as an alignment aid.
12. Proceed with care because the glass cover slip is very thin and fragile. Apply pressure to efficiently seal it with the DSA layer.
13. Other materials can be used as an optical window. PMMA and COC have similar optical properties, especially absorption. Depending on the strength of the fluorophore used and your optical configuration, it might be desirable to stick to

glass for the top window. However, if sensitivity is not a concern, a thicker window of plastic is also appropriate.

14. Establish a consistent naming scheme that allows later sequential batch image analysis through the creation of macros within the Image J environment.
15. In order to use the macro given in **Note 16**, save the images in different folders for each flow cell, each folder named fc1, fc2, fc3, etc. Within each folder, each image is saved as "CD45_"+j+"-001.tif", where 'j' corresponds to a given field of view.
16. This macro is given as an example of a simple algorithm that allows counting. Refinement might be necessary, depending on staining efficiency and quality of the flow cell and instrumentation used. For automated counting and minimum modifications to the macro provided here, save your images to "C:\\Documents and Settings\username\MMDDYY\" root directory.

```
// analysis of CD45 data
CountsCD45=newArray(1000);
H1=newArray(1000);
Xcoord=newArray(1000);
Ycoord=newArray(1000);
pic=0;
for (i=1;i<4;i++) {
for (j=1;j<6;j++) {
open("C:\\Documents and Settings\\username\\MMDDYY\\fc"
+i+"\\CD45_"+j+"-002.tif"); run("RGB Split");
close();
run("FFT Filter", "filter_large=40 filter_small=3
  suppress=none tolerance=5 autoscale saturate");
//run("Threshold...");
run("Clear Results");
run("Measure");
m=getResult("Mean",0);s=getResult("StdDev",0);
mr=round(m);sr=round(s);twos=mr+sr;
setThreshold(twos, 255);
run("Threshold", "thresholded remaining black");
run("Clear Results");
run("Analyze Particles...", "minimum=40 maxi
mum=500 bins=10 show=Masks display exclude clear");
initcountsg=nResults;totalcountsg=0;
for (n=1;n<nResults+1;n++) {
Circ=getResult("Circ.", n-1);
if (Circ>0.68) totalcountsg=totalcountsg+1;
print (Circ);
}
pic=pic+1;
CountsCD45[pic]=totalcountsg;
close();close();close();
```

```
}
}
for (n=1;n{LT}pic+1;n++) {
totalcount=totalcount+CountsCD45[n]; print (CountsCD45[n]);}
average=totalcount/pic;
print ("Average: "+average);
selectWindow("Log"); run("Text...", "path=' C:\\Documents
and Settings\\username\\MMDDYY\\Quantitative CD45.txt'");
```

Acknowledgments

We wish to acknowledge Glennon Simmons and Andrea Stewart for their help with the fabrication of the microfluidic structures and Dr. Dwight Romanovicz for acquiring scanning electron micrographs of the white blood cells on the membrane. Research described in this chapter was supported by the National Institutes of Health (Saliva grant no. U01-DEO015017-03), the Welch Foundation (F-1193), Philip Morris USA Inc., and Philip Morris International (grant no. UTA02/400, AMD3).

References

1. Houwen, B. (2001) The differential cell count. *Lab. Hematol.* **7,** 89–100.
2. Hoffman, R. A., Maino, V. C., Recktenwald, D. J., and Webster, H. K. (2002) BD Biosciences contributions in CD4 counting and immune status for HIV/AIDS. *Cytometry* **50,** 129–132.
3. Rabellino, E. M., Forman, M. A., Howes, J. C. G., Mills, R. A., Quintana, J. A., Roth, P. A., and Wilkinson, J. G. (2002) Beckman Coulter and CD4+ T cells. *Cytometry* **50,** 127–128.
4. Brown, M., and Wittwer, C. (2000) Flow cytometry: principles and clinical applications in hematology. *Clin. Chem.* **46,** 1221–1229.
5. Cohen, J. (2004) Monitoring treatment: At what cost? *Science* **304,** 1936–1936.
6. Helbert, M. and Breuer, J. (2000) Monitoring patients with HIV disease. *J. Clin. Pathol.* **53(4),** 266–272.
7. Kvale, D., Aukrust, P., Osnes, K., Muller, F., and Froland, S. S. (1999) CD4+ and CD8+ lymphocytes and HIV RNA in HIV infection: high baseline counts and in particular rapid decrease of CD8+ lymphocytes predict AIDS. *AIDS* **13,** 195–201.
8. Laurence, J. (1993) Review: T-cell subsets in health, infectious disease, and idiopathic CD4+ T lymphocytopenia. *Ann. Intern. Med.* **119,** 55–62.
9. Janossy, G., Jani, I. V., Kahan, M., Barnett, D., Mandy, F., and Shapiro, H. (2002) Precise CD4 T-cell counting using red diode laser excitation: For richer, for poorer. *Cytometry* **50,** 78–85.
10. Earley, M. C., Vogt, R. F., Shapiro, H. M., et al. (2002) Report from a workshop on multianalyte microsphere assays. *Cytometry* **50,** 239–242.
11. Ahn, C. H., Choi, J. W., Beaucage, G., et al. (2004) Disposable Smart lab on a chip for point-of-care clinical diagnostics. *Proc. IEEE* **92,** 154–173.

12. Auroux, P. A., Iossifidis, D., Reyes, D. R., and Manz, A. (2002) Micro total analysis systems. 2. Analytical standard operations and applications. *Anal. Chem.* **74,** 2637–2652.
13. Broyles, B. S., Jacobson, S. C., and Ramsey, J. M. (2003) Sample filtration, concentration, and separation integrated on microfluidic devices. *Anal. Chem.* **75,** 2761–2767.
14. de Mello, A. J. and Beard, N. (2003) Dealing with 'real' samples: sample pretreatment in microfluidic systems. *Lab on a Chip* **3,** 11N–19N.
15. Landers, J. P. (2003) Molecular diagnostics on electrophoretic microchips. *Anal. Chem.* **75,** 2919–2927.
16. Liu, J., Hansen, C., and Quake, S. R. (2003) Solving the "world-to-chip" interface problem with a microfluidic matrix. *Anal. Chem.* **75,** 4718–4723.
17. Manz, A., and Eijkel, J. C. T. (2001) Miniaturization and chip technology. What can we expect? *Pure Appl. Chem.* **73,** 1555–1561.
18. Manz, A., Graber, N., and Widmer, H. M. (1990) Miniaturized total chemical-analysis systems—a novel concept for chemical sensing. *Sensors Actuators B-Chem.* **1,** 244–248.
19. McCarley, R. L., Vaidya, B., Wei, S. Y., et al. (2005) Resist-free patterning of surface architectures in polymer-based microanalytical devices. *J. Am. Chem. Soc.* **127,** 842–843.
20. McClain, M. A., Culbertson, C. T., Jacobson, S. C., and Ramsey, J. M. (2001) Flow cytometry of *Escherichia coli* on nucrifluidic devices. *Anal. Chem.* **73,** 5334–5338.
21. McDonald, J. C. and Whitesides, G. M. (2002) Poly(dimethylsiloxane) as a material for fabricating microfluidic devices. *Accounts Chem. Res.* **35,** 491–499.
22. Minc, N. and Viovy, J. L. (2004) Microfluidics and biological applications: the stakes and trends. *Comptes Rendus Physique* **5,** 565–575.
23. Pamme, N., Koyama, R., and Manz, A. (2003) Counting and sizing of particles and particle agglomerates in a microfluidic device using laser light scattering: application to a particle-enhanced immunoassay. *Lab on a Chip* **3,** 187–192.
24. Sia, S. K. and Whitesides, G. M. (2003) Microfluidic devices fabricated in poly(dimethylsiloxane) for biological studies. *Electrophoresis* **24,** 3563–3576.
25. Situma, C., Wang, Y., Hupert, M., Barany, F., McCarley, R. L., and Soper, S. A. (2005) Fabrication of DNA microarrays onto poly(methyl methacrylate) with ultraviolet patterning and microfluidics for the detection of low-abundant point mutations. *Anal. Biochem.* **340,** 123–135.
26. Tudos, A. J., Besselink, G. A. J., and Schasfoort, R. B. M. (2001) Trends in miniaturized total analysis systems for point-of-care testing in clinical chemistry. *Lab on a Chip* **1,** 83–95.
27. Verpoorte, E. (2003) Beads and chips: new recipes for analysis. *Lab on a Chip* **3,** 60N–68N.
28. Verpoorte, E. and De Rooij, N. F. (2003) Microfluidics meets MEMS. *Proc. IEEE* **91,** 930–953.
29. Vilkner, T., Janasek, D., and Manz, A. (2004) Micro total analysis systems. Recent developments. *Anal. Chem.* **76,** 3373–3385.

30. Rodriguez, W. R., Christodoulides, N., Floriano, P. N., et al. (2005) A microchip CD4 counting method for HIV monitoring in resource-poor settings. *Plos Med*. **2,** 663–672.
31. Rasband, W. S. (2006) Image, U.S., National Institutes of Health, Bethesda, MD, U.S.A., http://rsb.info.mih.gov/ij/,1997–2006.
32. Piruska, A., Nikcevic, I., Lee, S. H., et al. (2005) The autofluorescence of plastic materials and chips measured under laser irradiation. *Lab on a Chip* **5,** 1348–1354.

6

Microchips for the Diagnosis of Cervical Cancer

Anja Gulliksen and Frank Karlsen

Summary

Cancer affects more people than any other disease. About one-third of the world's population is likely to get this diagnosis during their lifetime. Currently, the diagnostic methods for cancer detection are based on visual inspection. The lack of high analytical and clinical specificity and sensitivity makes these methods in many cases inferior to recently developed molecular methods. The increased clinical specificity and sensitivity of these new molecular approaches have great benefits, such as the possibility of implementing the molecular methods in miniaturized systems and enabling easier and faster point-of-care or bedside diagnostics. This chapter provides an introduction to performing clinical trials, screening, and molecular diagnostics against cancer-related markers. In addition, an example of molecular diagnosis of cervical cancer within a microsystem concept will be presented.

Key Words: Cancer; human papilloma virus; nucleic acid sequence-based amplification; molecular diagnostics; mRNA; point-of-care microsystems.

1. Introduction

1.1. Cancer

Every year more than 11 million people are diagnosed with cancer. By the year 2020, it is estimated that there will be 16 million new cases every year. Cancer causes 7 million deaths every year–or 12.5% of the deaths worldwide ***(1)***. Cancer is defined as uncontrolled growth and spread of cells. These cells can invade nearby tissues and are able to spread through the bloodstream and lymphatic system to other parts of the body. Cancer cells that spread to other organs are similar to those of the original tumor; therefore, these secondary (metastatic) cancers are named for their primary site although they may have invaded a different organ. Lung, colorectal, and stomach cancer are among the

From: *Methods in Molecular Biology, Vol. 385: Microchip-Based Assay Systems: Methods and Applications*
Edited by: Pierre N. Floriano © Humana Press Inc., Totowa, NJ

five most common cancers in the world for both men and women. For men, lung and stomach cancer are the most common cancers, whereas among women breast and cervical cancers are most common worldwide.

There are several main types of cancer:

- Carcinoma derives from epithelial tissue, skin, or in tissues that line or cover internal organs. This is the most common type of cancer.
- Sarcoma originates in bone, cartilage, fat, muscle, blood vessels, or other connective or supportive tissues.
- Leukemia starts in blood-forming tissue such as the bone marrow and causes large numbers of abnormal blood cells to be produced and enter the bloodstream.
- Lymphoma and multiple myeloma begin in the cells of the immune system.

1.1.1. The Causes of Cancer

Factors influencing a person's biological susceptibility to cancer include age, sex, immune status, nutritional status, genetics, and ethnicity. Today we have enough knowledge about the causes of cancer to prevent at least one-third of all cancers. Proven risk factors contributing to the development of cancer are tobacco, alcohol consumption, occupational exposures, environmental pollution, food contaminants, medicinal drugs, radiation, diet and nutrition, chronic infections, immunosuppression, genetic susceptibility, reproductive factors, and hormones.

In addition, infectious agents such as viruses, bacteria, and parasites are responsible for almost 22% of cancer deaths in the developing world and 6% in industrialized countries ***(1)***. Examples of infectious agents that contribute to the development of cancer are, among others, viral hepatitis B and C (liver) ***(2,3)***, human papilloma virus (HPV; cervix) ***(4–9)***, and the bacterium *Helicobacter pylori* (stomach) ***(10,11)***. Preventive measures include vaccination and prevention of infection and infestation.

1.1.2. Mechanisms of Tumor Development

Cancer may evolve from mutations, which include additions, deletions, substitutions, and rearrangements of certain genes or chromosomes that allow the cells to begin uncontrolled growth. Other factors contributing to instability and uncontrolled growth of the cells may be caused by changes in, for example, the immune defense system, loss or modification of transcription/translation regulation mechanisms, or changes in the different RNA substrates. The development of cancerous cells from healthy cells is called transformation. The factors influencing a person's susceptibility to develop cancer can be either inherited or acquired. Acquired changes may happen spontaneously, or they may be caused by repeated exposure to carcinogens such as different chemicals, viruses, or ultraviolet rays. In most cases the changes cause no permanent

damage to the cells because of the cells' own repair mechanisms. However, repeated carcinogenic exposure may eventually result in mutations or altered gene expression in key genes called oncogenes and tumor-suppressor genes. Thus, normally there is a latency period of years or decades between exposure to a carcinogen and the appearance of cancer.

The oncogenes produce growth factors that signal a cell to grow and divide into daughter cells. Normal cells have a limited life span, which is controlled by the telomere gene. As a result, normal tissue is growth limited, and therefore cell reproduction is equal to cell death. Feedback controls limit cell divisions after a certain number of cells have developed, allowing for tissue repair but not expansion. However, cancer cells contain telomerase, an enzyme that maintains telomere length and allows the cell to continue to divide without any feedback regulation. Tumor-suppressor genes, on the other hand, produce negative growth factors, which tell a cell when to stop dividing. If either the abnormally inactivated tumor-suppressor gene or the abnormally activated oncogene is inherited by any of the original cell's daughter cells in the cell division, a tumor develops.

Tumors may be benign or malignant. Benign tumors remain localized as a discrete mass. They may differ significantly from normal tissue in structure and excessive growth of cells, but are rarely fatal. However, even benign tumors may grow large enough to interfere with normal function. Benign tumors are usually treated by complete surgical removal. Cells of malignant tumors are what are referred to as a cancerous state. The tumors consist of undifferentiated or unspecialized cells that show an atypical cell structure and do not function like the normal cells from the organ from which they derive. Unlike normal cells, cancer cells lack inhibition mechanisms. Consequently, the malignant cells are invasive, which means that they can infiltrate the surrounding normal tissue. In addition, the malignant cells can metastasize, that is, spread via blood and the lymph system to other tissues and organs.

Cancer tissue, growing without limits, competes with normal tissue for nutrients and oxygen, eventually killing normal cells by nutritional deprivation. Cancerous tissue can also cause secondary effects, in which the expanding malignant growth puts pressure on surrounding tissue or organs.

1.2. Diagnosis of Cancer

Diagnosis is the determination of the nature of a disease or ailment. The pathologists' studies of cause of disease are based on modifications in cellular function and changes in cellular structure produced in any cell, organ, or part of the body caused by disease. Clinical diagnoses are built on the medical history and physical examination of the patient. In diagnostic tests, the blood, urine, tissues, smears, and other excretions and secretions of the body are

examined for evidence of chemical imbalance, cellular change, and the presence of pathogenic organisms.

Recognizing possible warning signs of cancer and taking prompt action lead to early diagnosis, which provides better odds for saving human lives. The major component of early detection of cancer is knowledge in order to promote analyses for early diagnosis and screening. Screening refers to the use of simple tests across a healthy population in order to identify individuals who have disease, which in most cases do not yet have symptoms. Examples of screening programs target breast cancer using mammography and cervical cancer using cytology screening methods. Importantly, the earlier and more precise the diagnosis, the better the prognosis will be.

Cancers that are caught and treated before they metastasize have better cure rates. However, the majority of cancer patients are in an advanced stage of cancer development when the disease is discovered. In these cases, the only realistic treatment option is pain relief and palliative care. Currently, cancer is mainly treated by surgery, chemotherapy, radiation therapy, hormonal therapy, and immunotherapy. Thus, new drugs and techniques are constantly being researched and developed.

1.2.1. Conventional Diagnosis

Normally, tumors are localized and identified by using magnetic resonance imaging (MRI), computed tomography (CT), X-ray, ultrasound, or bone scans. The microscope is the main instrument for detecting tissue changes, especially in the examination of small sections of tissue (biopsies) removed for diagnosis. However, this is a highly subjective interpretation where the results are entirely dependent on the individual interpreter and on the quality of the sample collection and preparation. Cancerous cells are usually identified by having an enlarged nucleus, abnormal cell morphology, irregular concentration of cells in the tissue, rearrangements, and loss of chromosomes. However, clinicians have different practices in the management of patients, which may result in different diagnostic interpretations. A system has been devised to classify malignant tissue according to the degree of malignancy, from grade 1, barely malignant, to grade 4, highly malignant. In practice, it is not always possible to determine the degree of malignancy, and it may be difficult even to determine whether a particular tumor tissue is benign or malignant.

These visualizing techniques have poor reproducibility with a consequent trade-off between diagnostic sensitivity and specificity. Therefore, in recent years these methods have often come under attack because of a growing awareness of their imperfections, including irreproducibility and frequent occurrence of false-negative results. Consequently, it is argued that there is a

great need for more objective and cost-effective screening methods with improved accuracy.

1.2.2. Molecular Diagnosis

Little doubt remains that cancer is connected to changes in the construction of the genetic elements. Many scientists believe that accumulation of a certain number of mutations and alterations of genetic elements is how the cell achieves a malignant phenotype. However, abnormal amounts of mRNA, modified splicing events, or stabilized pre-mRNA that is not directly related to mutation may also have a very important role. An estimated 5–15% of all cancers are hereditary ***(12,13)***. In these cases, mutations are present in every single cell in the body, thereby resulting in occurrences of cancer in the family. In the case of acquired cancer, the defect is present only in a single peripheral cell and the genetic defect is only passed on to the descendants of this specific cell. Molecular diagnosis of inherited disease will make it possible to study inherited mutations and identify the ones that are relevant for causing cancer. It has been shown that in most cases the same genes underlying the inherited syndromes are also involved in the sporadic cases of the same cancer type. Acquired cancer disease has been much more difficult to study and to make diagnostics methods for, and this area in particular has been opened because of the new findings in the field of proteomics and RNomics.

Because of the genetic complexity of cancer, it is normally insufficient to analyze a single sequence. Cancer development is often manifested by a multitude of genetic changes. Therefore, the advances in bioinformatics and high-throughput technologies such as microarray analysis ***(14)*** are bringing about a revolution in our understanding of the molecular mechanisms underlying normal and dysfunctional biological processes. This opens possibilities for the design of analytical tools to identify the disease state and disease susceptibility. Gene expression profiling has enabled the measurement of thousands of genes, both cellular and viral, in a single RNA sample. This technology also stimulates the discovery of new targets for the treatment of disease, which is aiding drug development, immunotherapeutics, and gene therapy. However, today this technology is mostly used as a research tool.

The essential molecular techniques used by leading clinicians and expert researchers for diagnosing and monitoring tumors currently are polymerase chain reaction (PCR) ***(15)*** and other nucleic acid amplification methods, fluorescent *in situ* hybridization (FISH) and other *in situ* hybridizations techniques, comparative genomic hybridization (CGH) ***(16)***, Southern analysis ***(17)***, sequencing ***(18)***, fingerprinting ***(19)***, and single-strand conformation polymorphism (SSCP) ***(20)***. However, other molecular methods may play a more important role in cancer diagnostics based on our knowledge and experi-

ence in the field of functional genomics, RNomics, and proteomics. These new technologies are gaining acceptance in modern laboratories and could become the future technology for cancer diagnostics ***(21)***.

1.2.3. mRNA vs DNA or Protein as Target for Routine Diagnostics

DNA is a passive target that contains the coding sequence for RNA and protein molecules, which are actually performing the work in a biological system. RNA has the same coding sequence as DNA, but is either directly or indirectly involved in the processes in the machinery of a cell. RNA is not only the basis for translation to proteins; in addition, different RNA (e.g., siRNA, RNAi, tRNA, rRNA) molecules form three-dimensional structures that are directly involved in the regulation or activation of the biological processes in the cell. In contrast to DNA, mRNA gives important clinical information about the different activities of the genes regulating the cells, bacteria, and viruses. The main challenge using protein as a target for routine diagnostics has been low sensitivity, reproducibility, and specificity. The main challenge using DNA as a target for routine diagnostics has been the lack of information about biological or clinical activity.

During recent decades, microarray technology and varied amplification methods have shown that mRNA is valid as a target for routine molecular diagnostics and for future point-of-care (POC) testing ***(22,38)***. Using mRNA as a target for routine diagnostics may give information about clinical activity, regulation, or processes in addition to higher or equal sensitivity, reproducibility, and specificity to DNA. DNA-detection methods have been criticized because of their lack of clinical specificity and positive predictive value (PPV). Many types of DNA lesions such as mutation, rearrangements, instability, and ploidy have been discovered. However, the main challenge in most precancer lesions is the complexity of the cells with abnormalities. Multiplex routine diagnostics of the molecular changes involved in the combination of different multiple DNA lesions has been very difficult because of the high number of variables involved.

There are several methods for amplification and detection of different DNA and mRNA molecules: reverse transcriptase polymerase chain reaction (RT-PCR) and other variants of PCR, ligase chain reaction (LCR) ***(23)***, strand displacement amplification (SDA) ***(24–26)***, nucleic acid sequence-based amplification (NASBA) ***(27–29)***, transcription-mediated amplification (TMA) ***(30)***, branched DNA (bDNA) ***(31,32)***, hybrid capture II (HCII) ***(33)*** and rolling circle amplification (RCA) ***(34,35)***. The most commonly used method is RT-PCR. However, the main disadvantage of RT-PCR for amplification of mRNA is the possible contamination of sample DNA and accordingly the challenge of finding specific primer sets and probes. Quantification of mRNA has been difficult because of the widely used semi-quantitative methods (mostly RT-

PCR) including calibrators that are not similar to the whole coding mRNA sequence area.

1.3. NASBA

NASBA is a transcription-based method that can amplify any single-stranded RNA sequence isothermally (41°C) by the simultaneous use of the activities of three enzymes: avian myeloblastosis virus reverse transcriptase (AMV-RT), RNase H, and T7 RNA polymerase. A schematic diagram of the NASBA reaction is shown in **Fig. 1**. NASBA can yield 10^9 RNA amplicons in about 2 h even with a background of genomic DNA ***(27)***. Target sensitivity and specificity are dependent on the hybridization kinetics of the primers and molecular beacon probes, three-dimensional polymer structures surrounding the target, and target sample quality ***(29,36)***. Primer 1 contains a 3'-terminal sequence that is target specific and a 5'-terminal T7 promoter sequence that can be recognized by T7 RNA polymerase. Primer 2 may be entirely a target specific sequence. The molecular beacon probe has a DNA stem-and-loop structure with a covalently linked FAM fluorophore at the 5'-terminal end and a dabsyl quencher on the 3'-terminal end. The probe will only fluoresce when the target specific sequence in the loop structure of the molecular beacon hybridizes to the target.

NASBA enables detection of RNA molecules down to 10–100 copies. To avoid contamination, it is necessary to perform the amplification and detection in separate areas of individual liquid plugs.

1.4. Miniaturized Systems for Detection of Cancer

Today almost all clinical samples of tissue, blood, etc. taken from patients at the local doctor's office are sent to remote labs for diagnosis. This is costly and takes time, it increases patient anxiety, and it delays the start of treatment. Ideally, these diagnoses should be carried out directly at the local doctor's office using fully automatic and accurate microfluidic Lab-on-a-Chip (LOC) systems. Clinical molecular diagnostics is predicted to be one of the most promising applications for miniaturized systems, in particular related to POC testing ***(37,38)***. In most cases the most important benefits of miniaturization are smaller sample requirement, hands-free operations, reduced reagent consumption, decreased analysis time, and higher levels of throughput and automation.

A diagnostic microsystem for detection of cancer requires extensive verification and validation, which will include cohort studies, normal population studies and follow-up, and prognostic studies. The verification studies must include analysis of robustness, reproducibility, stability, performance, analytical sensitivity, and specificity, whereas validation studies have to be performed by an independent group comparing the system against the best available diagnostic system in representative clinical samples.

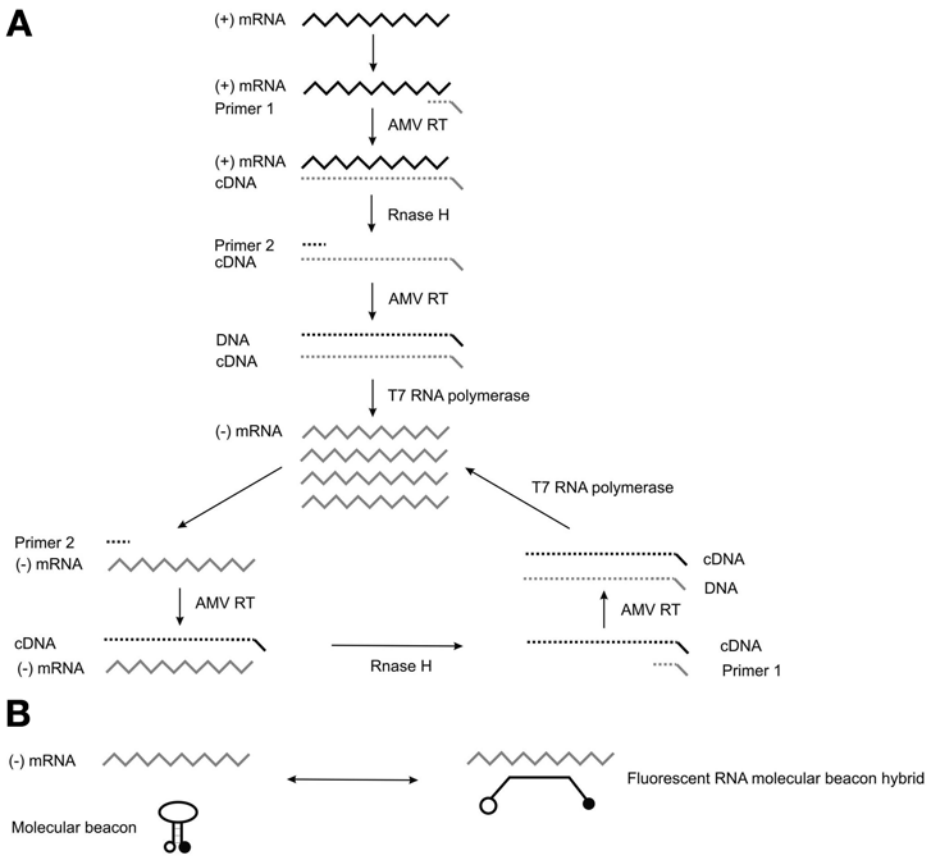

Fig. 1. **(A)** Schematic diagram of the principle of nucleic acid sequence-based amplification. Primer 1 anneals to the target RNA and is followed by an elongation of the primer with avian myeloblastosis virus reverse transcriptase (AMV-RT). A RNA:cDNA hybrid is then formed. The RNase H degrades the RNA of the hybrid, which allows annealing of primer 2 to the cDNA. Primer 2 is extended by AMV-RT to form a double-stranded DNA with a functional T7 promoter. T7 RNA polymerase recognizes the T7 promoter sequence and may generate between 100 and 1000 antisense RNA molecules from the double-stranded DNA sequence. The new antisense RNA molecules are in turn templates for the synthesis of double-stranded hybrid DNA molecules, except this time the amplification process starts with primer 2. **(B)** The amplification reaction is possible to monitor in real time because of the fluorescent light produced by the molecular beacon probes when they hybridize to the amplified antisense RNA. When monitoring a positive NASBA reaction in real time, a sigmoid curve is obtained. At the point of exponential increase in mRNA, the amplification reaction enters the cyclic phase, where the molecular beacon probes starts to hybridize to the copies of antisense RNA formed in the amplification process. A negative NASBA reaction will give rise to a straight horizontal line on a constant fluorescence level.

As already stated, the methods for diagnosing cancer are many. Cancer detection covers several different aspects, which include sample collection, concentration and preparation, collection of representative tissue, definition of disease, identification of the cause of cancer, identification of precancer markers, identification of the risk of developing cancer, detection of prognostic markers, primary or secondary screening, and detection of markers important before and after treatment.

Joi et al. ***(40)*** and Robison et al. ***(41)*** have recently highlighted the importance of using microarray technology in clinical studies before any real-life application may be discovered. Microarray technology and sequencing of the human genome has provided comprehensive molecular and genetic profiling of cancers. It has been confirmed that cancers are considerably more heterogeneous than can be predicted by traditional histopathological methods. Gene expression signatures for tumors have been classified and correlated to important clinical parameters, which also may revolutionize cancer medicine. Certainly, the greatest improvements in patient care will come through tailored therapies as genomics is coupled with clinical trials that randomize cohorts to different treatments. A major challenge is to make the technology available for routine, bedside, or POC diagnostics. The challenges lie in refining the use of the technology, proper validation of discoveries, and the large-scale collaborative efforts necessary for the incorporation of genomic and functional genomics knowledge into the design and conduct of clinical trials. In order to implement these assays on a large scale, there will need to be standardization of sample procurement, preparation, and analysis. In the end this will lead, ultimately, to user-friendly applications and tools for everyday patient care.

Many companies are involved in the development of microarray technology, including Affymax, Affymetrix, Agilent, Amersham, ArrayFox, Axon Instruments, Biodot, Bioneer, Cartesian, Corning, GeneMachine, Genespotter, GeneSpring, Genetix, Genometrix, GeSim, HT-Array, ImaGene, Incyte, Majer Precision, Microfab, Nanogen, Perkin Elmer, Robodesign, synQUAD Products, Telechem, TIGR, and Vysis. The companies provide all kinds of solutions for evaluation of gene expression. The different arrays make it possible to analyze transcription signatures from tens of thousand of genes of different species. The new data have disclosed many of the molecular mechanisms for gene expression. However, the method cannot reveal the complete complexity of transcription, splicing of transcripts, translation, abnormal splicing processes ***(42)***, transcriptional regulation, the difference of natural transcription in clinical samples and artificial cell lines, raft cultures, or animal models. Microarray technology may therefore still miss important markers for detection of precancerous stages or even the cancer disease itself. Examples of this could be long

or abnormal pre-mRNA or siRNA, which in one way or another may be directly involved in the carcinogenic process. One of the main problems with microarray analysis is the lack of single target analytical sensitivity. Even the use of preamplified material gives problems related to analytical sensitivity in real clinical samples, in particular, large numbers of clinical samples with limited amounts of material or representative material. Another problem with microarray technology is that very few standards, mainly generated by the RT-PCR-related companies, are used for quantification purposes. These standards may create a systematic wrong level of expression from many genes. Another challenge for microarray technology is the inability to analyze the complete sequence of long mRNA strands.

There are already more than 9000 publications describing or using microarray technology. About 2800 studies have been performed with the goal of evaluating the usefulness of microarrays in order to assess carcinogenesis and to discover cancer treatment and diagnostics options. However, very few have been able to demonstrate usefulness of the selected hotspots in early cancer routine diagnostics. Indeed, the microarray technology has opened many new doors in oncology, but there is still a need to evaluate the new findings in large population studies, cohort studies, head-to-head analysis, and prognostic and retrospective studies.

Several companies and academic research institutes are involved in microsystem technologies, which are focusing on microfluidics, biotechnology and health-based microsystems, bioMEMS, and LOC technologies. The main challenges for these companies and institutes are to deliver systems dedicated for more than research. POC, bedside, hands-free devices, system for the whole process of diagnostics, same-time diagnostics, hands-free collection, or sample preparation devices are examples of systems that are very important for future health services. An important demand for such diagnostics systems is to give high enough clinical sensitivity, specificity, odds ratio (OR), relative risk (RR), positive predicative value (PPV), and negative predicative value (NPV). The clinical specificity and PPV has to be compared with gold standards giving specificity higher than 70–80% and PPV higher than 30%. For biomarkers to be selected there must be an optimal correlation between the prevalence of the disease and the prevalence of the test. Today there are no examples of fully automatic operative working miniaturized systems that handle diagnoses of cancers or precancer disease. No microsystem has been developed so far for large-scale clinical trials.

Leading cancer researchers worldwide have contributed to a discussion about standardization of methods for cancer detection. An extract of how this should proceed further can be found at the National Cancer Institute website ***(39)***.

1.5. Fluorescent Detection of mRNA in Microchips for Diagnosis of Cervical Cancer

Our goal is to develop a miniaturized total analysis system (μTAS) for POC diagnostics. The sample will be injected into the system, and in the end a result will be revealed after the analysis is finished. Detection of multiple target molecules from one sample is a requirement and a necessity because many diseases may depend on several different factors. Hotspot sequences for different cancers markers, identified by microarray technology, would be ideal in this kind of a microsystem concept, which is intended for routine and POC diagnostics. The diagnostic test is aimed to be low in cost and time saving as a result of the combination of reduced consumption of reagents, fully automatic analysis, and disposable mass-produced polymer chips. Two separate microchip modules will constitute the final device. The first module handles the sample preparation, while the second amplifies and detect nucleic acids.

Cervical cancer is the second most common cancer among women worldwide *(6)*. Several studies have demonstrated that the presence of HPV is a prerequisite for the development of cervical cancer *(6,7)*. The activity of this virus has the potential to start the production of harmful proteins, which might stimulate growth of cervical cells leading to lack of cell cycle control.

Cervical cancer is mainly diagnosed by cytology, a method with poor reproducibility and specificity and limited sensitivity *(43)*. Thus, first-time cytology has a false-positive rate of between 50 and 75%. A molecular-based diagnostic LOC system, placed at the local doctor's office, would quickly identify multiple high-risk HPV mRNA transcripts of all women with persistent transforming infection with higher accuracy and reproducibility in comparison with conventional cytology *(8,9,44)*.

This chapter describes an approach to detect cancer markers by means of nucleic acid sequence-based amplification (NASBA) *(27–29)* in disposable polymer microchips. NASBA was chosen because of its high level of sensitivity and specificity. mRNA obtained from SiHa cell line samples (incorporates human papilloma virus, HPV, type 16) is used as a model system for detection of cervical cancer marker in the microchip-based assay.

The practical use of this model system is demonstrated by the detection of full-length abnormal mRNA coding for the E6 protein of the high-risk HPV type 16, one of the most important factors associated with the risk of development of cervical cancer *(7)*.

2. Materials

2.1. Sample Preparation Chip

Efficient sample pretreatment is one of the paramount tasks in the context of microsystems. Above all, reliable high-quality concentration devices are

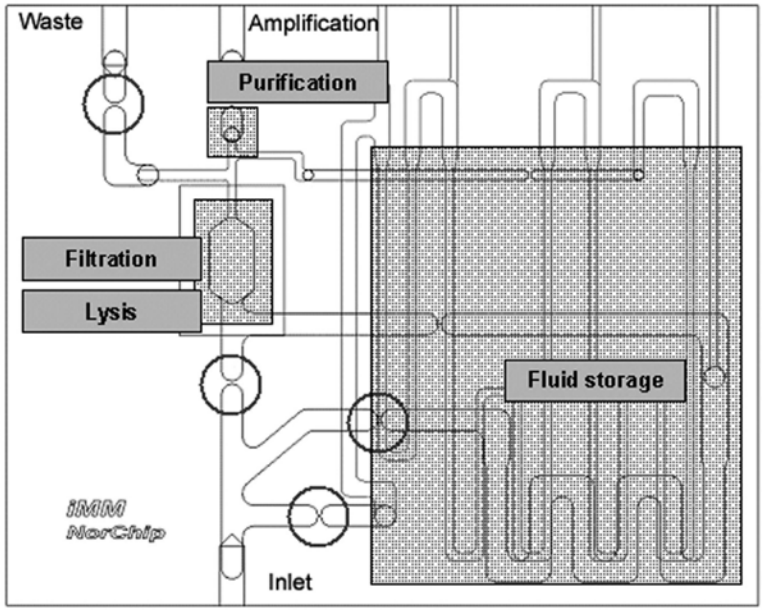

Fig. 2. The sample preparation chip is made with the intention of being disposable; hence it is fabricated in cyclic olefin copolymer. The chip contains all reagents needed for nucleic acid extraction and isolation. The elution for the chip is 100 µL. Integrated valves (circles) and pressure-driven flow (syringes) distribute the reagents within the chip throughout the procedure.

needed in order to enable detection of low numbers of specific cells, bacteria or viruses, present in biological samples. The quality of the assay is very dependent on how the sample material is handled and processed before the analysis takes place. It is important that the targets of interest are not destroyed in any way before performing the analyses. In most cases the sample preparation step is the most difficult part of the procedure, and the end result will strongly depend on the quality of this step alone (*see* **Note 1**).

The sample preparation chip (**Fig. 2**) for isolation of nucleic acids from epithelial cells has been designed to follow the procedures of Boom et al. ***(45–47)***. The key steps for the method are as follow:

1. Lysing the cells with lysing buffer containing guanidinium thiocyanate (GuSCN).
2. High GuSCN concentration causes the nucleic acids to adsorb to silica beads.
3. A washing buffer containing GuSCN is used to remove impurities.
4. Additional washing steps with ethanol and acetone removes proteins, lipids, and impurities from the silica beads.

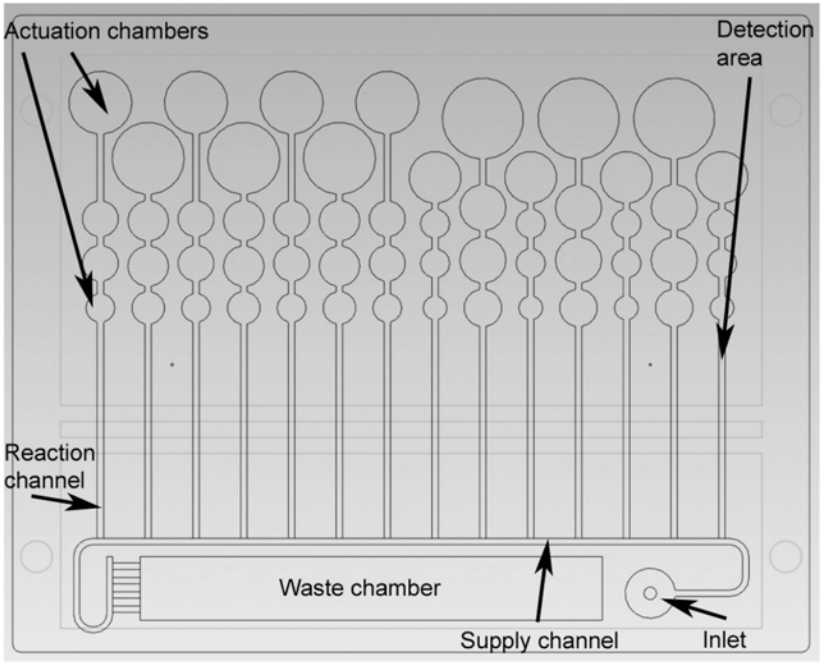

Fig. 3. Sketch of the amplification and detection chip. The chip is half the size of a credit card.

5. A drying step at 56°C is included to remove all acetone that can affect the end result.
6. An elution buffer is used to elute the nucleic acids from the silica beads.

2.2. Amplification and Detection Chip

The amplification chip is fabricated using cyclic olefin copolymer (COC) because of favorable optical and chemical properties of this polymer. The chip has an incorporated inlet hole for the nucleic acid sample, a supply channel, reaction channels, actuation, and waste chambers (*see* **Fig. 3**; and **Notes 2** and **3**).

Each reaction channel has a detection area corresponding to a volume of 80 nL ($400 \times 2000 \times 100$ μm^3). The parallel reaction channels are designed with the purpose to detect several targets simultaneously on one sample, which in many diagnostic relations are necessary. As in the case of cervical cancer, there are five main types of high-risk HPV (16, 18, 31, 33, and 45), which constitute 97% of all cervical carcinomas in Europe and North America ***(8,50)***. To be able to make a complete diagnosis for cervical cancer, it will therefore be necessary to look for several different targets.

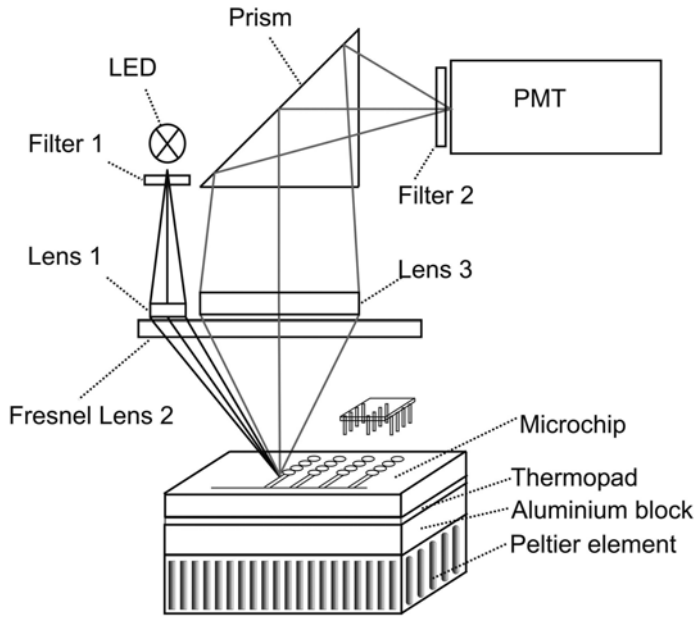

Fig. 4. Instrument setup. LED, light-emitting diode; PMT, photomultiplier tube.

In the fabrication of the amplification and detection chip, several steps are required:

1. Washing the injection-molded polymer chip with isopropanol to remove inhibiting agents.
2. Coating the network of channels with polyethylene glycol (PEG).
3. Depositing the reagents in the reaction channels.
4. Mounting a filter in the waste chamber.
5. Sealing the chip with a COC membrane.

2.3. Instrumentation

To control the function of the chip, an instrument with both an optical detection system and a heat-regulation module is required. The instrumental setup is illustrated in **Fig. 4**.

1. Light-emitting diodes (LED) (Lumileds, San Jose, CA), with 130 mW centered at 470 nm.
2. Bandpass filters (Chroma Technologies Corp, Brattleboro, VT), 465–500 nm and 500–545 nm.
3. Lenses (Melles Griot, Santa Clara, CA), ∅12.5 mm/f30 mm and ∅25 mm/f100 mm.
4. Fresnel lens (Melles Griot), ∅50 mm/f25 mm.

5. Prism (Melles Griot).
6. Photomultiplier tube (PMT) (Hamamatsu, Shizuoka, Japan).
7. Data is collected and processed using MATLAB (The MathWorks Inc., Natick, MA).
8. Peltier elements (Marlow Industries Inc., Dallas, TX) with aluminum blocks mounted on top formed the chip holder.
9. Thermal pad (Chomerics, Marlow, UK) is placed on the blocks for thermal contact to the chip.
10. A thermocouple is integrated into the chip holder, with feedback to the Peltier elements.
11. Two servomotors (Omron Electronics, Kyoto, Japan) are regulated by a physical signaling sublayer (PLS) (Saia-Burgess Electronics AG, Murten, Switzerland), which is programmed with PG 5 (Saia-Burgess Electronics AG, Murten, Switzerland).

2.4. Reagents for the Sample Preparation Chip

1. Lysis buffer/Washing buffer (bioMérieux, Boxtel, The Netherlands): 5.25 *M* GuSCN, 50 m*M* Tris-HCl (pH 6.4). Store at room temperature.
2. Size-fractioned (1–5 µm) silica particles (bioMérieux) suspended in lysis buffer (32% w/v). Store at room temperature.
3. Elution buffer contained 10 m*M* Tris-HCl and 1 m*M* ethylene diamine tetraacetic acid (EDTA) with pH 8.0 (bioMérieux). Store at room temperature.
4. 70% Ethanol (bioMérieux). Store at room temperature.
5. Acetone (bioMérieux). Store at room temperature.

2.5. Reagents for the Amplification and Detection Chip

The PreTect™ HPV–Proofer kit (NorChip AS, Klokkarstua, Norway) contains all the reagents needed to perform the NASBA reaction. Store at –20°C. Bring all reagents to room temperature before use. This is the final concentration of reagents in the reaction mixture ***(53)***. The reagents will be deposited directly on chip in the reaction channels:

1. 40 m*M* Tris-HCl, pH 8.5.
2. 70 m*M* KCl.
3. 12 m*M* $MgCl_2$.
4. 5 m*M* Dithiothreitol.
5. 1 m*M* dNTP, 2 m*M* rATP, 2 m*M* rCTP, 2 m*M* rUTP, 1.5 m*M* rGTP, 0.5 m*M* ITP.
6. 0.2 µ*M* Primers, PreTect™ HPV–Proofer kit (NorChip AS).
7. 0.4 µ*M* Molecular beacon probe, PreTect™ HPV–Proofer kit (NorChip AS).
8. 375 m*M* Sorbitol.
9. 0.105 g/L Bovine serum albumin.
10. 15% (v/v) Dimethylsulfoxide.
11. 6.4 U AMV-RT.
12. 32 U T7 RNA polymerase.
13. 0.08 U RNase H (*E. coli*).

3. Methods

3.1. Microchip-Based Preparation of Sample

1. The sample, in this case a cell suspension of cervical epithelial cells, is to be applied to the chip through the inlet hole.
2. A filter with defined pore size collects the cells.
3. Excess liquid is passed on to a waste chamber.
4. The lysis buffer stored on the chip is flushed over the filter to destroy the membranes of the cells with the resulting release of the nucleic acids.
5. The cell material released is transported to a bed of silica beads, where the nucleic acids absorb to the solid surface (*see* **Note 4**).
6. The silica particles are washed repeatedly in a chaotrophic washing buffer, and proteins such as RNase and DNase are denatured by the chaotropic agent ***(48,49)***.
7. Ethanol and acetone are flushed over the beads to remove impurities from the silica beads and to remove all biological material such as lipids, carbohydrates, and proteins (*see* **Note 5**).
8. The washing steps are followed by a drying step.
9. Finally, the nucleic acids are eluted in RNase-, DNase-, and protease-free elution buffer (*see* **Note 6**).
10. A processed sample may then be transferred directly from the sample preparation chip to the next chip module, where the amplification of the high-risk HPV transcripts will be identified.

3.2. Amplification and Detection Chip

1. The microchip is placed into the instrument and placed on top of the heat-regulating Peltier element. An aluminum block distributes the temperature evenly over the whole chip. A thermocouple is integrated into the chip holder, with feedback to the Peltier elements. The overall temperature accuracy of the system is within ±1°C.
2. Four pin rows are pushed down automatically by the instrument into the actuation chambers at the back of the microchip to enable microfluidic actuation.
3. When the nucleic acid sample is applied to the inlet hole of the chip, capillary forces cause the supply channel to fill completely.
4. The sample is distributed and metered into the parallel reaction channels by automatically releasing the first pin row, which pressed down the membranes in the first actuation chamber at the back of each reaction channel (**Fig. 3**) (*see* **Note 7**).
5. After the metering of the liquid plugs into the reaction channels, the supply channel is drained of sample.
6. Releasing the next three pin rows makes the sample plugs move along the channel on the way to the detection area. Deposited reagents containing different markers in the parallel reaction channels will make it possible to detect several target molecules simultaneously. The amplification of mRNA is performed at the detection area.

3.3. Protocol for Data Acquisition

1. The excitation light (494 nm) from the light-emitting diode (LED) excites the fluorophores of the amplification reaction in the 2×2 mm^2 detection area, corresponding to a detection volume of 80 nL (*see* **Fig. 3**).
2. The fluorescent light (525 nm) is collected, focused, and filtered before it reaches the detector, a photomultiplier tube (PMT).
3. The fluorescence in each channel is measured for 1 s on each scanning cycle, using a digital lock-in system operating at 1 kHz.
4. Data are sampled at a frequency of 100 kHz with a 12-bit AD converter.
5. Sequential measurements of the reaction chambers are performed by moving the chip underneath the optical unit using a servomotor in the instrument.
6. A complete chip cycle lasts for 90 s.
7. Data are collected and processed using MATLAB ***(52)***.
8. The experimental data are then handled by PreTect Data Analyzer (NorChip AS), which utilize polynomial regression algorithms. A user-friendly interface for interpretation of the results is revealed on a laptop connected to the instrument. A positive amplification reaction shows a sigmoid curve, while a negative sample has no change in the fluorescent level and gives a horizontal straight line. **Figure 5** shows a typical NASBA result. The figure depicts clearly the different results obtained on a SiHa cell line with integrated HPV 16 and a negative control of DNase and RNase free water. In both cases all 10 reaction channels on the microchips are of the same quality. The detection limit of the optical detection system has been found to be comparable with conventional systems for the same application, although the detection volume is 250 times smaller ***(52)***. An integration of the amplification and detection microchip, with the sample preparation microchip, would therefore constitute a fully automatic, laboratory-independent diagnostic system, resulting in an overall reduction in time and cost for the whole analysis.

4. Notes

1. A problem that can easily be identified for these kinds of devices is clogging of the system in critical steps such as the filtration. Cells may absorb to the channel walls or pass through the filters because of the flexible cell membranes.
2. In the case of the amplification chip, it is critical that all components are RNase and DNase free. RNases and DNases will degradate the target and also inhibit the amplification reaction.
3. In addition, the internal walls of the system have to be coated because of the polymers' hydrophobic surface. PEG gives a hydrophilic surface, which will prevent the enzymes to absorb to the surface of the system. BSA is added as a dynamic coating to prevent the amplification enzymes to be adsorbed on the microchip channel walls because of the increased surface-to-volume ratio in comparison with conventional tubes. In addition, serum albumin is known as a scavenger of PCR inhibitors ***(51)***.

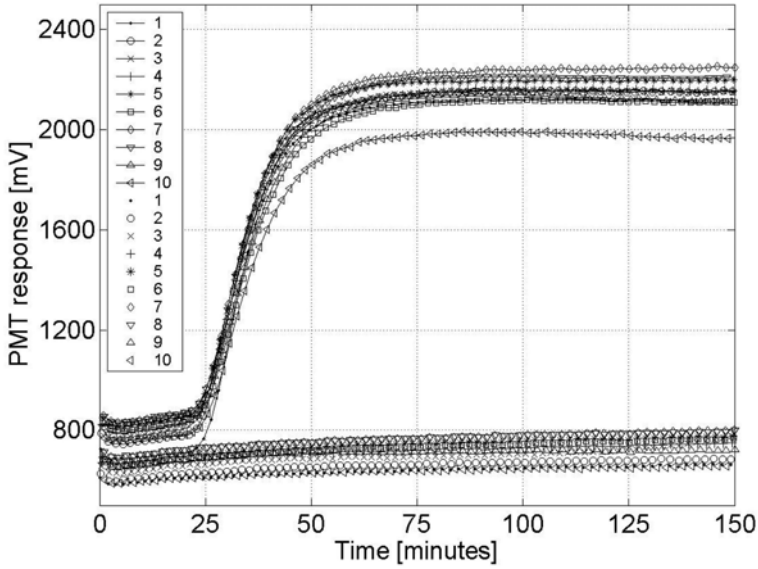

Fig. 5. Detection of SiHa cells (2000 cells/μL) on a microchip. Solid lines characterize positive amplification reactions, while no lines represent negative controls. The key numbers indicate the reaction channels on the microchip from left to right. PMT, photomultiplier tube.

4. The lysis buffer contains the chaotropic agent GuSCN, which at high concentrations causes the nucleic acids to bind to silicon dioxide particles, the size of which control the efficiency of the nucleic acid extraction from the sample.
5. Guanidine ions may disturb the amplification reaction and have to be washed away properly. Ethanol removes proteins and lipids that may have bound unspecifically to the silica particles ***(46)***. Acetone removes any other remaining impurities from the silica.
6. RNase inhibitors (e.g., RNAsin or vanadyl–ribonucleoside complexes) may be added. However, the presence of these inhibitors in the elution buffer is not strictly necessary in order to preserve the native RNA.
7. The liquid plugs are metered and moved along the channels because of the additional volume revealed by the deflected membranes. The volume expansion will reduce the pressure in front of the plug, causing the plug to move to equalize the pressure difference on each side.

Acknowledgments

We would like to acknowledge Dr. H. Rogne, Dr. I.-R. Johannessen, B. G. Fismen, H. Schumann-Olsen, and A. Ferber at SINTEF (Oslo, Norway) for the

development of the custom-made instrument incorporating heat regulation and optical detection. Dr. F. Schönfeld, Dr. K. S. Drese, and O. Sörensen at the Institut für Mikrotechnik Mainz GmbH (IMM, Germany) designed and fabricated the polymer microchips. We also thank Prof. R. Sirevåg (University of Oslo, Norway) and Dr. E. Hovig (Norwegian Radium Hospital, Norway) for valuable discussions.

References

1. www.who.int/cancer/en/ (July 2005).
2. Zuckerman, A. J. (1979) Role of the hepatitis B virus in primary liver cancer. *J. Toxicol. Environ. Health* **5,** 275–280.
3. Hadziyannis, S. J. (1981) Primary liver cancer and its relationship to chronic infection with the hepatitis B virus. *Springer Semin. Immunopathol.* **3,** 473–485.
4. Marx, J. L. (1986) Human papilloma virus and cervical cancer. *Science* **231,** 920.
5. Longworth, M. S. and Laimins, L. A. (2004) Pathogenesis of human papillomaviruses in differentiating epithelia. *Microbiol. Mol. Biol. Rev.* **68,** 362–372.
6. Muñz, N., Bosch, F. X., de Sanjosé S., et al. (2003) Epidemiologic classification of human papillomavirus types associated with cervical cancer. *N. Engl. J. Med.* **348,** 518–527.
7. Walboomers, J. M. M., Jacobs, M. V., Manos, M. M., et al. (1999) Human papillomavirus is a necessary cause of invasive cervical cancer worldwide. *J. Pathol.* **189,** 12–19.
8. Kraus, I., Molden, T., Ernø L. E., Skomedal, H., Karlsen, F., and Hagmar, B. (2004) Human papillomavirus oncogenic expression in the dysplastic portio; an investigation of biopsies from 190 cervical cones. *Br. J. Cancer* **90,** 1407–1413.
9. Cuschieri, K. S., Whitley, M. J., and Cubie, H. A. (2004) Human papillomavirus type specific DNA and RNA persistence—implications for cervical disease progression and monitoring. *J. Med. Virol.* **73,** 65–70.
10. Marwick, C. (1990) Helicobacter: new name, new hypothesis involving type. *JAMA* **264,** 2724–2727.
11. Graham, D. Y. (2000) Helicobacter pylori infection is the primary cause of gastric cancer. *Gastroenterology* **35 (Suppl 12),** 90–97.
12. Houlston, R. S., Collins, A., Slack, J., and Norton, N. E. (1992) Dominant genes for colorectal cancer are not rare. *Ann. Hum. Genet.* **56,** 99–103.
13. de la Chapelle, A. (1999) Testing tumors for microsatellite instability. *Eur. J. Hum. Genet.* **7,** 407–408.
14. Wang, D. G., Fan, J.bB., Siao, C.-J., et al. (1998) Large-scale identification, mapping, and genotyping of single-nucleotide polymorphisms in the human genome. *Science* **280,** 1077–1082.
15. Saiki, R. K., Scharf, S., Faloona, F., et al. (1985) Enzymatic amplification of β-globin genomic sequences and restriction site analysis for diagnosis of sickle cell anemia. *Science* **230,** 1350–1354.

16. Solinas-Toldo, S., Lampel, S., Stilgenbauer, S., et al. (1997) Matrix-based comparative geniomic hybridization: biochips to screen for genomic imbalances. *Genes Chromos. Cancer* **20,** 399–407.
17. Southern, E. M. (1975) Detection of specific sequences among DNA fragments separated by gel electrophoresis. *J. Mol. Biol.* **98,** 503–507.
18. Sanger, F., Nicklen, S., and Coulson, A. R. (1977) DNA sequencing with chain-terminating inhibitors. *Proc. Natl. Acad. Sci. USA* **74,** 5463–5467.
19. Jeffreys, A. J., Wilson, V., and Thein, S. L. (1985) Individual-specific "fingerprints" of human DNA. *Nature* **316,** 76–79.
20. Orita, M., Iwahana, H., Kanazawa, H, Hayashi, K., and Sekiya T. (1989) Detection of polymorphisms of human DNA by gel electrophoresis as single strand conformation polymorphisms. *Proc. Natl. Acad. Sci. USA* **86,** 2766–2770.
21. Becich, M. J. (2000) The role of the pathologist as tissue refiner and data miner: the impact of functional genomics on the modern pathology laboratory and the critical roles of pathology informatics and bioinformatics. *Mol. Diagn.* **5,** 287–299.
22. Lockhart, D. J. and Winzeler, E. A. (2000) Genomics, gene expression and DNA arrays. *Nature* **405,** 827–836.
23. Barany, F. (1991) Genetic disease detection and DNA amplification using cloned thermostable ligase. *Proc. Natl. Acad. Sci. USA* **88,** 189–193.
24. Walker, G. T., Little, M. C., Nadeau, J. G., and Shank, D. D. (1992) Isothermal in vitro amplification of DNA by restriction enzyme/DNA polymerase system. *Proc. Natl. Acad. Sci. USA* **89,** 392–396.
25. Spargo, C. A., Fraiser, M. S., Van Cleve, M., et al. (1996) Detection of *M. turberculosis* DNA using thermophilic strand displacement amplification. *Mol. Cell Probes* **10,** 247–256.
26. Nycz, C. M., Dean, C. H., Haaland, P. D., Spargo, C. A., and Walker, G. T. (1998) Quantitative reverse transcription strand displacement amplification: quantitation of nucleic acids using an isothermal amplification technique. *Anal. Biochem.* **259,** 226–234.
27. Compton, J. (1991) Nucleic acid sequence-based amplification. *Nature* **350,** 91–92.
28. Deiman, B., van Aarle, P., and Sillekens, P. (2002) Characteristics and Applications of the nucleic acid sequence-based amplification (NASBA). *Mol. Biotechnol.* **20,** 163–179.
29. Leone, G., van Schijndel, H., van Gemen, B., Kramer, F. R., Schoen, C. D. (1998) *Nucleic Acids Res.* **26,** 2150–2155.
30. Pasternack, R., Vuorinen, P., and Miettinen, A. (1997) Evaluation of the Gen-Probe *Chlamydia trachomatis* transcription-mediated amplification assay with urine specimens from women. *J. Clin. Microbiol.* **35,** 676–678.
31. Horn, T. and Urdea, M. (1989) Forks and combs and DNA: the synthesis of branched oligodeoxyribonucleotides. *Nucleic Acids Res.* **17,** 6959–6967.
32. Horn, T., Chang, C.-A., and Urdea, M. S. (1997) Chemical synthesis and characterization of branched oligodeoxynucleotides (bDNA) for use as signal amplifiers in nucleic acid quantification assays. *Nucleic Acids Res.* **25,** 4842–4849.

33. Manos, M. M., Kinney, W. K., Hurley, L. B., Sherman, M. E., et al. (1999) Identifying women with cervical neoplasia: using human papillomavirus DNA testing for equivocal Papanicolaou results. *JAMA* **281,** 1605–1610.
34. Fire, A. and Xu, S.-Q. (1995) Rolling replication of short DNA circles. *Proc. Natl. Acad. Sci. USA* **92,** 4641–4645.
35. Liu, D., Daubendiek, S. L., Zillmann, M. A., Ryan, K., And Kool, E. T. (1996) Rolling circle DNA synthesis: small circular oligonucleotides as efficient templates DNA polymerases. *J. Am. Chem. Soc.* **118,** 1587–1594.
36. Tyagi, S. and Kramer, F. R. (1996) Molecular beacons: probes that fluoresce upon hybridisation. *Nat. Biotechnol.* **14,** 303–308.
37. Tüdő, A. J., Besselink, G. A. J., and Schafoort, R. B. M. (2001) Trends in miniaturized total analysis systems for point-of-care testing in clinical chemistry. *Lab Chip* **1,** 83–95.
38. Verpoorte, E. (2002) Microfluidic chips for clinical and forensic analysis. *Electrophoresis* **23,** 677–712.
39. www.nci.nih.gov
40. Loi, S., Desmedt, C., Cardoso, F., Piccart, M., and Sotiriou, C. (2005) Breast cancer gene expression profiling: clinical trial and practice implications. *Pharmacogenetics* **6,** 49–58.
41. Robison, J. E., Perreard, L., and Bernard, P. S. (2004) State of the science: molecular classifications of breast cancer for clinical diagnostics. *Clin. Biochem.* **37,** 572–578.
42. Lukas, J., Gao, D.-Q., Keshmeshian, M., Wen, W.-H., Tsao-Wei, D., Rosenberg, S., and Press, M. F. (2001) Alternative and aberrant messenger RNA splicing of the *mdm2* oncogene in invasive breast cancer. *Cancer Res.* **61,** 3212–3219.
43. Jenkins, D. (2001) Diagnosing human papillomaviruses: recent advances. *Curr. Opin. Infect. Dis.* **14,** 53–62.
44. Gulliksen, A., Solli, L., Karlsen, F., et al. (2004) Real-time nucleic acid sequence-based amplification in nanoliter volumes. *Anal. Chem.* **76,** 9–14.
45. Boom, R., Sol, C. J. A., Salimans, M. M. M., Jansen, C. L., Wertheim-van Dillen, P. M. E., and van der Noordaa, J. (1990) Rapid and simple method for purification of nucleic acids. *J. Clin. Microbiol.* **28,** 495–503.
46. Boom, R., Sol, C. J. A., Beld, M., Weel, J., Goudsmit, J. and Wertheim-van Dillen, P. (1999) Improved silica-guanidiniumthiocyanate DNA isolation procedure based on selective binding of bovine alpha-casein to silica particles. *J. Clin. Microbiol.* **37,** 615–619.
47. Beld, M., Sol, C., Goudsmit, J. and Boom, R. (1996) Fractionation of nucleic acids into single-stranded and double-stranded forms. *Nucleic Acids Res.* **24,** 2618–2619.
48. Hatefi, Y. and Hanstein, W. G. (1969) Solubilization of particulate proteins and nonelectrolytes by chaotropic agents. *PNAS Biochem.* **62,** 1129–1136.
49. von Hippel, P. H. (1964) Neutral salts: The generality of their effects on the stability of macromolecular conformations. *Science* **145,** 577–580.
50. Lie, A. K., Risberg, B., Borge, B., Sandstad, B., Delabie, J., Rimala, R., Onsrud, M. and Thoresen, S. (2005) DNA versus RNA based methods for human papillomavirus detection in cervical neoplasia. *Gynecol. Oncol.* ***97,*** 908–915.

51. Kreader, C. A. (1996) Relief of amplification inhibition in PCR with bovine serum albumin or T4 gene 32 protein. *Appl. Environ. Microbiol.*. **62,** 1102–1106.
52. Gulliksen, A., Solli, L. A., Drese, K. S., Sœnsen, O., Karlsen, F., Rogne, H., Hovig, E. and Sirevåg, R. (2005) Parallel nanoliter detection of cancer markers using polymer microchips. *Lab Chip* **5,** 416–420.
53. van Strijp, D. and van Aarle, P. (1998) NASBA—a method for nucleic acid diagnostics, in *Diagnostic Virology Protocols* (Stephenson, J. R. and Warnes, A., eds.), Humana Press Inc., Totowa, NJ.

7

DNA Microchips to Identify Molecular Signatures in Cervical Cancers

Yick Fu Wong, Tony K. H. Chung, Vivian W. Wang, and David I. Smith

Summary

Cervical cancer is still the leading cause of gynecological cancer deaths worldwide in spite of the advent of early diagnosis with the Pap smear. Ninety-five percent of cervical cancers are of squamous cell origin. Cervical carcinoma is almost always associated with infection from oncogenic subtypes of human papillomavirus (HPV). However, HPV infection alone is insufficient for malignant transformation; other genetic events independent or in conjunction with HPV infection are required. The early studies of genetics in cervical cancer were often hampered because only a few genes or genetic events could be evaluated at a time. Therefore, the interactions of multiple genes throughout the genome could not be evaluated. Gene-expression profiling utilizing microarrays allows quantitative measurement of the expression of thousands to all human expressed genes simultaneously. Here we describe how to obtain information on global genetic events in cervical cancer using oligonucleotide microarrays in combination with real-time reverse transcriptase polymerase chain reaction (RT-PCR). This facilitates understanding of the gene expression differences that underlie cervical neoplastic development and progression and can identify molecular signatures that can potentially be used in cervical cancer diagnosis and prognosis. This technology also represents a leap forward in the goal to eventually provide tailored therapy to individual patients and offers a genetic blueprint for gauging the potential effectiveness of all common cervical cancer treatments.

Key Words: Gynecological cancer; molecular signature; gene expression profiling; microarray.

1. Introduction

Central to the understanding of the molecular mechanisms underlying cervical carcinogenesis is the availability of a comprehensive catalogue of the gene aberrations in cervical cancer cells. The advent of DNA microarrays allows the analysis of gene alterations across the entire human genome ***(1,2)***. Although

From: *Methods in Molecular Biology, Vol. 385: Microchip-Based Assay Systems: Methods and Applications*
Edited by: Pierre N. Floriano © Humana Press Inc., Totowa, NJ

conventional gene studies have yielded a wealth of knowledge, these studies are only capable of examining a minute fraction of the 27,000 estimated genes in the mammalian genome. Because genes interact with each other through various feedback mechanisms, the absence of a global picture on genetic changes restricts our understanding of the carcinogenesis process.

Genetic profiling of malignancies has proven invaluable in the identification of molecular pathways of tumor development and progression ***(3–5)***. Genetic alterations that correlate with disease status can be used to develop targeted therapies or to identify novel tumor markers, which can be used to monitor treatment response or disease recurrence ***(6,7)***. The hybridization of labeled cDNAs to an array of oligonucleotides representative of several thousand genes allows the identification and quantification of many expressed genes simultaneously ***(1,2)***. The comparison of gene-expression patterns (the transcriptome) in cells representing distinct phenotypes, e.g., normal and malignant cervical cells, will help to link the cellular phenotype with the transcriptome and could therefore uncover biologically and clinically significant patterns of gene expression in cervical cancer. The questions that would be addressed in such a study are as follow: (1) What are the upregulated and downregulated genes in invasive cervical cancer? (2) Which genes are potentially involved in the development and progression of cervical cancer? and (3) What is the clinico-pathological significance of these molecular characteristics in cervical neoplasms? This research can provide unprecedented information on global genetic events in cervical neoplasms. Genetic changes crucial to the development, progression, and metastasis of cervical malignancy may also then become apparent. This chapter presents the protocol to search for candidate molecular signatures in cervical cancer using oligonulceotide chips in combination with real-time RT-PCR. This work may serve as an engine for further characterization of these genes, which will allow them to be exploited in diagnosis, prognosis, molecular classification, and potential therapeutic targets of cervical cancer.

2. Materials

2.1. Patient and Tissue Sample

1. Patients presenting with squamous cell carcinoma and undergoing radical hysterectomy or radiotherapy are included in the study.
2. Women with benign conditions and undergoing total hysterectomy are recruited for the isolation of normal cervical epithelium as controls.
3. Ethics approval is obtained from the Institutional Ethics Board, and an informed consent form is obtained from each patient before the study begins.
4. Cervical tissue specimens are collected during surgical treatment or from biopsies.

5. The histopathological diagnosis and grading of cervical tumor is according to World Health Organization criteria ***(8)***, while the clinical staging of the tumor is made according to International Federation of Gynecology and Obstetrics criteria ***(9)***.
6. Clinical data for patients, including follow-up information, are collected from the medical records.
7. A deep freezer (–70°C) and Tissue-Tek® Optimal Cutting Temperature (OCT) compound (Ted Pella, Redding, CA) are required for storage of tissue samples.
8. A hematoxylin-and-eosin (H&E) staining set is needed for frozen-sectioned tissue staining.

2.2. RNA Extraction

RNA is extracted from the tumor and normal specimens using the RNeasy Mini Kit obtained from Qiagen. Tissue samples are homogenized into lysis buffer using the Rotor-stator prior to purification with the RNeasy Mini Kit.

1. RNeasy Mini Kit and proteinase K (Qiagen Inc., Valencia, CA).
2. Rotor-stator (IKA Works, Cincinnati, OH).
3. β-Mercaptoethanol (Sigma-Aldrich, St. Louis, MO).

2.3. Microarray

A number of different platforms can be utilized for microarray analysis. However, the majority of microarrays are run on Affymetrix GeneChips. The Human Genome U133 2.0 arrays contain oligonucleotide probes for the majority of expressed human genes. Each gene is interrogated with 11 perfect match 25-mer oligonucleotide probes and 11 mismatch primers containing a single mismatch at position 13 in the oligonucleotides. Affymetrix GeneChips are usually run in Microarray Core facilities that have considerable experience working with this platform.

1. GeneChip® Human Genome U133 2.0 Arrays (Affymetrix, Santa Clara, CA).
2. GeneChip® Scanner 3000 and GeneChip Operating Software (GCOS) for high-resolution scanning and scanning patch, which enables feature extraction (Affymetrix, Santa Clara, CA).

2.4. Data Analysis

There are also many different software packages available for the analysis of microarray data. Generally the data are first analyzed to quantitate the expression of each gene by comparing the signal of the 11 perfect match primers to those of the 11 mismatch primers. However, there are a number of programs that only utilize the perfect match primers to quantitate message levels. Subsequent analysis utilizes various known molecular pathways to attempt to determine the key pathways that might be involved in the process you are studying.

1. DNA-Chip Analyzer (dChip) (www.dchip.org) ***(10)***.
2. PathwayAssist version 3.0 software (Iobion Informatics LLC, La Jolla, CA) ***(11)***.

2.5. Real-Time RT-PCR

Microarray analysis is merely the first step in the identification of key genes. Once a number of candidate genes have been identified, the next step is to precisely determine the amount of transcript present for these genes. This is most easily performed using real-time RT-PCR analysis ***(12)***.

1. SuperScript II RNase H- Reverse Transcriptase (Invitrogen, Carlsbad, CA).
2. Random primers (3 µg/µL) (Invitrogen, Carlsbad, CA).
3. dNTP mix (10 m*M* each) (Roche, NJ).
4. RNaseOUT recombinant ribonuclease inhibitor (40 U/µL) (Invitrogen, Carlsbad, CA).
5. Human Universal Reference Total RNA (BD Biosciences Clontech, Palo Alto, CA).
6. 384-Well clear optical reaction plate (Applied Biosystems, Foster City, CA).
7. ABI PRISM optical adhesive cover (Applied Biosystems, Foster City, CA).
8. TaqMan gene expression assays (predesigned, gene-specific TaqMan probe and primer sets for quantitative gene expression studies of human genes) (Applied Biosystems, Foster City, CA).
9. ABI Prism 7900 sequence analyzer (Applied Biosystems, Foster City, CA).
10. SDS2.1 software (Applied Biosystems, Foster City, CA).

3. Methods

3.1. Collection of Tissue Sample for RNA Extraction

1. Dissected tissue specimens obtained from cervical tumor or normal cervix are placed in a sterile plastic-capped jar on ice and are immediately sent to the laboratory.
2. For cervical tumors, a portion of specimen is cut and placed into a sterile microtube and snap-frozen in liquid nitrogen; another portion is sliced into several pieces (making sure that the thickness of the pieces are not more than 1 mm), embedded in OCT, and snap-frozen in liquid nitrogen.
3. For normal cervix samples, the whole specimen, after recognizing the precise position of the epithelium surface, is cut into several slices. One slice is taken to be embedded in OCT and snap-frozen in liquid nitrogen; the remainder is placed into microtubes, one slice per tube, and snap-frozen in liquid nitrogen.
4. All above specimens are stored at –70°C before use to limit RNA degradation.
5. A frozen section (5 µm) from both OCT-embedded cervical tumor and normal cervix is prepared and stained with H&E, which is used to corroborate the diagnosis of squamous cell carcinoma and to identify normal squamous cell epithelia. Only those cases with cervical squamous cell carcinoma in which the proportion of tumor cells in the tumor samples is greater than 80% are included in this study.

6. Before starting the total RNA-extraction procedure, several slices of tumor tissue sample from storage are obtained (making sure that the tissue sample weighs less than 30 mg) and placed into a suitably sized vessel for homogenization.
7. Normal cervix samples are taken from storage and placed on dry ice. After recognizing where the cervix epithelium side is, use a forceps to orient the specimen and use a scalpel to scrap the surface of cervix gently three times; the normal cervix epithelium is then scraped into a microtube.

3.2. Total RNA Extraction and Quantitation

Total RNA is extracted from cervical tissue using the RNeasy Mini Kit according to the manufacturer's protocol (*see* **Notes 1** and **2**).

1. Six hundred microliters of buffer RLT are added to the microtube containing the cervical tissue sample. The sample is disrupted and homogenized immediately using a conventional rotor-stator homogenizer until the specimen is uniformly homogeneous.
2. The homogenate is centrifuged for 3 min at maximum speed ($\geq$8000*g*) in a microcentrifuge to remove large particulates**.** The supernatant is then transferred into a new microtube by pipetting.
3. One volume of 70% ethanol is added to the cleared lysate. It is mixed well by pipetting five times, but should not be centrifuged.
4. Seven hundred microliters of buffer RW1 are added to the RNeasy column. The tube is closed gently and centrifuged for 15 s at $\geq$8000*g* to wash the column. The flow-through and collection tube are discarded.
5. The RNeasy column is transferred into a new 2-ml collection tube. fove hundred microliters of buffer RPE from kit are added onto the RNeasy column. The tube is closed gently and is centrifuged for 15 s at $\geq$8000*g* to wash the column. The flow-through is discarded.
6. Another 500 µL of buffer RPE are added to the RNeasy column. The tube is closed gently and is then centrifuged for 2 min at $\geq$8000*g* to dry the RNeasy silica-gel membrane.
7. The RNeasy column is placed onto a new 2-mL collection tube. This is centrifuged in a microcentrifuge at full speed for 1 min ($\geq$8000*g*).
8. The RNeasy column is transferred to a new 1.5-ml collection tube. Thirty to 50 µL of RNase-free water are directly added onto the RNeasy silica-gel membrane to elute the RNA. The tube is closed gently and is centrifuged for 1 min at $\geq$8000*g* to elute.
9. If the expected RNA yield is >30 µg, the elution step is repeated as described with a second volume of RNase-free water. It is eluted into the same collection tube.
10. The concentration of RNA is determined by measuring the absorbance at 260 nm (A_{260}) in a spectrometer. The absorbance ratio of the reading at 260 nm (A_{260}) and 280 nm (A_{280}) provides an estimate of the purity of RNA with respect to contamination that absorbs in the UV, such as protein. Pure RNA used in this study should have a ratio between 1.9–2.1 in 10 m*M* Tris-HCl, pH 7.5. The integrity and size

distribution of total RNA purified are checked by denaturing agarose gel electrophoresis and ethidium bromide staining. The respective ribosomal bands should appear as sharp bands on the stained gel. The intensity of the 28S ribosomal RNA bands should be approximately twice that of the 18S RNA band.

11. The total RNA obtained is stored at -70°C pending use in microarray hybridization and real-time RT-PCR.

3.3. Microarray Hybridization and Data Collection

The RNA samples are then sent to the Microarray Core Facility. The samples are analyzed on an Agilent Bioanalyzer (Palo Alto, CA), which provides greater information about overall RNA quality than conventional gel electrophoresis. Samples that look good are then used to synthesize fluorescently labeled cDNA for hybridization to the Affymetrix Chips. Prior to placing samples on the relatively expensive U133 Plus 2 arrays, they are tested with Affymetrix test microarrays which contain probes for a number of control genes. The probes are derived from different portions (not just the extreme 3' end as are the oligos on the U133 Plus 2 chips) of the test genes and by analyzing the results from this test array and comparing the intensity of signals at different portions along these genes (middle vs 3' end and 5' end vs 3' end), one can determine if the labeled cDNA is intact enough for hybridization to the U133 Plus 2 arrays. The samples are then hybridized to the U133 Plus 2 arrays and washed as described by Affymetrix. The chips are then scanned using a laser scanner, and the raw data of signal intensities are obtained.

3.4. Microarray Data Analysis

The dChip software package ***(10)*** is used for probe-level and high-level analysis of the Affymetrix gene-expression microarrays. At the probe level, the model-based approach allows pooling information across multiple arrays and automatic probe selection to handle cross-hybridization and image contamination. High-level analysis in dChip includes comparing samples and hierarchical clustering. Gene expression data obtained from microarrays including those for cervical carcinoma and normal cervical epithelia are normalized with the dChip program. Only those microchips that have no outliers greater than 5% from the study set are allowed to undergo further high-level evaluation with dChip (*see* **Notes 3–5**).

1. Use an Affy CEL file-converting tool to convert the latest binary-format (Version 4) CEL file to the text-format (Version 3) CEL file so dChip can read. (For better model fitting and outlier detection, the number of arrays in a dChip group should be more than five.)
2. Use dChip software for normalization and model-based expression value computation from probe-level data. We first use an Invariant Set Normalization method to normalize arrays at the probe cell level to make them comparable and then use

a model-based method for probe selection and for computing expression values. Gene-expression data obtained from all microarrays is normalized. Model based expression index is calculated with PM-only model (meaning that only the perfect match oligos are considered with this program). Use "Analysis/Normalize" to normalize the expression values using the Invariant Set Normalization method (Version 1.0 uses a simplified ISN method with fixed rank difference threshold 50 without iteration). The standard error attached to an expression value is scaled by the ratio of the expression values before and after normalization. Afterwards, high-level analysis can be applied. "Analysis/Compare Samples" and "Analysis/Hierarchical Clustering" can then be performed as usual.

3. Click "OK" to read in the data file. If successful, the "Modeled" indicator will appear in the lower right corner to indicate that expression data are available for high-level analysis. The "Normalized" indicator will not be shown, and if the data have been normalized one can proceed to high-level analysis.
4. Use lower confidence bounds of fold changes to conservatively estimate the real fold changes. Genes with increased or decreased expression more than twofold (lower confidence bound) can then be selected for further study.
5. Use hierarchical clustering analysis to group genes with similar expression patterns.
6. Prepare "Gene information files" specified at the "Open group/Other information" dialog to be used in dChip. They are tab-delimited text files (with .XLS extension for easy opening in Excel) providing annotation information to probe sets and have the following columns: Probe set name, Identifier (Accession number), LocusLink ID, Gene name, Gene Ontology terms, Protein domain terms, Pathway terms, Chromosome terms, and Gene description. These annotation terms allow dChip to find significant gene clusters or classify a gene list.
7. Use Annotation CSV files to convert the quarterly updated NetAffx annotation files to dChip information files. The input information files need to be downloaded to local computers. Download and unzip the Annotation CSV files for a described array type (you need a free NetAffx account to do this); make sure to use the CSV file as it is without resaving it in Excel in a different format. Also, download the three Gene Ontology (GO) structure files: function ontology, process ontology, component ontology (save in text format with name "function.ontology.txt" etc.). Use the "Gene list file" in the "Analysis/Hierarchical clustering" dialog for clustering analysis and in the "Tools/Export data/Expression value" dialog for exporting expression values for only these genes. For unsupervised gene selection, the filtering criteria are varied across samples: P call % in the array used $\geq$20%. Unsupervised hierarchical clustering of the genes thus filtered shows if each of the cancer and normal samples can be separated based upon their expression profiles. For supervised selection: *t*-test with *p*-value < 0.01 is used to select genes that showed more than twofold change (90% lower bound) and mean difference of >100 between normal and cancer samples. Probe sets are obtained with 0% median false discovery rate (FDR) assessed by at least 50 permutations, which indicates that these genes are very likely to be of real biological interest.

8. After a list of genes is obtained by "Compare samples" or "Filter genes," use the "Tools/Classify Genes" dialog to classify these genes into different groups according to GeneOntology or other annotational terms. Gene groups have header lines such as "Found 15 GeneOntology 'response to external stimulus' genes in a 120-group (all: 1068/7734, PValue: 0.661181)." The *p*-values are calculated in the same way as for the significant gene clusters. Here 120 is the number of genes having GeneOntology annotation in the input gene list, thus there may be fewer than the actual number of genes in the list. Note that at "Tools/Classify genes"; the whole gene list is considered to assess the significant enrichment; while at clustering, every gene that clusters with at least four annotated genes is considered. Thus, the former gives fewer significant gene groups than the latter. Significant *p*-values as defined in the "Tools/Options/Clustering" dialog are suffixed by stars ("***") in the output file. Also, one may check the "Only report significant results" box to output only gene groups with significant *p*-values. The additional data columns such as expression values or fold changes of the "gene list file" will be copied into the output "classified file."
9. To better examine the possibility that cervical tissue samples could be separated into two distinct sets (normal cervical epithelium and cervical cancer) on the basis of gene-expression profiles, unsupervised hierarchical clustering is performed
10. Use supervised hierarchical clustering to pick up genes associated with cancer and genes correlated to different clinico-pathological features, including tumor grade, clinical stage, disease status, and total survival time. To identify co-regulated pathways contributing to the distinct biology associated with cervical cancer, probe sets can be identified as differentially regulated at least more than twofold relative to normal cervix ($p < 0.01$) using PathwayAssist version 3.0 software. This software package contains more than 140,000 documented protein interactions acquired from PubMed using the natural language processing algorithm MEDSCAN. This proprietary database is used to develop a biological association network (BAN) to identify putative signaling pathways. By overlaying expression data over the BAN, co-regulated genes defining specific signaling pathways can be identified. In our analysis of cervical tumors ***(13)***, we identified SPP1, VEGF, CDC2, and CKS2 as genes that were coordinately differentially regulated between normal cervical epithelium and cervical cancers (**Fig. 1**). These genes encode for proteins that are part of a signaling pathway associated with tumor cell "Cell survival and apoptosis" as well as regulation of signal transduction. These interacting genes could constitute a potentially important signaling pathway involved in the development of cervical cancer.

3.5. Real-Time RT-PCR

Quantitative real-time RT-PCR analysis is performed using a fluorescence temperature cycler ABI Prism 7900 Sequence Analyzer. cDNA is synthesized with Superscript II using total RNA. This machine can hold 96- or 384-well plates, and with the 384-well plates offering the ability to analyze many more

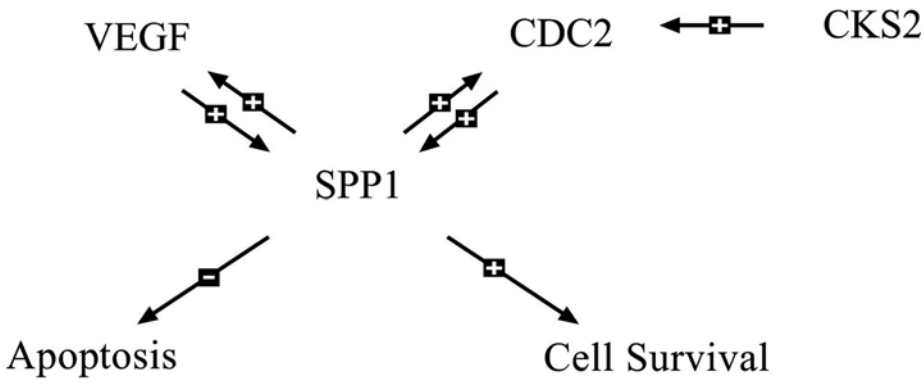

Fig. 1. A potential signaling pathway involved in the development and progression of cervical squamous cell carcinoma. Four genes—SPP1, VEGF, CDC2, and CKS2—are overexpressed in cancer compared to its normal counterpart.

samples with a much smaller reaction volume for each sample (*see* **Notes 6** and **7**).

1. The extracted RNA is thawed on ice, and other reverse transcription reagents, except enzymes, are thawed at room temperature.
2. To 1 µg of total RNA, 250 ng of random primers and 1 µL of 10 m*M* dNTP mix are added, and then ddH_2O is added up to 12 µL. The mixture is heated to 65°C for 5 min and quickly chilled on ice. This mixture is briefly centrifuged to spin down the solution.
3. 4 µL of 5 × First-Strand Buffer, 2 µL 0.1 *M* dithiothreitol, and 1 µL RNaseOUT recombinant ribonuclease inhibitor (40 U) are added to the mixture. The tube is mixed gently and incubated at 25°C for 2 min.
4. 1 µL of SuperScript II RT (200 units) is added and mixed by pipetting gently up and down five times. The mixture is incubated at 25°C for 10 min, then at 42°C for 50 min, and the reaction is inactivated by heating at 70°C for 15 min. The final reaction volume is 20 µL.
5. To construct standard curves for 18S ribosomal RNA and candidate genes, serial dilution of cDNAs is prepared from the Human Universal Reference Total RNA. Standard curves need to be optimized for each individual gene.
6. All samples are done in duplicate. To prepare a PCR reaction master mix, 2.5 µL TaqMan Universal PCR Master Mix (2x), 0.25 µL TaqMan Gene Expression Assay (20x), and 1.25 µL ddH_2O are added for each sample and mixed thoroughly. Three to four additional reactions are included in the calculations to provide excess volume for the loss that occurs during reagent transfers.
7. 1 µL of cDNA template is added to the bottom of the specified well of a 384-well clear optical reaction plate and then 4 µL PCR Master Mix are aliquoted to the well. The final reaction volume is 5 µL. This can be compared to 50-µL reac-

tions, which are usually performed in the 96-well clear optical reaction plates. The plate is tapped to bring the solutions down toward the bottom of the wells.

8. The 384-well plate is covered with an ABI PRISM optical adhesive cover. The cover should be pressed firmly on the wells and at the edges to avoid evaporation. The reaction is mixed gently and centrifuged at 2000 rpm for 1–2 min to bring down the solution and to eliminate any bubbles.
9. The reaction plate is placed in the ABI PRISM 7900HT Sequence Detection System. The thermal cycling conditions are set as at 50ºC for 2 min, 95ºC for 10 min, followed by 45 cycles of 95°C for 15 s and 60°C for 1 min, and the reaction volume is set as 5 µL to start the run.
10. The increase in fluorescence signal is monitored by the 7900HT system, and the data are interpreted by SDS2.1 software when the run is finished. The comparative Ct method ***(14)*** is used to calculate amplification fold as specified by the manufacturer. Each reaction is run in duplicate.
11. The amount of target and 18S ribosomal RNA is determined from the corresponding standard curve. The fluorescence from 18S ribosomal RNA is used as an endogenous reference control to normalize the fluorescent signal of the target genes. Normalization is done by dividing the target amount to the 18S ribosomal RNA amount. The normalized amount of target is then compared to the control group to obtain the expression fold changes. Negative controls without template are produced for each run.

3.6. Making Sense of the Data

The most important issue that plagues most individuals performing microarray data is how to make sense of the data that is generated. Once a list of consistently dysregulated genes is obtained, there could be several hundred to over a thousand genes on those lists. In our analysis of 29 cervical cancers vs 18 normal cervix samples, we found 237 individual genes that satisfied all the necessary criteria. Of those, 98 were upregulated and 139 were downregulated. However, what proportion of these genes is actually important in the development of cervical cancer? This is, unfortunately, one of the greatest problems with microarray analysis as a tool to understand cancer, because changes in a single transcription factor during cancer development could change the expression of many other downstream genes, most of which may not be important at all in the overall process. As a result of these difficulties, a number of different programs have been developed that attempt to determine the pathways of genes that are aberrantly regulated. This includes Pathway Assist, Genespring, and Ingenuity. These programs attempt to determine important gene pathways as well as protein interactions based upon data obtained from the literature, and they can be used to identify putative signaling pathways that might be important in cervical cancer development.

An important resource for the scientific community interested in gene expression in cancers is Oncomine (http://www.oncomine.org) ***(15)***, which was

developed by Dr. Arul Chinnaiyan and colleagues at the University of Michigan. Oncomine sends out requests for microarray data on any cancer contained in any publication. This is a resource that can only improve over time as more microarray data from larger numbers of cancers are incorporated into the database. It also offers the ability to compare the list of genes you obtain in your microarray experiment to those obtained from other investigators both within the same tumor type and between different tumor types.

4. Notes

1. Great care should be taken to avoid inadvertently introducing ubiquitous RNases into the RNA samples during or after the isolation procedure. The use of sterile, disposable polypropylene tubes is recommended throughout the procedure. To ensure that it is RNase-free, glassware can be treated with 0.1% diethyl pyrocarbonate (DEPC) (allowed to stand 12 h at 37°C and then autoclaved or heated to 100°C for 15 min to eliminate residual DEPC) before use; 0.1% DEPC treated water is used for solution preparation.
2. β-Mercaptoethanol must be added to buffer RLT before use. β-Mercaptoethanol is toxic. It should be dispensed in a fume hood—10 µL is added per 1 mL of buffer RLT.
3. To prevent multiple probe sets for the same gene from biasing as a result of the functional significance computation, it is best to check "Analysis/Open group/Options/Analysis/Mask redundant probe sets" to exclude the redundant probe sets (identified by LocusLink ID) from a gene list. This can also be done at "Tools/Options/Analysis/Mask redundant probe sets," but redoing "Analysis/Open group" is desired since the array background information on gene annotation is computed after reading in the "gene information file." An "array summary file" is saved after all arrays are read in. Clicking the Excel icon in the left pane will start Excel to view this file. As with most other files exported by dChip, the format of this file is a tab-delimited text file with "xls" extension for easy access of the file by Excel. At this stage the summary file looks as follows: the last two columns are the median probe intensity and the "P call %" (the percentage of probe sets called "Present" in an array). The median intensity is computed using unnormalized probe values by selecting a probe for every 5×5 region on the array. Some arrays may have an unusually low "P call %" (<10%). One may check the "Image View" for potential problems. Good images have dark backgrounds and bright foreground signals, while problematic sample preparation, hybridization, or scanning may result in the high background noise that overwhelms the real signals. Sometimes it is necessary to exclude these arrays from further analysis by moving those files out of the data directory and redoing "Analysis/Open group."
4. When gene-expression analysis using microarray was first developed, it became clear that there were a number of important technical challenges to obtaining reproducible data. The first consideration is having a resource of tissue specimens that are going to be analyzed. These specimens should be fresh-frozen because

paraffin-embedded tissues have considerable degradation of RNA, making traditional microarray analysis close to impossible. However, new technologies are being developed, such as cDNA-mediated annealing, selection, extension, and ligation assay (shortened to DASL) from Illumina, specifically to analyze gene expression of samples stored in paraffin. One disadvantage of most resources of fresh-frozen specimens is that they traditionally have less clinical follow-up than long-stored paraffin sections; hence, unless your fresh-frozen resource contains samples with long-term follow-up, important clinical data such as the overall survival of the patient will be lacking. The fresh-frozen samples should be frozen as quickly as possible to prevent any unnecessary degradation of RNA, and only those samples that yield good-quality RNA should be used for microarray experiments. The second important consideration is the overall purity of the tumor specimens analyzed. It is absolutely essential to carry out this work with skilled pathologists who can provide accurate information about the overall purity of the tumor specimens that will be analyzed. A third consideration that used to be important is variability in different lots of microarray chips. Similarly, there also used to be a concern about which individual actually ran the microarray experiment and which day they ran it. In the last few years, however, these issues have been resolved so that there is less variability between different lots of chips (certainly from Affymetrix), and most experienced microarray core laboratories now have personnel who are sufficiently skilled such that different microarrays run by different individuals on different days still produce highly reproducible and comparable data. A more important consideration is what one is hoping to obtain with microarray data. Depending on the samples analyzed, one can obtain important information, not just about genes that are consistently up- or downregulated during the development of cervical cancer. For example, by comparing early-stage to late-stage ovarian cancers, you can obtain important information about genes that are dysregulated early vs those that are dysregulated later in the development of cervical cancer. Alternatively, a microarray experiment can be set up to compare cervical cancers with a good prognosis vs those with a poor overall prognosis. It is actually possible to examine all these variables, in which case a larger number of cervical specimens needs to be examined. It is also important that the measurements obtained in a sufficiently large enough sample of tumor specimens can be compared to the expression in multiple normal cervical epithelial specimens so that information about the range of expression of each gene in each normal sample can be compared to the tumor samples.

5. Different programs have been developed to take the raw DAT data files and determine the relative level of expression of each gene. Affymetrix uses their own program to measure the difference between the intensities of the sequence-specific perfect match probe set and the mismatch probe set to make measurements for each gene. Other programs have been developed, some which only use the perfect match primers for their analysis, whereas others use both the perfect match and the mismatch primers (such as GC-RMA). All these programs attempt to average the signal obtained from all the probes to get a measurement of expression for each gene.

What is important to realize is that the same set of microarray data can generate completely different lists of aberrantly regulated genes when different analysis programs are utilized. Once one has decided which program to use to measure gene expression, the next step is to determine which genes are aberrantly regulated when comparing the group of normal cervical samples to the group of cervical tumor samples. Fold-change analysis is performed, in which the ratio of the geometric means of the expression intensities of the relevant gene fragments is computed. This ratio is reported as the fold change (either up or down). However, because so many genes are being analyzed in any microarray experiment, it is possible that some genes will appear to differ between normal samples and tumors. As a result, *p*-values are calculated for each gene. We have used a two-sided Welch modified two-sample *t*-test, and only *p*-values 0.01 are considered significant, i.e., the relative expression of each gene is compared between the normal and tumor samples, and those genes that have less variability in the normal and tumor groups will have the highest *p*-values. By incorporating both fold differences in expression and *p*-values, there is a greater probability of obtaining genes that are actually aberrantly regulated during cervical cancer development. A problem with this approach, however, is that any genes with highly variable expression within the normal samples and, more importantly, within the tumor samples will generate lower *p*-values and may be excluded from further analysis. This group of genes could contain a number of genes that are important in the development of a proportion of the cervical tumor samples, but which would be excluded from further analysis because their calculated *p*-values would be greater than 0.01. If *p*-values are not considered, then there is uncertainty about the lists of genes obtained in terms of which genes are actually aberrantly regulated in a proportion of the cervical tumors vs those that appear simply by statistical chance. Another important consideration is what fold change between normal and cervical tumor specimens is significant and worthy of further consideration. We have generally assumed the cut-off for consideration for those genes that are more than twofold up- or downregulated. Lowering that threshold can produce much larger lists of potentially dysregulated genes, but then there is considerably less certainty as to which genes on that list are potentially important in the development of cervical cancer. Conversely, making the threshold higher will generate considerably smaller lists of dysregulated genes, but one runs the risk of excluding a number of important genes simply because their overall level of dysregulation is below the cut-off point. There are other ways to identify dysregulated genes than simply comparing normal cervical epithelium samples to cervical tumors. For example, one can compare low-stage to high-stage tumors or tumors associated with HPV16 infection vs other oncogenic HPV-subtypes. Alternatively, one could compare tumors with dramatically different clinical outcomes. When these types of analyses are complete, it is possible to obtain lists of genes that by gene expression profiling appear to be significantly different between the two groups that one is analyzing (whatever those groups are). The next step in this type of analysis is to choose a group of genes that are potentially interesting and then to determine precisely the level of message for those genes. This is most conveniently

done with real-time PCR. This will help to determine which candidate genes are actually aberrantly expressed (at the mRNA level) and exactly how aberrantly expressed each gene is. Microarray analysis is much more of a qualitative-comparison technique between different samples and does not generate quantifiable numbers for message abundance. Real-time PCR analysis also offers the ability to analyze large numbers of samples quickly, and even samples in paraffin (which may be associated with longer clinical follow-up and outcome measures) can be used in these analyses.

6. Take RNaseOUT recombinant ribonuclease inhibitor and SuperScript II RT out of the freezer just prior to use and refreeze immediately after use. cDNA can also be kept at –20°C for prolonged storage.
7. cDNA templates and PCR Master Mix are added to the reaction plate quickly to avoid evaporation of solution.

Acknowledgments

The study on cervical cancer summarized in a paper published in the *International Journal of Cancer* is supported by the Research Grant Council of the Hong Kong Special Administration Region: grant number CUHK4084/01M. All of the microarray experiments that we performed on cervical cancer were done in the microarray core facility at the Mayo Clinic, which now has 5 yr of experience working with Affymetrix microarrays. The authors are also grateful to all staff at the Gynaecologic Cancer Research Laboratory, The Chinese University of Hong Kong, for their excellent experimental work.

References

1. DeRisi, J., Penland, L., Brown, P. O., et al. (1996) Use of a cDNA microarray to analyze gene expression patterns in human cancer. *Nat. Genet.* **14,** 457–460.
2. Brown, P. O. and Botstein, D. (1999) Exploring the new world of the genome with DNA microarrays. *Nat. Genet.* **21,** 33–37.
3. Alizadeh, A. A., Eisen, M. B., Davis, R. E., et al. (2000) Distinct types of diffuse large B-cell lymphoma identified by gene expression profiling. *Nature* **403,** 503–511.
4. Perou, C. M., Sorlie, T., Eisen, M. B., et al. (2000) Molecular portraits of human breast tumours. *Nature* **406,** 747–752.
5. Sorlie, T., Perou, C. M., Tibshirani, R., et al. (2001) Gene expression patterns of breast carcinomas distinguish tumor subclasses with clinical implications. *Proc. Natl. Acad. Sci. USA* **98,** 10,869–10,874.
6. Jazaaeri, A. A., Awtrey, C. S., Chandramouli, G. V., et al. (2005) Gene expression profiles associated with response to chemotherapy in epithelial ovarian cancers. *Clin. Cancer Res.* **11,** 6300–6310.
7. Pittman, J., Huang, E., Dressman, H., et al. (2004) Integrated modeling of clinical and gene expression information for personalized prediction of disease outcomes. *Proc. Natl. Acad. Sci. USA* **101,** 8431–8436.

8. Scully, R. E. and Poulsen, H. E. (eds.) (1994) *Histological Typing of Female Genital Tract Tumours*, Springer-Verlag, New York.
9. International Federation of Obstetrics and Gynecology. (1987) News. *J. Gynecol. Obstet.* **25,** 87.
10. Li, C. and Wong, W. H. (2003) DNA-chip analyzer (dChip), in *The Analysis of Gene Expression Data, Methods and Software* (Parmigiani, G., Garret, E. S., Irizary, R., and Zeger, S. L., eds.) Springer-Verlag, New York.
11. Donninger, H., Bonome. T., Radonovich, M., et al. (2004) Whole genome expression profiling of advance stage papillary serous ovarian cancer reveals activated pathways. Oncogene **23,** 8065–8077.
12. Bustin, S. A. (2000) Absolute quantitation of mRNA using real-time reverse transcription polymerase chain reaction assays. *J. Mol. Endocrinol.* **25,** 169–193.
13. Wong, Y. F., Cheung, T. H., Tsao, G. S. W., et al. (2006) Genome wide gene expression profiling of cervical cancer in Hong Kong women by oligonucleotide microarray. *Int. J. Cancer* **118,** 2461–2469.
14. Livak, K. J. and Schmittgen, T. D. (2001) Analysis of relative gene expression data using real-time quantitative PCR and the $2^{-\Delta\Delta C}{}_T$ method. *Methods* **25,** 402–408.
15. Rhodes, D. R., Yu, J., Shanker, K., et al. (2004) ONCOMINE: a cancer microarray database and integrated data-mining platform. *Neoplasia (New York)* **6,** 1–6.

8

Impedimetric Detection for DNA Hybridization Within Microfluidic Biochips

Louise Lingerfelt, James Karlinsey, James Landers, and Anthony Guiseppi-Elie

Summary

A fully integrated biochip for the performance of microfluidic-based DNA bioassays is presented. A microlithographically fabricated circumferential interdigitated electrode array of 1- to 5-μm critical line and space dimensions, with associated large area counterelectrode (1000 × WE) and reference electrode (Ag/AgCl), has been developed as a four-electrode system for the electrochemical detection of DNA hybridization using any of the techniques of amperometry, voltammetry, potentiometry, and impedimetry. This is presented as an alternative to optical detection with an emphasis on label-free impedimetric detection of hybridization. A micro total analysis system (μTAS) is presented, using fluidic channels to connect integrated reaction domains with downstream electrochemical detection. This is accomplished by bonding a patterned poly(dimethylsiloxane) (PDMS) substrate to the biochip or by adhesive bonding of the chip to channels fabricated within glass and plastic microfluidic cards, adding increased functionality to the device.

Key Words: DNA hybridization; electrochemical impedance spectroscopy; DNA diagnostics; oligonucleotide; silanes; DNA immobilization; biochips; poly(dimethylsiloxane); micro total analysis system (μTAS).

1. Introduction

Low-density arrays that directly detect DNA hybridization have tremendous potential for applications in human health care ***(1,2)***, forensics ***(3)***, and national security. Current technology for DNA hybridization detection is most commonly based on optical measurements and generally uses fluorescence ***(4)***. These optical methods require costly labeling strategies that use bleachable fluorescent probes and expensive optical equipment. Electrochemical methods (amperometry, voltammetry, potentiometry, and impedimetry) for the detec-

From: *Methods in Molecular Biology, Vol. 385: Microchip-Based Assay Systems: Methods and Applications*
Edited by: Pierre N. Floriano © Humana Press Inc., Totowa, NJ

tion of DNA hybridization are being developed as a way to reduce cost, eliminate fluorescent labeling of DNA targets, and reduce the overall complexity and size of the instrument footprint ***(5)***. Specifically, electrochemical impedance spectroscopy (EIS) has been demonstrated as an effective analytical technique for detecting and monitoring DNA hybridization at an electrode/electrolyte interface ***(5–7)***. We have previously demonstrated significant differences in impedance measurements before and after hybridization of 30- and 50-mer oligonucleotides, suggesting EIS as an effective method for detection in fully integrated Lab-on-a Chip (LOC) systems.

EIS is a radiofrequency technique that is widely used for the characterization of charge transfer kinetics at electrified interfaces and for the study of transport of ions in electrolytes. The technique uses a sinusoidally varying voltage that is both nonperturbating and interrogating (typically 20–50 mV p-t-p). The voltage is applied between a pair of opposing working and counterelectrodes that span the medium of interest. The inclusion of a third or reference electrode and an appropriate potentiostat allows the sine wave to be superimposed on the quiescent or other offset potential of the working electrode. Under these circumstances, the ensuing current informs on both the coupled mass transport and charge transfer kinetics of electrochemically dischargeable species and of the movement of ions under the influence of the oscillating electric field. When potentials are selected that do not electrochemically discharge redox active moieties of DNA (such as guanine) and possess a single frequency that is larger that the heterogeneous charge transfer rate of typical electrochemical reactions associated with the medium under interrogation, then the technique of electrochemical impedance (EI) measures the ability of DNA to support ionic mobility. EI has been demonstrated as an effective analytical technique for understanding the way in which charge migration is impeded or conducted through an interface that is decorated with oligonucleotides. Illustrated schematically in **Fig. 1**, EIS seeks to measure the change in ion density before and after probe hybridization with its complementary target. The inclusion of a fourth, large-area (>100 times) counterelectrode enables the implementation of the interrogation technique of the Electroactive Polymer Sensor Interrogation System (EPSIS) ***(8)*** and the use of electroactive polymer layers to amplify impedance signal associated with hybridization ***(9,10)***.

A convenient format for the immobilization of oligonucleotide probes and for the delivery of the interrogating sine wave is the co-planar interdigitated microsensor electrode (IME) shown in **Fig. 2** (*see also* **Fig. 4**). IMEs are fabricated using state-of-the-industry microlithography techniques and present a well-defined fringing electric field from which impedance changes may be measured. Direct measurements of DNA hybridization by electrochemical detection have shown much greater sensitivity to smaller sample quantities compared to optical methods ***(11)***.

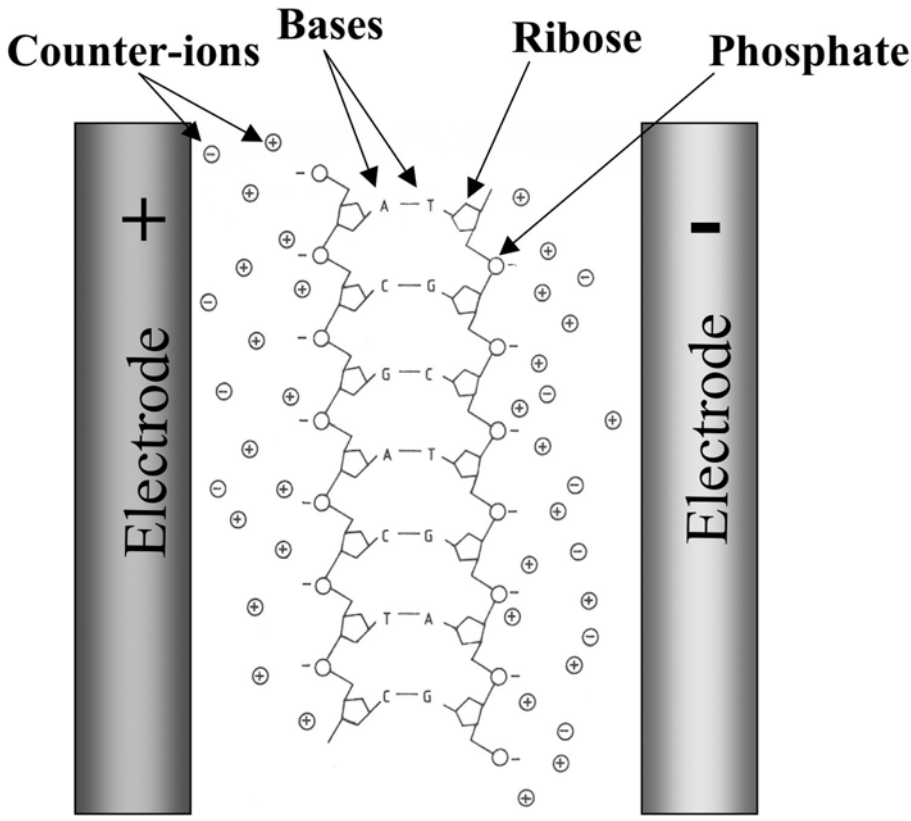

Fig. 1. Representation of DNA hybridization between a pair of electrodes. Increased impedance following hybridization is associated with a reduction of the density of water molecules and ions within the electric field.

DNA hybridization is based on the hydrogen bonding between single strands in a manner consistent with the DNA complementarity principle described by Watson and Crick in the 1950s. For detection based on EI or EIS, synthetic oligomeric probe DNA sequences taken from the 3' end that represent specific genes are covalently immobilized to the chip surface between opposing interdigitated electrodes, as shown in **Fig. 2** ***(5)***. Diffusive mass transfer is used to transport the target DNA (polymerase chain reaction [PCR] or reverse transcriptase product) to the immobilized probe on the substrate. Hybridization results in an overall increase in impedance because of the reduction of ionic conductivity surrounding the double-helical DNA relative to the single-stranded counterpart. The influence of the ionic hybridization buffer is minimized by the fact that the fringing electric field is within the diffusion boundary layer.

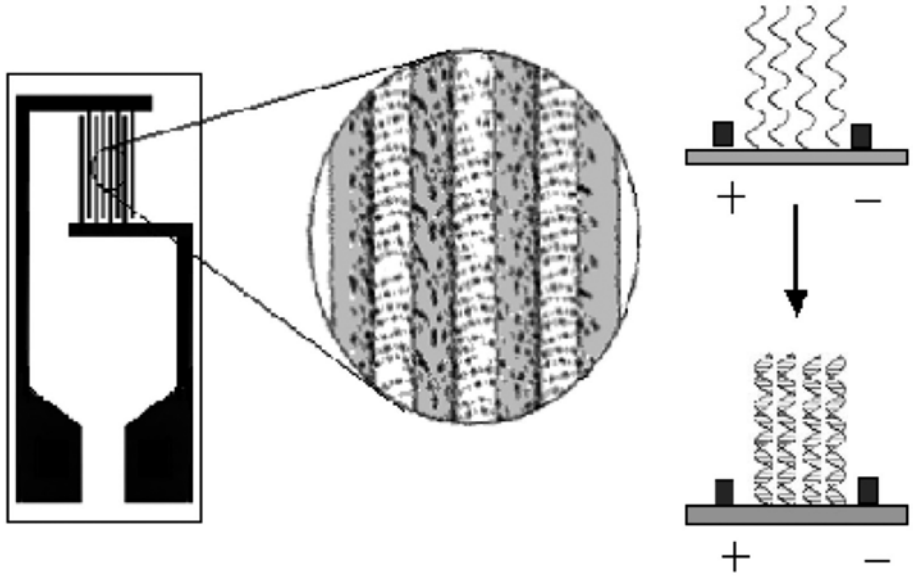

Fig. 2. Interdigitated microsensor electrode device showing the lines of force of the fringing electric field and of hybridization between interdigitated electrodes.

In solution, electric fields are typically created by the application of a voltage between a set of immersed electrodes ***(12)***. The electric field drives the transport of ions through the solution, generating an electric current. At small field strengths, the current generated is directly proportional to the strength of the electric field. The proportionality constant is known as the electrical conductivity and represents an intrinsic property of the electrolyte that is dependent on the concentration, valence state, and electrophoretic mobility of the ions present in solution. EI and EIS are based on applying an alternating sinusoidal voltage ($V = V_{max}$ sine ωt), rather than a fixed potential, over a wide frequency range, measuring the ensuing current ($I = I_{max}$ sine $\omega t+\theta$), and extracting the transfer function (V/I) ***(10)***.

Impedance is a complex electrical property comprised of two components: the real component, also known as the resistance, R, and the imaginary component, also known as the reactance, X, and is often presented as a Nyquist plot ***(13)***.

Impedance profiles also may be described by the resultant magnitude, $|Z|$, and phase angle, θ, of the real and imaginary components, as shown in **Fig. 3**. Bode plots are used to present the relationship of $|Z|$ to θ. For a pair of co-planar interdigitated electrodes bearing oligomeric DNA immobilized between them and immersed in a hybridization buffer, such an electrified system may,

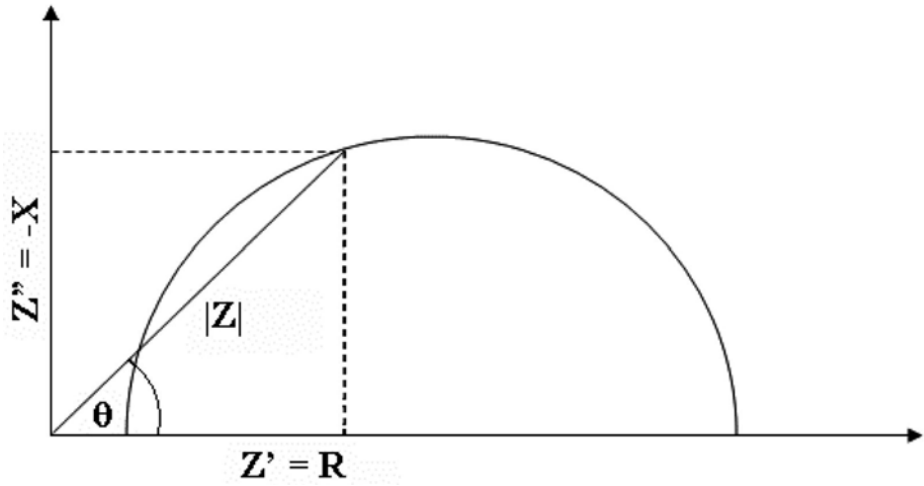

Fig. 3. Nyquest plot of frequency dependent real (*x*) and imaginary (*y*) components of the complex impedance and the corresponding magnitude, |*Z*|, and phase, θ, at given a single frequency.

in its simplest response, behave like a parallel resistor-capacitor (R-C) network. The reactance term then describes that part of the system that behaves as a capacitor while the resistance term describes that part of the system that behaves as a resistor ***(14)***. Frequency-dependent EIS has as one of its goals the identification of an appropriate frequency to be used with time-dependent EI from which the kinetics and equilibrium hybridization characteristics of probe–target and probe–mismatch pairs may be obtained.

Figure 4 shows a microfabricated electrochemical cell-on-a chip (ECC IME) developed by ABTECH Scientific, Inc. (Richmond, VA) for integration and use within microfluidic channels of micro total analysis systems (μTAS). This chip is available with several different conductors—gold, platinum, and indium tin oxide—the latter being used for its transparency and hence compatibility with optical detection systems. The available lines and spaces of interdigitation include 1, 5, 10, 15, and 20 μ. These ECC IME devices may be decorated with oligomeric DNA probes that are covalently bound to the interdigit space of the device shown in **Fig. 5**. To achieve DNA immobilization, the ECC IME devices must first undergo surface activation, surface modification, and then derivatization with the DNA probe before integrated bioanalytical measurements are performed. Surface activation of the borosilicate glass is required to expose the hydroxyl functional groups and is typically performed by using a brief and mild alkaline etch treatment (RCA clean: 1- to 10-s immersion in 5:1:1 solution of H_2O:NH_4OH:H_2O_2 followed by immediate,

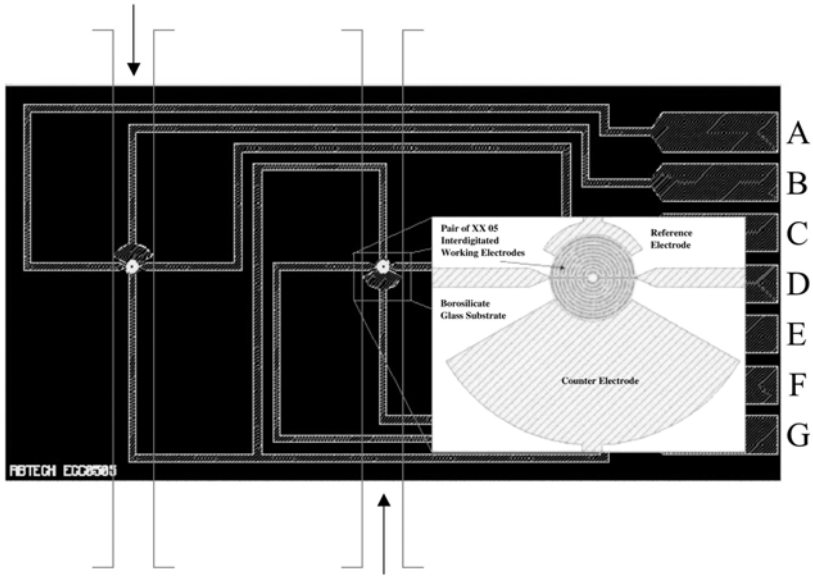

Fig. 4. Schematic illustration of a microfabricated, dual-channel, electrochemical cell-on-a-chip interdigitated microsensor electrode (ECC IME) device showing the fluid flow over the microelectrode arrays: **A** = C2W2, **B** = C2CE, **C** = C2W1, **D** = C1W1, **E** = C1CE, **F** = C1W2, **G** = REF. C2, Cell 2; C1, Cell 1; W, working electrode; CE, counterelectrode; RF, reference electrode.

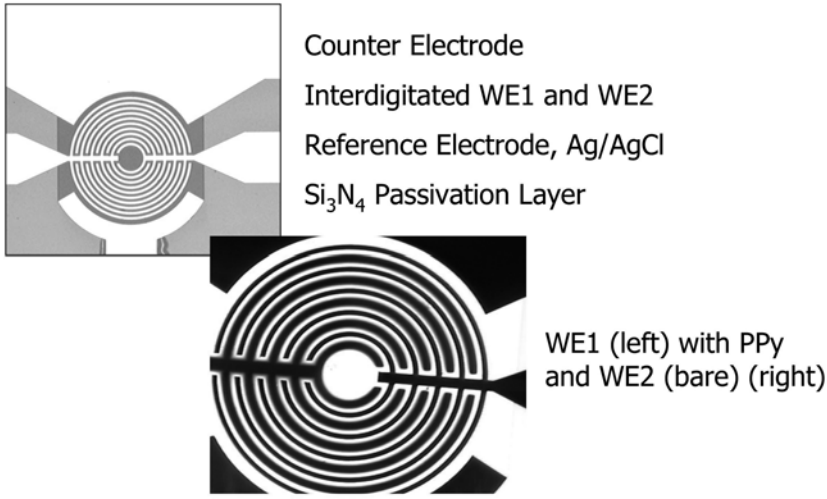

Fig. 5. Micrographs (×50) showing one channel (Cell 1) of the microfabricated, electrochemical cell-on-a-chip interdigitated microsensor electrode (ECC IME) device. **(A)** Various electrodes of the individual cell; **(B)** C1W1 with electropolymerized polypyrrole (PPy)—C1W2 serves as an opposing driving electrode.

profuse washing with deionized [DI] water) of the IME device. Following surface activation, the hydroxyls are modified using an organosilane. Silanization of the borosilicate glass has proven to be a simple and effective method for DNA immobilization ***(14,15)***. Common silanizing agents include 3-aminopropyltrimethoxysilane (APS), 3-mercaptopropyltrimethoxysilane (MPS), and 3-glycidoxypropyltrimethoxysilane (GPS), with terminal amino, mercapto, and epoxy moieties, respectively, which react and are coupled through the modified terminal group on the nucleotide. For GPS, the terminal amino group of the NH_2-C6-DNA probe reacts with the epoxy functionality of the silane compound, resulting in covalent attachment ***(16)***, and has been shown to be superior to other methods of direct covalent immobilization ***(17)***. Because organosilanes form siloxane polymers that deposit coherently and indiscriminately over the complete device, the electrodes (digits) must be subsequently cleaned to remove the polysiloxane. Subsequent covalent attachment via derivatization of the ω-terminus of the silane is a particularly effective method of DNA immobilization, and one that ensures effective probe alignment and surface coverage ***(6,7)***.

Following the necessary surface modifications, hybridization occurs when the complementary strand of DNA binds to the immobilized probe under the appropriate conditions. EIS measurements are performed before, during, and after hybridization, with the sensitivity of the detection determined by the effective change in the temporal impedance measurement ***(6,7)***. Both single- and multiple-frequency measurements can be made based on EIS detection. Single-frequency measurements are more rapid but require specific knowledge of an appropriate and effective frequency for measurement of the system of interest.

In order to incorporate the hybridization array into an integrated device that contains additional sample preparation steps (e.g., cell sorting, DNA extraction, polymerase chain reaction ampification, etc.), it is necessary to pattern additional flow channels and chambers that must be fluidically sealed. Much success has been reported with sealing PDMS to glass surfaces—this can be performed either reversibly or irreversibly (with additional surface treatment). PDMS is an ideal substrate because it is nontoxic, can be reproduced with high fidelity by replica molding, cures at low temperatures, is elastomeric, and its surface can be adapted for a range of chemistries.

2. Materials

2.1. Electrochemical Cell-on-a-Chip Interdigitated Microsensor Electrode: Cleaning, Silverization, and Platinization

1. Electrochemical Cell-on-a-Chip interdigitated microsensor electrodes (ECC IMEs) and STC 7 Test Clip (ABTECH Scientific Inc., Richmond, VA) consisting

of five pairs of opposing platinum electrodes several micrometers wide and several millimeters long (*see* **Note 1**).
2. Trichloroethylene (Sigma Aldrich, St. Louis, MO).
3. Acetone (Sigma Aldrich, St. Louis, MO).
4. Isopropyl alcohol (Sigma Aldrich, St. Louis, MO).
5. Ultraviolet (UV)/Ozone Cleaner (Boekel Industries, Inc.)
6. Alkaline etch cleaning solution: 5:1:1 solution of H_2O:NH_4OH:H_2O_2 (30% solution).
7. Acidic activiation solution: 4:1 concentrated H_2SO_4:H_2O_2 (30% aqueous solution).
8. DI, distilled water.
9. Silverizing solution: Silver Cy-less II Ready-to-Use (http://www.technic.com) electroplating solution (Technic, Inc.).
10. Platinizing solution: YSI 3140 (YSI, Inc., Yellow Springs, OH).
11. Potentiostat/Galvanostat PAR Model 283 (AMETEK Princeton Applied Research).
12. Ag/AgCl, 3 *M* Cl^- reference electrode (RE 803). (ABTECH Scientific, Inc., Richmond, VA),

2.2. Surface Modification via Silanization of ECC IME Device

1. Silanizing agent: 3-glycidoxypropyltrimethoxysilane as 0.1% by volume in anhydrous toluene (Sigma Aldrich, St. Louis, MO) (*see* **Note 2**).
2. Anhydrous toluene (Sigma Aldrich, St. Louis, MO).
3. Water bath (42°C).
4. Vacuum oven (120°C).

2.3. Cathodic Cleaning of ECC IME Device

1. Phosphate-buffered saline (PBS) (0.15 *M* NaCl, 0.1 *M* NaH_2PO_4 at pH 7.4).
2. Potentiostat/Galvanostat PAR Model 283 (AMETEK Princeton Applied Research).

2.4. DNA Probe Immobilization

1. Spotting buffer (0.5X standard sodium citrate [SSC] buffer, 1.5 *M* betaine, pH 5.4).
2. 50-mer NH_2-C6-Oligonucleotide and complementary sequence (Integrated DNA Technologies, Coralville, IA).
3. Water bath (42°C).
4. Controlled atmosphere oven (50°C, 50% RH) (Custom Built).

2.5. DNA Target Hybridization Detection With EIS

1. Hybridization buffer (20 µL phosphate-buffered KCl solution and 100 µL MWG hybridization buffer).
2. MWG Hybridization buffer comprised of 50% formamide, 6X SSC, 0.5% sodium dodecyl sulfate, 50 m*M* Na_3PO_4, and 5X Denhardt's reagent at pH 8.8 (MWG Biotech Inc.).

3. Synthetic, single-stranded, 50-mer oligonucleotides complementary, noncomplementary (random) and single, double, and multiple mismatch sequences (MWG Biotech Inc.) (*see* **Note 3**).
4. PBS (0.1 *M* KCl, 0.33 m*M* NaH_2PO_4 at pH 7.2).
5. DI, distilled water.
6. Perkin-Elmer Princeton Applied Research M283 Potentiostat/Galvanostat.
7. Solartron Schlumberger 1260 Frequency Response Analyzer (FRA).

2.6. Fabrication of a Flow-Through Device

1. Silicon monitor wafer (100 mm) (MEMC Electronic Materials, St. Peters, MO).
2. Silanizing agent: 1,1,1,3,3,3-hexamethyldisilazane (HMDS) (Acros Organics, Morris Plains, NJ).
3. Photoresist: NANO SU-8 25 (MicroChem, Newton, MA) (*see* **Note 4**).
4. Spin coater: WS-400-6NPP-LITE (Laurell Technologies Corporation, North Wales, PA).
5. Photomask (Pixels, Charlottesville, VA) (*see* **Note 5**).
6. UV lamp.
7. Developer: 2-(1-methoxy)propyl acetate (PGMEA) (Acros Organics, Morris Plains, NJ).
8. PDMS elastomer: Sylgard 184 base and curing agent (Dow Corning, Midland, MI).
9. Plasma cleaner/sterilizer (Harrick Scientific, Ossining, NY).

3. Methods

3.1. Cleaning of Microfabricated ECC IME

*3.1.1. Standard Wash for Grease and Solvent Removal (*see ***Note 6****)*

1. Set up a water bath to accommodate wash solvents.
2. Immerse ECC IME chip in boiling trichloroethylene (TCE) for 3 min.
3. Immerse ECC IME chip in boiling acetone for 3 min.
4. Ultrasonicate the ECC IME chip in 2-propanol for 3 min
5. Wash the ECC IME chip in flowing DI water for 3 min.

3.1.2. Activation of Borosilicate Glass Surface and Removal of Residual Organic/Ionic Contamination

1. Heat the 5:1:1 solution of H_2O:NH_4OH:H_2O_2 (30% aqueous) to 75–80°C in a water bath.
2. Immerse the ECC IME device in the heated 5:1:1 solution of H_2O:NH_4OH:H_2O_2 for 1–10 s (*see* **Note 7**).
3. Wash immediately in flowing DI water for 3 min.

3.1.3. Clean the ECC IME Device Using UV-Ozone

1. Clean the ECC IME device for 10–25 min in an UV/Ozone Cleaner to remove adsorbed organics (*see* **Note 8**).
2. Wash the UV-cleaned IME device by ultrasonic washing for 1 min in 2-propanol.

3. Dry the device in an air-filtered convection oven at 80°C from 30 min to 1 h for the complete evaporation of water from the surface.

3.2. Surface Activation of Metallic Digits (Au and Pt)

1. Immerse ECC IME device in 4:1 concentrated H_2SO_4:H_2O_2 (30% aqueous solution) at 80°C for 1–10 s (*see* **Note 9**).
2. Wash immediately in flowing DI water for 3 min and dry in the air-filtered convection oven.

3.3. Silanization of ECC IME Devices

1. Immerse the ECC IME device in 0.1% by volume 3-glycidoxypropyl-trimethoxysilane (GPS) in anhydrous toluene at room temperature for 2 h (*see* **Note 10**).
2. Wash the ECC IME device three times with anhydrous toluene.
3. Oven-cure the polysiloxane on the ECC IME device for 10 min at 110°C in the air-filtered vacuum oven.

3.4. Cathodic Cleaning

1. Set up a three-electrode electrochemical cell arrangement with the ECC IME connected via the STC-7 Test Clip, an external platinum mesh counterelectrode, and the external Ag/AgCl, 3 *M* Cl reference electrode to the PAR 283 Potentiostat/Galanostat.
2. Using the Multimeter, check that the electrode bonding pads on the chip are in contact with the leads on the STC 7 Test Clip. The working electrode to be cathodically cleaned is the shorted version of all the electrodes (A–F) of the ECC IME device (*see* **Note 11**).
3. Submerge the two active regions of the ECC IME device into the pH = 7.4 PBS solution at room temperature.
4. Cycle the electrodes between –1.2 and –2.0 V at a scan rate of 50 mV/s for 5–8 min. For an 8-min cycling, 15 cycles should occur.
5. Gently tap the electrode handle to dislodge any bubbles attached to the electrode surface.
6. Rinse the electrodes with DI, distilled water.

3.5. Silverization of ECC IME Reference Electrodes by Galvanostatic Deposition

1. Set up a three-electrode electrochemical cell arrangement with the ECC IME connected via the STC-7 Test Clip and the external Ag/AgCl, 3 *M* Cl to the PAR 283 Potentiostat /Galanostat.
2. Using the Multimeter, check that the electrode bonding pads on the chip are in contact with the leads on the STC 7 Test Clip. Set the electrode to be silverized (G = REF) as the working electrode and short the large area electrodes (B = C2CE and E = C1CE) as the counterelectrode and place the Ag/AgCl, 3 *M* Cl to serve as the external reference electrode.

3. Submerge the two active regions of the ECC IME device into the Technic Silver Cy-less II Ready-to-Use electroplating solution at room temperature.
4. Calculate the appropriate current (I) and time (t) for silverization based on the known or calculated working electrode area and the charge density of 6456 mC/cm^2 at a current density of 5.38 mA/cm^2.
   - I (current setting, mA) = Total REF electrode area of ECC IME XX05 (cm^2) * Current density (5.38 mA/cm^2)
   - Q (total charge, mC) = Charge density of 6,456 mC/cm^2 * Total REF electrode area of ECC IME XX05 (cm^2)
   - t (duration, s) = Q (mC)/I (mA)
   - For ECC IME 1005, t = 2,368.5 mC/cm^2 * 0.000454 cm^2/0.000454 cm^2 * 5.38 mA/cm^2 = 1200 s or 20 min (*see* **Note 12**)
5. Apply the calculated current for the calculated duration vs Ag/AgCl to achieve silverization.
6. Verify siliverization by checking the potential difference between the silverized REF electrode and the external Ag/AgCl, 3 *M* Cl^- using the Multimeter. The ΔE should be close to zero and steady.
7. Rinse the ECC IME device with DI, distilled water.

3.6. Platinization of ECC IME Working Electrodes by Galvanostatic Deposition

1. Set up a three-electrode electrochemical cell arrangement with the ECC IME connected via the STC-7 Test Clip and the external Ag/AgCl, 3 *M* Cl to the Potentiostat/Galanostat.
2. Using the Multimeter, check that the electrode bonding pads on the chip are in contact with the leads on the STC 7 Test Clip. Short (connect together) the electrodes to be platinized (WE_{TOT} = A + C + D + F, where A = C2W2, C = C2W1, D = C1W1, F = C1W2) as the working electrode, and short the large-area counter-electrodes (CE_{TOT} = B + E, where B = C2C2 and E = C1CE) as the counter-electrode and the recently silverized electrode (G = REF) as reference electrode.
3. Submerge the two active regions of the ECC IME device into the YSI 3140 Platinizing Solution at room temperature.
4. Calculate the appropriate current (I) and time (t) for platinization based on the known or calculated working electrode area and the charge density of 6000 mC/cm^2 at a current density of 59.0 mA/cm^2.
   - I (current setting, mA) = Total working electrode area (WE_{TOT}) of ECC IME XX05 (cm^2) * Current density (59.0 mA/cm^2)
   - Q (total charge, mC) = Charge density of 6000 mC/cm^2 * Total working electrode area (WE_{TOT}) of ECC IME XX05 (cm^2)
   - t (duration, s) = Q (mC) / I (mA)
   - For ECC IME 1005 (10 µm line and space), t = (6,000 mC/cm^2 * 2 * 0.000946 cm^2) / (2 * 0.000946 cm^2 * 59.0 mA/cm^2) = 102 s or 1.70 min (*see* **Note 12**)
5. Apply the calculated current for the calculated duration vs Ag/AgCl to achieve platinization.

6. Rinse the ECC IME device with DI, distilled water and dry in the air-filtered convection oven.
7. Verify there is no short-circuit of the electrode digits by checking the resistance between the digits with the Multimeter set to Ohms. The resistance should still correspond to open circuit. Verify the quality and distribution of the platinization by inspection under an optical microsope.

3.7. DNA Probe Immobilization

1. Prepare a 150-µ*M* solution of the oligonucleotide probe in a pH 5.4 spotting buffer (0.5X SSC buffer and 1.5 *M* betaine) (*see* **Note 13**).
2. Incubate single-strand oligonucleotide probes on GPS-modified ECC IME surface overnight at 50°C in pH 5.4 spotting buffer.
3. Wash for 15 min with DI, distilled water at 50°C to remove unreacted DNA probe.
4. Repeat the cathodic cleaning (**Subheading 3.4.**) to remove nonspecifically adsorbed oligonucleotide probes from the metallic digits.
5. For storage, dry the ECC IME device in a desiccator for several hours and store in a sterile DNAse-free container before use. To use stored DNA chips, rehydrate in hybridization buffer.

3.8. Preparing a Photoresist Master

The preparation of the master follows conventional photolithography methods for a negative SU-8 photoresist on a silicon wafer ***(18)***. The process is illustrated in **Fig. 4**.

1. The silicon wafer is blown with a stream of air to remove any dust on the surface and then placed in a sealed container containing HMDS to promote adhesion of the resist.
2. The wafer is then placed on the spin coater chuck and held in place with vacuum. SU-8 photoresist is added dropwise from a medicine dropper into the center of the wafer and spun at 1000 rpm for 40-µm thickness (*see* **Note 14**).
3. The wafer is then transferred to a hotplate and soft-baked for 15 min at 95°C to set the resist (*see* **Note 15**).
4. A photomask containing an image of the microfluidic pattern is placed directly on top of the resist-coated wafer and illuminated under UV light (*see* **Note 16**).
5. A postexposure bake is then performed at 95°C for 4 min (*see* **Note 17**).
6. The wafer is then placed in the developer for a recommended time of 6 min for 40 µm (*see* **Note 18**). Following development, the wafer is rinsed with 2-propanol and dried with a stream of air. The positive relief formed on the wafer acts as the master (*see* **Note 19**).

3.9. Making the PDMS Replica

The preparation of the replica follows conventional processing methods for PDMS ***(19)***. The process is illustrated in **Figs. 6** and **7**.

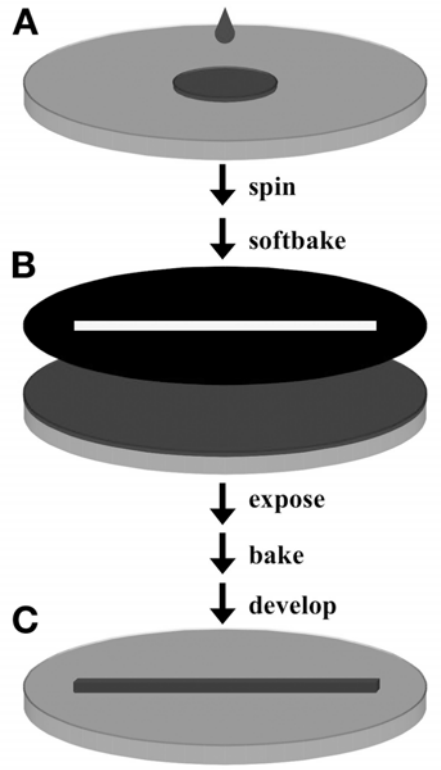

Fig. 6. Preparation of the master mold: **(A)** Photoresist added dropwise in the center of the silicon wafer. **(B)** After spinning the resist to achieve the desired thickness, photomask containing the desired features is brought into contact with the surface and the features are illuminated. **(C)** After removing the unexposed photoresist, the patterned features are left on the wafer as positive relief.

1. The PDMS elastomer base and curing agent are mixed in a 10:1 ratio as per manufacturer's instructions. The mixture is stirred thoroughly and poured over the master.
2. The master and elastomer are placed in a dessicator, and vacuum is applied to remove any air bubbles from the PDMS. The combination is then transferred to an oven for 45 min at 100°C to set the elastomer (*see* **Note 20**).
3. The resulting PDMS replica can then be peeled off from the master, yielding a negative relief containing the microfluidic network.

3.10. PDMS–Glass Bonding

The PDMS will form a reversible seal by bringing it into contact with a clean glass surface, and this may suffice. However, to ensure a good fluidic

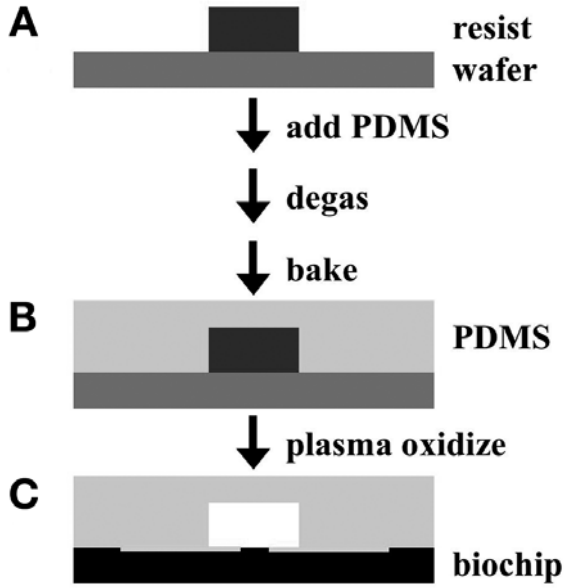

Fig. 7. Making the poly(dimethylsiloxane) (PDMS) replica: **(A)** End-on view of feature in resist master. **(B)** PDMS is poured onto the master, degassed, and baked to set. **(C)** Once the PDMS is set, it is removed from the master, plasma-oxidized, and bonded to the biochip.

seal and prevent leakage, the elastomer surface is plasma-oxidized to form an irreversible seal against the glass. The surface is exposed to the plasma for approx 1 min before being removed from the chamber and brought into contact with the array chip (*see* **Note 21**).

3.11. Integrated System Assembly and Test

1. Gently apply the PDMS fluidic chamber to the surface of the chip such that the electrochemical cells sit within and form the base of a designated channel.
2. Introduce buffer under pressure-driven or electroosmotic flow and check for leaks.

3.12. DNA Hybridization

1. Dissolve 8.22 µ*M* oligonucleotide target in hybridization buffer (20 µL phosphate-buffered KCl solution and 100 µL MWG hybridization buffer) for 4 h at 42°C.
2. Introduce target DNA into the microfluidic DNA detector and commence electrochemical impedance measurements.

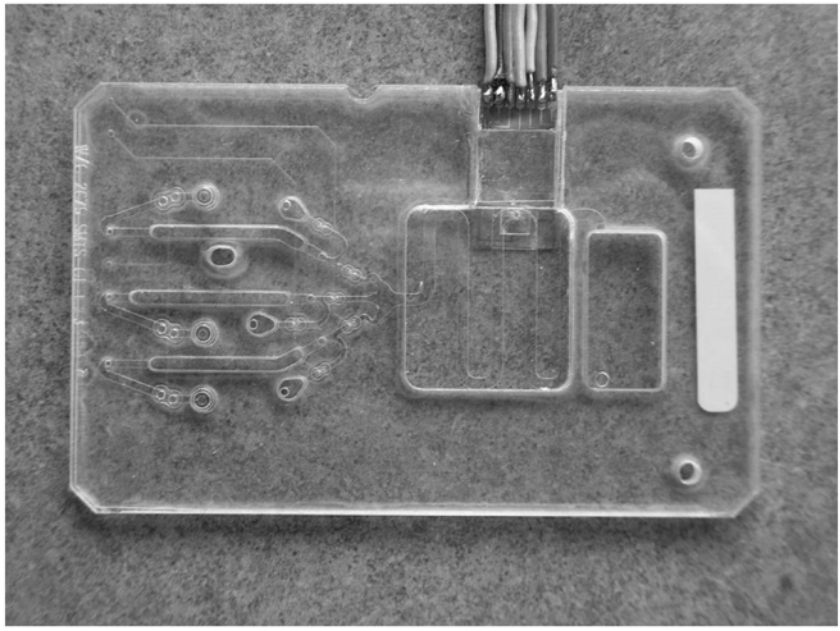

Fig. 8. An integrated biochip showing the microfabricated pattern of electrodes bonded and sealed into the Micronics' microfluidic T-cassette.

3.13. Electrochemical Impedance Measurements

1. Set the two members of the interdigitated pair of electrodes of any one fluidic detector to the working electrode (e.g., WE = D = C1W1) and the counter-electrode (CE = F = C1W2) and connect the reference electrode to the silverized electrode (G = REF). **Figure 8** shows an example of an integrated biochip with a Micronics Microflow T-cassettte.
2. Check the quality of the connections using the Multimeter set at 40MΩ and activating the range with the audio on.
3. Electrochemical impedance measurements may be taken before, during, and following the hybridization event in hybridization buffer.
4. Impedance measurements should be performed in the hybridization buffer.
5. The frequency-dependent electrochemical impedance spectra may be obtained before (t = 0) and after (t = ~16 h) using a 10 mV amplitude sine wave over the frequency range of 10 mHz – 1.0 GHz at 20 ± 1°C using the Perkin-Elmer Princeton Applied Research M283 Potentiostat/Galvanostat coupled with a Solartron Schlumberger 1260 FRA.
6. Temporal impedance measurements are made at 10 mV amplitude sine wave at a frequency of 4 kHz.

4. Notes

1. Each borosilicate glass chip consisted of two discrete electrochemical cells over which channels were constructed. Each cell comprised a pair of circumferential presented interdigitated microsensor electrodes, a silverized reference electrode (0.1 × WE area), and a counterelectrode (10 × WE area). Each digit of the IME was 5 μm wide and was separated from its nearest opposing digit by 5 μm space. (Part number ECC IME 0505-Pt-U; ABTECH Scientific, Inc.)
2. The bottle of 3-glycidoxypropyl-trimethoxysilane must be degassed before storage by gently flowing nitrogen or argon gas over the top of the bottle for approx 5 min. Nitrogen or argon is used to displace air (moisture), which will initiate polymerization without displacement. Alternatively, a canular may be used.
3. Complementary, noncomplementary (random), single, and multiple mismatched target oligonucleotides are used to compare effects on EIS between specific and nonspecific hybridization.
4. In addition to the photoresist used in this work, different SU-8 formulations are available for a wide range of thickness with high aspect ratio features.
5. A local printing company was used to obtain a high resolution (3600 dpi) transparency. The microfluidic features were designed using Adobe Illustrator (San Jose, CA) software. When using a negative resist, the desired features are transparent in the mask.
6. This procedure is a general degreasing method that should be performed in sequence without much delay between steps.
7. This procedure is an aggressive alkaline etch of the glass; it removes trace organics and physically adsorbed monolayers of adventitious organics that are not removable by the procedure described in **Subheading 3.3.** *Caution*: Do not exceed the recommended 10 s because this etch may undercut the delicate microfabricated electrodes.
8. This procedure removes monomolecular layers of bound organics on metallic and oxide surfaces. This procedure removes chemisorbed and covalently bound self-assembled monolayers of adventitious organics, alkane thiols, and silane layers. This method is not applicable to thick organic films.
9. This procedure provides addition cleaning and activates the surface by producing a uniform concentration of hydroxyl groups at the surface.
10. Fresh solution should be made for each silanization reaction.
11. Cathodic cleaning is necessary to remove covalently attached GPS on the electrodes.
12. By adjusting the applied constant current to the area of the candidate electrode, the time to achieve the required charge density is always 1.7 min.
13. Spotting buffers are used in the fabrication of oligonucleotides microarrays.
14. The manufacturer recommends approx 1 mL of resist per 25 mm wafer diameter. An initial spread cycle is used to ensure uniform coverage, and it consists of a 100 rpm/s ramp to 500 rpm. To achieve the desired thickness, the wafer is ramped at 300 rpm/s to the appropriate spin speed and held for 30 s.
15. A prebake is recommended before the soft bake, although this will require either a second hotplate for temperature stepping or a programmable hotplate for

ramping. When a second hotplate is used, a 5-min prebake is recommended at 65°C. This allows the solvent to evaporate out of the resist film at a more controlled rate to ensure coating fidelity.

16. The manufacturer offers suggestions for wavelength and exposure dose as a function of desired thickness, but recommends using 350–400 nm.
17. A 1-min prebake at 65°C is recommended to minimize resist cracking.
18. Development time is approximate, as it will vary with such parameters as agitation and temperature.
19. While SU-8 has good mechanical properties, it may be desirable to perform a hard bake to preserve the integrity of the master. This will require a ramp or step to 150–200°C, with bake times of approx 30 min being sufficient.
20. The degassing step takes approx 30 min, and any bubbles remaining on the surface can be removed with a sharp utensil. As an alternative to the oven, the PDMS can be left out of the oven to cure overnight at room temperature.
21. If the glass–PDMS bond does not seal after oxidation, it may help to oxidize both of the surfaces to be bonded.

Acknowledgments

This work was supported by the consortium for the Center for Bioelectronics, Biosensors and Biochips, Virginia Commonwealth University (C3B) and by the Commonwealth Technologies Research Fund (CTRF) Grant no.: SE2002-02.

References

1. Guiseppi-Elie, A. (2003) Biochip platform for DNA diagnostics. *PharmaTech* **87,** 1–6.
2. Landers, J. P. (2003) Molecular diagnostic analysis using electrophorectic microchips. *Anal. Chem.* **75,** 2919–2927.
3. Breadmore, M. C., Wolfe, K. A., Arcibal, I. G., et al. (2003) Microchip-based purification of DNA from biological samples. *Anal. Chem.* **75,** 1880–1886.
4. Schena, M., ed. (1999) *DNA Microarrays: A Practical Approach*, Oxford University Press, New York.
5. Guiseppi-Elie, A. and Lingerfelt, L. (2005) Impedimetric detection of DNA hybridization: towards near patient DNA diagnostics, in *Immobilisation of DNA on Chips 1*(Wittmann, C., ed.), Springer-Verlag, New York.
6. Gheorge, M. and Guiseppi-Elie, A. (2003) Electrical frequency dependent characterization of DNA hybridization. *Bios. Bioelectron.* **19,** 95–102.
7. Hang, T. C. and Guiseppi-Elie, A. (2004) Frequency dependent and surface characterization of DNA immobilization and hybridization. *Bios. Bioelectron.* **19,** 1537–1548.
8. Guiseppi-Elie, A., Wallace, G. G., and Matsue, T. (1998) Chemical and biological sensors based on electrically conducting polymers, in *Handbook of Conducting Polymers* (Skotheim, T. A., Elsenbaumer, R. L., and Reynolds, J. R., eds.), Marcel Dekker, Inc., New York.

9. Gheorge, M. and Guiseppi-Elie, A. (2000) Low-density arrays of DNA-doped polypyrrole. *Proc. Am. Chem. Soc. PMSE* **83,** 550–551.
10. Lei, C., Gheorge, M., and Guiseppi-Elie, A. (2000) DNA immobilization and bioelectric detection based on conducting polymers. *Proc. Am. Chem. Soc. PMSE* **83,** 552–553.
11. Popovich, N. D., Eckhardt, A. E., Mikulecky, J. C., Napier, M. E., and Thomas, R. S. (2002) Electrochemical sensor for detection of unmodified nucleic acids. *Talanta* **56,** 821–828.
12. Sheppard, J. and Guiseppi-Elie, A. (1998) Enzyme sensors based on conductimetric measurement, in *Enzyme and Microbial Biosensors: Techniques and Protocols* (Mulchandani, A. and Rogers, K. R., eds.), Humana Press, Totowa, NJ.
13. Kell, D. B. (1987) The principles and potential of electrical admittance spectroscopy: an introduction, in *Biosensors: Fundamentals and Applications* (Turner, A., Karube, I., and Wilson, G. S., eds.), Oxford University Press, Oxford, pp. 427–468
14. Lamture, J. B., Beattie, K. L., Burke, B. E., et al. (1994) Direct detection of nucleic acid hybridization on the surface of a charge coupled device. *Nucleic Acids Res.* **22,** 2121–2125.
15. Maskos, U. and Southern, E. M. (1992) Oligonucleotide hybridizations on glass supports: a novel linker for oligonucleotide synthesis and hybridization properties of oligonucleotides synthesized in situ. *Nucleic Acids Res.* **20,** 1679–1684.
16. Sales, J. A. A., Prado, A. G. S., and Airoldi, C. (2002) The incorporation of propane-1,3-diamine into silylant epoxide group through homogenous and heterogeneous routes. *Polyhedron* **21,** 2647–2651.
17. Taylor, S., Smith, S., Windle, B., and Guiseppi-Elie, A. T. (2003) Impact of surface chemistry and blocking strategies on DNA microarrays. *Nucleic Acids Res.* **31,** e87.
18. Duffy, D. C., McDonald, J. C., Schueller, O. J. A., and Whitesides, G. M. (1998) Rapid prototyping of microfluidic systems in poly(dimethylsiloxane). *Anal. Chem.* **70,** 4974–4984.
19. Lorenz, H., Despont, M., Fahrni, N., LaBianca, N., Renaud, P., and Vettiger, P. (1997) SU-8: a low-cost negative resist for MEMS. *J. Micromechan. Microeng.* **7,** 121–124.

9

Applications of Functional Protein Microarrays

Identifying Protein–Protein Interactions in an Array Format

Matthew A. Coleman, Peter T. Beernink, Julio A. Camarero, and Joanna S. Albala

Summary

The use of protein arrays and their importance in proteomic applications continues to be at the forefront of scientific discovery and innovative technology development. To date, array-based approaches have proven to be a powerful tool for protein expression profiling, novel biomarker discovery, and the examination of protein, DNA, and small molecule interactions. Our laboratory has developed several approaches for characterizing protein–protein interactions using protein microarrays for a variety of different biological applications. Here we describe the identification of protein–protein interactions using a microarray format.

Key Words: Protein microarray; *in vitro* expression; fluorescence; green fluorescent protein; protein interactions.

1. Introduction

The use of a microarray format to analyze molecular interactions provides a unique method of high-throughput screening for functional analysis, basic biology, and novel biomarker discovery (for review, *see* **refs. *1–3***). Protein microarrays utilize a genomic scale approach for identifying or characterizing proteins and have now been well adapted for studying protein–protein interactions ***(4,5)***. These developments enable extremely small-scale expression screening, either directly using labeled proteins or indirectly by immunological detection ***(6)***, and are performed in a parallelized and miniaturized format ***(7)***. The development of protein microarray strategies for analysis of dynamic protein-related interactions such as those found associated with chromatin will greatly propel our understanding of processes involved in transcription, translation, and DNA repair. This protocol was specifically developed for identify-

From: *Methods in Molecular Biology, Vol. 385: Microchip-Based Assay Systems: Methods and Applications*
Edited by: Pierre N. Floriano © Humana Press Inc., Totowa, NJ

ing potential relationships between novel DNA repair proteins and chromatin components. To this end, we employed protein interaction microarrays to examine possible protein–protein interactions between the chromatin remodeling Swi/Snf-like proteins and those involved in DNA repair *(8)*.

In order to develop more rapid protein expression screening approaches, we have combined the attributes of high-throughput protein expression with rapid and sensitive fluorescence labeling and detection systems. Our laboratory has developed high-throughput expression screening methods in both cell-free *(9)* and whole cell expression systems *(10)* that produce proteins in a miniaturized format amenable to array-based approaches. These high-throughput protein expression systems have been used to identify highly expressed proteins for structural studies and for the generation of a variety of proteins for biochemical assays and interaction analyses *(8,11)*. Fluorescence-based protein expression screens have been implemented in several formats—microplate, dot blot, and protein microarray—that utilize fluorescent–labeling to enable rapid, reproducible detection of proteins with high sensitivity and a wide dynamic range *(9)*. These approaches facilitate extremely small-scale expression screening either directly using fluorescently labeled amino acid into the protein or indirectly by fluorescence-based immunoassay.

Our approach for using microarrays to study protein interactions has evolved into an assembly line that takes advantage of multiple molecular techniques (**Fig. 1**). First, methods were developed for producing recombinant proteins. To accomplish this we have applied two protein expression technologies, using both in vitro and in vivo (baculovirus) techniques *(9,10)*. In vitro transcription/translation (IVT) is faster than cell-based methods and has the ability to produce proteins that are difficult to obtain because they are toxic or subject to proteolysis using in vivo systems. Baculovirus expression systems provide high levels of protein expression and are capable of accurate posttranslational modification/processing of proteins. Second, methods for arraying and protein attachment were devised using commercially obtained glass slides for arraying the proteins. Third, detection strategies requiring the use of fluorescently–labeled molecules were employed. The following section outlines in detail the methods developed for studying protein–protein interactions by microarray. Linkage of these methodologies will be important for achieving future automation.

2. Materials

2.1. Protein Expression and Screening

1. *E. coli* clones from the LLNL-IMAGE Consortium cDNA collection *(12)*.
2. pIVEX-2.4b (Roche), GFPfolder *(16)*, pETBlue-2 (Novagen).
2. *Tgo* DNA polymerase (Roche).

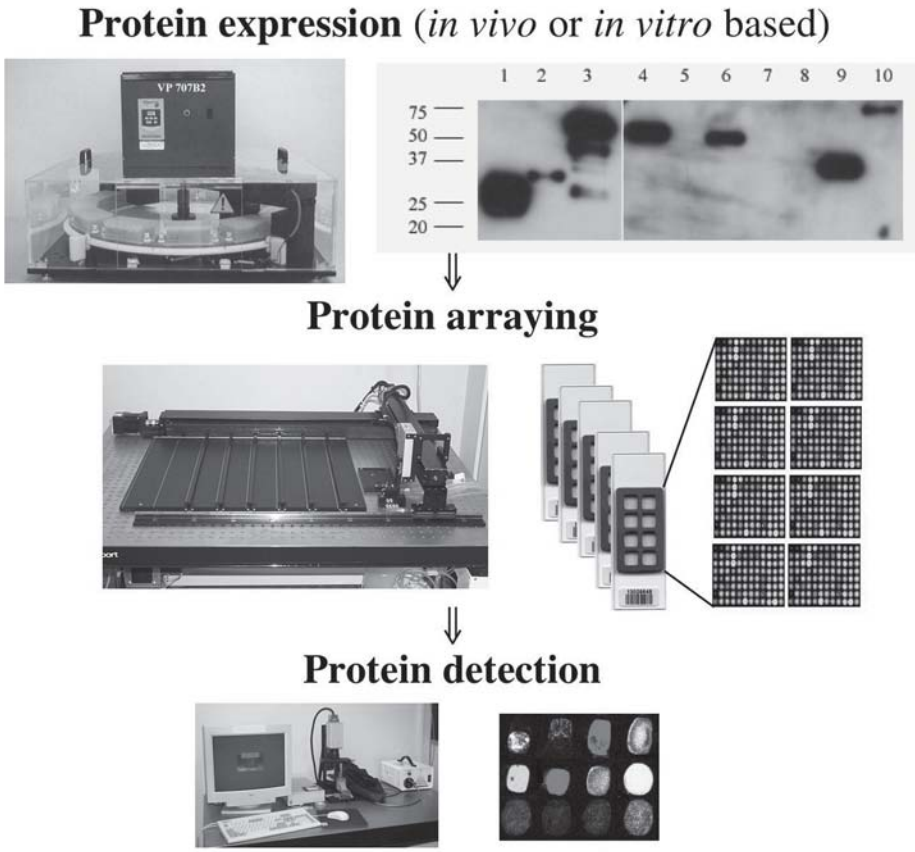

Fig. 1. Protein expression (*in vivo* or *in vitro* based): scheme for automated protein expression, arraying, and characterization. Illustrated are the respective steps involved starting from protein production and purification (protein expression) to microarray spotting (protein arraying) and, finally, protein characterization (protein detection). Using in vitro transcription technologies. this entire process is automatable and can be performed in less than 8 h. The robotics included a Carousel Levitation Stirrer (V & P Scientific) for recombinant protein expression in baculovirus, a robotic arrayer (Norgren Systems). and a detector (ScanArray 5000 XL, Perkin Elmer).

3. PicoGreen dsDNA Quantification Kit (Molecular Probes).
4. RTS-100 and RTS-500 HY IVT systems (Roche).
5. Baculovirus system ***(13)***.

2.2. Protein Array Printing and Imaging

1. Barcoded glass slides coated with γ-aminopropylsilane (GAPS II™; Corning).
2. Robotic arrayer (Norgren Systems).

3. Spotting buffer: 50 m*M* hydroxyethyl piperazine ethane sulfonate (HEPES) pH 7.5, 5% glycerol, 50 m*M* KCl.
4. Bovine serum albumin (BSA).
5. Cy3- and Cy5-labeled DNA (Molecular Probes).
6. Laser-based confocal scanner (ScanArray 5000 XL; Perkin Elmer).

2.3. Microarray-Based GFP Immunoassays

1. Hybridization chamber (Schleicher & Schuell).
2. Blocking buffer: 1X PBS, 1% Tween-20, 100 µg/mL BSA.
3. Wash buffer: 50 m*M* Tris-HCl pH 7.5, 50 m*M* NaCl, 2 m*M* dithiothreitol (DTT), 0.5% NP-40.
4. GFP antibody (BD Clontech Living Colors).
5. Rhodamine-labeled goat anti-mouse 2° antibody (Santa Cruz Biotechnology).
6. ScanArray 5000 XL (Perkin Elmer) with QuantArray software (Packard Bioscience).

2.4. Identifying Protein–Protein Interactions Using Microarrays

1. Spotting buffer: 50 m*M* HEPES·KOH pH 7.5, 5% glycerol, 50 m*M* KCl.
2. Barcoded glass slides coated with γ-aminopropylsilane (GAPS II™; Corning).
3. Hybridization chamber (Schleicher & Schuell).
4. Blocking buffer: 3% fat-free milk powder, 1X PBS, 1% Tween-20, 100 µg of BSA (10X PBS: 80 g NaCl, 2 g KCl, 14.4 g Na_2HPO_4, 2.4 g KH_2PO_4, adjust pH to 7.4 with HCl).
5. Wash buffer: 50 m*M* Tris-HCl, pH 7.5, 50 m*M* NaCl, 2 m*M* DTT, 0.5% NP-40.
6. FITC and rhodamine-labeled goat anti-mouse 2° antibody (Santa Cruz Biotechnology).

3. Methods

3.1. Cell-Free Protein Expression Screening

Cell-free or IVT production of proteins has become widely accepted as a means to overcome bottlenecks in protein expression and purification in support of high-throughput structural proteomics applications ***(11)***. Importantly, cell-free protein expression can bypass many of the difficulties often associated with other recombinant protein expression methods such as cloning, cell transfection, and cell growth by eliminating several steps of the process ***(14)***. This approach can accelerate protein production and is easily amenable to robotic automation for high-throughput production. Cell-free systems also allow for unique strategies for protein labeling and tagging for downstream visualization of protein interaction or function by directly incorporating the fluorescent label in to the protein. However, more complex mammalian proteins containing multiple posttranslational modifications often require a eukaryotic environment for recombinant protein production. We have there-

fore also utilized a baculoviral expression system to produce proteins using an insect cell-based system as previously described ***(10,13,15)***.

1. Selected cDNAs were cloned into expression vector of interest (*see* **Note 1**): for example, pIVEX-2.4b (Roche Applied Science), GFPfolder ***(16)***, or pETBlue-2 (Novagen).
2. Polymerase chain reaction (PCR) reactions were performed with primers specific to the T7 promoter (GCGCGCGAGATCTCGATCCCGCGAAATTAA TACGAC) and terminator (GCGCGCGTATCCGGATATAGTTCCTCCTTTCAG) regions using *Tgo* DNA polymerase (Roche).
3. PCR products were quantified using the PicoGreen dsDNA Quantitation Kit (Molecular Probes) or by agarose gel electrophoresis.
4. IVT reactions were performed using the RTS 100 HY Kit (Roche) and approx 100-ng PCR product.
5. Reactions were incubated at 30°C for 3 h.
6. IVT products were spotted as described below (*see* **Note 2**).

3.2. Protein Array Printing and Imaging

We have used contact microarray spotting technology to attach proteins to a glass slide in an array format for multiple functional genomics studies ***(8,17,18)***. Our current microarrayer is capable of arraying proteins on 100 slides at densities as high as 10^4 array elements per centimeter squared. In addition, we are developing future capabilities for the immobilization and presentation of proteins that use "expressed protein ligation" for the creation of protein microarrays ***(18)***. By this technique, proteins are site-specifically immobilized on the surface of the slide using an intein-based chemistry allowing control of the orientation of the proteins on the array.

1. Glass slides were spotted with protein samples using a robotic arrayer.
2. Proteins were diluted to concentrations ranging from 5 ng/mL to 1 mg/mL in spotting buffer.
3. A single print head was used to deposit approx 1 nL of diluted protein solution on the slide (*see* **Note 3**).
4. Proteins were spotted in duplicate or triplicate, generating approx 300-µm-diameter spots with a spot-to-spot distance of approx 350 µm.
5. BSA served as nonfluorescent control, while Cy3- and Cy-5 labeled DNA were used as position controls to mark the four corners of the array.
6. After spotting, the slides were stored in the dark at 4°C (*see* **Note 4**).
7. GFP fusion proteins were imaged with a laser-based confocal scanner (ScanArray 5000 XL; Perkin Elmer) using the 488-nm Ar laser to detect fluoroscein-labeled fusion proteins, a GHeNe 543 nm laser for Cy3-labeled DNA, and a HeNe 594 nm laser for detection of Cy5-labeled DNA.
8. Images were collected and analyzed using mean pixel intensities with QuantArray™ software (Packard Bioscience).

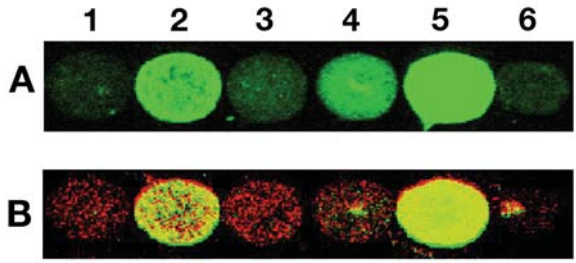

Fig. 2. Microarray-based detection of green fluorescent protein (GFP) expression: **(A)** Image from a protein microarray showing in vitro transcription (IVT)-expressed GFP fusion proteins and controls that were spotted with a center to center spot distance of 350 µm. Each spot is approx 200 µm in diameter. The sources of template DNA (plasmid or polymerase chain reaction product) for the IVT reaction were as follows: (1) lysate control, (2) TN1331, (3) RAD23A, (4) LcrG, (5) LcrH, (6) blank. **(B)** Immunological detection of GFP-fusion proteins on a microarray. Proteins were spotted as above and detected with an anti-GFP 1° antibody followed by a rhodamine-labeled 2° antibody. The GFP (green) and rhodamine (red) fluorescence were detected with 488 and 543 nm filters, respectively. A yellow spot indicates fluorescence from both GFP and the rhodamine-labeled 2° antibody (described in detail in **ref. *9***).

3.3. Microarray-Based GFP Immunoassays (Western-Based Detection)

An obvious application of high-throughput protein expression is the identification of proteins expressed from hypothetical genes and the production of highly expressed recombinant proteins for functional analysis. An efficient screening process to identify highly expressed proteins (or variants of a single protein) is of potential value, because obtaining homogeneous, soluble protein is the major bottleneck in structural genomics projects ***(11)***. The combined use of IVT and fusion protein tags enable extremely small-scale expression screening either directly using GFP fusion constructs or indirectly by immunoassay. As shown in **Fig. 2**, several GFP fusion constructs were detected by both inherent green fluorescence (**Fig. 2A**) and rhodamine-based immunofluorescence resulting in a combined yellow signal in two channels (**Fig. 2B**).

1. For immunological detection of fusion proteins, spotted arrays were covered with a hybridization chamber (Schleicher & Schuell) and filled to a total volume of 300 µL with blocking buffer.
2. The arrays were incubated for 30 min at 25°C with gentle shaking.
3. Wash buffer was applied to the slides three times for 5 min each at 25°C.
4. After the final wash, mouse anti-GFP 1° antibody (BD Clontech Living Colors) was diluted 1:500 in 400 µL of PBST (PBS with 1% Tween) and was incubated for 30 min at 25°C with gentle shaking.

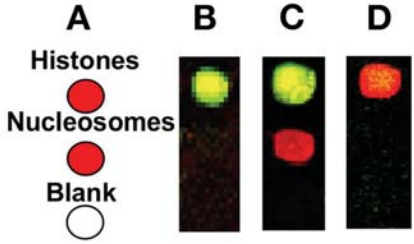

Fig. 3. Identification of protein–protein interaction by protein microarray. **(A)** Proteins arrayed on the slides for binding studies as shown in **C** and **D**. **(B)** Control protein shows no binding to histones or nucleosomes. The yellow spot represents the background fluorescence of the histone proteins. **(C)** The target protein SMARCAL1 binds to the nucleosome complex as indicated by the red spot. Slides were incubated with primary antibody to SMARCAL1 followed by incubation with a rhodamine-labeled secondary antibody. **(D)** The target protein Rad51B binds to histones and not nucleosomes on the array, as indicated by the red spot. Slides were incubated with primary antibody to Rad51B followed by incubation with a rhodamine-labeled secondary antibody (described in detail in **ref. *8***).

5. This was followed by three 5-min washes at 25°C.
6. Rhodamine-labeled goat anti-mouse 2° antibody (Santa Cruz Biotechnology) was diluted 1:250 in 400 µL of PBST and was incubated for 30 min at 25°C with gentle shaking.
7. The incubation with the 2° antibody was followed by three additional 5-min washes with gentle shaking.
8. Imaging and analysis of the arrays were performed on a ScanArray 5000 XL (Perkin Elmer) using QuantArray software (Packard Bioscience).

3.4. Identifying Protein–Protein Interactions Using Far-Western Assay Microarrays

The use of a chip/microarray format to analyze protein–protein interactions provides a unique method of high-throughput screening for functional analysis. Protein arrays allow multiplexed protein detection along with sensitive quantification in a miniaturized format ***(19)***. Our laboratory has utilized the microarray format for studying a variety of novel protein–protein interactions as shown in **Fig. 3**, where protein arrays were utilized to examine a chromatin remodeling protein, SMARCAL1, and the DNA repair enzyme, Rad51B ***(8,17)***.

1. Purified proteins and IVT-expressed proteins were resuspended in spotting buffer at concentrations ranging from 0.01 to 10 ng/nL.
2. Proteins were spotted in duplicate on aminopropyl triethoxysilane- and/or polylysine-coated glass slides using a robotic arrayer.

3. After spotting, the arrays were dried at 25°C and then stored at 4°C until use.
4. Spotted arrays were covered with a hybridization chamber and filled to a total volume of 300 mL of blocking buffer.
5. Slides were blocked for 15 min at 25°C with gentle shaking.
6. Wash buffer (50 m*M* Tris pH 7.5, 50 m*M* NaCl, 2 m*M* DTT, 0.5% NP-40) was then used to wash the slides three times for 5 min at 25°C.
7. After the final wash, 50 ng of target protein was diluted in 300 µL of interaction buffer and added to the array for 30 min at 25°C with gentle shaking.
8. The slides were washed three times in wash buffer for 5 min at 25°C.
9. Primary antibody against the target protein was diluted in 400 mL of buffer and incubated for 30 min at 25°C with gentle shaking.
10. Following this incubation, the slides were washed three times for 5 min in wash buffer.
11. A fluorochrome-labeled secondary anti-goat or anti-rabbit antibody was diluted in buffer and incubated for 30 min at 25°C with gentle shaking.
12. This was followed by three 15-min washes with gentle shaking at room temperature.
13. Scanning and analysis were performed on a 4 laser ScanArray 5000 XL (Perkin Elmer) using QuantArray (Packard BioScience).

3.5. Conclusion

Protein arrays are highly amenable to miniaturization and portability and therefore have potential applications in basic biological research, genomic annotation, identification of disease biomarkers, as well as for diagnostics ***(20–22)***. Coupled with high-throughput methods to express and purify proteins, protein arrays have the potential to identify and characterize newly discovered proteins and protein complexes. Production of proteins to provide content for protein microarrays remains a challenge, as does providing quality control for proteins on the array. Furthermore, use of antibodies for array-based proteomics relies on the availability of highly sensitive and specific antibodies that are often expensive or hard to produce. Nonetheless, array-based approaches are a powerful tool for studying protein, DNA, and small molecule interactions. Our laboratory has developed several approaches for producing proteins and characterizing their interactions using microarrays. Future plans to fully automate the process through linking of these methodologies could advance the screening and characterization of these proteins and further our understanding of the cellular proteome.

4. Notes

1. Both plasmid-based and PCR products encoding a T7 promoter can be used in this process.
2. IVT reactions can be quickly assessed for protein production using the following dot blot protocol: (1) The tRNA-Lysine-BODIPY conjugate FluoroTect Green$_{Lys}$ (Promega) is added at a ratio of 1 µL of FluoroTect per 50 µL IVT reaction

volume. After the reactions are complete, a 5-µL sample is diluted with 100 µL urea lysis buffer (8 *M* urea, 10 m*M* Trizma base, $NaPO_4$ pH 8.0) and applied to a PVDF membrane by vacuum. (2) This is followed by washes with urea lysis buffer (200 µL) and PBS (200 µL). (3) The membrane is dried and washed in PBS for up to 1 h prior to detection. (4) Fluorescence detection is accomplished by imaging the washed PVDF membrane on a FluorImager 595 (Molecular Dynamics) using an excitation wavelength of 488 nm and an emission wavelength of 510 nm.

3. We have determined that robotic spotting is best when the humidity is greater than 30%.
4. In our experience, slides remain stable at 4°C when printed with GFP for approx 1 yr, but we prefer to use our slides within 1 mo of printing.

Acknowledgments

The authors would like to thank Christa Prange for critical evaluation of this manuscript. This work was performed under the auspices of the U.S. Department of Energy by the University of California, Lawrence Livermore National Laboratory under Contract W-7405-Eng-48.

References

1. Albala, J. S. (2001) Array-based proteomics: the latest chip challenge. *Exp. Rev. Mol. Diag.* **1(2),** 145–152.
2. Cahill, D. J. (2001) Protein and antibody arrays and their medical applications. *J. Immunol. Methods* **250(1–2),** 81–91.
3. Poetz, O., Schwenk, J. M., Kramer, S., et al. (2005) Protein microarrays: catching the proteome. *Mech. Ageing Dev.* **126(1),** 161–170.
4. MacBeath, G. and Schreiber, S. L. (2000) Printing proteins as microarrays for high-throughput function determination. *Science* **289(5485),** 1760–1763.
5. Zhu, H., Klemic, J. F., Chang, S., et al. (2000) Analysis of yeast protein kinases using protein chips. *Nat. Genet.* **26(3),** 283–229.
6. Ramachandran, N., Hainsworth, E., Bhullar, B., et al. (2004) Self-assembling protein microarrays. *Science* **305(5680),** 86–90.
7. Haab, B. B., Dunham, M. J., and Brown, P. D. (2001) Protein microarrays for highly parallel detection and quantitation of specific proteins and antibodies in complex solutions. *Genome Biol.* **2(2),** research 0004.1–0004.13.
8. Coleman, M. A., Miller, K. A., Beernink, P. T., et al. (2003) Identification of chromatin-related protein interactions using protein microarrays. *Proteomics* **3(11),** 2101–2107.
9. Coleman, M. A., Lao, V. H., and Segelke, B. W. (2004) High-throughput, fluorescence based screening for soluble protein expression. *J. Proteome Res.* **3(5),** 1024–1032.
10. Albala, J. S., Franke, K., McConnell, I. R., et al. (2000) From genes to proteins: high-throughput expression and purification of the human proteome. *J. Cell Biochem.* **80(2),** 187–191.

11. Segelke, B. W., Schafer, J., Coleman, M. A., et al. (2004) Laboratory scale structural genomics. *J. Struct. Funct. Genomics* **5(12),** 147–157.
12. Lennon, G., Auffray, C., Polymeropoulos, M., et al. (1996) The I.M.A.G.E. Consortium: an integrated molecular analysis of genomes and their expression. *Genomics* **33,** 151–152.
13. Gilbert, M., Edwards, T. C., and Albala, J. S. (2004) Protein expression arrays for proteomics. *Methods Mol. Biol.* **264,** 15–23.
14. Murthy, T. V., Wu, W., Qiu, Q. Q., et al**.** (2004) Bacterial cell-free system for high-throughput protein expression and a comparative analysis of *Escherichia coli* cell-free and whole cell expression systems. *Protein Expr. Purif.* **36(2),** 217–225.
15. Gilbert, M. and Albala, J. S. (2002) Accelerating code to function: sizing up the protein production line. *Curr. Opin. Chem. Biol.* **6(1),** 102–105.
16. Waldo, G., Standish, B. M., Berendzen, J., and Terwilliger, T. C. (1999) Rapid protein-folding assay using green fluorescent protein. *Nat. Biotechnol.* **17(7),** 691–695.
17. Rao, R. S., Visuri, S. R., McBride, M. T., Albala, J. S., Matthews, D. L., and Coleman, M. A. (2004) Comparison of multiplexed techniques for detection of bacterial and viral proteins. *J. Proteome Res.* **3(4),** 736–742.
18. Camarero, J. A., Kwon, Y., and Coleman, M. A. (2004) Chemoselective attachment of biologically active proteins to surfaces by expressed protein ligation and its application for "protein chip" fabrication. *J. Am. Chem. Soc.* **126(45),** 14,730–14,731.
19. Zhou, H., Bouwman, K., Schotanus, M., et al**.** (2004) Two-color, rolling-circle amplification on antibody microarrays for sensitive, multiplexed serum-protein measurements. *Genome Biol.* **5(4),** R28.
20. Kononen, J., Bubendorf, L., Kallioniemi, A., et al. (1998)Tissue microarrays for high-throughput molecular profiling of tumor specimens. *Nat. Med.* **4(7),** 844–847.
21. Huang, J. X., Mehrens, D., Wiese, R., et al. (2001) High-throughput genomic and proteomic analysis using microarray technology. *Clin. Chem.* **47(10),** 1912–1916.
22. Pawlak, M., Schick, E., Bopp, M. A., et al. (2002) Zeptosens' protein microarrays: a novel high performance microarray platform for low abundance protein analysis. *Proteomics* **2(4),** 383–393.

10

A Microchip-Based Assay for Interleukin-6

Nicolaos Christodoulides, Priya Dharshan, Jorge Wong, Pierre N. Floriano, Dean Neikirk, and John T. McDevitt

Summary

The electronic taste chip (ETC) assay system is a lab-on-a-chip technology that offers a microchip platform on which bead-based immunoassays are performed. Each bead within the array serves as its own independent self-contained "microreactor" system, with its selectivity determined by the specificity of the antibody that it hosts. The bead-loaded chip is sandwiched between two optically transparent polymethylmethacrylate inserts, packaged within a metal casing described here as the "flow cell." This flow cell allows for delivery of sample and detecting reagents to the microchip and the associated beads. Images of fluorescent beads are captured with a digital video chip and analyzed to facilitate detection and, ultimately, quantitation of analytes in complex fluids. This chapter describes the application of the ETC system for the detection and measurement of interleukin (IL)-6.

Key Words: Coronary heart disease; interleukin-6; electronic taste chip; bead-based immunoassay; lab on a chip; inflammation.

1. Introduction

Interleukin (IL)-6 is a pleiotropic cytokine with a broad range of humoral and cellular immune effects relating to inflammation, host defense, and tissue injury. It is produced in response to several factors, including infection, IL-1, interferon–γ, and tumor necrosis factor (TNF) ***(1)***. IL-6 is an important mediator of the acute-phase response and a primary determinant of hepatic production of C-reactive protein (CRP) ***(2,3)***, a well-established acute-phase reactant and a powerful biomarker for the development of atherosclerosis and coronary heart disease ***(4,5)***. Plasma levels of IL-6 are elevated, with CRP, in apparently healthy individuals at risk for a future cardiac event ***(6)***.

There is also evidence that links IL-6 with certain conditions of the central nervous system (CNS). Increased concentrations of IL-6 in the compromised human CNS have been associated with Alzheimer's disease ***(7)***, brain tumors

From: *Methods in Molecular Biology, Vol. 385: Microchip-Based Assay Systems: Methods and Applications*
Edited by: Pierre N. Floriano © Humana Press Inc., Totowa, NJ

(8), multiple sclerosis, *(9)* Parkinson's disease *(10)*, stroke *(11)*, and traumatic brain injury *(12)*. Even though some of the factors directly responsible for IL-6 upregulation in each of these conditions have been identified, there is still ongoing research, utilizing primary cultures of neural cells (such as astrocytes) and in vitro models of CNS injury, aimed in identifying other molecules effecting the IL-6 response *(13)*. It is therefore imperative to be able to measure IL-6 levels in an accurate and cost-effective manner for diagnostic as well as research-based applications.

Measurements of IL-6 are currently performed with commercially available kits based on enzyme-linked immunoSorbent assay (ELISA) methodology. ELISA has indeed become the gold standard for immunoassays, with a high degree of accuracy, precision, and sensitivity. Nonetheless, this established methodology requires long incubation times, large amounts of expensive reagents, and a trained technician to complete multiple steps of a procedure that cannot be easily implemented in an automated fashion.

Using the ETC assay system developed in our laboratory, immunoassays are performed on beads, which are positioned in micromachined wells on a silicon chip enclosed within a metal casing defined as the "flow cell" *(14,15)*. A fluid delivery system is used to deliver a series of reagents to the flow cell and hence to all of the beads located within. Fluorescent signals generated by antigen/antibody reactions on the beads are visualized with a modified microscope, captured on a charge-coupled device (CCD), and then digitally analyzed and quantified.

In this chapter we describe an ETC-based assay for IL-6. Here, a "sandwich" type of immunoassay is employed within the sensor array. Beads coupled to antibodies specific for IL-6 are sequentially exposed to the sample and IL-6-detecting antibody solutions. Fluorescent signals derived from each of the beads are observed through the microscope optics. These images are permanently captured using a CCD and then processed for analysis in an automated fashion. The ability to regenerate IL-6-sensitized beads and use them in successive assay cycles facilitates the development of an automated, high-throughput microchip-based bead-based IL-6 immunoassay with short analysis time, small sample volumes, and markedly reduced reagent costs suitable for both research and diagnostic applications.

2. Materials

2.1. Fabrication of Silicon Microchips

1. 250-µm Double-sided polished p-type 4–in. single crystal silicon (100) wafer.
2. Piranha solution: 3:1 H_2SO_4/H_2O_2, 70°C.
3. KOH solution (Transene silicon etchant PSE-200) (*see* **Note 1**).
4. Oxygen (O_2) and carbon tetrafluoride gas (CF_4).
5. Silane (SiH_4).

2.2. Creation of Bead Sensor Elements

2.2.1. Fabrication of Polymer Microbeads

1. Agarose powder (type I-B), D-mannitol, and divinyl sulfone were purchased from Sigma Corporation (St. Louis, MO).
2. Suspending solution: 10 mL Span 85 diluted with hexanes to 100 mL.
3. 250- to 280-μm Mesh size wire screen sieves (W. S. Tyler; Mentor, OH).
4. 1:1 Water/ethanol solution.
5. Automated high-throughput particle analysis/sorting instrument (Union Biometrica; Sommerville, MA) (*see* **Note 2**).
6. 0.5 *M* Potassium hydrogen phosphate, pH 12.3.
7. Sodium hydroxide, pH 12.3.
8. Sodium borohydride purchased from Fisher Scientific (Fair Lawn, NJ).

2.2.2. Activation of Agarose Microbeads

1. 1 *M* Sodium hydroxide
2. Sodium borohydride.
3. Glycidol.
4. 0.16 *M* Sodium periodate aqueous solution.
5. Supersize (250–350 μm) agarose beads (Agarose Bead Technology, ABT, Tampa, FL) (*see* **Note 3**).

2.2.3. Coupling of Agarose Microbeads to Antibody Reagents

1. 0.44 *M* Aqueous solution of sodium cyanoborohydride.
2. Capturing antibody (mouse anti-human IL-6) (R & D Systems, cat. no. MAB 206, 0.5 mg/mL).
3. 3 mg/mL Isotypic, irrelevant to IL-6, anti-TNF-α monoclonal antibody (R&D Systems, cat. no. AB210NA).
4. Trizma base (Sigma-Aldrich), 50 m*M* Tris-HCl, pH 7.1.

2.3. Assay Reagents

1. BupH modified Dulbeccos's phosphate-buffered saline (PBS) pack (Pierce, cat. no. 28374).
2. 1% Bovine serum albumin (BSA; Sigma-Aldrich), in PBS. Dissolve 0.1 g of BSA in 10 mL of PBS.
3. Detecting antibody: monoclonal anti-human IL-6 clone 8H12 (Cell Sciences, cat. no. CM1302).
4. Alexa Fluor® 488 monoclonal antibody labeling kit (Molecular Probes, cat. no. A-20181).
5. IL-6 standard (eBioscience, cat. no. 14-8069), 100 μg/mL.

2.4. Flow Cells

1. Two circular 1/16-in.-thick machined polymethylmethacrylate inserts (top and bottom) with holes drilled on their side and surface (**Fig. 1A**).

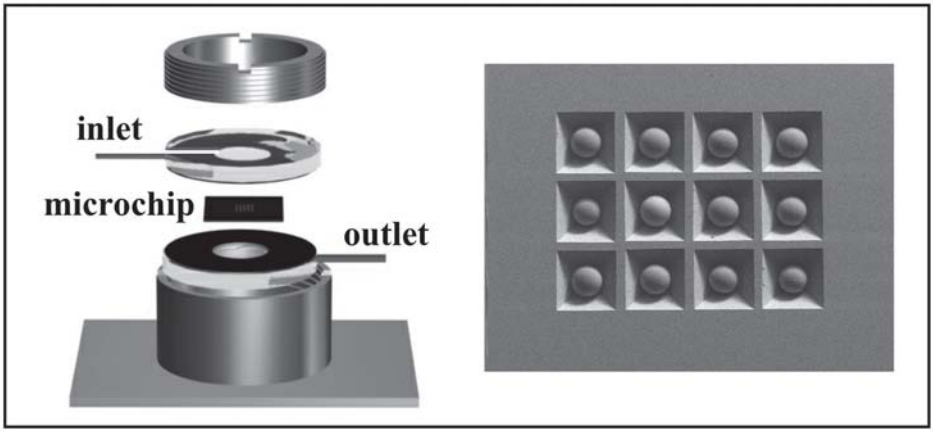

Fig. 1. Assay platform of electronic taste chip system. **(A)** The bead-loaded microchip is sandwiched between two poly(methylmethacrylate) inserts and packaged within a casing to create the analysis flow cell of the system. **(B)** A scanning electron micrograph of the microchip with a microetched array of addressable wells that host beads sensitized to the analyte of interest.

2. Stainless steel casing.
3. 1-in. cut, 0.039-in.-diameter stainless steel tubing.
4. 1/32-in. ID, 3/32-in. OD silicone tubing.
5. 60- to100-µm Single-sided adhesive cut to serve as gasket material.
6. Silicon microchip microfabricated as described in **Subheading 2.1.**

2.5 Instrumentation and Software

1. Modified Olympus BX2 compound microscope (Olympus America Inc., Melville, NY) equipped for both epifluorescence and transmission measurements.
2. Fluoroisothiocyanate (FITC) filter cube (480 nm excitation, 505 nm long pass beam splitter dichroic mirror, and 535 ± 25 nm emission) to image the Alexa Fluor® 488-IL-6 on beads (Chroma 41003).
3. FIAlab custom four-pump system with auto-sampler. This custom-built system consists of four peristaltic pumps (model) and an AIM 2500 auto-sampler, both of which are controlled by software. Even though these components may be programmed to function in an automated fashion, each assay step can be completed in a manual mode, if desired.
4. FIAlab Labview-based software. The complete assay sequence can be modified easily through the assay builder interface.
5. Digital video camera (DVC) color CCD (DVC Corporation, Austin, TX) outputting RGB channels.

6. Bead-loading microscope: Olympus SZX12 stereo microscope (Olympus America Inc., Melville, NY).
7. Image Pro Plus 4.0 software (Media Cybernetics, Silver Spring, MD).
8. Microsoft® Excel (Microsoft Corporation).
9. SigmaPlot® (www.spssscience.com).

3. Methods

3.1. Silicon Chip Fabrication

A typical taste chip (**Fig. 1B**), as used in our laboratories, is made through bulk micromachining of silicon using anisotropic etching. Inverted square-based pyramid wells are chemically etched in a square arrayed pattern on silicon wafers (230–380 μm thick). This design serves as a chamber to contain the beaded sensing element while allowing both bottom-illuminated light to be transmitted through the bead and fluid to flow perpendicular through the wafer. Furthermore, patterns of these wells have been etched to create 3 × 3, 3 × 4, 4 × 5, 5 × 7, or 10 × 10 arrays.

This process has been described in the literature by our group and others. Although not fully understood (parameters such as atomic lattice packing density and attached H_2O molecules play an important role), anisotropic etching of silicon is characterized with the very highly preferential etching of silicon along the (111) surface, allowing the fabrication of microstructures with a great level of control. The complete sequence is shown in **Fig. 2**. Briefly, here is the succession of steps required for the fabrication:

1. Deposit Si_3N_4 on a 4-in. silicon wafer using low-pressure chemical vapor deposition (LPCVD) techniques. A layer of ~1000 is created by reacting ammonia (NH_3) and dichlorosilane ($SiCl_2H_2$) gas with a flow rate of 3.5:1, i.e., 70:20 cm^3/min, at 830°C and 200 mtorr (*see* **Note 4**).
2. Move the wafer to a photolithography cleanroom environment.
3. Remove the mask layer from one side of the silicon substrate by protecting the other side with photoresist and plasma-etching (CF_4 and O_2 at 100 W) the Si_3N_4 layer. This is achieved by reactive ion etching (RIE) with a flow rate of 20:1 CF_4:O_2 (80 cm^3/min:4 cc/min). An etching rate of ~1000 /min is observed with 100 W radiofrequency power and 50 mtorr of pressure.
4. Dip the wafer into a 40% KOH solution at 79 C for 9 h in order to etch the substrate (*see* **Note 5**). This creates the square-based pyramidal wells with an angle of 54.7° with respect to the surface of the silicon (*see* **Figs. 1B** and **2**).
5. After completion of the KOH etch, completely remove the nitride masking layer from both sides of the silicon substrate using plasma etching.
6. Soak the completed device in 30% H_2O_2 for 15–20 min to form a thin SiO_2 layer on the surface of the silicon. This improves surface-wetting characteristics. Typically, an ~750-μm-thick SiO_2 layer is deposited by reaction of silane and oxygen gas with a flow rate of 5:6 (25:30 cm^3/min) at 530°C and 110 mtorr.
7. Once etching is complete, the wafers are diced into chips of the desired size.

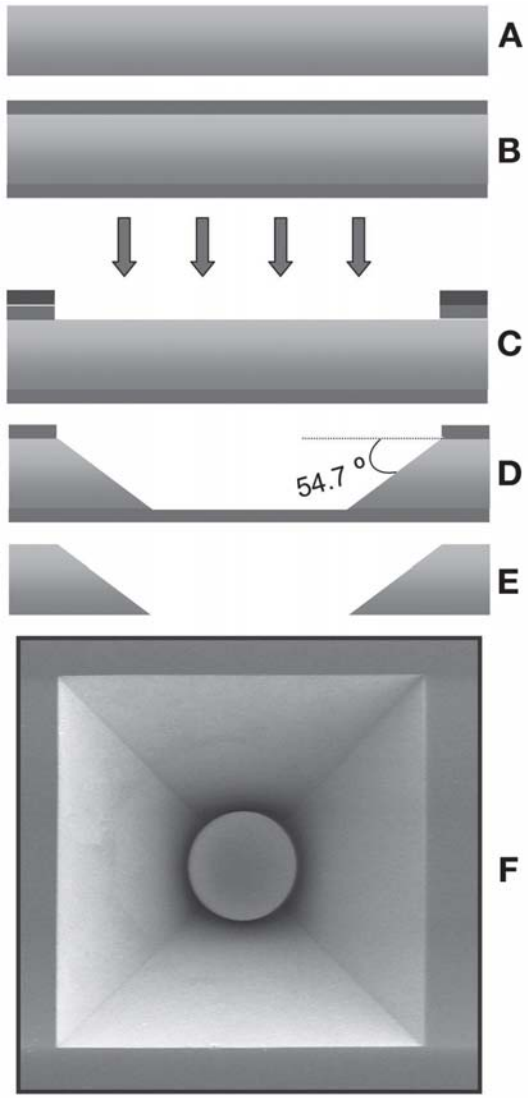

Fig. 2. **(A)** A silicon wafer is cleaned with pirhana solution. **(B)** Deposition of Si_3N_4 is achieved using low-pressure chemical vapor deposition techniques. **(C)** Alignment of the photoresist mask and reactive ion etching of the Si_3N_4 in a cleanroom environment. **(D)** The wafer is dipped into a KOH solution in order to etch the substrate. Square-based pyramidal wells with an angle of 54.74° with respect to the silicon surface are created. **(E)** After completion of the KOH etch, the Si_3N_4 layer is completely removed from both sides of the silicon substrate by using plasma etching. **(F)** Scanning electron micrograph top view of a well created through this process hosting one bead.

3.2 Bead Development

3.2.1. Production of Agarose Beads

Agarose beads were prepared by adapting a procedure previously described ***(16–18)***.

1. Prepare an agarose solution by heating approx 1 g of agarose in 50 mL of water to 95°C.
2. Stir the solution slowly and let it cool to 60°C.
3. Heat to 60°C a solution consisting of 10 mL Span 85 and 90 mL hexanes (suspending solution). Adjust stirring speed in order to obtain desired bead size range.
4. Add agarose solution to the suspending solution while stirring continuously for 1 min at 59°C.
5. Let the reaction cool to 25°C
6. Stop the stirring.
7. Transfer the resulting mixture to a wire screen sieve and wash with water.
8. Wash with the water/ethanol solution
9. Using 250- and 280-µm mesh size sieves, isolate particles with diameters ranging between 250 and 280 µm.
10. Cross-linking of agarose renders stability to the agarose matrix. Resuspend 1 mL of beads in 5 mL of 0.5 *M* potassium hydrogen phosphate at pH 12.3.
11. Add 60 µL of 0.7 *M* sodium borohydride and 35 µL of divinyl sulfone.
12. Shake the mixture for 18 h.
13. Wash the beads with 5 mL of sodium hydroxide pH at 12.3. Repeat procedure four times and resuspend the beads in 11 mL of sodium hydroxide solution.
14. Add 22.5 mg mannitol to hydroxylate nonreacted divynil sulfone termini.
15. Mix gently with agitation for 4 h.
16. Wash with excess water.

3.2.2. Agarose Bead Sorting, Activation, and Conjugation

1. A second round of sieving is optional but may help further narrow the size distribution of the beads, especially if already cross-linked beads from a commercial source are used. Use a series of graded sieves to obtain a population of beads that is uniform in diameter. This strategy is the same whether samples from a commercial source or freshly prepared beads are utilized.
2. Further narrowing of the bead size distribution can be obtained by subjecting the obtained bead fraction to an automated high-throughput particle analysis/sorting instrument (Union Biometrica, Sommerville, MA). The instrument parameters are set to analyze the size distribution of beads and sort the population according to predefined criteria. As a result, a population of beads can be obtained with a variation in diameter of approx 5%.
3. To generate reactive aldehyde groups within the agarose matrix, add 1 mL of settled beads of consistent size (2.0 mL total liquid volume) to 1.2 mL of a solution made from 10 mL 1 *M* sodium hydroxide, 20 mg sodium borohydride, and 3 mL glycidol.

4. Shake the obtained solution gently for 18 h.
5. Further wash with copious amounts of water.
6. Add 0.7 mL of a 0.16 *M* sodium periodate solution to the washed beads to achieve a final volume of 3.2 mL.
7. Shake gently the mixture for 1 h and follow with successive water washes (*see* **Note 6**).

3.3. Coupling of the IL-6-Specific Capturing Antibody on the Agarose Microbeads

Analyte-specific capture antibodies are coupled to the aldehyde-activated beads via established reductive amination procedures ***(14)***, as described below:

1. Isolate an ~500-µL aliquot of aldehyde-functionalized agarose beads (settled volume) in an individual capped microcentrifuge tube.
2. Pool 10- to 100-µL vials of 0.5 mg/mL mouse anti IL-6 antibody to a final volume of 1 mL and a final concentration of 5 mg/mL.
3. Mix the 500-µL bead aliquot with 1 mL of the 5 mg/mL and 4.8×10^{-4} mol $NaCNBH_3$.
4. In a parallel reaction, substitute IL-6-capturing antibody with an isotypic, irrelevant to IL-6 antibody. These beads serve as negative controls for the assay.
5. Let the beads settle on the bottom of the tube and then immediately remove a 50-µL aliquot from the supernatant portion of the mixture. Use this aliquot as the "before" sample to evaluate efficiency of antibody conjugation to the bead.
6. Incubate mixtures overnight at room temperature with end-over-end tumbling.
7. The next day, let beads settle at the bottom of the tube and save another 50-µL aliquot as the "after-conjugation" sample.
8. Rinse beads with at least three volume washes of PBS.
9. The remaining active sites are deactivated with the amine-containing TRIS-buffered saline and a similar amount of $NaCNBH_3$ by tumbling for 1 h.
10. Rinse the beads with three volume washes of PBS and evaluate antibody coating on the beads either using Coomassie blue protein stain or by spectrophotometric evaluation of the antibody concentration in the "before" and "after" samples.
11. Using the Coomassie approach, qualitatively assess the presence of the antibody on the beads with a blue color.
12. When using the spectrophotometric method, quantitatively assess conjugation efficiency of the antibody on the bead. This is achieved by comparison of the before and after sample measurements to a standard dose–response curve generated with serial dilutions of capturing antibody in PBS.

3.4. Conjugation of IL-6-Detecting Antibody to Alexa Fluor® 488

The procedure below follows protocols given by kit manufacturers.

1. Bring the Alexa Fluor® 488 reactive dye and the capturing monoclonal antibody to which the dye will be conjugated at room temperature for 30 min.
2. Meanwhile, resuspend the dried sodium bicarbonate as provided by the manufacturer in 1 mL of nanopure water and repeat-pipet until the reagent is fully dissolved.

3. In an Eppendorf vial, mix 50 µL of the sodium bicarbonate solution with one vial of the capturing antibody (0.5 mg of Ab in 0.5 mL).
4. Resuspend reactive dye with 100 µL of the antibody–sodium bicarbonate solution and incubate the mixture at room temperature for 60 min while gently inverting the tube to facilitate mixing every 15 min.
5. While the antibody–Alexa Fluor® 488 mix is incubating, add approx 1.5 mL purification resin to the spin column.
6. Place the spin column in one of the collection tubes and centrifuge for 5 min at 1100*g* to allow excess buffer to drain away.
7. At the end of the hour, load the 100 µL of dye mixture into the column dropwise, and let it absorb into the resin. Once entire sample is within the resin, place the column into an empty collection tube and centrifuge for 5 min at room temperature at 1100*g*.
8. Collect Alexa Fluor® 488-conjugated antibody from the bottom of the collection tube (*see* **Note 7**).

3.5. Preparation of IL-6 Standards

The steps below describe how to perform a serial dilution of the antigen for generation of a standard curve.

1. On the day of the assay, thaw 100 µg/mL of the IL-6 stock antigen standard.
2. Dilute to a working concentration of 1000 ng/mL of IL-6 by mixing 10 µL of the 100 µg/mL IL-6 stock antigen standard with 990 µL of 1% BSA/PBS.
3. Using 1% BSA/PBS as a diluent, prepare 10-fold serial dilutions of antigen stock to generate IL-6 concentrations ranging from 1 to 1000 pg/mL in 1% BSA/PBS diluent.
4. One vial with 1% BSA/PBS is used as the zero (no antigen) calibrator solution (*see* **Note 8**).

3.6. Description of Assay Run

The IL-6 assay on the microchip system is a sandwich-type immunoassay. Here, beads sensitized with a capturing antibody specific for IL-6 are used to sequester IL-6 on the bead. A fluorescently labeled antibody is then used to detect the captured analyte on the bead, as shown in **Fig. 3**. The procedure described below applies to assay steps necessary for both the creation of a calibration curve (using IL-6 standards) and analysis of the unknown. Prior to attempting these assay steps, the pumps of the fluid delivery system need to be calibrated (*see* **Note 9)**

1. Load fresh beads onto a 3 × 4 chip array with sharp etched forceps (*see* **Note 10**).
2. Monitor the bead-loading procedure under a microscope to ensure placement of selected beads to predetermined positions (i.e., analyte-sensitized reactive beads designated to specific location/address in the array).
3. Encase the bead-loaded chip into a fluid flow cell, within the stainless steel housing.

4. Ensure that the flow cell is maintained at a fixed position with regards to the CCD throughout the duration of the assay run (*see* **Note 11**).
5. Prime PBS, detecting antibody, BSA blocking agent, and antigen tubing lines. This procedure minimizes the introduction of air bubbles to the analysis area.
6. Connect tubing from fluidic delivery system to the inlet of the flow cell and connect the outlet to a waste line.
7. Adjust and maintain focusing on the bead array.
8. Block the inner walls of the fluidic tubing lines, the flow cell, and the beads by delivering 3% BSA in PBS at a flow rate of 0.07 mL/min for 5 min.
9. Follow with a washing step with PBS delivered for 1 min at 2 mL/min.
10. Deliver either IL-6 standard (prepared as described in **Subheading 3.5.**) or the unknown sample destined for analysis at a flow rate of 0.03 mL/min for 20 min.
11. Follow with a washing step with PBS delivered for 1 min at 2 mL/min.
12. Detect the presence of captured analyte by delivering the Alexa Fluor® 488-labeled detecting antibody (as prepared in **Subheading 3.4.**) diluted to an optimized concentration at a flow rate of 0.03 mL/min for 10 min (*see* **Note 7**)
13. Follow with a washing step with PBS delivered for 1 min at 2 mL/min.
14. Acquire an image of the beads with the CCD camera, save with a descriptive name for each run, and analyze as described in **Subheading 3.7.**

3.7. Image and Data Analysis: Construction of a Standard Curve and Determination of IL-6 Concentrations in Unknowns

Digital information from each array/run is obtained by using Image Pro Plus software and analyzed with SigmaPlot. The concentration of the unknown sample is extrapolated from the generated standard curve, as described below.

1. Within Image Pro Plus, open all relevant micrographs and draw an area of interest (AOI) on the periphery of each bead (**Fig. 3B**) of the array for each run (*see* **Note 12**).
2. Measure the intensity in the green channel for each bead, for each standard and unknown, as density of green (average intensity per pixel).
3. Export results for all beads to a SigmaPlot datasheet.
4. Average the signal intensity obtained for the nine beads of the array that are conjugated to the IL-6-specific antibody for each assay run.
5. Discard outliers by using a Q-test.
6. Organize the mean data into three columns (column 1: IL-6 standard concentration; column 2: mean fluorescence intensity for each standard; column 3: mean fluorescence intensity for each unknown).

Fig. 3. **Electronic taste chip-based immunoassay for interleukin (IL)-6.** (*opposite page*) **(A)** The relevant immunocomplexes of the bead-based IL-6 assay are shown in schematic form. Here, an IL-6-specific capturing antibody sequesters IL-6 on the bead. Detection of the captured analyte is achieved with an Alexa Fluor® 488®-conjugated antibody. **(B)** An image showing a population of approx 280-mm-bead

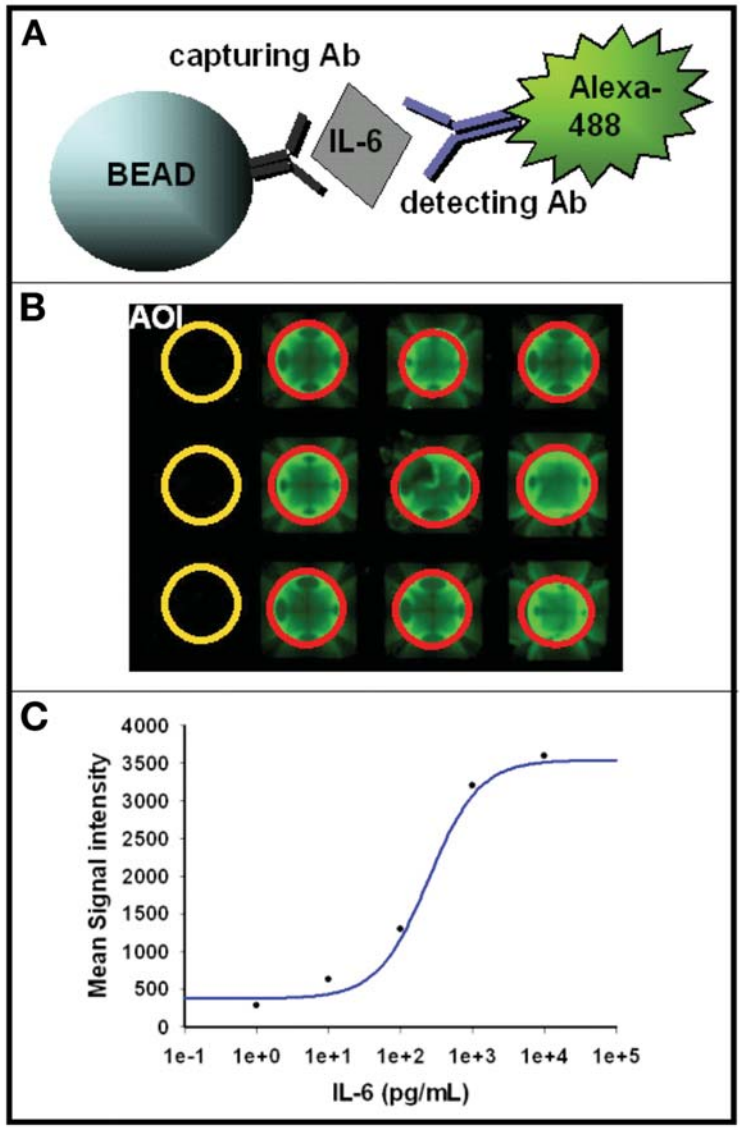

Fig. 3. (*continued*) microreactor elements is captured digitally and analyzed in an automated fashion with a macro that measures the signal intensity of an area of interest (AOI) around each bead in the array. Data from all beads are then exported to a SigmaPlotÆ datasheet. The signal intensity obtained from redundant beads of the array is averaged for each assay run. A Q-test is then applied to identify and discard outliers. The remaining data are analyzed using a four-parameter logistic equation process within the SigmaPlot environment to generate a standard dose–response curve (**C**), which is used to predict concentrations of the unknowns.

7. Highlight all data from the three columns and from the "standard curves analysis" function found under the "Pharmacology" tab, and perform a four-parameter logistic equation analysis within the SigmaPlot environment. Make sure that the "Log X axis scale" and "Predict unknowns" buttons are selected. Such a standard curve is shown in **Fig. 3C**.
8. Retrieve predicted value for the unknowns.

4. Notes

1. Other etchants can be used such as hydrazine–water solution, ethylene diamine pyrocatechol/water (EDP), and tetramethylammonium hydroxide (TMAH)
2. Use of this instrument is optional. The mechanical sieving methods provided in this chapter produce beads of consistent size within approx 7%. The use of the bead sorter can further improve the size homogeneity of the bead population to less than approx 5%.
3. The intended use of the beads as provided by commercial sources is immuno-affinity chromatography, for which there is not as tight a requirement for size homogeneity of the beads. In contrast, for our application, size homogeneity of the beads is associated with the precision and accuracy of the assay. Likewise, the level of activation (glyoxylation) is as important as sieving in producing consistent populations of beads and needs to be monitored with a great level of control.
4. Thickness control is very important because KOH etches not only the silicon substrate but also the silicon nitride layer. On the other hand, if the thickness is too great, the tensile strength of the SiN_3 layer is such that the patterns will be affected.
5. Successful patterning requires that a highly stable temperature be maintained throughout the etch process.
6. Our experience has shown that beads that appear opaque under examination with brightfield microscopy perform significantly better than those that are transparent. In order to assess the opacity, place samples of aldehyde-functionalized agarose beads on glass microscope slides in aqueous solution and discard the beads that appear transparent.
7. Use a small aliquot (~10 µL) to assess conjugation efficiency as per kit manufacturer's instruction. If the conjugation procedure is successful, aliquot and store the detecting antibody frozen (at –20°C) until use. On the day of use, thaw, and dilute the final product (previous experience with this assays suggest that a 1:250 to 1:1000 dilution in 1% BSA/PBS is likely to be optimal).
8. IL-6 is very labile, so both standards and samples should be aliquotted and stored frozen at –80°C until analysis.
9. Depending on the pump manufacturer and software used, flow rates might be expressed in terms of percentage and need to be calibrated. As an indication, we are giving here the optimal flow rates for the particular pumps we are using with this notation.

   Antigen 20 min @ 5% flow rate
   PBS wash 1min @ 100% flow rate

Detecting antibody 10 min @ 5% flow rate
PBS wash 1 min @ 100% flow rate

10. Dose–response curves can be generated by using either a fresh batch of beads or beads regenerated after each assay run. Bead regeneration can be accomplished with a solution phase exposure to 0.1 *M* glycine–HCL buffer (pH 2.5) and then re-equilibration with PBS. This procedure breaks antigen–antibody interaction without affecting the functional integrity of the capturing antibody, thus allowing for the bead to be re-used in successive assay cycles.
11. It is not necessary to keep the flow cell in the same position throughout the analysis, but doing so facilitates analysis procedures, as AOIs on the beads can be registered and used for all the assays, and analyzed with a simple macro that can be written within the Image Pro Plus environment.
12. Simple macros can be written to facilitate data analysis steps, such as automated registration of the location of the beads, selection of bead parameters (diameter, area, pixel values, density), and export of numerical values to data-sheet environment.

Acknowledgments

We wish to acknowledge Dr. Dwight Romanovicz for acquiring the scanning electron micrographs of the silicon microchip. Research described in this article was supported by the National Institutes of Health (Saliva grant # U01-DEO015017-03), the Welch Foundation (F-1193), Philip Morris USA Inc., and Philip Morris International (Grant #UTA02/400, AMD3).

References

1. Papanicolaou, D. A., Wilder, R. L., Manolagas, S. C., and Chrousos, G. P. (1998) The pathophysiologic roles of interleukin-6 in human disease. *Ann. Intern. Med.* **128,** 127–137.
2. Baumann, H. and Gauldie, J. (1990) Regulation of hepatic acute phase plasma-protein genes by hepatocyte stimulating factors and other mediators of inflammation. *Mol. Biol. Med.* **7,** 147–159.
3. Heinrich, P. C., Castell, J. V., and Andus, T. (1990) Interleukin-6 and the acute phase response. *Biochem. J.* **265,** 621–636.
4. Ridker, P. M., Buring, J. E., Shih, J., Matias, M., and Hennekens, C. H. (1998) Prospective study of C-reactive protein and the risk of future cardiovascular events among apparently healthy women. *Circulation* **98,** 731–733.
5. Ridker, P. M., Cushman, M., Stampfer, M. J., Tracy, R. P., and Hennekens, C. H. (1997) Inflammation, aspirin, and the risk of cardiovascular disease in apparently healthy men. *N. Engl. J. Med.* **336,** 973–979.
6. Ridker, P. M., Rifai, N., Stampfer, M. J., and Hennekens, C. H. (2000) Plasma concentration of interleukin-6 and the risk of future myocardial infarction among apparently healthy men. *Circulation* **101,** 1767–1772.
7. Bauer, J., Ganter, U., Strauss, S., et al. (1992) The participation of interleukin-6 in the pathogenesis of Alzheimers disease. *Res. Immunol.* **143,** 650–656.

8. Borg, S. A., Kerry, K. E., Royds, J. A., Battersby, R. D., and Jones, T. H. (2005) Correlation of VEGF production with IL1α and IL6 secretion by human pituitary adenoma cells. *Eur. J. Endocrinol.* **152,** 293–300.
9. Filion, L. G., Graziani-Bowering, G., Matusevicius, D., and Freedman, M. S. (2003) Monocyte-derived cytokines in multiple sclerosis. *Clin. Exp. Immunol.* **131,** 324–334.
10. Nagatsu, T. and Sawada, M. (2005) Inflammatory process in Parkinson. *Curr. Pharm. Design* **11,** 999–1016.
11. Waje-Andreassen, U., Krakenes, J., Ulvestad, E., et al. (2005) IL-6: an early marker for outcome in acute ischemic stroke. *Acta Neurol. Scand.* **111,** 360–365.
12. Maier, B., Laurer, H. L., Rose, S., Buurman, W. A., and Marzi, I. (2005) Physiological levels of pro- and anti-inflammatory mediators in cerebrospinal fluid and plasma: a normative study. *J. Neurotrauma* **22,** 822–835.
13. Penkowa, M., Giralt, M., Lago, N., et al. (2003) Astrocyte-targeted expression of IL-6 protects the CNS against a focal brain injury. *Exp. Neurol.* **181,** 130–148.
14. Goodey, A., Lavigne, J. J., Savoy, S. M., et al. (2001) Development of multianalyte sensor arrays composed of chemically derivatized polymeric microspheres localized in micromachined cavities. *J. Am. Chem. Soc.* **123,** 2559–2570.
15. Lavigne, J. J., Savoy, S., Clevenger, M. B., et al. (1998) Solution-based analysis of multiple analytes by a sensor array: Toward the development of an "electronic tongue." *J. Am. Chem. Soc.* **120,** 6429–6430.
16. Gustavsson, P.-E., Axelsson, A., and Larsson, P.-O. (1999) Superporous agarose beads as a hydrophobic interaction chromatography support. *J. Chromatography A* **830,** 275–284.
17. Gustavsson, P.-E. and Larsson, P.-O. (1996) Superporous agarose, a new material for chromatography. *J. Chromatography A* **734,** 231–240.
18. Gustavsson, P.-E., Mosbach, K., Nilsson, K., and Larsson, P.-O. (1997) Superporous agarose as an affinity chromatography support. *J. Chromatography A* **776,** 197–203.

11

Allergen Microarrays for the Diagnosis of Specific IgE Against Components of Cow's Milk and Hen's Egg in a Multiplex Biochip-Based Immunoassay

Christian Harwanegg, Sabine Hutter, and Reinhard Hiller

Summary

Over the last few decades, the prevalence of allergic diseases has increased dramatically in developed nations. The resulting burden on health care systems worldwide has provoked a whole series of research initiatives among allergy experts and commercial companies that aim to develop novel tests to improve the diagnostic risk assessment and early preventive treatment of the disease. The advent of protein microarray technology has inspired the development of miniaturized immunological applications that permit the simultaneous analysis of huge numbers of disease-related parameters. Allergen microarrays have been developed for the monitoring of patient-specific antibody profiles to a previously unknown variety of allergens in a single analytical step. This has been accomplished by the successful adaptation of solid-phase antibody assays for the detection of surface-bound allergens to the microarray format, the development of appropriate assay conditions, and the improvement of software-guided microarray image analysis. Here we report a protocol for the development and analysis of food allergen microarrays.

Key Words: Allergy; microarray; biochip; fluorescence; solid-phase immunoassay; image analysis.

1. Introduction

IgE-mediated type I allergic diseases are among the most common causes of chronic illness in the populations of industrialized countries. Particularly in the last few decades, the prevalence of allergy has increased dramatically and the costs for disease treatment represent a major burden for the health care system of the affected nations ***(1)***. After having been sensitized upon the first contact with an allergy-eliciting molecule (allergen), a patient's condition frequently aggravates by serial subsequent exposure to the same allergen, which is accompanied by the development of the well-known symptoms of allergy (e.g.,

From: *Methods in Molecular Biology, Vol. 385: Microchip-Based Assay Systems: Methods and Applications*
Edited by: Pierre N. Floriano © Humana Press Inc., Totowa, NJ

rash of the skin, hay fever, or chronic asthma). Hence, the identification of the origin of the allergic reaction is a key step in the accurate diagnosis and the choice of a proper treatment.

Since the discovery of immunoglobulin E (IgE) as the key mediator of the allergic response in a patient's immune system *(2)*, the routine determination of circulating IgEs has improved the diagnosis of allergy significantly. In contrast to in vivo provocation, in vitro testing of allergen-specific IgEs reduces the risk of adverse reactions (e.g., anaphylactic shock) towards the allergen preparation being applied. In concert with a sound anamnesis, determining serum IgE levels is often sufficient to reliably identify the causative agent of allergy.

In the 1990s, novel test formats for the massively parallel analysis of gene expression became available by the advent of microarray technology. Today, state-of-the-art applications (e.g., Affymetrix GeneChips®) permit the study of several thousand transcripts on a (nearly) whole-genome-wide scale, and in 2004 the first microarray-based in vitro diagnostic tests became available for the parallel detection of single nucleotide polymorphisms in drug-metabolizing enzymes, used to improve the efficacy of treatment by determining the metabolizer state of a particular patient. Concomitantly, the development of protein microarray technology has raised the expectations for novel multianalyte immunological tests that permit the simultaneous detection of large numbers of disease-related parameters.

Allergen microarrays are a prominent example of biochip-based applications, demonstrating the applicability of protein microarray technology for clinical purposes by adopting the principle of the allergosorbent test to a miniaturized format *(3–7)*. Typically, a preparation of allergenic material is immobilized onto a solid-phase carrier and incubated with the serum of an allergic patient. The binding of allergen-specific IgEs is monitored subsequently by the addition of a specific anti-IgE antibody in combination with an appropriate signal amplification protocol and readout procedure. For in vitro diagnostic (IVD) purposes, quantification of analytes (e.g., IgE antibodies) in a patient's sample is facilitated by the parallel determination of the analytes contained in a calibrator (e.g., a serum containing well-defined concentrations of allergen-specific IgE antibodies). Subsequently, the calibrator results are utilized for heterologous interpolation of the sample signals and (semi-) quantitative test results are being generated.

Here, we describe the fabrication and assay of allergen microarrays for the fluorescence-based detection of selected food allergens.

2. Materials

2.1. Allergens

The protocol developed here has been optimized for the spotting of cow's milk and hen's egg allergens. The corresponding proteins have been purchased from Sigma-Aldrich (Vienna, Austria).

1. Cow's milk allergens:
   Lactoferrin
   Lactalbumin
   Lactoglobulin
   Immunoglobulin G
   Bovine serum albumin
   Casein
2. Chicken's egg allergens:
   Ovomucoid
   Ovalbumin
   Conalbumin
   Lysozyme.

2.2. Equipment

1. Home-made slides or CodeLink™ activated slides (Amersham Biosciences, Uppsala, Sweden) are used as microarray substrates (*see* **Note 1**).
2. For spotting, we have used an Affymetrix 418 microarrayer (Affymetrix, Santa Clara, CA) or an analogous microarraying device (*see* **Note 2**).
3. Custom-made humid chamber for incubation of 12–36 microarray slides (VWR International, Vienna, Austria) (*see* **Fig. 1A**).
4. Two glass troughs for microscopy slides with slide baskets made of glass (holding 10 slides). Each trough is suited to hold up to 220 mL of liquid (Sigma-Aldrich, no. S-6141 (s*ee* **Fig. 1B**).

2.3. Buffers and Solutions

1. Assay buffer: 150 m*M* sodium chloride, 10 m*M* Tris-HCl, 0.5% Tween-20, pH 8.0 (*see* **Note 2**).
2. Blocking solution: 1% w/v of anti allergic skim milk powder to the assay buffer (*see* **Note 3**).
3. Allergen printing buffer: 150 m*M* sodium phosphate buffer, pH 8.5.

2.4. Detection Antibody and Detection Antibody Solution

1. Choose a commercially available anti human IgE detection antibody.
2. For the preparation of the fluorescence-labeled anti-IgE detection antibody, we recommend the Alexa Fluor 546 antibody labeling kit (Invitrogen, Carlsbad, CA); refer to the manufacturer's homepage for ordering (www.probes.com). You may also use a commercially available fluorescence-labeled anti-human IgE antibody.
3. Following the labeling procedure, prepare a working dilution of the detection antibody in the blocking solution (*see* **Note 4**).

2.5. Microarray Scanner

For the analysis of allergen microarrays, we recommend the use of confocal laser scanners, especially instruments from the ScanArray series (Perkin Elmer

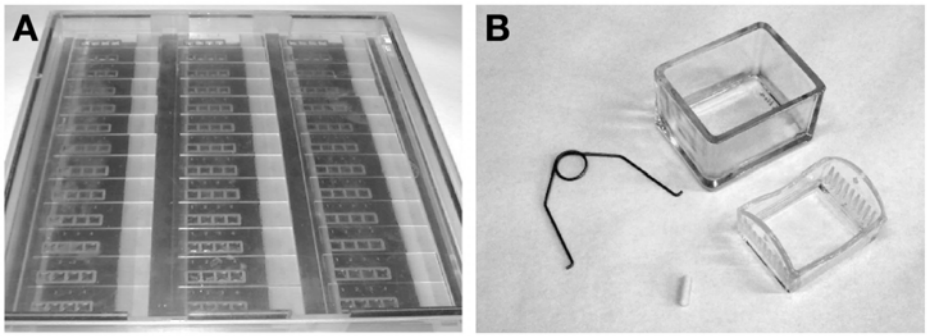

Fig. 1. Custom-made humid chamber **(A)** and glass troughs for microscopy slides **(B)**.

Life Sciences, Boston; MA), the Affymetrix 428 series (Affymetrix, Santa Clara, CA), or the LS 400 series (Tecan Instruments, Salzburg, Austria) (*see* **Note 5**).

2.6. Microarray Image Analysis Software

Basically, several commercially available software packages are compatible with the analysis of allergen microarray images. In our facility, the GenePix package (Axon, Union City, CA) and the QuantArray package (Perking Elmer, Boston, MA) are employed regularly for image analysis. Both packages produce output files using the GPR (Genepix Result File) standard (*see* **Note 6**).

3. Methods

3.1. Production of Allergen Microarrays

1. For producing custom-made microarray substrates, incubate conventional microscopy glass slides in a 1:1 mixture of methanol and concentrated hydrochloric acid overnight, followed by short sonication in acetone in order to remove surface contaminations.
2. Render the surface amine-reactive by using conventional silane and crosslinker chemistry. For an exemplary protocol, *see* **ref. *3***. We also recommend CodeLink™ activated slides for the spotting of allergen microarrays (Amersham Biosciences, Uppsala, Sweden). (*See also* **Note 1**).
3. Dissolve allergens to a final concentration of up to 2 mg/mL in allergen printing buffer. Each allergen may require buffer optimisation in terms of pH value, protein concentration, or dissolving procedure.
4. Spot allergens in replicates onto the surface in each reaction well of the glass slide. Spotting of the allergens in an ordered array can be accomplished by any available microarraying device, e.g., the GMS 417 Microarrayer (Affymetrix, Santa Clara, CA) (*see* **Note 7**).

5. After spotting, store allergen chips at room temperature for at least 3 h. For prolonged storage, store desiccated under vacuum.

3.2. Allergen Microarray Assay

3.2.1. Preparation of Allergen Microarrays

1. Remove the chips from the vacuum storage/use directly after spotting without getting in contact with the surface where the allergens are immobilized.
2. Put the allergen microarray(s) into a glass trough containing an appropriate amount of assay buffer (approx 200 mL) in a glass basket together with a magnetic stir bar.
3. Place the basket onto a magnetic stirrer and stir vigorously (600 rpm or two-thirds of maximum) for 60 min.
4. Remove the glass basket containing the microarray slides and put it into a glass trough containing double-distilled or high-performance liquid chromatography (HPLC)-grade water. Add a stir bar and stir vigorously on a magnetic stirrer (600 rpm) for 5 min.
5. Remove the glass basket containing the allergen microarrays and place it onto a paper towel to air-dry. Wait until the slides are completely dry (15 min). Continue with the test protocol immediately afterwards (*see* **Note 8**).
6. Discard all used washing solutions.
7. Place a fresh paper towel on the bottom of the humid chamber and soak the towel with double-distilled or HPLC-grade water (*see* **Note 9**).
8. Close the lid of the humid chamber to prevent it from evaporation until further use.

3.2.2. Sample Preparation and Incubation

1. Remove the sample sera and the calibration serum from a –20°C refrigerator and thaw it on ice. Wait until the sera have thawed completely.
2. Vortex briefly and quickly spin off the sample for 10 s in a benchtop centrifuge.
3. Place the prepared allergen microarrays in the humid chamber with the reaction sites up.
4. Pipet 20 µL of the calibration serum onto reaction site 1 and 20 µL of the sample sera onto reaction sites 2, 3, and 4 of the allergen microarray, respectively. Make sure that the microarray is placed in the humid chamber properly. Close the humid chamber without mingling the sera (*see* **Note 10**).
5. Incubate at room temperature for 120 min.
6. Remove the allergen microarray slides from the humid chamber carefully without mingling the sera.
7. Dip the slides briefly into a container filled with double-distilled or HPLC-grade water to remove the sera.
8. Wash the slide(s) with assay buffer for 15 min (*see* **Subheading 3.2.1**).
9. Wash the slide(s) with double distilled or HPLC-grade water for 5 min (*see* **Subheading 3.2.1.**).
10. Let the washed slides air-dry for approx 15 min (*see* **Subheading 3.2.1.**).
11. The allergen microarray slide(s) are now ready for the incubation of the detection antibody solution.

12. Place the dry slides in the humid chamber with the reaction sites upwards.
13. Discard all used washing solutions.
14. Pipette 20 µL of detection antibody solution onto the reaction sites of the allergen microarray slides, respectively.
15. Make sure that the slides are placed in the humid chamber properly. Close the humid chamber.
16. Incubate at room temperature for 60 min.
17. Remove the slides from the humid chamber carefully.
18. Dip the slides briefly into a container filled with double-distilled or HPLC-grade water.
19. Wash the slides with assay buffer for 15 min (*see* **Subheading 3.2.1.**).
20. Wash the slides with double-distilled or HPLC-grade water for 5 min (*see* **Subheading 3.2.1.**).
21. Let the washed slides air-dry for approx 15 min (*see* **Subheading 3.2.1.**).
22. The slide(s) are now ready for scanning. Use directly for data acquisition in a biochip reader (microarray scanner) or store in the dark for subsequent scanning (*see* **Note 11**).

3.3. Allergen Microarray Scanning

1. If necessary, adjust the scanning focus level following the instructions of the scanner software to obtain identical settings for each allergen microarray image (*see* **Note 12**).
2. Select the proper scan area inside each Teflon mask for each individual reaction site to reduce the scanning time and the file size of the Tagged Image File Format (TIFF) image obtained.
3. Choose the proper settings for the microarray scanning (*see* **Note 13**).
4. Acquire the first scan image and save the file by using an appropriate description.
5. Acquire the second scan image and save the file by using an appropriate description.
6. If necessary, acquire additional images of your experiments.

3.4. Allergen Microarray Data Analysis

Raw data acquisition includes all software-guided steps required to obtain fluorescence intensity (FI) values corresponding to the individual spots of the allergen microarray(s).

3.4.1. General Procedure for the Allergen Microarray Data Acquisition

1. Create an array list file. For allergen microarray analysis, the position as well as the description of the individual spots contained in the allergen microarray (allergens, human IgE, guide dots) must be defined. For this purpose the GAL (Genepix Array List) file has been established as a widespread standard format.

2. Analyze the allergen microarray image. Based on the existing GAL file, the software generates the raw data from an allergen microarray image. The output file should contain the parameters listed above (*see also* **Note 6**).
3. Save the data. The resulting data should be saved in an adequate file (e.g., text-based or appropriate database format) (*see* **Note 14**).

3.4.2. General Procedure for Interpolating the Data of the Images Into One Final Raw Data Set

Calculate the interpolation factor between the two images using the following algorithm:

1. For each spot that is not saturated in the image scanned with the higher scanning power, calculate the fluorescence intensity ratio between the two images. The expected ratio should be between 2 and 10.
2. Calculate the median of all individual spot interpolation factors.
3. Interpolate each spot if necessary.
4. For each spot that appears saturated in the image scanned with the higher scanning power (>65,000 pixels), replace the saturated fluorescence intensity with the value obtained from the image scanned with low-power settings multiplied by the interpolation factor (*see* **Note 15**).

3.4.3. General Procedure for Calculating the Mean Value of Each Triplicate

Filter the raw data by two criteria:

1. Eliminate spots that are below the threshold you have defined for your experiments. Determine the necessary threshold by performing a series of negative controls (e.g., by applying buffer samples instead of patient sera), and calculate the mean signals obtained for each allergen. Add 2 standard deviations to this mean value.
2. Eliminate spots that were not automatically detected by the software (spots flagged as absent or not found).
3. Calculate the triplicate means by applying the following rules:
   a. If at least two replicates were found,but the third replicate is below the defined threshold or was not identified by the software, calculate the mean of the two remaining spots.
   b. If fewer than two replicates were found or are below the threshold, the according allergen-specific FI value should be considered as 0 (negative) (*see* **Note 16**).

3.4.4. FI Data Normalization and Class Assignment

With the aid of the calibration serum (provided separately), the raw data are arranged into four classes, which in turn correlate with the conventional RAST classes. Based on this mathematical transformation, information of the specific IgE titer contained in a patient's serum becomes available.

3.4.5. Guideline for FI Value Normalization

1. In addition to the patient's serum, a calibration serum must be assayed in parallel.
2. The calibration serum must contain IgE specific for at least six individual allergens contained in an allergen microarray.
3. The IgE concentrations corresponding to these particular allergens have to be determined using a state-of-the-art instrument (e.g., UniCAP, Pharmacia Diagnostics, Uppsala, Sweden).
4. The specific IgE values should be distributed across the full range of the RAST classes (1–6) in order to enable a reliable FI value normalization.

3.4.6. General Procedure for FI Value Normalization

1. Perform a linear extrapolation of the log of the FI values obtained from the calibration serum against the log of the determined IgE titers of the individual allergens.
2. Calculate the corresponding regression parameters (slope, axis intercept), e.g., by using Microsoft Excel linear regression functions. The coefficient of correlation (R^2) obtained by this procedure should be in the range of 0.85 to 1.0.

Using the regression parameters calculated above, the IgE titers (normalized values) for all of the allergen spots contained in the protein microarray can be determined by using the following formula:

$$\text{IgE titer (kUA/l)} = \text{inv log (log FI x a + b)}$$

where FI is the calculated allergen fluorescence intensity, a is the slope, b is the axis intercept of the regression curve, kUA/L: is kilo units allergen/L, and inv log is inverse logarithm.

Based on the calculation in **step 2**, the individual values can be arranged into four classes:

1. Negative values (0 kUA/L) are allocated to NEGATIVE.
2. Extrapolated values lying within RAST 1–2 (0.35–3.5 kUA/L) are allocated to LOW.
3. IgE values between 3.5 and 0.0 kUA/L are classified as INTERMEDIATE.
4. Higher values (>50,0 kUA/L) are categorized as HIGH.

4. Notes

1. To produce chips containing several identical allergen microarrays, we use customized slides containing a Teflon mask (SPI Technologies, Westchester, USA), designed to create 7 × 7 mm rectangular glass areas representing four individual reaction wells surrounded by 2-mm Teflon. However, for simplicity, conventional substrates containing amino-reactive crosslinkers (e.g., from TeleChem) may be used as well.
2. You may use contact or noncontact microarrayers for spotting of allergen microarrays. In general, the choice for a certain substrate type as well as the

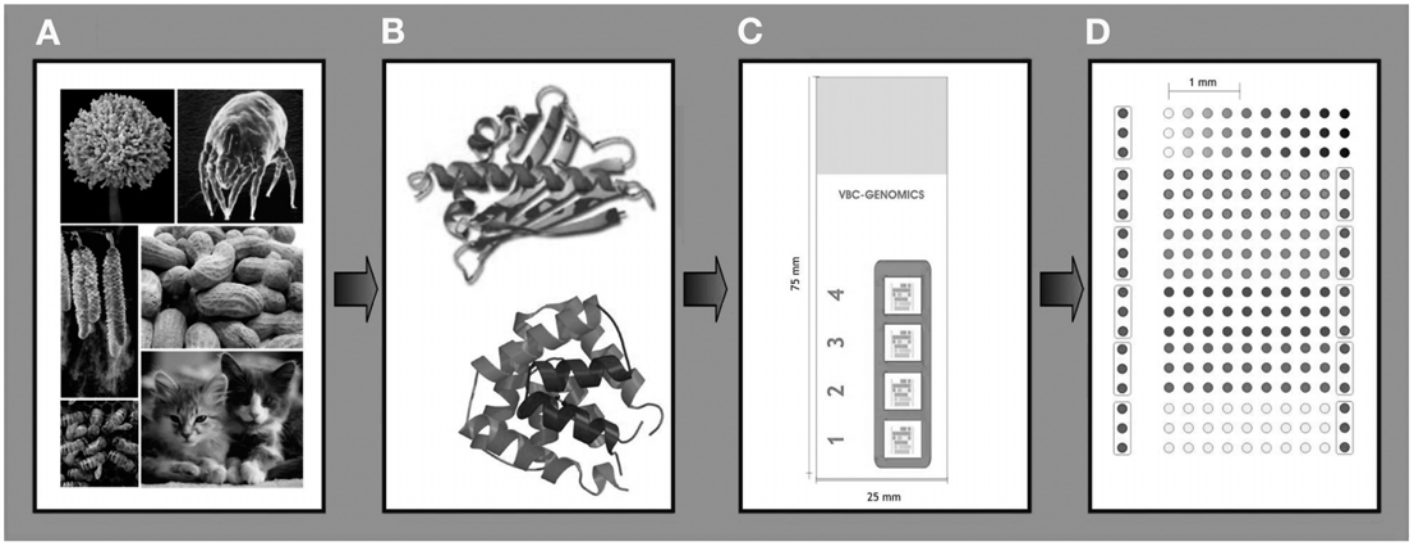

Fig. 2. Production of allergen microarrays. **(A)** Allergens from various biological sources (e.g., molds, mites, pollen, nuts, animals) can be obtained in native form by purification or by recombinant production in suitable host organisms (e.g., *E. coli*, *Pichia pastoris*) **(B)**. **(C)** Allergen microarrays are produced by spotting of allergen proteins onto functionalized glass slides containing amino-reactive groups (e.g., epoxysilanized glass). **(D)** Each allergen is immobilized in triplicate (spot size in the range of 50–150 µm), together with a group of serially diluted purified human IgE antibodies (top of allergen microarray layout) and guide dots (i.e., fluorescence-labeled proteins) for automated image analysis after microarray scanning

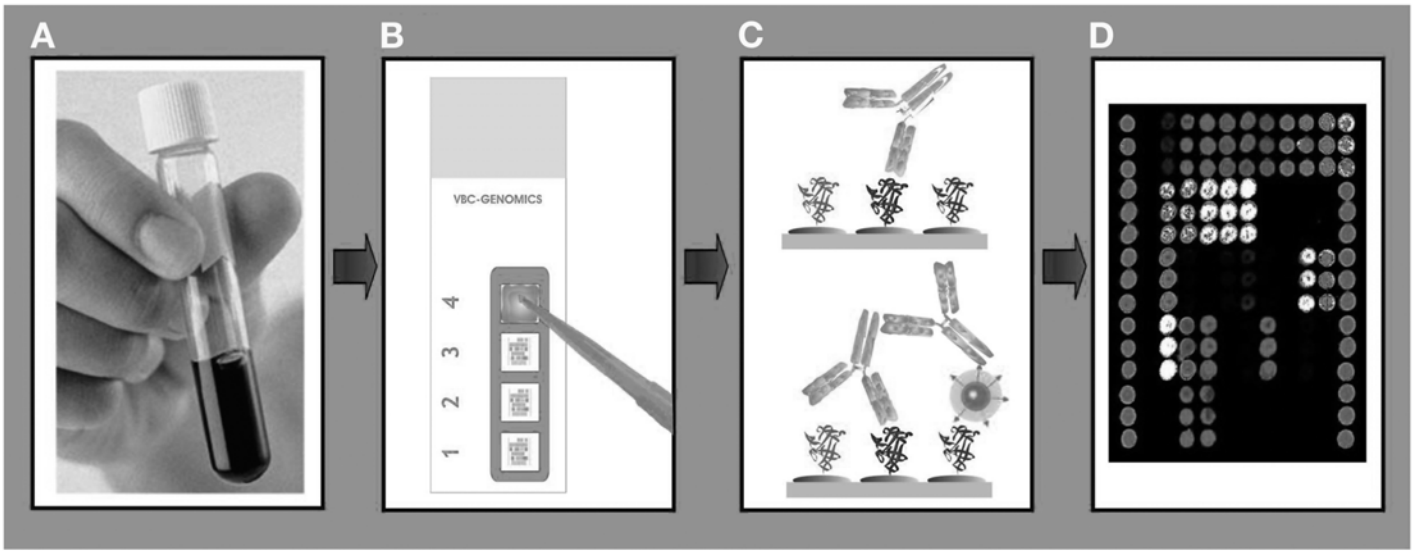

Fig. 3. Allergen microarray assay. **(A)** The basic source of the assay is human serum, which can be of venous or capillary origin. **(B)** Following the allergen microarray preparation, serum is pipetted directly into an individual reaction site, whereas a calibration serum is always incubated in reaction site 1. **(C)** Allergen-specific binding is monitored using the principle of solid-phase immunoassays: Individual allergens are attached covalently to the surface of the functionalized glass slide in the form of microarray spots (size ~50–150 µm). IgE antibodies contained in the serum of an allergic patient bind to the individual allergens, and this event is monitored by the addition of a secondary, fluorescence-labeled anti-human IgE antibody. **(D)** The results are analyzed by scanning in a microarray reader. A typical allergen microarray image contains several to many fluorescence signals with variable intensities. Depicted here is a false-color image displaying various strong (white), intermediate (green/yellow), and low (blue/dark blue) signals.

sample material used for spotting should be considered and may influence the decision as to which device to use. For example, to spot antibody microarrays, a noncontact spotter and a membrane or gel-like substrate might be the most promising option.

3. Incubate blocking solution at room temperature with gentle agitation for 60 min to dissolve the powder. Be sure that the blocking solution is completely dissolved. The blocking solution will have a turbid appearance. Prepare only the volume necessary for the assay. Store the blocking solution at 4°C for no longer than a week. When stored at 4°C, the assay buffer can be used for 4 wk.
4. Determine the optimal working dilution of the detection antibody on your detection system (e.g., a fluorescence scanner) by preparing serial antibody dilutions and measuring the resulting signal-to-noise ratios in the corresponding assays. Choose the working dilution with the optimum signal-to-noise ratio.
5. The most relevant specifications of scanners for proper allergen microarray analysis are, in our experience:
   Instrument optics: confocal laser scanning microscope
   Minimal resolution: 10 µm
   Minimal linear range: 4 log
   Minimal detection limit: 0.02 fluorescence molecules per μm^2
   Image format: TIFF
   Color depth: 16 bit
   Manual or automated focusing enabled

   Usage of charge-coupled device camera-based instruments is not recommended! They are prone to producing artefacts during scanning and frequently display an insufficient linear range.
6. If other software packages are being used, an option for GPR output files should be available. Also, a customized software package can be licensed from VBC-GENOMICS for simple image and data analysis (www.vbc-genomics.com).
   Major features of the software for allergen microarray image analysis include:
   The software must contain a feature that enables the loading of a file that contains information about spot position and description (e.g., GAL file).
   The software must contain a feature to automatically identify spots within a microarray as well as an algorithm to distinguish actual spots from background.
   The software must have a feature to identify/calculate the following parameters:
   a. Spot position (x, y)
   b. Spot diameter
   c. Spot description (or name)
   d. Mean of FI values (minus background)
   e. Median of FI values (minus background)
   f. Flag present/absent (spot found or not found)
7. For good array-to-array and batch-to-batch reproducibility, try to control as many parameters as possible during the spotting process (e.g., humidity, temperature, time, device calibration). We also recommend producing the arrays with guide dots as well as positive and negative assay controls. Guide dots can

be spots of labeled proteins that facilitate finding the correct array position during the image analysis. In case of allergen microarrays, we recommend using purified human IgE in increasing concentrations as positive controls and buffer dots or dots containing nonallergenic proteins as negative controls (e.g., human serum albumin).

8. The glass microarray surface must be completely dry. Residues of water at the margin of the glass slide can be removed with a paper towel.
9. Incubation with small volumes such as on the allergen microarray format requires preventing evaporation during the assay, otherwise samples will dry out.
10. Avoid direct contact of the pipet tip to the microarray surface when dispensing the sera. Always pipet the calibration serum onto reaction site 1!
11. Proceed to the next topic on "Allergen Microarray Scanning." Make sure that the scanning is started directly after completing the assay to ensure optimal results, or store microarrays desiccated or under argon and protected from light to prevent bleaching of fluorescence signals.
12. As a result of inhomogeneities of the glass surface or an improper adjustment of the scan focus, FI values contained in an image might be inaccurate or irreproducible if not adjusted for every microarray individually.
13. Each allergen microarray is scanned twice at two independent scanner settings to obtain different images of an identical allergen microarray. The first scan should display no saturated signals according to your scanner's dynamic range. You might also use the "Auto-Adjust" function of your scanner to choose the optimum scanning settings. The second scan should be performed with higher laser power or photomultiplier settings to obtain a high sensitivity (*see also* **Fig. 4**). If – after the second scan with low scanning power – saturated signals still appear on the allergen microarray, a third scan should be performed in order to acquire an image with only nonsaturated signals.
14. Because each microarray is scanned at least twice, each of the two (or more) images must be analyzed separately. Most software packages, however, allow overlaying at least two images and acquiring the raw data of both images in one analysis step, which are saved as one result file.
15. Each allergen or IgE standard is spotted in triplicate to provide highly reliable testing conditions. Therefore, further calculations of feature mean values are necessary.
16. In the following steps, proceed with allergen mean values for all calculations.

References

1. The UCB Institute of Allergy (1999) European Allergy White Paper: allergic diseases as a public health problem in Europe. http://www.theucbinstituteofallergy.com/IoaImages/247_13_SUMM_tem75–5866.pdf.
2. Ishizaka, K. and Ishizaka, T. (1967) Identification of gamma-E-antibodies as a carrier of reaginic activity. *J. Immunol.* **99,** 1187–1198.
3. Deinhofer, K., Sevcik, H., Balic, N., et al. (2004) Microarrayed allergens for IgE profiling. *Methods* **32,** 249–254.

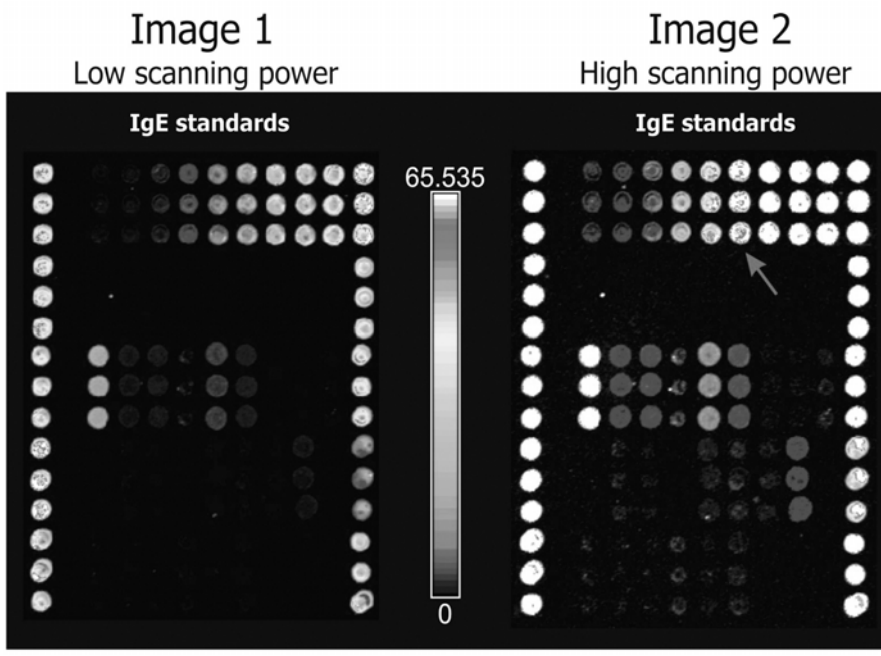

Fig. 4. Typical results of allergen microarray scanning: Image 2 is obtained at a high scan power. As a reference for the settings, acquire an image where each of the microarray guide dots as well as the five highest concentrations of the IgE concentration series are saturated (**Fig. 3**). The lower concentration of the IgE standard must not be saturated, as will be most of the individual allergen spots (**Fig. 3**). In order to acquire Image 1, the scan power is reduced such that none of the standard IgE spots as well as none of the allergen spots contain saturated fluorescence intensity pixels. Usually, the scan power for Image 1 is reduced 5- to 10-fold when compared to that in Image 2 (*see* **Fig. 2**).

4. Hiller, R., Laffer, S., Harwanegg, C., et al. (2002) Microarrayed allergen molecules: diagnostic gatekeepers for allergy treatment. *FASEB J.* **16,** 414–416.
5. Jahn-Schmid, B., Harwanegg, C., Hiller, R., et al (2003) Allergen microarray: comparison of microarray using recombinant allergens with conventional diagnostic methods to detect allergen-specific serum immunoglobulin E. *Clin. Exp. Allergy* **33,** 1443–1449.
6. Kim, T. E., Park, S. W., Cho, N. Y., et al (2002). Quantitative measurement of serum allergen-specific IgE on protein chip. *Exp. Mol. Med.* **34,** 152–158.
7. Wiltshire, S., O'Malley, S., Lambert, J., et al. (2002) Detection of multiple allergen-specific IgEs on microarrays by immunoassay with rolling circle amplification. *Clin. Chem.* **46,** 1990–1993.

12

Surface Plasmon Resonance Imaging on Polypyrrole Protein Chips

Application to Streptavidin Immobilization and Immunodetection

Emilie Mercey, Ludivine Grosjean, André Roget, and Thierry Livache

Summary

Initially developed for the construction of DNA chips, the polypyrrole approach has been extended to other biochemical compounds (mainly proteins and oligosaccharides). This method allows one to copolymerize a pyrrole monomer with a biomolecule bearing a pyrrole group; this reaction is based on an electrochemical process allowing a very fast coupling of the biomolecule (probe) to a gold layer used as a working electrode. Fluorescence-based detection processes are classically used for evidence biorecognition on biochips; in order to avoid the labeling of the targets, we propose an alternative method—surface plasmon resonance imaging (SPRi).

Surface plasmon resonance (SPR) is a typical label-free method for real-time detection of the binding of biological molecules onto functionalized surfaces. This surface-sensitive optical method is based upon evanescent wave sensing on a thin metal layer. The SPR approach described herein is performed in an imaging geometry that allows simultaneous monitoring of biorecognition reactions occurring on an array of immobilized probes (chip). In a SPRi experiment, local changes in reflectivity are recorded with a charge-coupled device (CCD) camera and are exploited to monitor up to 100 different biological reactions occurring on the molecules linked to the polypyrrole matrix. This method will be applied to protein recognition.

Key Words: Antibody; polypyrrole; protein array; surface plasmon resonance imaging.

1. Introduction

In the past 10 years there has been increasing interest in biochips bearing a high number of probes (DNA, proteins, etc.). A number of techniques have been developed to immobilize these probes on a high variety of supports. A comparison of different supports by Angenendt et al. ***(1)*** showed high signal

From: *Methods in Molecular Biology, Vol. 385: Microchip-Based Assay Systems: Methods and Applications*
Edited by: Pierre N. Floriano © Humana Press Inc., Totowa, NJ

uniformity and reproducibility of most plain glass and plastic slides. These arrays were realized in different ways, mainly spotting by physical methods: ink jet *(2)* or activation of a support and postfunctionalization *(3)*. *In situ* synthesis was also described for DNA and peptide arraying *(4–6)*. Immobilization of DNA or proteins can also be done on a polypyrrole support. Oligonucleotide arrays can be built either by *in situ* DNA synthesis *(7)* or by postfunctionalization *(8,9)*. Another approach is the entrapment of DNA or protein during the electrosynthesis of the polymer *(10,11)*. Chemical modification of DNA or protein by a pyrrole moiety (**Fig. 1**, **step 1**) has allowed us to construct biochips by electrocopolymerization of these biological molecules with pyrrole *(12–14)*. This straightforward method allows one to make DNA or protein immobilization in one step, avoiding the support activation. This electrochemical reaction is highly reproducible and allows one to control the density of the immobilized probe as well as polypyrrole film growth. An efficient method has been developed to make DNA or protein biochips by a simplified electrochemical process, electrospotting (**Fig. 1**, **step 2**) *(15)*; it allows the preparation of spots bearing biomolecules on a nonstructured conducting layer (homogeneous gold film).

With these methods, arrays of proteins, antigens, or antibodies have been prepared and used to perform biological recognition. The efficiency of the immunological response can be checked by fluorescence (**Fig. 1**, **step 3**), which is a highly sensitive *(16,17)* reference method. However, this approach is an end-point method and needs a labeled target that can modify the activity of the protein. For these reasons, label-free methods have been investigated; among them, surface plasmon resonance (SPR) seems to be very promising and has been used to detect antigen–antibody or, more generally, protein–protein interactions *(18)*. In order to be compatible with the analysis of protein array, SPR imaging (SPRi) was developed, which makes it possible to measure multispot parallel interactions in one experiment *(19)*. The result is a quantified comparison of various interactions with positive and negative spots within the same experiment and, therefore, improved consistency.

2. Materials

2.1. Synthesis of the Linker Pyrrole N-Hydroxysuccinimidyl (6-(Pyrrol-yl)-Caproate)

1. 2,5-Dimethoxytetrahydrofuran, mixture of *cis* and *trans* isomers 99% (Acros Organics).
2. 6-Aminocaproic acid 99+% (Acros Organics).
3. 1,4-dioxan, synthesis grade (Aldrich).
4. Acetic acid, purex analytical grade (Aldrich).
5. *N*-Hydroxysuccinimide 97% (Aldrich).

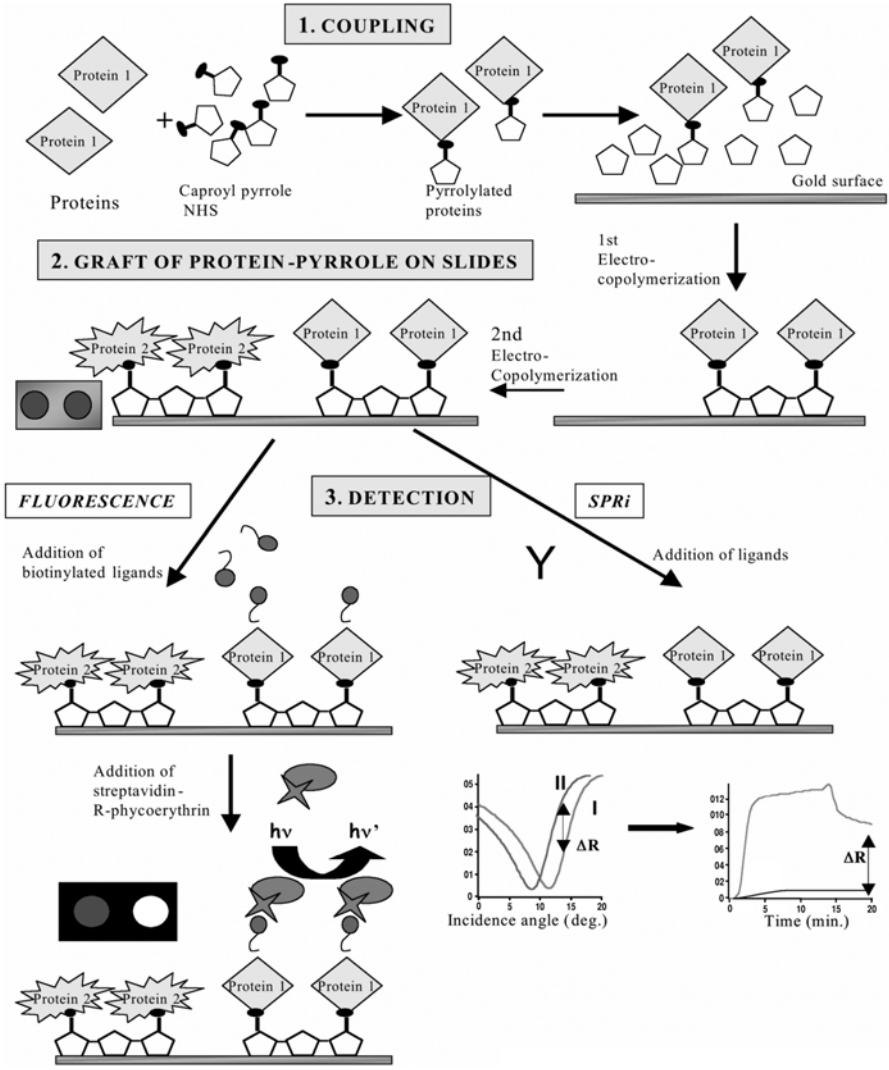

Fig. 1. Procedure to build protein biochips. **Step 1:** Coupling between proteins and caproyl pyrrole NHS; **step 2:** grafting of protein pyrrole on the gold layer by electro-copolymerization; **step 3:** detection by (left) fluorescence process and (right) surface plasmon resonance imaging experiment to study the dynamic interaction.

6. *N*,*N*'-Dicyclohexylcarbodiimide 99% (Acros Organics).
7. *N*,*N*-Dimethylformamide (DMF) for analysis (Carlo Erba).
8. Dimethylsulfoxide, analytical reagent (Prolabo).

9. Dichloromethane (CH_2Cl_2) purex for analysis (Aldrich).
10. Ethyl alcohol anhydrous (EtOH), for analysis (Carlo Erba).
11. Silica gel PF_{254} containing Ca SO_4 for preparative layer chromatography (Merck).
12. Chloroform-d, 99.9 atoms % D, stabilized with 0.5 wt silver foil (Aldrich).

2.2. Preparation of Pyrrolylated Proteins

1. Dimethylsulfoxide (DMSO) analytical reagent (Prolabo).
2. N-Hydroxysuccinimidyl (6-(pyrrol-yl)-caproate) synthesized in the laboratory, diluted in DMSO with different concentrations.
3. DMF for analysis (Carlo Erba).
4. Streptavidin from *Streptomyces avidinii* (Sigma) is dissolved in phosphate-buffered saline (PBS) buffer at 1 mg/mL.
5. Lysozyme (from egg white), 50,000 U/mg cryst. Hydrochloride for biochemistry called HEL Merck Lipha) is dissolved in PBS buffer at 1.39 mg/mL (100 μ*M*).
6. Antibody anti-HEL, called F10, monoclonal (produced in the P. Marche laboratory) is dissolved in PBS at 0.76 mg/mL.
7. Coupling buffer: PBS 0.01 *M* (PBS tablets from Sigma).
8. Electrocopolymerization buffer: 50 m*M* phosphate buffer, 50 m*M* NaCl, pH 6.8.
9. Vivaspin 0.5 mL concentrator with polyether sulfone membrane (5000 MWCO PES membranes) from Vivascience.

2.3. Preparation of Biotinylated Lysozyme

1. Use the same materials (*see* **Subheading 2.2.**).
2. EZ-link® NHS-Biotin, 100 mg, ref. 20217 from Pierce.

2.4. Copolymerization of Streptavidin–Pyrrole on SPRi Slides

1. Glass prisms covered by 50-nm gold thin films by vacuum-evaporation are from Genoptics® (Orsay, France).
2. Microelectrochemical cell: a 0.6-mm-diameter platinum wire is inserted in a 200-μL pipet tip.
3. Electrocopolymerization buffer: 50 m*M* phosphate buffer, 50 m*M* NaCl, pH 6.8.
4. EG&G Princeton Applied Research model 283 potentiostat.
5. 8300 Schlumberger X/Y recorder.

2.5. Fluorescence Detection

1. Washing buffer: 0.01 *M* PBS (tablets from Sigma), 0.05% Tween 20 (v/v) (Tween 20 in vitro test [10 mL] from Cis bio International).
2. Blocking buffer: 0.01 *M* PBS, 1% bovine serum albumin (BSA) (w/v) (BSA [initial fractionation by heat shock], fraction V minimum 98% [electrophoresis] from Sigma), 0.05% Tween 20 (v/v).
3. Regeneration buffer: buffer 0.1 *M* glycine (0.1 *M* glycine, electrophoresis reagent minimum 99% from Sigma), HCl (hydrochloric acid 1 *N* from SDS), pH 2.3.
4. Dako Cytomation Pen, ref. S2002 (to draw the hydrophobic line).

5. Biotinylated HEL (*see* **Subheading 3.3.**).
6. F10 antibody (*see* **Subheading 2.2.**).
7. Anti-Rabbit IgG (whole molecule) biotin conjugate B-8895 0.5 mL (from Sigma).
8. Streptavidin, R-phycoerythrin conjugates 1 mg/mL in 0.1 *M* $NaPO_4$, 0.1 *M* NaCl, pH 7.5, 2 m*M* azide (from Molecular Probes).
9. R-Phycoerythrin, biotin-XX conjugate 4 mg/mL in 0.1 *M* $NaPO_4$, 0.1 *M* NaCl, pH 7.5, 2 m*M* azide (from Molecular Probes).
10. Cover glasses 24 × 24 mm (n°1) (from Marienfeld).
11. Epifluorescence microscope BX 60 Olympus equipped with a Peltier cooled CCD camera (Hamamatsu) and an image analysis software (ImagePro Plus, Media Cybernetics).

2.6. SPRi Interaction Monitoring

1. SPRi lab: SPR imaging system and Software Genovision (Genoptics®, Orsay, France).
2. Syringe pump model A-99 from Bioblock Scientific.
3. Regeneration buffer: 0.1 *M* glycine, HCl pH 2.3.
4. Biotinylated SDF-1 (chemokine) at 100 µ*M* obtained from H. Lortat-Jacob from the Institut de Biologie Structurale (Grenoble, France).

3. Methods

3.1. Synthesis of N-Hydroxysuccinimidyl 6-(Pyrrol-yl)-Caproate (= Caproyl Pyrrole NHS)

1. A mixture of 2,5-dimethoxytetrahydrofuran (490 mmol, 64.85 mL),6-aminocaproic acid (430 mmol, 56.33 g), acetic acid (430 mL), and 1,4-dioxan (570 mL) is heated under reflux for 4 h and stirred at room temperature overnight ***(20)***.
2. The volatiles are removed under reduced pressure; the residue is dissolved in ethanol (2 × 100 mL) to eliminate acetic acid.
3. Product **1** (**Fig. 2**) is obtained with a yield of 86% after chromatographic purification on silica gel (500 g) column; CH_2Cl_2/EtOH as eluents. The elution starts by 500 mL CH_2Cl_2, then 300 mL 98% CH_2Cl_2/2% EtOH, then 400 mL 95%/5% EtOH; product **1** goes out the column for a gradient of 90%/10% EtOH. This product **1** is a brownish oil.
4. M.S. product **1** (m/z) = 182.1 (M+).
5. ^{1}H-RMN product **1** (200 MHz; $CDCl_3$/TMS) δ (ppm): 1.72 (m, 6H, -CH_2-(C**H2**)$_3$-CH_2-); 2.34 (t, 2H, -C**H2**-CO_2H); 3.87 (t, 2H, -C**H2**-N); 6.13 (dd, 2H, 3-**H** and 4-**H** pyrrole); 6.64 (dd, 2H, 2-**H** and 5-**H** pyrrole).
6. Product **1** (144 mmol, 26.05 g), *N*-hydroxysuccinimide (144 mmol, 16.56 g), *N*,*N*'-dicyclohexylcarbodiimide (159 mmol, 32.75 g), and DMF are mixed, at room temperature, overnight.
7. The mixture is filtered to eliminate *N*,*N*'-dicyclohexylurea.
8. The volatiles are removed under reduced pressure. Product **2** is used without any other purification.

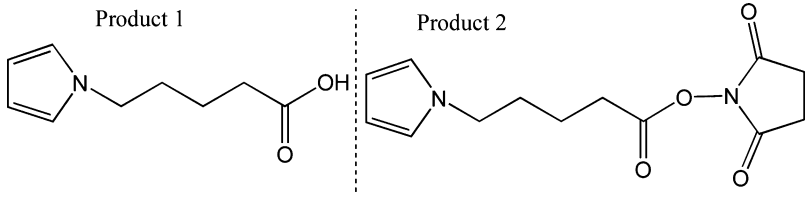

Fig. 2. Product 1: 6-pyrrolyl caproic acid; product 2: caproyl pyrrole NHS.

9. ^{1}H-RMN product **2** (200 MHz ; $CDCl_3$/TMS) δ (ppm): 1.72 (m, 6H, -CH_2-(C**H2**)$_3$-CH_2-); 2.34 (t, 2H, -C**H2**-CO); 2.88 (tt, 4H, -CH_2-CH_2-: NHS); 3.87 (t, 2H, -C**H2**-N); 6.13 (dd, 2H, 3-**H** and 4-**H** pyrrole); 6.64 (dd, 2H, 2-**H** and 5-**H**: pyrrole).

3.2. Preparation of Pyrrolylated Proteins

The coupling between the pyrrole and proteins is made by the use of the effect of the activated ester on the amine function of the proteins.

3.2.1. Pyrrolylation of Streptavidin

In order to find the IMR allowing the best coupling between the two molecules, the samples are prepared in different initial molar ratios (IMR = 0, 10, 20, 40, and 60).

1. 200 µL Streptavidin (1 mg/mL) is added to the caproyl pyrrole NHS diluted in DMSO at different concentrations (386 µ*M*, 773 µ*M*, 1.54 m*M*, or 3.1 m*M*). For example, for IMR = 20, 200 µL streptavidin (1 mg/mL) and 86 µL caproyl pyrrole NHS (773 µ*M*) are mixed for 2 h at room temperature.
2. The samples are then centrifuged on Vivaspin filters at 6000*g* for 25 min at 15°C to eliminate the small molecules in excess and the solvent DMSO.
3. The samples are then rinsed with 100 µL of electrocopolymerization buffer, centrifuged, and rinsed again, three times.
4. The samples are recovered and diluted in electrocopolymerization buffer at 20 µ*M* (~50 µL electrocopolymerization buffer).

3.2.2. Pyrrolylation of the Lysozyme HEL

HEL lysozyme (100 µL, 1.39 mg/mL) is added to the caproyl pyrrole NHS diluted in DMSO at different concentrations (15 or 30 m*M*). The samples are prepared in different initial molar ratios (IMR = 0, 10, 20).

1. For example, for IMR= 20, 100 µL HEL (1.39 mg/mL) and 7 µL caproyl pyrrole NHS (30 m*M*) are mixed for 2 h at room temperature (*see* **Note 1**).
2. The samples are then centrifuged on vivaspin filters at 6000*g* for 25 min at 15°C to eliminate the small molecules in excess and the solvent DMSO.
3. The samples are then rinsed with 100 µL of electrocopolymerization buffer, centrifuged, and rinsed again, three times.

4. The samples are recovered and diluted in electrocopolymerization buffer at 100 μ*M* (~200 μL electrocopolymerization buffer).

3.2.3. Pyrrolylation of F10 Antibody

F10 antibody (200 μL, 4.3 μ*M*) is added to the caproyl pyrrole NHS diluted in DMSO at different concentrations (375 μ*M*, 750 μ*M*, or 1.5 m*M*). Some samples are prepared in different initial molar ratios (IMR = 0, 5, 10, 20) to find the IMR allowing the best coupling between the two molecules.

1. For example, for IMR = 20, 200 μL of F10 antibody (4.3 μ*M*) and 12 μL of caproyl pyrrole NHS (1.5 m*M*) are mixed for 2 h at room temperature (*see* **Note 1**).
2. After the reaction, the samples are centrifuged at 6000*g* for 25 min at 15°C to eliminate the small molecules in excess and the solvent DMSO.
3. The samples are then rinsed with 100 μL of electrocopolymerization buffer, centrifuged, and rinsed again, three times.
4. The samples are recovered and diluted in electrocopolymerization buffer at 20 μ*M* (~45 μL electrocopolymerization buffer).

3.3. Preparation of Biotinylated HEL Lysozyme

1. 100 μL HEL lysozyme (1.39 mg/mL) is added to 7 μL biotin–NHS ester diluted in DMF at 30 m*M* and mixed for 2 h at room temperature.
2. The sample is centrifuged at 6000*g* for 25 min at 15°C to eliminate the small molecules in excess and the solvent DMF.
3. The sample is rinsed with 100 μL electrocopolymerization buffer.
4. The samples are centrifuged and rinsed again, three times.
5. The sample is recovered and diluted in electrocopolymerization buffer at 140 μ*M* (~70 μL electrocopolymerization buffer).

3.4. Copolymerization of Protein–Pyrrole on SPRi Slides

1. The electrochemical copolymerization was carried out by the "electrospot" method ***(19)*** on the gold layer through the use of a 200-μL pipet tip as the electrochemical cell.
2. Electrical contact was established inside the tip by inserting a platinum wire used as a counterelectrode.
3. The tip was filled with 10 μL of polymerization solution containing 15 μ*M* pyrrole–streptavidin and 20 m*M* pyrrole monomers and was then applied to a precise location on the gold layer used as the working electrode.
4. This electrochemical system was connected to a potentiostat and to an X/Y recorder. The polypyrrole film was synthesized by electrocopolymerization on the gold layer by a 2.4 V electrochemical pulse for 0.5 s (the voltage is defined with the respect to the platinum counterelectrode).
5. Following the electrosynthesis, the tip was emptied and rinsed with water.
6. The successive polymerizations were carried out by the same process with the different concentrations and different IMR of streptavidin–pyrrole (7.5 μ*M*,

IMR = 0, 20, 40, 60) to be copolymerized on spatially defined areas of the gold slide.
7. When all the samples spots were synthesized, the slide was disconnected and rinsed with washing buffer (*see* **Notes 2** and **3**).

3.5. Fluorescence Detection

The step of fluorescence detection ***(16,17)*** is generally used to control the quality of the chip (presence of the protein spots, biological activity). It also makes it possible to find the best IMR and the best concentration of protein pyrrole. The protocols for all proteins used are essentially the same.

3.5.1. Streptavidin–Pyrrole

1. Draw a hydrophobic line with a Dako Pen around the location of the spots.
2. Add 50 µL of a solution of 1% BSA diluted in the washing buffer (blocking buffer) and wait for 30 min to allow the disposition of BSA on the gold surface. This step allows one to reduce nonspecific fluorescence between the gold surface and the fluorescent tag.
3. Rinse the slide with 1 mL of washing buffer to eliminate BSA excess on the surface.
4. Add 50 µL of biotin–R-phycoerythrin 10% (v/v) for 20 min protected from the light.
5. Rinse again with 1 mL of washing buffer.
6. The slide is placed under the microscope (objective ×1.25 or ×4 and exposition time of 1 s or less) and the image recorded.

Figure 3 shows that IMR 20 gives the best result. Moreover, the polypyrrole spots and the gold layer do not interact with the fluorescent tag. We choose, for the next SPRi experiments, IMR = 20 and a streptavidin–pyrrole concentration of 15 µ*M*.

3.5.2. Antibody F10–Pyrrole

1. Draw a hydrophobic line with a Dako Pen around the location of the spots.
2. Add 50 µL of blocking buffer and wait for 30 min to block the surface with BSA. This step allows one to reduce nonspecific binding.
3. Rinse the slide with 1 mL of washing buffer to eliminate BSA excess on the surface.
4. Add 50 µL of biotinylated HEL 1.5 µ*M* for 30 min to do the biological recognition.
5. Rinse again with 1 mL of washing buffer.
6. Add 50 µL of streptavidin–R-phycoerythrin (SAPE) 5% (v/v) for 20 min protected from the light.
7. Rinse again with 1 mL of washing buffer.
8. The slide is placed under the microscope (objective ×1.25 or ×4 and exposition time of 1 s or less) and the image recorded.

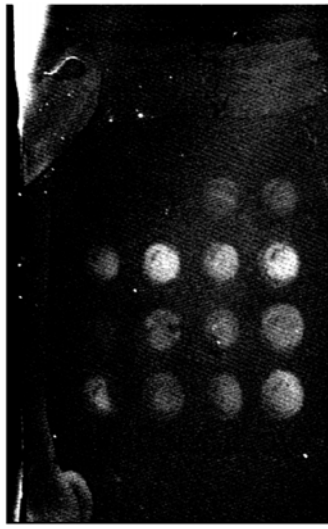

ppy **45**	ppy **54**	IMR = 0 *7.5µM* **81**	IMR = 0 *15µM* **94**
IMR = 20 *7.5µM* **99.4**	IMR = 20 *15µM* **135**	IMR = 20 *7.5µM* **114**	IMR = 20 *15µM* **153**
IMR = 40 *7.5µM* **60**	IMR = 40 *15µM* **87**	IMR = 40 *7.5µM* **89**	IMR = 40 *15µM* **105**
IMR = 60 *7.5µM* **105**	IMR = 60 *15µM* **47**	IMR = 60 *7.5µM* **99**	IMR = 60 *15µM* **122**

Fig. 3. Slide bearing streptavidin–pyrrole spots: image exposed for 1 s, objective ×1.25.

Figure 4 shows that the nonspecific background is very low. The streptavidin spot (IMR = 20, 15 µ*M*) is a plot allowing one to control HEL biotinylation (*see* **Subheading 3.3.**). The signal seen on the spot F10 IMR = 0 is a result of interaction with pyrrole polymer during the copolymerization. These results show that the best IMR for the coupling is 20, with a concentration of 10 µ*M*.

3.5.3. HEL Antigen–Pyrrole

1. Draw a hydrophobic line with a Dako Pen around the location of the spots.
2. Add 50 µL of blocking buffer and wait for 30 min to block the surface with BSA. This step allows one to eliminate nonspecific binding.
3. Rinse the slide with 1 mL of washing buffer.
4. Add 50 µL of F10 antibody 100 n*M* for 30 min.
5. Rinse again with 1 mL of washing buffer.
6. Add 50 µL of biotinylated anti-rabbit IgG 3.4 µg/mL for 30 min.
7. Rinse again with 1 mL of washing buffer.
8. Add 50 µL of streptavidin–R-phycoerythrin (SAPE) 5% (v/v) for 20 min protected from the light.
9. Rinse again with 1 mL of washing buffer.
10. The slide is placed under the microscope (objective ×1.25 and exposition time of 1 s or less) and the image recorded.

Figure 5 shows that the nonspecific background is very low. SA spots and F10 spots allow one to confirm that the anti-rabbit antibody used is biotinylated

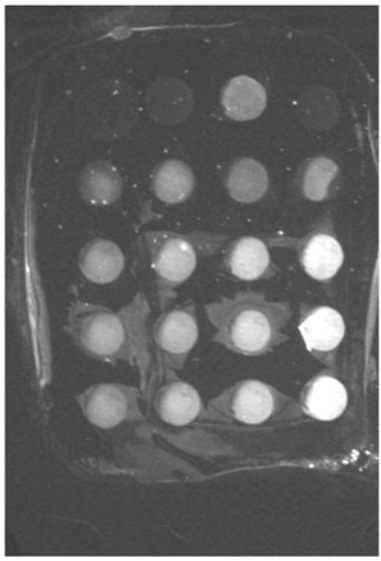

Ppy **28**	Ppy **32**	SA, 20 15µM **87**	HEL, 10 15µM **33**
IMR = 0 1.25µM **71**	0 2.5µM **99**	0 5µM **78**	0 10µM **98**
IMR = 5 1.25µM **101**	5 2.5µM **127**	5 5µM **149**	5 10µM **177**
IMR = 10 1.25µM **113**	10 2.5µM **126**	10 5µM **152**	10 10µM **190**
IMR = 20 1.25µM **103**	20 2.5µM **132**	20 5µM **151**	20 10µM **196**

Fig. 4. Slide bearing F10–pyrrole spots: (left) image exposed for 1 s, objective ×0.25; (right) table explaining location, initil molar ratio (IMR), spotting concentrations, fluorescence intensities of each spot.

(interaction between SA and IgG biotin) and that this antibody is active and recognizes F10.

HEL spots have an increasing intensity proportionally with the spotting HEL concentration. HEL spots with IMR = 0 have a signal intensity higher than the background, because HEL, like F10 (*see* **Subheading 3.5.2.**), may interact with the pyrrole during the electrocopolymerization. The best IMR seems to be in the range of 10–20.

3.6. SPRi Interaction Monitoring

The SPRi reader was from Genoptics (Orsay, France), and the optical setup was as described elsewhere ***(19,21)*** . Briefly, the interactions produce changes in the refractive indexes near the gold surface, which result in the changes of the reflectivity recorded by a 12-bit CCD camera as grey-level contrasts. During experiments, images were recorded at fixed intervals of time (0.1 s). All the images captured are analyzed on a PC computer with Genovision Software (Genoptics).

The biological interactions are carried out in an 8-µL Teflon cell connected to a push syringe in washing buffer at room temperature. The flow rate of running solutions within the cell was 70 µL/min (*see* **Note 4**).

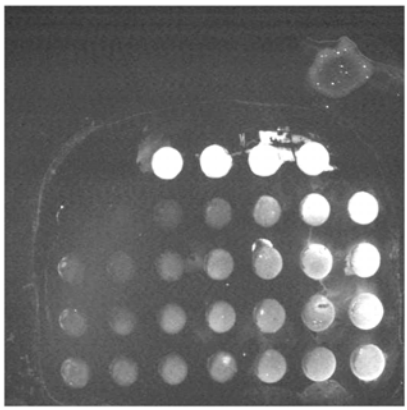

Ppy **30**	Ppy **30**	SA **228**	F10 (5) 10µM **232**	F10 (10) 10µM **196**	F10 (20) 10µM **243**	
0 0.3µM **32**	0 0.6µM **37**	0 1.25µM **40**	0 2.5µM **49**	0 5µM **73**	0 10µM **123**	0 20µM **192**
5 0.3µM **47**	5 0.6µM **46**	5 1.25µM **32**	5 2.5µM **64**	5 5µM **72**	5 10µM **88**	5 20µM **127**
10 0.3µM **49**	10 0.6µM **49**	10 1.25µM **62**	10 2.5µM **70**	10 5µM **72**	10 10µM **81**	10 20µM **114**
20 0.3µM **53**	20 0.6µM **53**	20 1.25µM **60**	20 2.5µM **66**	20 5µM **72**	20 10µM **78**	20 20µM **98**

Fig. 5. Slide of HEL–pyrrole spots: (left) picture exposed at 1 s, objective ×0.25; (right) table explaining the location of each spot on the slide, its initial molar ratio, spotting concentration, and fluorescence intensity.

3.6.1. With Streptavidin–Pyrrole

1. For the experiment, the plots of streptavidin–pyrrole are electrospotted on a glass prism covered by 50-nm gold thin film. Here, the studied spots are two strepatvidin–pyrrole IMR = 20 at 15 µ*M*, one polypyrrole spot, and the gold layer.
2. We put the prism into the SPR imaging, as described by the manufacturer. With the use of the syringe pump, the washing buffer runs in the cell.
3. To show that this technique allows one to use any biotinylated biological molecule, a solution of 500 µL biotinylated SDF-1 (chemokine) at 400 n*M* is injected for 7 min with a flow rate of 70 µL/min. The observed signal increases showing that the biotinylated SDF is bound on the streptavidin.
4. To know if the chemokine is still active, a 500-µL solution of 10 µ*M* heparan sulfate (HS) is injected for 7 min, and then regeneration buffer is injected to dissociate the SDF–HS complex to allow to the signals to return to baseline.

An increase in the signal can be observed in **Fig. 6**, which shows that there has been a real interaction between the fixed SDF and HS. The use of streptavidinated surface allows the grafting of different biotinylated biomolecules; in this way, it could be used as a versatile support, i.e., the grafting of bacteria ***(22)***.

3.6.2. SPRi Interactions Between HEL Antigen and F10 Antibody

For the experiment, spots of F10–pyrrole, HEL–pyrrole, and streptavidin–pyrrole are spotted on a glass prism covered by 50-nm gold thin film; **Fig. 7** shows the matrix and localization of each spot and its IMR and concentration.

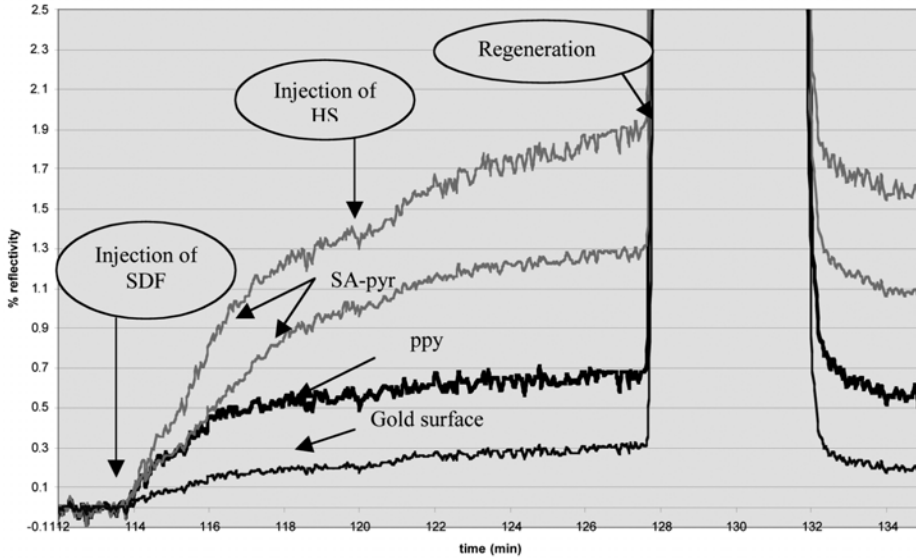

Fig. 6. Sensorgram of injection of biotinylated chemokine SDF. First step: injection of 500 µL biotinylated SDF-1 at 400 n*M*; second step: injection of 500 µL heparan sulfate (HS) at 10 µ*M*; third step: regeneration with injection of 500 µL regeneration buffer to dissociate totally the protein–oligosaccharide complex.

The prism is put into the SPRi instrument, as described by the manufacturer. Using a syringe pump, the washing buffer runs into the cell at a constant flow rate of 70 µL/min.

The experiment is started by two injections of 500 µL of blocking buffer to avoid proteins sticking anywhere on the surface (curves not shown). After the blocking step, protein is injected in the cell and one can observe the possible biological interactions.

To obtain the results displayed in **Fig. 8**, the following protocol must be followed:

1. 500 µL HEL at 625 n*M* is injected for 8 min. The signals increase corresponding to the F10 plots with IMR = 10 or 20. The signal observed on HEL spots can result from a nonspecific interaction and an optical index shift.
2. Wash for 5 min; the dissociation of HEL–F10 interaction can be observed.
3. Inject 280 µL of regeneration buffer for 4 min to totally dissociate the interactions and to go back to the baseline. After this first injection (*see* **Fig. 8**), the curves corresponding to F10 spots with IMR = 10 and 20 (encircled curves) increase during the HEL injection (specific interaction), whereas the other spots show just a background level during the interaction phase and no residual sig-

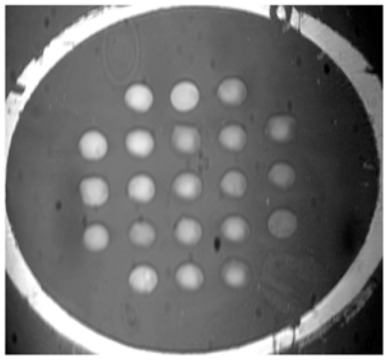

	F10 **10**/10µM	SA **20**/15µM	HEL **10**/25µM	
F10 **20**/10µM	F10 **10**/10µM	HEL **20**/25µM	HEL **10**/12.5µM	Ac n°36 0/5µM
F10 **20**/10µM	F10 **10**/5µM	HEL **20**/25µM	HEL **0**/10µM	ppy
F10 **20**/5µM	F10 **0**/5µM	HEL **20**/12.5µM	AB n°36 20/5µM	ppy
	SA **20**/15µM	HEL **10**/25µM	AB n°36 20/5µM	

Fig. 7. (Left) Picture of the plot matrix; (right) description of each spot: initial molar ratio, concentration, localization. AB n°36 is a monoclonal IgG1 from mouse that does not recognize HEL.

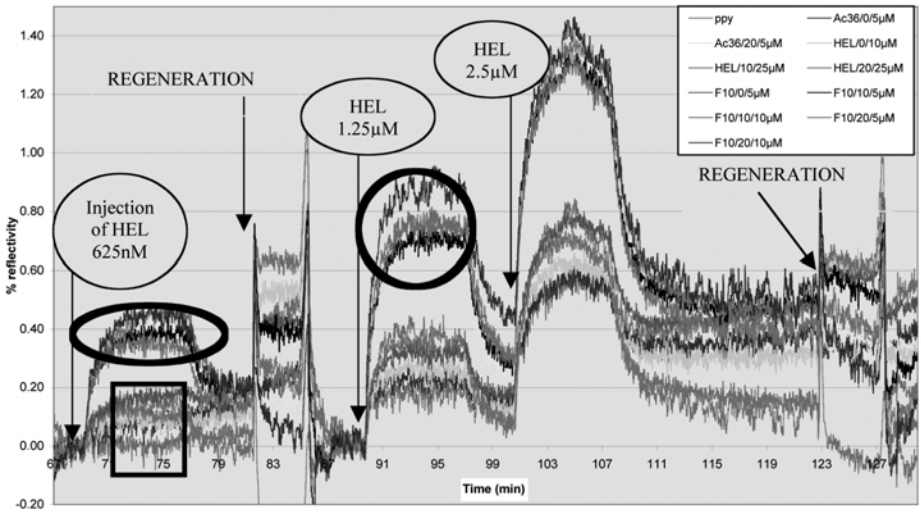

Fig. 8. Sensorgram of HEL injections at different concentrations. The circled curves on the graph are the F10 spots (initial molar ratio [IMR] = 10 at 5 µ*M* and 10 µ*M* and IMR = 20 at 5 and 10 µ*M*); the curves in the rectangle are the other spots: F10/IMR = 0/5 µ*M*, HEL/IMR = 10/25 µ*M* First injection: 625 n*M* HEL for 8 min; inject washing buffer (5 min) and regeneration buffer for 4 min; second injection: injection of HEL 1.25 µ*M* for 8 min, washing (4 min), then second injection of HEL 2.5 µ*M* (8 min), washing (15 min), and regeneration for 4 min.

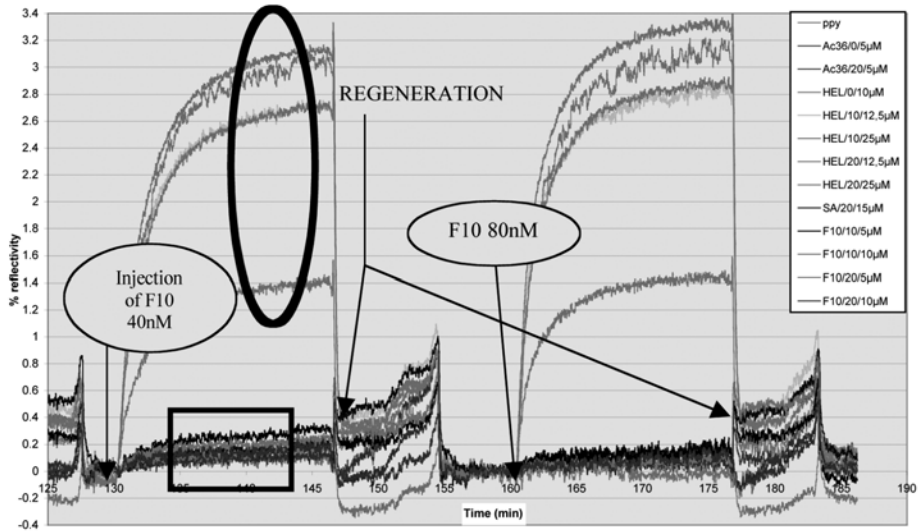

Fig. 9. Sensorgram of F10 injections at two different concentrations. The circled curves on the graph are all the HEL spots; the curves in the rectangle are the other spots: F10, SA (streptavidin) and AB n°36. First injection: 40 n*M* F10 for 8 min, washing (8 min), and regeneration for 4 min; second injection: F10 at 80 n*M* for 8 min, washing (8 min), and regeneration for 4 min.

nal after the washing step. The same result can be observed for the second injection.

4. Second injection: 500 µL HEL, 1.25 µ*M* for 8 min.
5. Wash for 4 min.
6. Inject 500 µL HEL at 2.5 µ*M* for 8 min.
7. Wash for 15 min.
8. Use 280 µL of regeneration buffer for 4 min. After the different HEL injections, two F10 concentrations are injected into the cell to see if interaction between HEL spots and F10 in solution are possible (*see* **Fig. 9**).
9. 500 µL F10 is injected at 40 n*M* for 8 min; three HEL spots with IMR = 10 and 20 and concentrations = 12.5 µ*M* and 25 µ*M* recognize specifically the injected antibody (plateau value at ~3%); the HEL spot with IMR = 0 and concentration = 10 µ*M* can recognize the target at a lower level (plateau value at ~1.4%). This shows that the pyrrolylation of the HEL increases its grafting and its recognition with the F10 antibody. None of the other spots (ppy, SA, AB n°36, or F10) recognize the antibody.
10. Even if a washing step is done for 8 min, dissociation of HEL–F10 interaction cannot be seen.

11. The surface is regenerated by the injection of 280 µL of regeneration buffer for 4 min, the interaction is dissociated, and all the curves again join the baseline.
12. 500 µL F10 at 80 n*M* (twice) is injected for 8 min; no increase in signal shows that the saturation level has been obtained.
13. The cell is washed without observation of a decrease in the signal intensities; dissociation of HEL–F10 interaction cannot be seen.
14. The experiment is finished with 280 µL of regeneration buffer for 4 min.
15. At the end of the experiment, the running buffer is stopped and the prism is removed.

4. Notes

1. Coupling: for HEL or F10, do not increase DMSO percentage above 5% (*see* **Subheading 3.2.2.**).
2. Following electropolymerization, wait at least for 20 min before rinsing the biochip to avoid nonfixed proteins sticking on the gold layer around the spot (*see* **Subheading 3.4.**).
3. Following electrocopolymerization, do not dry the gold surface to avoid protein denaturation. Following spotting, the surface is rinsed with PBS, Tween 20 at 1% (v/v) and the prism is stored at 4°C (*see* **Subheading 3.4.**).
4. All buffers used in SPRi experiments must be filtered (0.20 µm) and degazed (ultrasound) in order to avoid air bubbles in the cell during the experiment (*see* **Subheading 3.6.**).

Acknowledgments

We thank Genoptics SA for the DRT grant (LG).

References

1. Angenendt, P., Glökler, J., Murphy, D., Lehrach, H., and Cahill, D. J. (2002) Toward optimized antibody microarrays: a comparison of current microarray support materials. *Anal. Biochem.* **309,** 253–260.
2. Yershov, G., Barsky, V., Belgovskiy, A., et al. (1996) DNA analysis and diagnostics on oligonucleotide microchips. *Proc. Natl. Acad. Sci. USA* **93,** 4913–4918.
3. Sheldon, M., Briggs, J., Bryan, R., et al. (1993) Matrix DNA hybridization. *Clin. Chem.* **39,** 718–719.
4. Blanchard, P., Kaiser, R. J., and Hood, L. E. (1996) High-density oligonucleotide arrays. *Biosens. Bioelectron.* **11(6–7),** 687–690.
5. Pease, A. C., Solas, D., Sullivan, E J., Cronin, M. T., Holmes, C. P., and Fodor, S. P. A. (1994) Light-generated oligonucleotide arrays for rapid DNA sequence analysis. *Proc. Natl. Acad. Sci. USA* **91,** 5022–5026.
6. Fodor, S. P., Read, J. L., Pirrung, M. C., Stryer, L., Lu, A. T., and Solas, D. (1991) Light-directed, spatially addressable parallel chemical synthesis. *Science* **251(4995),** 767–776.

7. Roget, A. and Livache, T. (1999) In situ synthesis and copolymerization of oligonucleotides on conducting polymers. *Mikrochim. Acta* **131,** 3–8.
8. Korri-Youssoufi, H., Garnier, F., Srivastava, P., Godillot, P., and Yassar A. (1997). Toward bioelectronics: specific DNA recognition based on an oligonucleotide-functionalized polypyrrole. *J. Am. Chem. Soc.* **119,** 7388–7389.
9. Röckel, H., Huber, J., Gleiter, R., and Schuhmann, W. (1994) Poly(dithienylpyrrole) derivatives and their application in synthesis of functionalized amperometric biosensors**.** *Adv. Mat.* **6(7–8),** 568-571
10. Wang, J., Jiang, M., Fortes, A., and Muckherjee, B. (1999) New label-free DNA recognition based on doping nuceic-acid probes within conducting polymers films. *Anal. Chim. Acta* **402,** 7–12.
11. Thanachasai, S., Furukawa, H., Yoshida, S., and Watanabe, T. (2003) Determination of enzyme immobilized into electropolymerized polymer films. *Chem. Lett.* **32(2),** 176–177.
12. Livache, T., Roget, A., Dejean, E., Barthet, C., Bidan, G., and Teoule, R. (1994) Preparation of a DNA matrix via an electrochemically directed copolymerization of pyrrole and oligonucleotides bearing a pyrrole group. *Nucleic Acids Res.* **22,** 2915–2921.
13. Livache, T., Bazin, H., Caillat, P., and Roget, A. (1998) Electroconducting polymers for the construction of DNA or peptide arrays on silicon chips. *Biosens. Bioelectron.* **13,** 629–634.
14. Wolowacz, S. E., Yon Hin, B. F. Y., and Lowe C. R. (1992) Covalent electropolymerisation of glucose oxydase in polypyrrole. *Anal. Chem.* **64,** 1541–1545.
15. Livache, T., Guedon, P., Brakha, C., Roget, A., Levy, Y., and Bidan, G. (2001) Polypyrrole electrospotting for the construction of oligonucleotide arrays compatible with a surface plasmon resonance hybridization detection. *Synth. Methods* **121(2–3),** 1443–1444.
16. Haab, B. B., Dunham, M. J., and Brown, P. O. (2001) Protein microarrays for highly parallel detection and quantitation of specific proteins and antibodies in complex solutions. *Genome Biol.* **2(2),** 04.1–4.13.
17. Templin, M. F., Stoll, D., Schrenk, M., Traub, P. C., Vohringer, C. , and Joos, T. O. (2002) Protein microarray technology. *Trends Biotechnol.* **20,** 160–166.
18. Parsons, I. D. and Stockley, P. G. (1997) Quantitation of the *Escherichia coli* methionine repressor-operator interaction by surface plasmon resonance is not affected by the presence of a dextran matrix. *Anal. Biochem.* **254,** 82–87.
19. Guedon, P., Livache, T., Martin, F., et al. (2000) Characterization and optimization of a real-time, parallel, label-free, polypyrrole-based DNA sensor by plasmon resonance imaging. *Anal. Chem.* **72,** 6003–6009.
20. Jirkowski, I. and Baudy, R. (1981) A facile large scale preparation of 1H-pyrrole-1-ethanamine and syntheses of substituted pyrrolo[1,2-a]pyrazines and hydro derivatives thereof. *Synthesis* 481–483.
21. Nelson, B. P., Grimsrud, T. E., Liles, M. R., Goodman, R. M., and Corn, R. M. (2001) Surface plasmon resonance imaging measurements of DNA and RNA hybridization adsorption onto DNA microarrays. *Anal. Chem.* **73,** 1–7.

22. Da Silva, S., Grosjean, L., Ternan, N., Mailley, P., Livache, T., and Cosnier, S. (2004) Biotinylated polypyrrole films: an easy electrochemical approach for the reagentless immobilization of bacteria on electrode surfaces. *Bioelectrochemistry* **63,** 297–301.

13

Protein Array-Based Multiplexed Cytokine Assays

Cheng C. Wang

Summary

We have demonstrated a microarray format immunoassay using HydroGel-coated slides. HydroGel is a porous substrate based on a polymer matrix that provides a three-dimensional hydrophilic environment similar to free solution suitable for biomolecular interactions. This substrate has been used to develop fluorescence-based multiplexed cytokine immunoassays. Forty-three monoclonal antibodies (mAbs) of cytokines and chemokines are printed at a volume of 350 pL per spot using a PerkinElmer BioChip Arrayer®. Cytokines that are captured by the arrayed mAb are detected using another biotinylated mAb, following by the addition of a Texas red conjugated streptavidin. The fluorescent images of arrays are recorded using a PerkinElmer ScanArray™ 5000 confocal slide scanner and quantitated using PerkinElmer QuantArray™ software. Experiments demonstrate that 43 cytokines can be simultaneously screened and quantitated in conditioned culture media, cell lysate, and human plasma. Using this chip, we have examined cytokine expression in breast cancer cells and identified the chemokines associated with human cervical cancers.

Key Words: Microarray; protein chip; chemokine; cytokine; immunoassay; multiplex assays; HydroGel.

1. Introduction

Miniaturization and multiplexing assays with protein microarrays allow for a dramatic reduction in the amount of sample required (typically in the 10- to 100-µL ranges), an increase in the number of analytes that can be measured simultaneously, and increased throughput potential. This increased information attained by quantitatively measuring many analytes in parallel maintains relative expression levels within the same sample and may enable determination of relationships between diverse proteins involved in many pathways in response to the same environment ***(1)***.

From: *Methods in Molecular Biology, Vol. 385: Microchip-Based Assay Systems: Methods and Applications*
Edited by: Pierre N. Floriano © Humana Press Inc., Totowa, NJ

There have been several recent developments in microarray-based enzyme-linked immunosorbent assay (ELISA) for cytokine assays. Antibodies spotted into glass-bottomed microwell *(2)* or polystyrene 96-well plates *(3)*, glass slides *(4–6)*, membranes *(7–9)*, and antibody-coated beads *(10)* have been used to simultaneously detect multiple antigens in a miniature format. In general, proteins are more sensitive to their environment than nucleic acids. The hydrophobicity of many glass and plastic surfaces may cause protein denaturation, and thus render lower sensitivity and high noise-to-signal ratios. Consequently, substrate choice is a major consideration when designing protein microarray experiments. HydroGel-coated slides are based on a specialized polyacrylamide formulation that offers several advantages for protein applications including a high probe-binding capacity, very low inherent and assay-dependent background, and a hydrophilic environment *(11)*. We printed 43 cytokine antibodies on HydroGel-coated slides for simultaneously screening and quantitating cytokines in supernatants of cell culture, conditioned media, cell lysate, and human blood plasma.

Cytokines and growth factors mediate a wide range of physiological processes, including hematopoiesis, immune responses, wound healing, and general tissue maintenance *(12,13)*. Many factors contribute to the complexity of cytokine quantitation *(14)*. Measuring cytokines in biological fluids and tissues is fascinating because these mediators are involved in many pathological manifestations of inflammatory, infectious, and immunological diseases. Developing an accurate and sensitive method for the measurement of cytokines in body fluids is an absolute prerequisite for the proper use of these mediators in clinical practices.

Breast cancer cells have a higher density of high-affinity interleukin (IL)-6 receptors than normal tissue. IL-6 has a pleiotropic effect on breast cancer cells. IL-6 upregulates tumor necrosis factor (TNF)-α, IL-1α, and IL-1β expression *(15)*. Characterization of cytokine expression in breast cancer cell lines would reveal the relationship between serum IL-6 levels with poor prognosis in breast cancer.

The development of cervical cancer is initiated by the infection of cervical mucosa cells with high-risk human papillomavirus (HPV) types such as HPV-16 or -18. Monocyte chemoattractant protein (MCP)-1 is an important factor involved in the cross talk between mononuclear cells and HPV-infected cervical epithelia. In earlier studies the experimental model of a negative regulatory loop between the expression of the HPV oncogenes E6/E7 and the MCP-1 gene in vivo is proposed *(16)*. Since macrophages and macrophage-derived cytokines appear to be important in the transcriptional regulation of high-risk types of HPV, monitoring MCP-1 expression by in situ hybridization (ISH) in histologically distinct stages of cervical intraepithelial neoplasms (CIN), cer-

vical cancer, and non-HPV-associated cases of erosive endocervicitis indicated that dysregulation of MCP-1 gene expression may represent an important step during HPV-linked carcinogenesis, allowing the escape of virus-positive cells from local immune response ***(17)***.

We describe here protocols to use the chip to profile human cytokine expression of breast tumor cells and monitor human cytokine expression in clinical samples. Application of the chip to cervical cancer is also described. Potential clinical diagnosis application indicates a great future for protein arrays.

2. Materials

2.1. Reagents

1. Recombinant human cytokines, anti-cytokine capture antibodies, biotinylated anti-cytokine detection antibodies, anti-bovine IgG (goat) antibody, biotinylated anti-bovine IgG (goat) antibody, Texas red-conjugated bovine IgG fraction, and Texas red-conjugated streptavidin are from R & D systems (Minneapolis, MN) and Invitrogen (Carlsbad, CA). All antibodies and proteins are reconstituted according to the manufacturers' recommendations.
2. Stock cytokine solutions and subsequent serial dilutions are prepared using Dulbecco's Modified Eagle's (DME) culture medium supplemented with 10% fetal bovine serum (FBS).
3. FBS and DME media are from Hyclone (Logan, UT).
4. HydroGel slides are made in PerkinElmer with a licensed technology ***(11)*** (*see* **Note 1**).
5. All other biochemicals are from Sigma-Aldrich (St. Louis, MO).
6. Frame-Seal™ gasketed chambers and 384-well comical bottom plate are from Bio-Rad (Hercules, CA).

2.2. Buffers

1. Incubation and antibody dilution buffer: phosphate buffered saline (PBS): (0.14 *M* NaCl, 0.003 M KCl, 0.01 *M* sodium phosphate, pH 7.2).
2. Assay washing buffer: PBST (PBS containing 0.1– 0.5% Tween 20, pH 7.2).
3. Slide blocking and storage buffer: Pierce Endogen SuperBlock™.
4. Slide washing buffer: distilled water (dH_2O).

2.3. Samples

1. Cancer cell lines (MDA-MB-231 cells) ***(18)*** are obtained from ATCC and grown in DME's medium containing 10% fetal calf serum and a mixture of glutamine, penicillin, and streptomycin.
2. Patient blood sera are collected in Emory University Hospital.

2.4. Equipment and Software

1. PerkinElmer BioChip Arrayer®
2. PerkinElmer ScanArray™ 5000 confocal scanner.

3. PerkinElmer QuantArray™ software.
4. Statistica software (StatSoft, Tulsa, OK).
5. SigmaPlot software (SPSS, Chicago, IL).
6. Microsoft Excel (Microsoft, Seattle, WA).
7. Hybridization incubator (Robbins Scientific, Sunnylvale, CA).
8. Swinging bucket plate centrifuge (Sigma, St. Louis, MO).
9. Humidity chamber (Espec, Hudsonville, MI).

3. Methods

3.1. Antibody Array on HydroGel Substrate

3.1.1. Cytokine Array Design

Cytokines and chemokines are arranged in functional groups on the slides (**Fig. 1**).

1. Group 1 (A2– A10): CC, C, and CX3C chemokines.
2. Group 2 (A11, A12 and B2–B5): CXC chemokines.
3. Group 3 (B6–B11): hematopoietic factors.
4. Group 4 (B12): chronic inflammatory mediator.
5. Group 5 (C2–C8): growth and angiogenic factors.
6. Group 6 (C9, C10): IL-6 family.
7. Group 7 (C11, C12): TNF family.
8. Group 8 (D1, D2): IL-1s.
9. Group 9 (D4– D11): immunomodulating interleukins.

Controls are as follows:

1. Positive assay control: A11 (ENA-78).
2. Negative control: bovine serum albumin (BSA) at 1 mg/mL (D12).
3. Printing control: Texas red conjugated human IgG (row 13).
4. Detection control: biotinylated goat anti-bovine IgG (row 1).

3.1.2. Printing of the Antibody Array

1. Prior to printing, wash HydroGel-coated slides three times for 10 min each in dH_2O, dry by centrifugation and further in a 40°C oven for 20 min.
2. Cool the slides to room temperature for 5 min prior to printing.
3. Dilute capture antibody probes to a concentration of 0.5 mg/mL in PBS and add to 384-well comical bottom plate.
4. Print the monoclonal antibodies of 43 cytokines and chemokines in a 4-column by 13-row format as indicated in **Fig. 1** (four replicates for each probe at a pitch of 500 μm in the layout of 13×16 patterns on a 12×12 cm HydroGel pad).
5. Printing volume is 350 pL per spot using a PerkinElmer BioChip Arrayer (*see* **Note 2**).
6. Ultrasonically wash spotter tips in buffered surfactant (PBST) and between aspirates to eliminate carryover.

	A	B	C	D
1	Biotin-IgG	Biotin-IgG	Biotin-IgG	Biotin-IgG
2	RATEN	MIG	TGF-b	IL-1b
3	TARC	IL-8	MCSF	IL-1a
4	MIP-1g	GRO-a	VEGF	Leptin
5	MIP-1b	GRO	IGF-I	IL-15
6	MDC	TPO	EGF	IL-13
7	MCP-3	SCF	ANG	IL-12
8	MCP-2	IL-5	PDGF	IL-10
9	MCP-1	IL-3	OSM	IL-7
10	I-309	GCSF	IL-6	IL-4
11	ENA-78	GM-CSF	TNFb	IL-2
12	SDF	IFNg	TNFa	BSA
13	TR – IgG	TR - IgG	TR - IgG	TR – IgG

Fig. 1. Microarray layout. The antibody probes are printed at a volume of 350 pL per spot using a PerkinElmer BioChip Arrayer®. For each probe, four replicates are printed at a pitch of 500 μm as in the layout. Bovine serum albumin in printing buffer served as negative control. A series of replicate spots of biotinylated anti-bovine IgG (goat) antibody (10-fold decreasing intervals from A1 to D1) served as a detection control monitoring the ability of the immunoassay components to form a complex in the HydroGel matrix. Texas red-conjugated IgG spotted from A13 to D13 (10-fold increasing intervals) served as printing quantity controls. Epithelial Neutrophil Activating peptide-78 (A11) is set to be a positive control for cytokine assays.

7. Following printing, incubate HydroGel-coated slides overnight at 25°C in a humidified chamber (65% humidity).
8. Wash slides three times for 30 min each in PBS + 0.5% Tween 20, pH 7.2 (PBST) to remove any unbound probe and store the slide overnight in Pierce SuperBlock™ at 4°C.

3.2. Microarray Immunoassay

1. Rinse the slides three times in buffered surfactant wash buffer (PBST) to remove blocking solution.
2. Add 50 µL volume target samples to Frame-Seal™ gasket HydroGel chambers to prevent cross contamination of top and bottom arrays.
3. Incubate the slides for 1 h at room temperature in a gasketed and sealed frame on a rotating hybridization incubator.
4. Wash slides two times for 15 min each in wash buffer (PBS + 0.1% Tween, pH 7.2) followed by a 5-min wash in PBS, pH 7.2, to remove excess surfactant, and dry by brief centrifugation.
5. Apply 50µL aliquot of a cocktail of all 43 biotinylated detection antibodies at levels optimized for this system to the slides
6. Incubate the mixture for 1 h at room temperature.
7. Washing and centrifugation of slides as in **step 3**.
8. Finally, incubate the slides for 30 min at room temperature in an excess of Texas red-conjugated streptavidin (50 µL volume).
9. Wash and dry by the above procedure, followed by an additional 5-min rinse in PBS, pH 7.2, to remove detergent prior to imaging.

3.3. Slide Imaging and Data Analysis

1. Image the arrays in the Texas red channel using a PerkinElmer ScanArray 5000 confocal slide scanner.
2. Optimize the laser power and Photo Multiplier Tubes (PMT) settings for each substrate type such that the most intense spots for each analyte series are at approx 80% saturation. (Within an experiment, all slides of the same substrate type are scanned using the same settings.)
4. Determine the quantities of images using PerkinElmer QuantArray software.
5. Substrate baseline using the signals from the no-cytokine control from sample data.
6. Normalize the mean dialog box unit per pixel values for each array using the signal obtained from the detection antibody control, and calculate the data using Microsoft Excel.

3.4. Standard Curves Construction

1. Constitute a serial dilution of cytokine standards by spiking stock cytokines into cell culture media (DME) supplemented with 10% FBS.
2. Apply each dilute to two identical arrays on one slide. HydroGel pad contains a cytokine-free negative control and a detection control (biotinylated anti-bovine IgG).

Table 1
Using Analytic Software to Calculate the Dynamic Range, Slope, Coefficient of Determination (r^2 Value), and Theoretical Limits of Detection for Each Cytokine in Fig. 6

	TNF-α	IL-1β	IL-2	IL-6	IL-13	IFN-γ
y-Intercept	1.8	1.7	0.92	1.8	0.01	1.2
Slope	1.21	1.11	1.02	0.89	1.26	0.90
r^2	0.97	0.99	0.96	0.98	0.92	0.95

TNF, tumor necrosis factor; IL, interleukin; IFN, interferon.

Table 2
Quantitation of Cytokines Using Both Classical Well-Based ELISA and Array-Based ELISA

	IL-6	TNF-α
96-Well ELISA	96 pg/mL	52 pg/mL
Array ELISA	97 pg/mL	47 pg/mL
%	1.04	–9.62

ELISA, enzyme-linked immunosorbent assay; IL, interleukin; TNF, tumor necrosis factor.

3. Plot the baseline deducted data using Statistica software to determine dynamic range and dose response (*see* **Note 3**).
4. Determine the slope of the linear portion of each curve and the coefficient of determination (r^2) by trimming the curves and analyzing the resulting linear portion of each curve by linear regression using SigmaPlot software (*see* **Table 1**).

3.5. Quantitation of Cytokines in Human Serum

1. Spike the IL-6 and TNF-α into PBS containing 10% FBS.
2. Add 50 µL diluted samples to HydroGel pad.
3. Subject HydroGel to the standard array ELISA.
4. Calculate the cytokine concentration from the standard cytokine curve built at the same time (*see* **Table 2**).
5. Measure the cytokine concentration of the above samples following the R & D systems' single-well-plate ELISA.

3.6. Detecting Cytokine Expression in Clinical Samples

3.6.1. Breast Cancer Samples

1. Culture and stimulate human estrogen-receptor-negative MDA-MB231 breast tumor cells as described ***(18)***.
2. Separate the cells from supernatant by slow centrifugation, and subject to standard lysis procedure.

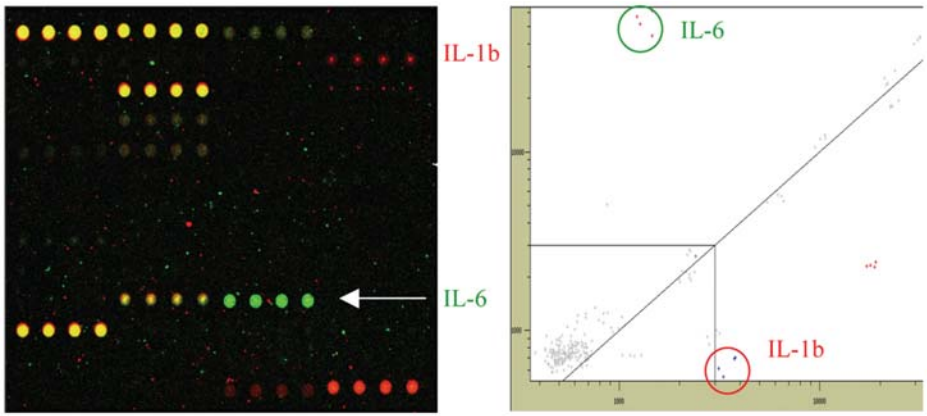

Fig. 2. Overlapping images of top and bottom arrays. Two identical 43-cytokine arrays are applied separately with cell lysate (red) and cell supernatant (green) from the same MDA-MB231 breast cancer cells. The yellow spots represent the occurrence of cytokines in both samples (red and green overlapped). Red spots indicate the cytokines presented in lysate only, and green spots represent the released cytokines in cell culture. Ratiometric analysis of overlapped images revealed that interleukin (IL)-6 is in cell supernatant and IL-1b is presented in cell lysate.

3. Add 50 µL cell culture supernatant to the top HydroGel pad.
4. Add 50 µL pelleted cell lysate to the bottom HydroGel pad (**Fig. 2**).

3.6.2. Cervical Cancer Samples

1. Apply 50 µL cancer plasma to the top HydroGel pad.
2. Add 50 µL normal plasma to the bottom HydroGel pad.
3. Repeat the standard array immunoassay procedures described in **Subheading 3.4.**
4. Analyze the data by overlapping the top and bottom images and comparing the metric ratio using PerkinElmer QuantArray software (**Fig. 3**).

4. Notes

1. HydroGel: The porous nature of the substrate enables probes, analytes, and detection molecules to form the necessary molecular interactions to generate stable complexes in immunoassays. The high loading capacity and hydrophilic environment of HydroGel slides may give an advantage over other microarray substrates. However, the structure of the HydroGel substrate is also sufficiently open for efficient washing of excess samples and detecting antibodies so that background noise and nonspecific binding activities are low. The three-dimensional substrate offers much better fluid performance. This contributes to the substrate's ability to achieve limits of detection comparable to what is commonly reached in traditional assays. This combination of physical attributes is unique to

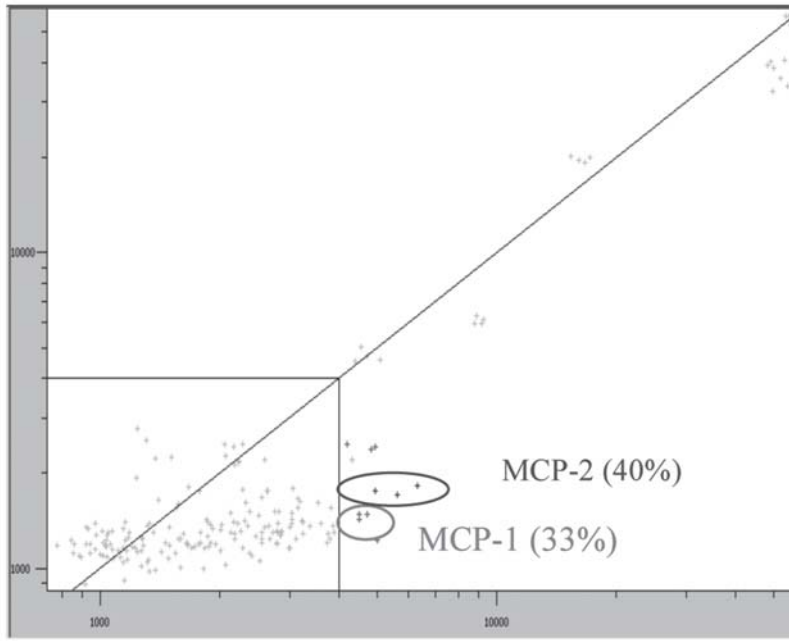

Fig. 3. Ratiometric plot of cervical intraepithelial neoplasm (CIN–II) blood against normal human blood. There are two 12 × 12 HydroGel pads in a slide. Identical arrays are printed on both pads. Plasma from normal persons is applied onto the top array, and patient plasma is assayed in the bottom array. After incubation and washing, both arrays are subject to the same postincubation immunodetection. The images from top and bottom arrays are overlapped, and a ratiometric plot is generated. The spots circled indicate MCP-1 decreased to 33% and MCP-2 to 40% in cancers compared to in normal persons.

HydroGel-coated slides, making them an excellent choice for protein microarray applications. Higher sensitivity is an important feature for applications analyzing proteins that have a broad expression range due to either physiological or pathological causes.

2. Substrate characterization: Currently, flat-surface-based chemical-treated glass slides ***(19)*** and nitrocellular-coated slides have been used to spot proteins ***(20)***. Thus, we compared HydroGel with these two substrates. The substrates chosen for comparison are an aldehyde-derivatized glass substrate and a three-dimensional nitrocellulose polymer-coated slide. When compared to HydroGel-coated slides (curve A, **Fig. 4**), the dynamic range of the aldehyde-derivatized glass substrate (curve B, **Fig. 4**) is short of lower concentration points because of the capture capacity. While the nitrocellulose-coated slide (curve C, **Fig. 4**) performs similarly to HydroGel-coated slides at the higher target concentrations, its sensitivity is much lower because of high levels of inherent fluorescent background.

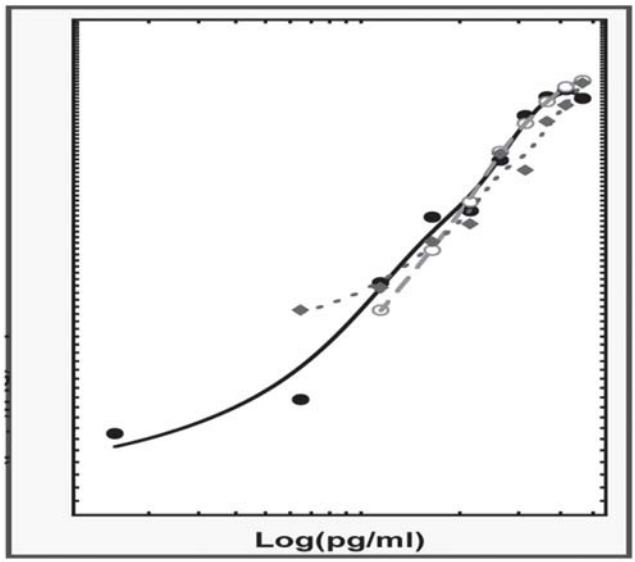

Fig. 4. Comparison of standard curves derived for interleukin-1b (pg/mL) performed with multiplex assays on three substrates. A multiplex assay is performed with six cytokine mixtures using arrays printed on HydroGel-coated slides and on two commercially available substrates. Cytokine concentrations ranged from 1.6 pg/mL to 50 ng/mL in 4 log steps. For imaging, the laser power and PMT settings of the ScanArray 5000 confocal slide scanner are optimized for each substrate. Detected signal is reported as DLU per pixel. HydroGel-coated slides (filled circles), aldehyde-derivatized glass slides (open circles), and nitrocellulose-coated slides (filled squares).

The data demonstrates that the higher probe-loading capacity of the HydroGel substrate in comparison to the two-dimensional substrate, coupled with the low inherent fluorescent background of HydroGel-coated slides, results in superior overall performance. Results show broad dynamic range for assays performed with HydroGel-coated slides and narrowed dynamic range on the other substrates because of the decreased response at the lower extremes of the curve.

3. Maintaining protein activity: Protein chips are made in much the same way as DNA microarrays, but getting all the elements to work is far more difficult than with DNA arrays ***(21)***. We achieve this by adopting two protein-arraying tools. A noncontact piezoelectric robotic dispenser, PerkinElmer BioChip Arrayer, is used to produce arrays. The small drops (350 pL) are pipetted out gently, which ensures that the protein is not denatured while printing. In addition to its three-dimensional network structure, HydroGel contains glycerin, a commonly used protein stabilizer. The high content of glycerol in HydroGel keeps the antibodies stable and hydrated after printing and long storage.

4. Assay optimization: Assays use the binding of antibodies to a ligand to detect specific interactions and result in quantization of that ligand. Immunoassays can be highly specific, quick, and simple to carry out and require little expensive machinery. In traditional well-plated ELISA, each target analyte has to be measured in a separate reaction. Consequently, ELISAs require milliliter volumes of sample to analyze multiple analytes. Although some of the time-consuming process can be carried out in an automated system, parallel analysis of several analytes for the same sample and at the same time is still a challenge. In the research, drug discovery, and diagnostic areas clinical samples are precise. The minimum sample requirement is a critical factor. Microarray-based parallel immunoassays enable simultaneous detection of many analytes from a small volume (50 μL or less) of sample fluid. The use of exceedingly small quantities of capture antibody immobilized in microspots facilitates ambient analyte assay conditions. Under these assay conditions, the fractional occupancy of capture antibody is independent of sample volume ***(22)***. Analyte concentrations are thus measured with greater sensitivity and potentially greater speed.
5. Cross-reaction: Unlike standard singleplex methods of analyte detection, assays performed in multiplex are potentially complicated by possible cross-reactivity from multiple capture-and-detection antibody pairs used in conjunction. To rule out this possibility, each cytokine is applied to an array individually and the signals of the unrelated probes are measured. The arrays tested for cross-reactivity showed no signals above background for any of the cytokines, suggesting that cross-reactivity is not a factor in this system (data not shown). A similar measure of cross- reactivity between the multiplex components is to compare standard curves for an analyte derived with microarrays when the analyte is alone in the capturing step or when it is in a mixture with other analytes. This is done with IL-6 as the detected analyte with the sixplex cytokine immunoassay chip in the presence of all six biotinylated antibodies. The resulting dose–response curves (**Fig. 5**) exhibits little difference in dose response or dynamic range, indicating essentially no interference from the other antibodies in the multiplexed system. However, multiplexed assays bear lower detection limits compared with singleplexed assays. Results for other cytokines are similar. The results simplified the detection antibody cocktail preparation.
6. Linear range: Standard curves produced with HydroGel-coated slides demonstrate a dynamic range of up to 3 log orders of magnitude and observed detection limits in the pg/mL range for five of the six cytokines tested in a model multiplexed array system (**Fig. 6**). Ongoing efforts to optimize relative levels of antibody pairs suggest that a four- to fivefold reduction in the detection limit is attainable without signal amplification. To approximate a typical cytokine immunoassay on tissue culture supernatants, the sixfold multiplex cytokine assay is run using cytokine-spiked DME medium supplemented with 10% FBS. The experiment is set up such that two arrays (on one HydroGel-coated slide) are incubated with a mix of all six cytokines at the same concentration. Nine concentrations (5 pg/mL to 50 ng/mL in 0.5 log steps) of each cytokine are tested to generate a standard

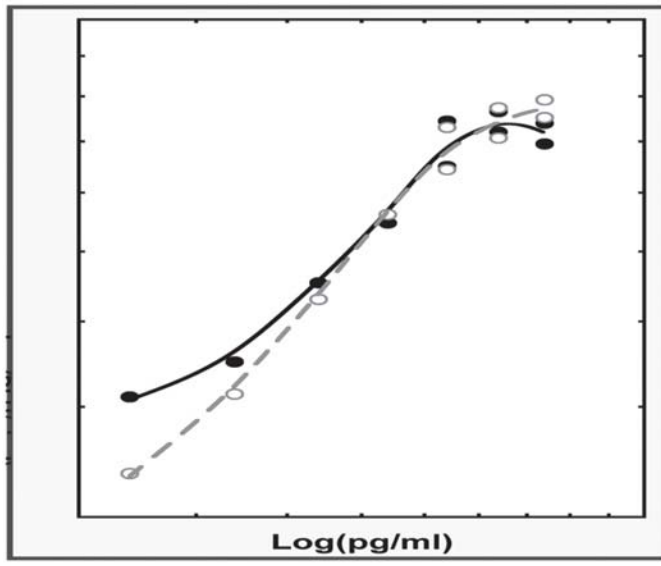

Fig. 5. Comparison of standard curves generated for interleukin-6 using arrays on HydroGel-coated slides with target cytokine applied either in multiplex (filled circles) or singleplex (open circles). All six biotinylated detection antibodies are present in both immunoassays. The assay is performed as stated in **Subheading 3.** with cytokines spiked into DME medium with 10% fetal bovine serum. Cytokine concentrations ranged from 50 pg/mL to 50 ng/mL. Curves show similar dose response and detection range, except for lower detection limits in the multiplex form, suggesting that the components of the multiplexed assay interfere little with specific analyte measurement.

curves. In addition, as a negative control, one slide is incubated with DME medium supplemented with 10% FBS only, followed by processing with the detection antibody mixture and Texas red-conjugated streptavidin, as described above. The standard curves are trimmed and the linear portion reflecting the dynamic range of the assay is used to calculate the slope of the dose response. The endpoints of each graph approximate the boundaries of the dynamic range for the detection of the target cytokine. The observed dynamic ranges ranged from a low of at least 2 log for IL-13 to a high of at least 3.0 log for IL-1B, IL-2, IL-6, and interferon (IFN)-γ (**Fig. 6**). The slope of the linear regression equation best represents the dose response for each cytokine. All six cytokines demonstrated pronounced dose responses, having slopes ranging from 0.89 to 1.26. These dose responses are suitable for quantitating the levels of the cytokines from an experimental sample when applied to these standard curves.

7. Reliability: The intravariability is determined by comparing the signals from 16 duplicated spots in the same array. The variability of spots from different slides

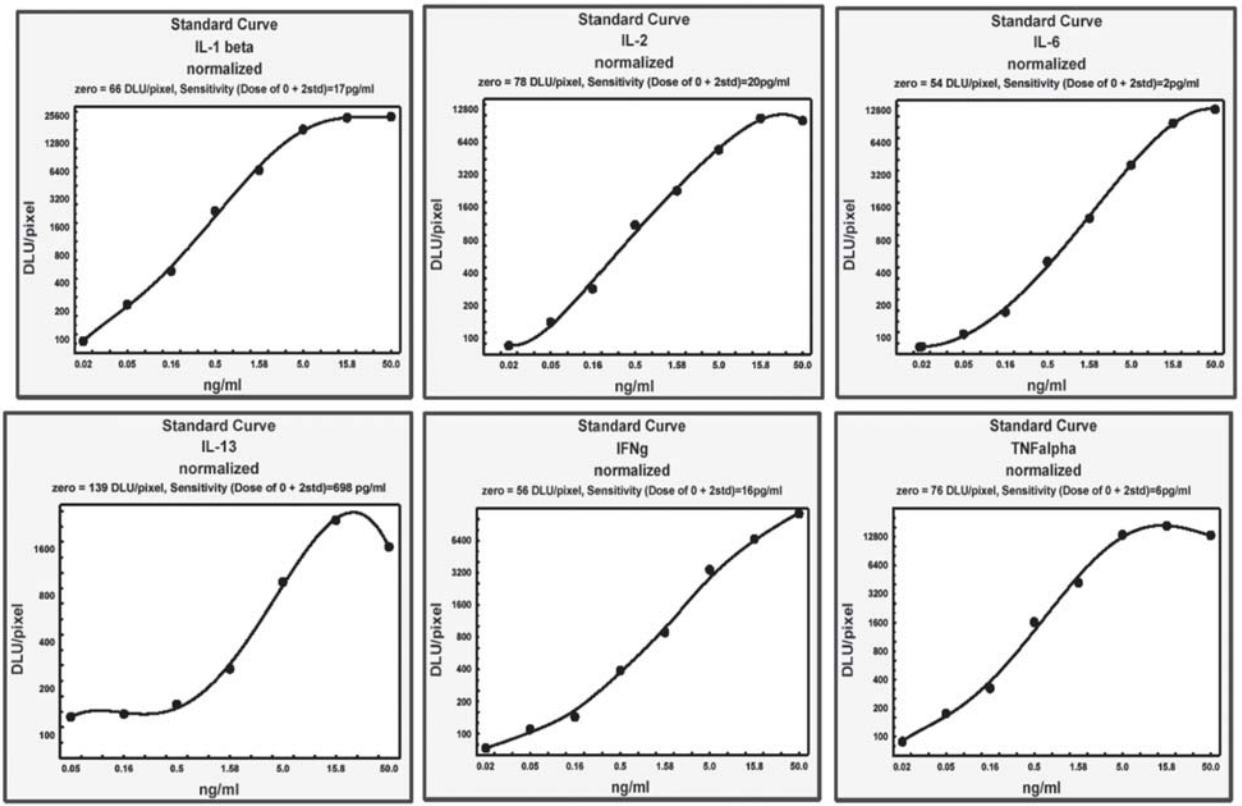

Fig. 6. Standard curves for six individual cytokines derived from serum-based assays performed in multiplex on HydroGel-coated slides. Slides are prepared and assays are performed as stated in **Subheading 3.** Images are collected using a ScanArray™ 5000 microarray scanner, and data is normalized to control spots, then baseline subtracted. Plots of the full range of data for six cytokines show a sigmoid curve of dose response typical of assays from this system.

(intervariability) is determined from four different arrays. The CV (standard deviation divided by average) is usually less than 10%, suggesting the reliability of our system.

8. Sensitivity: As seen in **Table 1**, the microarray-based cytokine assays on HydroGel-coated slides resulted in an observed sensitivity of less than 20 pg/mL for five out of six cytokines tested. This level of sensitivity results from the high degree of reproducibility of the data (CV% data not shown) and the low baseline values of the probes on the HydroGel substrate. The combination of sensitivity and broad dynamic range would allow for the discrimination between the healthy and diseased states associated with these cytokines and quantitation of cytokine level present in the pathological state. The detection limits for each cytokines are calculated by adding up the background and twice the standard deviations. IL-6 is the top performer with sensitivity at 2 pg/mL, followed by TNF-α at 6 pg/mL. IFN-γ (16 pg/mL) and IL-1β (17 pg/mL) are almost identical. IL-2 sensitivity is 20 pg/mL. IL-13 has demonstrated a slightly higher detection limits at 698 pg/mL because of the performance of the antibody pair. The high loading capacity of the HydroGel-coated slide substrate, with retained protein function, allows the researcher to choose from a broader range of capture antibody deposition than other commercially available substrates. This in turn enhances flexibility in choosing relative levels of matched pairs for multiplexed analysis and may enable the use of antibody pairs that would not be supported by other systems ***(23)***.

Acknowledgments

My gratitude is extended to Ruo-Pan Huang, Martin Sommer, Henry Lisoukov, Ruochun Huang, Ying Lin, and Jocelyn Burke for their original contribution to this project ***(24)***, to Q. Wang, F. E. Wiedmer, and J. Horn for their contributions in HydroGel slide production and array printing, and to R. Cavallo, T. Miller, F. Corden, K. Woodward, D. Shen, and F. Wang for their valuable discussions.

References

1. Zhu, H. and Snyder, M. (2003) Protein chip technology. *Curr. Opin. Chem. Biol.* **7(1),** 55–63.
2. Wiese, R., Belosludtsev, Y., Powdrill, T., Thompson, P., and Hogan, M. (2001) Simultaneous multianalyte ELISA performed on a microarray platform. *Clin. Chem.* **47(8),** 1451–1457.
3. Mendoza, L. G., McQuary, P., Mongan, A., Gangadharan, R., Brigna, S., and Eggers, M. (1999) High-throughput microarray-based enzyme-linked immunosorbent assay (ELISA). *Biotechniques* **27(4),** 778–780, 782–786, 788.
4. Moody, M. D., Van Arsdell, S. W., Murphy, K. P., Orencole, S. F., and Burns, C. (2001) Array-based ELISAs for high-throughput analysis of human cytokines. *Biotechniques* **31(1),** 186–190, 192–194.
5. Schweitzer, B., Wiltshire, S., Lambert, J., et al. (2000) Immunoassays with rolling circle DNA amplification: a versatile platform for ultrasensitive antigen detection. *Proc. Natl. Acad. Sci. USA* **97(18),** 10,113–10,119.

6. Haab, B. B., Dunham, M. J., and Brown, P. O. (2001) Protein microarrays for highly parallel detection and quantitation of specific proteins and antibodies in complex solutions. *Genome Biol.* **2(2),** RESEARCH0004 Epub.
7. Huang, R. P. (2004) Cytokine protein arrays. *Methods Mol. Biol.* **264,** 215–231.
8. Lin, Y., Huang, R., Chen, L. P., et al. (2003) Profiling of cytokine expression by biotin-labeled-based protein arrays. *Proteomics* **3(9),** 1750–1757.
9. Huang, R., Lin, Y., Wang, C. C., et al. (2002) Connexin 43 suppresses human glioblastoma cell growth by down-regulation of monocyte chemotactic protein 1, as discovered using protein array technology. *Cancer Res.* **62(10),** 2806–2812.
10. Carson, R. T. and Vignali, D. A. (1999) Simultaneous quantitation of 15 cytokines using a multiplexed flow cytometric assay. *J. Immunol. Methods* **227(1–2),** 41–52.
11. Mirzabekov, A. and Zlatanova, J. (2001) Gel-immobilized microarrays of nucleic acids and proteins. Production and application for macromolecular research. *Methods Mol. Biol.* **170,** 17–38.
12. Carding, S. R., Hayday, A. C., and Bottomly, K. (1991) Cytokines in T-cell development. *Immunol. Today* **12(7),** 239–245.
13. Murphy, P. M. (2001) Chemokines and the molecular basis of cancer metastasis. *N. Engl. J. Med.* **345(11),** 833–835.
14. Bienvenu, J., Monneret, G., Fabien, N, and Revillard, J. P. (2000) The clinical usefulness of the measurement of cytokines. *Clin. Chem. Lab. Med.* **38(4),** 267–285.
15. Haverty, A. A., Harmey, J. H., Redmond, H. P., and Bouchier-Hayes, D. J. (1997) Interleukin-6 upregulates GP96 expression in breast cancer. *Surg. Res.* **69(1),** 145–149.
16. Kleine-Lowinski, K., Gillitzer, R., Kuhne-Heid, R., and Rosl, F. (1999) Monocyte-chemo-attractant-protein-1 (MCP-1)-gene expression in cervical intra-epithelial neoplasias and cervical carcinomas. *Int. J. Cancer* **82(1),** 6–11.
17. Riethdorf, S., Riethdorf, L., Richter, N., and Loning, T. (1998) Expression of the MCP-1 gene and the HPV 16 E6/E7 oncogenes in squamous cell carcinomas of the cervix uteri and metastases. *Pathobiology* **66(6),** 260–267.
18. Huang, R. P., Fan, Y. de Belle, I., et al. (1997) Decreased Egr-1 expression in human, mouse and rat mammary cells and tissues correlates with tumor formation. *Int. J. Cancer* **72(1),** 102–109.
19. MacBeath, G. and Schreiber, S. L. (2000) Printing proteins as microarrays for high-throughput function determination. *Science* **289(5485),** 1760–1763.
20. Stillman, B. A. and Tonkinson, J. L. (2000) FAST slides: a novel surface for microarrays. *Biotechniques* **29(3),** 630–635.
21. Kodadek, T. (2001) Protein microarrays: prospects and problems. *Chem. Biol.* **8**, 105–115.
22. Ekins, R. P. (1989) Multi-analyte immunoassay. *J. Pharm. Biomed. Anal.* **7(2),** 155–168.
23. Service, R. F. (2001) Proteomics. Searching for recipes for protein chips. *Science* **294,** 2080–2082.

24. Wang, C. C., Huang, R. P., Sommer, M., et al. (2002) Array-based multiplexed screening and quantitation of human cytokines and chemokines. *J. Proteome Res.* **1(4),** 337–343.

14

Lectin Microarrays for Glycoprotein Analysis

Kanoelani T. Pilobello and Lara K. Mahal

Summary

Glycosylation is one of the most common posttranslational modifications, with more than half of all known proteins thought to be glycoproteins. Alterations in glycosylation play a role in a diverse set of biological phenomena including tumor cell metastasis, intracellular communication, and inflammation. The complexity of glycosylation at the molecular level and the lack of rapid analytical tools complicate the study of glycan function. We have recently developed a lectin microarray for the high-throughput analysis of glycosylation. Lectins are carbohydrate-binding proteins that have been used for decades as a detection method for glycans. By placing the lectins in a microarray format and using standard microarray printing and scanning technology, we have created a simple yet powerful technique for glycan profiling.

Key Words: Lectin microarray; glycomics; carbohydrate analysis; glycan profiling; array.

1. Introduction

Glycosylation plays a role in a diverse set of biological phenomena, including tumor cell metastasis, intracellular communication, and inflammation ***(1)***. More than half of all known proteins are predicted to be glycoproteins, making glycosylation one of the most ubiquitous posttranslation modifications ***(2)***. The complexity of carbohydrates presents a major analytical challenge, which has limited our understanding of the roles of glycosylation in biology. To address this, our laboratory has recently developed a new method for high-throughput glycoprotein analysis, the lectin microarray ***(3)***.

Lectins are carbohydrate-binding proteins that have been used for decades as a detection method for glycans ***(4)***. By creating a microarray of lectins with discrete and overlapping specificities, we obtain a lectin-based profile of a fluorescently labeled glycoprotein that yields information about its carbohy-

From: *Methods in Molecular Biology, Vol. 385: Microchip-Based Assay Systems: Methods and Applications*
Edited by: Pierre N. Floriano © Humana Press Inc., Totowa, NJ

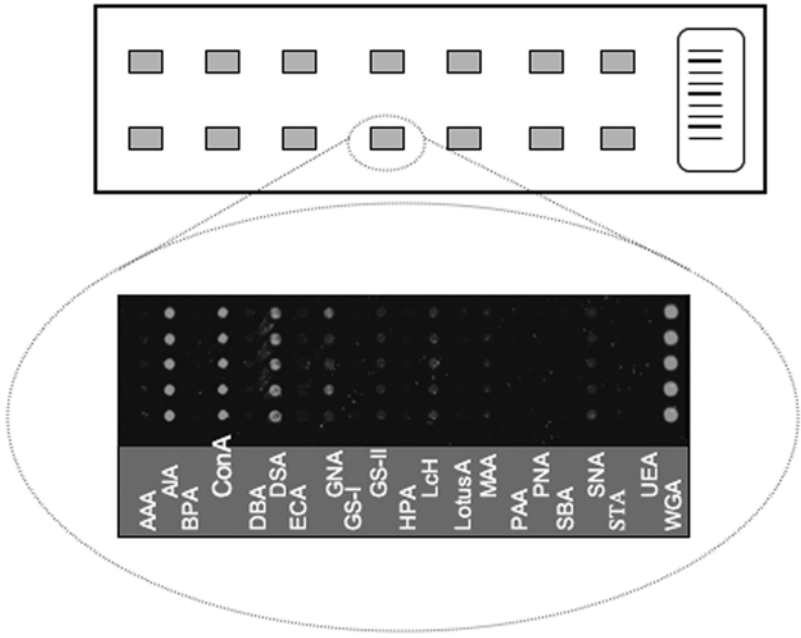

Fig. 1. Schematic of the 14 subarrays printed using the 16-well FAST format on a barcoded slide. Enlarged area shows data from a 21-lectin subarray hybridized with Cy3-ovalbumin (10 μg).

drate composition. Modifying existing microarray technology, we have been able to fit 14 lectin microarrays in discrete wells on a single slide, allowing us to analyze 14 samples simultaneously (**Fig. 1**). Our protocols use standard microarray printing and scanning instruments to create a simple yet powerful technique for glycan profiling.

2. Materials

2.1. Lectins, Cy-Dye Labeling of Glycoprotein Samples, and Standards

1. NHS-Cy3 and -Cy5 (monoreactive dye pack aliquotted for a 1-mg labeling reaction; Amersham Biosciences, Piscataway, NJ).
2. Cy buffer: sodium carbonate buffer (0.1 *M* $NaCO_3$ in H_2O, pH 9.3). A stock buffer may be made, but the pH will need to be readjusted periodically.
3. Slide-A-Lyzer® dialysis cassettes (Pierce, Rockford, IL) or other dialysis tubing (MWCO ≤ 20,000 Da).
4. Glycoproteins for standards (if desired): fetuin (fetal calf serum), ovalbumin (chicken egg), bovine submaxillary mucin (Type I-S), and porcine stomach mucin (Type II; Sigma, St. Louis, MO). These glycoproteins were chosen as "standards"

because of the large body of literature regarding their carbohydrate compositions and lectin binding ***(5–10)***.

5. Lectins (**Table 1**) (E.Y. Laboratories, San Mateo, CA).
6. Buffers designated in lectin product specification sheets or phosphate-buffered saline (PBS, 0.1 *M* NaH_2PO_4, 0.15 *M* NaCl, pH 7.3).

2.2. Lectin Printing

1. Python programming language (freely available for download at http://www.python.org).
2. Spotbot® Personal Microarrayer with SMP3 pins (Telechem Int., Sunnyvale, CA).
3. Nexterion H slides (SCHOTT North America, Elmsford, NY).
4. Lectins (*see* **Subheading 2.2.** and **Table 1**).
5. 10X Print buffer: 5 mg/mL bovine serum albumin, 10 m*M* monosaccharide in PBS. The choice of monosaccharide will depend on the lectin and is loosely based on its binding affinity (*see* **Table 1**).
6. Low-volume, conical-bottom 384-well plates (Whatman Inc., Middlesex, UK).
7. Ethanolamine solution: 50 m*M* ethanolamine solution in H_2O, pH 8.0 (*see* **Note 1**).
8. 16-Well FAST frame and cassette (Schleicher & Schuell, Keene, NH).
9. PBS with Tween (PBST): 0.1 *M* NaH_2PO_4, 0.15 *M* NaCl, 0.05% TWEEN 20, pH 7.2.
10. Centrifuge: either Slide Spinner microfuge (Labnet International, Edison, NJ), or a standard floor centrifuge with slide rack adaptors.

2.3. Hybridization to Array and Inhibition Experiments

1. Slides from **Subheading 3.4.**; samples and glycoprotein standards from **Subheading 3.1.**
2. 200-µL Multichannel pipettor.
3. PBS-2T: PBS + 0.1% TWEEN-20.
4. Monosaccharides for inhibition (typically *N*-acetyl-D-glucosamine (GlcNAc) and lactose, 200 m*M* in PBS-2T).

2.4. Data Analysis

1. Genepix Personal 4100A (Molecular Devices, Sunnyvale, CA) or similar Cy3/Cy5 slide scanner.
2. Genepix Pro 5.1 analysis software (Molecular Devices, Sunnyvale, CA) or equivalent.
3. Microsoft Excel or equivalent.

3. Methods

3.1. Labeling Glycoprotein Standards and Samples and Lectin Handling

1. Dilute glycoproteins to approx 8 mg/mL (two times final concentration) in Cy buffer. Like all proteins, the glycoproteins should be handled gently. Although gentle rocking at room temperature to aid in solubilization of the proteins is permissible, an effort to minimize agitation is good practice.

Table 1
Lectin and Their Codes, Specificities, Print Concentrations (Conc.), and Monosaccharides in Print Buffer (Monosacc.)

Lectin	Code	Specificity	Conc. (mg/mL)	Monosacc.
Anguilla anguilla	AAA	α-Fucose	1.0	Fucose
Artocarpus integrifolia	AIA	Gal α-OR	0.5	Galactose
Bauhinia purpurea	BPA	GalNAc/Gal	0.5	Galactose
Canavalia ensiformis	Con A	Mannose, GlcNAc	0.5	Mannose
Dolichos biflorus	DBA	GalNAc α-OR	0.5	Galactose
Datura stramonium	DSA	GlcNAc β-1,4GlcNAc oligomers	0.5	GlcNAc
Erythrina cristagalli	ECA	Gal β-1,4GlcNAc	1.0	Galactose
Galanthus nivalis	GNA	Terminal α-1,3 mannose	0.5	Mannose
Griffonia simplicifolia-I	GSI	α-Galactose	0.5	Galactose
Griffonia simplicifolia-II	GSII	Terminal GlcNAc	0.5	GlcNAc
Helix pomatia	HPA	α-GalNAc	0.5	Galactose
Lens culinaris	LcH	Complex	1.0	Mannose
Lotus tetragonolobus	Lotus A	Terminal α-Fucose, Le^x	0.5	Fucose
Maackia amurensis	MAA	α-2,3 Sialic acid	0.5	GlcNAc
Persea americana	PAA	Unknown	0.5	GlcNAc
Arachis hypogaea	PNA	Terminal Gal β-OR	0.5	Galactose
Glycine max	SBA	Terminal GalNAc	0.5	Galactose
Sambucus nigra	SNA	α-2,6 Sialic acid	0.5	GlcNAc
Solanum tuberosum	STA	GlcNAc oligomers	0.5	GlcNAc
Ulex europaeus-I	UEA-I	α-Fucose	0.5	Fucose
Triticum vulgare	WGA	β-GlcNAc, sialic acid, GalNAc	1.0	GlcNAc

2. One aliquot of Cy dye (either Cy3 or Cy5), is diluted with 500 µL of Cy buffer. This is enough dye to label two 250-µL (8 mg/mL) glycoprotein samples.
3. For each glycoprotein, 250 µL of sample is mixed with 250 µL of the diluted Cy dye such that the final glycoprotein concentration is approx 4 mg/mL. The diluted glycoproteins are then conjugated to Cy3 or Cy5 for 30 min at room temperature. Gentle agitation at this point is optional.
4. After a 30-min incubation, the glycoproteins are injected into Pierce Slide-A-Lyzer® cassettes (MWCO 7000, 0.1–0.5 mL capacity) and dialyzed against PBS overnight at 4°C (*see* **Note 2**).
5. After dialysis, the labeled glycoproteins are removed from the cassettes, aliquotted into 10-µL aliquots, and snap-frozen in liquid nitrogen. Samples may be stored at –80°C and used for a 3- to 6-mo period. It is important to note the lot number of the glycoproteins for future reference, as we have observed some lot-to-lot variation of the glycoproteins (*see* **Note 3**).
6. Lectins are typically dissolved in PBS or the recommended buffer at a concentration of 1 mg/mL. If necessary, lectins can be rocked gently overnight at 4°C (*see* **Note 4**).
7. Lectins are aliquotted (10- to 20-µL aliquots) and snap-frozen in liquid nitrogen. They may be stored at -80°C for up to 1 yr without loss in activity.

3.2. Reprogramming the SpotBot

The first generation SpotBot program provided with the instrument is unable to print slides in a 16-well hybridization format to match the FAST frame hybridization cassette wells. It should be noted that on our slides, 2 of the wells are occupied by a barcode, and thus we only create 14 functional microarrays (**Fig. 1**). The Spotbot is controlled by XML command lines. The program provided will generate the XML commands to print in a 16-well format for the number of slides and samples specified by the user.

The program was written in Python because of the simplicity of Python's documentation. Python tutorials are available through http://www.python.org. Python comes as part of the Mac OSX + distribution and can be accessed by typing "python" in the terminal. For Macintosh computers a text editor, GNU Emacs, is required to convert the file from text to the Python format (to download go to http://www.gnu.org/software/emacs/emacs.html). The program provided herein prints five replicate spots of each lectin onto multiple slides in a 16-well format. The program will preprint spots onto the slide adjacent to the slide that is printed, resulting in the ability to print up to seven full slides (*see* **Note 5**). To reprogram your Spotbot:

1. Open a new file in GNU Emacs.
2. Type in the following program. (Note that all comments with the symbol # before them are **NOT** part of the program and should be omitted when typing.)

```
sample = X                #X = desired number of lectins.
d = 22                    #optimized for FAST 16 well format
riter = 1
reit = 1
rslide = 1
slides = Y                #Y = desired number of slides to print.
num_platerows = 16        #  rows in a 384 well plate
num_platecolumns = 24     # columns in a 384 well plate
adj_num_platecolumns      #scaled “plate size”
  = num_platecolumns*
  (slides)
precolumn_offset = 16     # preslide offset
prerow_offset = 15
reit_offsets =
  {1 : 23, 2 : 28, 3 :
  33, 4 : 38, 5 : 43}
preslide = {1 : 8, 2 :
  9, 3 : 10, 4 : 11,
  5 : 12, 6 : 13, 7
  : 14}
num_prerows = 1
num_precolumns = 20
#Depending on the viscosity of your solutions and the arraying
  process you use, the number of #precolumns may need adjustment
  to get consistent spots.
num_subarray_rows = 7       #this value can be adjusted if
                              the program is modified for a
                            #format other than the 16 well.
                              Adjustment of the #multipier (44)
                              in “calculated row” (see below)
                              may be
                            #necessary
num_replicates = 5
num_samples_per_row = 5     # range:1-5.
def  do_replicate(rslide,column,e,row,d,s,riter,num_samples_
  per_row,column_offset=0): calculated_row = row+d+s*44+int
  ((riter-1)/num_samples_per_row)
  print """<SpotSlide><Number>%d</Number><Column>%d<Column>
  <Row>%d</Row><Time>0</Time></SpotSlide>"""%\
(rslide,column+e+column_offset,calculated_row)
def do_replicates(rslide,e,row,d,s,riter,num_replicates,
  num_samples_per_row,column_offset=0):
for column in range(num_replicates):
  do_replicate(rslide,column,e,row,d,s,riter,num_samples
    _per_row,0)
```

```
for column in range(num_replicates):
  do_replicate(rslide,column,e,row,d,s,riter,num_
    samples_per_row, column_offset=48)
def do_precolumn(precolumn,precolumn_offset,riter,prerow_off-
  set):
  g = preslide[rslide]
print """<SpotSlide><Number>%<Number><Column>%d</Column>
    <Row>%d</Row><Time></SpotSlide>"""%\
  (g,precolumn+precolumn_offset, riter+prerow_offset)
for platerow in range(num_platerows):
  for platecolumn in range(adj_num_platecolumns):
    if riter <= sample:
      calculated_platecolumn = (platecolumn/slides) + 1
      print  """<Wash><Time>0.5</Time></Wash><Dry><Time>0.5
        </Time>
      </Dry><Wash><Time>0.5</Time></Wash><Dry><Time>0.5
        </Time>
      </Dry><Wash><Time>0.5</Time></Wash><Dry><Time>0.5
        </Time>
      </Dry><Wash><Time>2</Time></Wash><Dry><Time>10
        </Time><Dry>
      <GetSample><Number>1</Number><Column>%</Column>
      <Row>%</Row><Time>3</Time><GetSample>"""%
        (calculated_platecolumn,platerow+1 for prerow in range
        (num_prerows):
  for precolumn in range(num_precolumns):
    do_precolumn(precolumn,precolumn_offset,
      riter,prerow_offset)
  e = reit_offsets(11)
  for s in range(num_subarray_rows):
    for row in range(1):
    do_replicates(rslide,e,row,d,s,riter,num_replicates,
      num_samples_per_row,\
      column_offset=0)
  if rslide < slides:
    rslide = rslide + 1
  else:
    riter = riter + 1
    rslide = 1
    reit = reit + 1
  if reit > num_samples_per_row:
    reit = 1 #contols print column.
else:
  break                    #(See Note 6).
```

3. Save buffer as the desired filename.py. This program will run in Python 2.2 and later versions (*see* **Note 7**).
4. For a Macintosh running OS X, open a terminal window (shell) and type "python filename.py > (name of text file to output to).txt". The output file is an XML command file.
5. The resulting XML command file can be cut and pasted into a Spocle file, the shell of which must be generated in Spoclegen (provided with the Spotbot). To create a Spocle dummy file:
   a. Open Spoclegen in the computer connected to the Spotbot. In the Start tab, accept the Factory Default Profile.
   b. In the Pins tab, select your pin type (SMP3) and the 1 × 1 pin configuration.
   c. Continue on to the Plates tab, and select partial last microplate. On the diagram that appears, use the mouse and click on the A1 position.
   d. In the microarrays tab, change the spot spacing to 200 μm.
   e. In the substrate tab, double click on the slide diagrams for slides 2–7 and 9–14 until their designation changes to "unused," and change the "Pre-print Spots per Sample" to 10. Both of these actions simply serve to make deletion easier in future steps.
   f. Select the default for both the Motion and Wash/Dry tabs.
   g. Select the default settings in the Finish tab and click finish. The generated shell file will be saved by date and time in the Spotbot folder. It must be further modified as shown below to create the final program on the Spotbot computer.
6. Open the Spocle dummy file in a text editor such as Microsoft Wordpad. Disable any autoformatting. Delete everything between the two comments in the program (ex. "Get sample…`</Command>`").
7. Open the XML command file previously generated with Python. Copy and paste the XML command line file in the space that was just deleted, i.e., between the two `</Comments>`. The file can be saved by selecting save or hitting the save button in the button bar. (Note: It must be saved in the text-only format. This file is your final printing program.)

3.3. Lectin Microarray Printing Protocol

1. Remove Nexterion H slides from –20°C and allow them to warm to room temperature.
2. Thaw lectins on ice. Dilute in PBS to 2 times their final concentration (**Table 1**).
3. Prepare 10X print buffers with the appropriate monosaccharides (**Table 1**).
4. Load the lectins in the 384-well plate in the order desired. The final concentrations of the lectins are given in **Table 1**. The volume of lectin solution used per well is 10 μL, therefore 1 μL per well of the 10x print buffer is used (*see* **Note 8**).
5. Centrifuge the plate at 50*g* using a swinging bucket rotor and plate adaptors (JS 5.3 rotor; Beckman-Coulter, Fullerton CA). The plate can be stored at –4°C while other preparations are being made.
6. Turn on the Spotbot. Remember to turn on the peristaltic pump, the Megasonic Wash Station, and the air compressor for the pin drying station. The chamber

should be kept at 50% humidity for the duration of the printing process, which may require use of the humidifier depending on ambient conditions.
7. Open the Spotbot program that was previously created and select the default plate type (MMP384).
8. At the first prompt, load any plain glass slides to be used as spacers, the preprint slide (which can be a plain glass slide or the back of an old slide), the Nexterion H slides to be printed, and the loaded 384-well plate, and insert a clean pin into the printhead at the 1 × 1 position (see Spotbot manual for more details).
9. After everything has been loaded, continue the Spocle program; this will start your print run (*see* **Note 9**).
10. Once printing is completed, slides are incubated in the Spotbot for 1 h (*see* **Note 10**). This is an ideal time to prepare the solutions for the hybridization step.
11. Slides are then dipped face down into the ethanolamine solution by hand and held there for approx 1 min prior to tranfer to a Coplin jar filled with the ethanolamine solution. Slides are incubated in the solution for 1 h at room temperature.
12. Following this incubation, the slides are rinsed 3 times with PBST and once with PBS. The slides are centrifuged at 50*g*.
13. The FAST 16-well format hybridization cassette is positioned over the slides and then inserted into the FAST frame to provide a discrete set of 14 wells, each containing a single lectin microarray (or subarray; **Fig. 1**). Each well can be used for a separate hybridization reaction.

3.4. Hybridization to Array and Inhibition Protocols

1. If an inhibition experiment with monosaccharides is desired, preincubate subarray wells with 50 µL of either PBS-2T (positive control) or monosaccharide solution and let incubate for 30 min at room temperature.
2. Add 50 µL of the appropriate Cy-labeled glycoprotein sample (200 µg/mL inPBS). The final concentration of glycoprotein is 100 µg/mL. If no inhibition experiment is desired, use 100 µL of a 100 µg/mL solution of Cy-labeled glycoprotein and omit **step 1**. Incubate the slide for 2 h at room temperature.
3. After 2 h, use a multichannel pipettor to aspirate the samples and to dispense 100 µL PBST to rinse the wells. Wash all subarray wells 3 times for 3 min with PBST (*see* **Note 11**).
4. Remove the slide from the FAST frame and cassette and incubate it in a Coplin jar with PBS for 5 min.
5. Centrifuge the slides at 50*g* for 5 min or until dry. At this point the slide is ready for analysis.

3.5. Data Analysis

1. Scan the slide using a microarray scanner (such as the Genepix Personal 4100A) and accompanying software (Genepix Pro 5.1; *see* **Note 12**).
2. After an initial autoalignment, the spots are scanned by eye and manually aligned if necessary.

3. Results are then exported as a text file and processed in Microsoft Excel or other spreadsheet software.

4. Notes

1. All H_2O used in this method is deionized water.
2. We have used Amersham Bioscience Hi-Trap desalting columns for removal of free Cy dye in the labeling protocol but have found that dialysis is preferable for complete removal of free dye, particularly from the mucins.
3. It is convenient to label large stocks of glycoprotein standards to provide a stable reference point for the slides. In addition, the exact molecular weight of the mucins is unknown, which complicates calculations, such as the dye:protein ratio, and is why we work in mg/mL instead of molarity.
4. The handling of the lectins is a difficult issue as some lots of lectin have solubility and potentially activity problems. We have found no clear answer to these concerns. Although raising the pH to solubilize the lectins is one option, their binding capacities may be affected. Pelleting any aggregates and reoptimizing the lectin concentration to give good signal on the microarray based on labeled glycoprotein standards is the best solution that we have found. Because of issues of solubility, we recommend that each new lot of lectin be tested on the microarray against an older lot to verify that the binding capacity is the same (i.e., to avoid lot to lot variation).
5. Contrary to the Telechem literature, the SpotBot can print seven full slides and seven half slides. We use the adjacent slide to each printed slide for preprinting to streamline the printing process. This is done under the assumption that the x,y movement of the printhead has the highest contribution to print time after the wash/dry cycle. The program is made to dip before printing on each slide, a simple solution to the problem of sample evaporation from the pin.
6. The alignment of statements in the program is important.
7. Filename refers to your chosen name for the program.
8. We typically load 21 lectins in alphabetical order by three-letter abbreviation. Although the lectin microarray shown herein consists of only 21 lectins, the array can be easily expanded by inclusion of more lectins and carbohydrate-specific antibodies. We have found that it is easier to observe misloading if the plate has been centrifuged (50*g*, 1 min). The use of a Combitip (0.1-mL tip, Eppendorf) greatly accelerates the pipetting process.
9. Occasionally, the wash station will not drain properly because of an air bubble in the export port. This can be solved by blowing into the port using extra tubing.
10. The slides can be removed from the Spotbot for this incubation,but they must be kept in a humidified environment and should be handled with extreme care.
11. Rocking the slides during each rinse is recommended. The practice of aspirating the rinses from opposing sides of the wells is also recommended.
12. If white pixels are observed (indicating saturation), lower the PMT gain of the microarray scan for more accurate data.

Acknowledgments

The authors would like to thank Anders N. Pearson for his advice and help in rewriting the SpotBot program and the Arnold and Mabel Beckman Foundation Young Investigator Program and the University of Texas at Austin for financial support.

References

1. Varki, A. (1993) Biological roles of oligosaccharides: all of the theories are correct. *Glycobiology* **3,** 97–130.
2. Apweiler, R., Hermjakob, H., and Sharon, N. (1999)On the frequency of protein glycosylation, as deduced from analysis of the SWISS-PROT database. *Biochim. Biophys. Acta* **1473,** 4–8.
3. Pilobello, K. T., Krishnamoorthy, L., Slawek, D., and Mahal, L. K. (2005) Development of a lectin microarray for the rapid analysis of protein glycopatterns. *ChemBiochem* **6,** 985–989.
4. Rudiger, H. and Gabius, H. J. (2001) Plant lectins: occurrence, biochemistry, functions and applications. *Glycoconj. J.* **18,** 589–613.
5. Weiskopf, A. S., Vouros, P., and Harvey, D. J. (1998) Electrospray ionization-ion trap mass spectrometry for structural analysis of complex N-linked glycoprotein oligosaccharides. *Anal. Chem.* **70,** 4441–4447.
6. Che, F. Y., Song, J. F., Shao, X. X., Wang, K. Y., and Xia, Q. C. (1999) Comparative study on the distribution of ovalloumin glycoforms by capillary electrophoresis. *J. Chromatogr. A* **849,** 599–608.
7. Johnson, W. V. and Heath, E. C. (1986) Evidence for posttranslational O-glycosylation of fetuin. *Biochemistry* **25,** 5518–5525.
8. Karlsson, N. G. and Packer, N. H. (2002) Analysis of O-linked reducing oligosaccharides released by an in-line flow system. *Anal. Biochem.* **305,** 173–185.
9. Schulz, B. L., Packer, N. H., and Karlsson, N. G. (2002) Small-scale analysis of O-linked oligosaccharides from glycoproteins and mucins separated by gel electrophoresis. *Anal. Chem.* **74,** 6088–6097.
10. Gerken, T. A., Gilmore, M., and Zhang, J. (2002) Determination of the site-specific oligosaccharide distribution of the O-glycans attached to the porcine submaxillary mucin tandem repeat. Further evidence for the modulation of O-glycans side chain structures by peptide sequence. *J. Biol .Chem.* **277,** 7736–7751.
11. Walz, A., Odenbreit, S., Mahdavi, J., Boren, T., and Ruhl, S. (2005) Identification and characterization of binding properties of *Helicobacter pylori* by glycoconjugate arrays. *Glycobiology* **15,** 700–708.

15

Interaction of HIV RNA With Peptides Detected by Acoustic Shear Wave Sensor Operated in an On-line Format

Anil K. Deisingh, Satie Siewah, Nardos Tassew, and Michael Thompson

Summary

Acoustic wave sensors are now widely used in various clinical applications because they allow real-time data to be rapidly obtained. In this chapter we describe the use of the thickness shear mode (TSM) acoustic wave sensor to study the interaction between the transactivation responsive region (TAR) of the HIV-1 mRNA and short peptides derived from the regulatory Tat protein as well as with two inhibitor molecules, namely neomycin and streptomycin. The interaction between the TAR-Tat system is a target for the development of antiviral drugs.

Key Words: Acoustic wave sensor, HIV-1, TAR-Tat, RNA-ligand binding, inhibitors, biosensors.

1. Introduction

The interactions between proteins and nucleic acids have been extensively studied by gel-shift assays and by the use of methods involving filter binding *(1,2)*. However, these approaches tend to be labor intensive and time consuming and may require the use of fluorescent dyes or radioisotopes for visualization purposes *(3)*. To eliminate these factors, biosensors can be employed to provide label-free and real-time detection of kinetic parameters.

One of the rapidly developing biosensors area involves the development of systems based on thickness shear mode (TSM) whereby ultrasonic waves in piezoelectric materials are generated (**Fig. 1**). Piezoelectric materials are sensitive to changes in mass, density, or viscosity, and therefore, frequency can be used as a sensitive transduction parameter. The most common piezoelectric substance is quartz, usually the AT-cut variety because of its excellent

From: *Methods in Molecular Biology, Vol. 385: Microchip-Based Assay Systems: Methods and Applications*
Edited by: Pierre N. Floriano © Humana Press Inc., Totowa, NJ

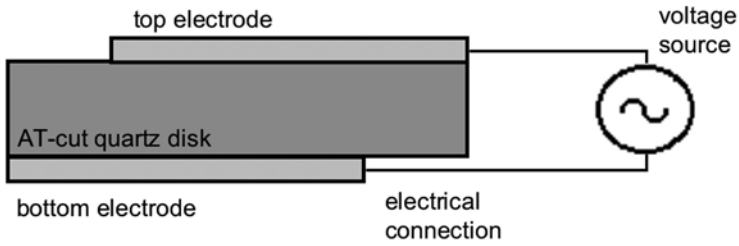

Fig. 1. Typical thickness shear mode sensor with electrode connection.

temperature coefficients. The type and angle of a quartz cut affects operating parameters such as frequency stability, which in turn is dependent on the plane or angle of the crystalline axes of the crystal. The plane is termed the "cut," the most common being referred to as the "AT" cut ***(4)***. The type of acoustic wave generated is determined by the crystal cut (an AT cut is 35° 15' relative to the plane) and the thickness of the material along with the geometry and configuration of the metal electrodes used to produce the electric field ***(5)***. These sensors are considered to be microchips and are widely used in clinical, food, and water applications ***(6)***.

In liquids the TSM sensor response is governed by several factors, which include the viscoelastic, interfacial acoustic coupling properties of a surface-bound film and the surrounding fluid and acoustoelectrical properties ***(3)***. This proves useful when the sensor is modeled as an equivalent circuit (**Fig. 2**) to generate parameters such as series resonance frequency (f_s), inductance (L_m), motional resistance (R_m), and static as well as motional capacitance (C_o and C_m). The network analysis (equivalent circuit) method is a system that was developed by Kipling and Thompson ***(7)***, and it provides almost complete characterization of the electrical information obtained when an acoustic wave device operates in liquids.

The coupling of a flow-injection analysis (FIA) procedure to an acoustic wave sensor (**Fig. 3**) allows the kinetic processes at the sensor surface to be monitored as well as providing real-time monitoring of binding interactions. Experiments using biosensors require the immobilization of a substrate on the surface, development of a baseline response in buffer, and injection of an analyte solution during association and dissociation of the analyte by washing with buffer ***(3)***.

In this chapter the interaction between the transactivation responsive region (TAR) of the HIV-1 mRNA and short peptides derived from the regulatory Tat

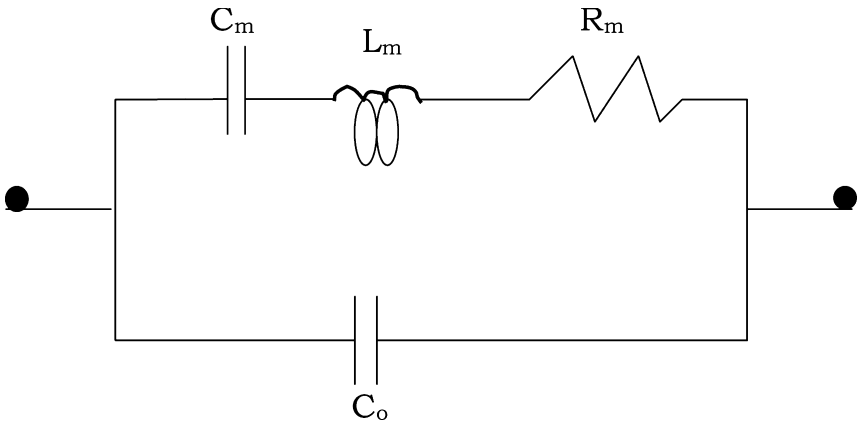

Fig. 2. Thickness shear mode sensor connected in a circuit.

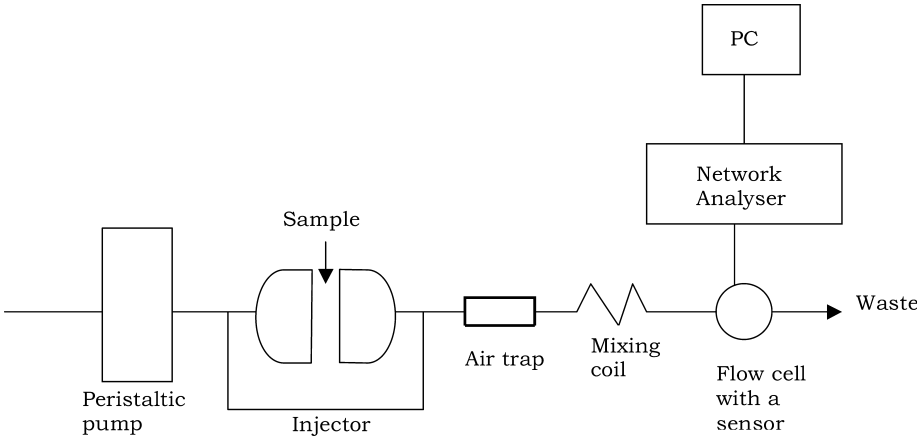

Fig. 3. Combination of flow-injection analysis with thickness shear mode.

protein and inhibitor molecules will be described. The HIV-1 Tat protein is a regulatory protein that stimulates transcription of the HIV virus by binding to the TAR at the 5' end of mRNA sections ***(8)***. The Tat protein contains 86 amino acids, and it is essential for the transcription of the whole virus ***(9)***. Thus, the

interaction between the TAR-Tat systems is a target for the development of antiviral drugs.

The use of a TSM sensor for studying RNA–protein and RNA–small molecule interaction at interfaces will be described. It has been shown that short, synthetic Tat peptides containing the arginine-rich basic region bind to TAR RNA with affinity and specificity similar to the full-length Tat protein, which makes them suitable for investigating TAR-Tat binding ***(9)***. In addition, the effect of inhibitors such as neomycin and streptomycin will be investigated.

2. Materials

2.1. TAR RNA Synthesis and RNA–Ligand Characterization (see *Note 1)*

1. A, U, G, and C phosphoramadites for RNA synthesis (Glen Research, Sterling, VA).
2. C-Biotin tetraethylene glycol (TEG) controlled pore glass columns for RNA synthesis (Glen Research, Sterling, VA).
3. Tetrazole/acetonitrile, 1-methylimidazole/tetrahydrofuran (THF), acetic anhydride/pyridine/THF, iodine/H_2O/pyridine, and anhydrous acetonitrile (Applied Biosystems, Mississauga, Ontario, Canada), aqueous ammonia, ethanol, tetrabutylammonium fluoride (TBAF), triethylamine, tetraethylammonium acetate (TEAA), trifluoroacetic acid (TFA), acetonitrile, and sterile water (Sigma-Aldrich, Oakville, Ontario, Canada).
4. A buffer composed of 1 *M* Tris-HCl (pH 7.5), 5 *M* NaCl ,and 0.5 *M* ethylene diamine tetraacetic acid (EDTA) (Sigma-Aldrich, Oakville, Ontario, Canada) (*see* **Note 2**).
5. Neomycin sulfate (Sigma-Aldrich, Oakville, Ontario, Canada) (*see* **Note 3**).
6. Streptomycin (Sigma-Aldrich, Oakville, Ontario, Canada).
7. 9 MHz AT-Cut piezoelectric quartz crystals, coated with polished gold electrodes on both sides (International Crystal Manufacturing, Oklahoma City, OK) (*see* **Note 4**).

2.2. Peptide Synthesis and Radiolabeling

1. Resins and amino acid residues (Advanced ChemTech, Louisville, KY).
2. Dimethylformamide, *N*-methylpyrolidone, piperidine, and *N*, *N*, *N*', *N*'-tetraethyluronium hexafluorophosphate (HATU) (Sigma-Aldrich, Oakville, Ontario, Canada).
3. T4 polynucleotide kinase and T4 polynucleotide buffer (New England Biolabs, Ipswich, MA) (*see* **Note 5**).
4. [γ-^{32}p] ATP (NEN Life Science Products, Boston, MA).
5. Sterilized water, anhydrous ethanol, sodium ethanoate, chloroform, EDTA (Sigma-Aldrich, Oakville, Ontario, Canada).
6. Scintillant vials (Fisher Scientific, Nepean, Ontario, Canada).

2.4. Flow Cell and Network Analyzer

1. The response of the TSM sensor in liquid was measured by an HP 4195 network spectrum analyzer (Hewlett-Packard, Palo Alto, CA).

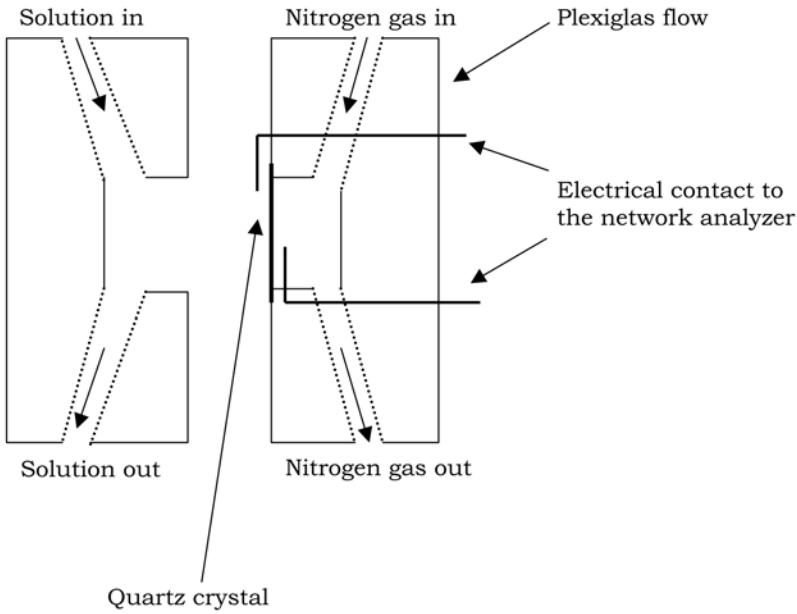

Fig. 4. Schematic of the thickness shear mode sensor flow cell assembly. AT-cut quartz crystal is sandwiched between the two halves of the flow cell. One face of the crystal is exposed to buffer and biochemical solutions, while the other face is kept dry under a flowing nitrogen gas.

2. The quartz crystal is placed between two halves of a Plexiglas flow cell with O-rings (**Fig. 4**) in such a way that the electrodes are in electrical contact with the network analyzer (*see* **Note 6**).
3. Only one face of the crystal is exposed to buffer and sample solutions while the other face of the crystal is kept dry by continuously flowing nitrogen gas (*see* **Note 7**).
4. Buffer and sample solutions are introduced in a flow-through format using a peristaltic pump (four-channel EVA pump model 1000).
5. Data points are collected every 30 s, and the values of the equivalent circuit element of the crystal are calculated internally by the analyzer from measured data. A PC is connected to the analyzer and the frequency response is displayed on the screen in real time.

3. Methods

3.1. TAR RNA Synthesis and Characterization

1. TAR RNA containing 31 bases (5'-GGC CAG AUC UGA GCC UGG GAG CUC UCU GGC C-3') was chemically synthesized using 2'-*tert*-butyldimethylsilyl and

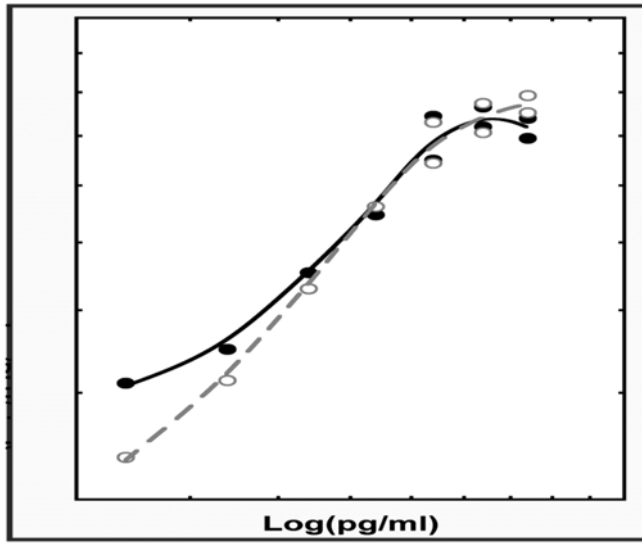

Fig. 5. Sequences of Tat peptide fragments contain the Arg-rich RNA-binding region.

5'-dimethoxytrityl- protected phosphoramadites on an Applied Biosystems 392 DNA/RNA synthesizer. Biotin was incorporated at the 3' end during the synthesis (*see* **Note 8**).
2. The oligoribonucleotides were desalted and detritylated using oligonucleotide purification cartridges (Poly Pak). The molecular mass was confirmed by MALDI-MS.
3. The RNA was dried and stored at –20°C and when required for use was resuspended in Tris buffer containing 10 m*M* Tris-HCl, 70 m*M* NaCl, and 0.2 m*M* EDTA, pH 5.5 (*see* **Note 9**).

3.2. Tat Peptide Synthesis

1. Tat peptides (**Fig. 5** shows a few examples) were synthesized using standard FMOC protocols.
2. The peptides were purified using a linear gradient from water (0.1% TFA) to 70% acetonitrile (0.1% TFA). The masses were confirmed by electrospray mass spectrometry.
3. The concentrations of the peptides were determined by spectroscopy from tyrosine absorbance in 6 *M* guanidine hydrochloride (275.5 nm, ε = 1475).

3.3. RNA–Ligand Interactions

1. The interactions of different Tat peptide fragments with immobilized Tar RNA were studied (*see* **Note 10**).

2. All measurements were obtained during a continuous flow, with the pump being stopped only for very short periods to allow switching of solutions (*see* **Note 11**).
3. A 500-µL solution of neutravidin in Tris buffer (1 mg/mL) was then injected followed by a wash with buffer to remove nonadsorbed protein (*see* **Note 12**).
4. After stabilization, a 500-µL solution of 3'-biotinylated Tar RNA (1 µ*M* in Tris buffer) was flowed through and the surface was washed with buffer until the frequency was once again stabilized (*see* **Note 13**).
5. 200 µL of analyte solution (Tat peptide, neomycin or streptomycin) were injected and the dependence of the frequency signal on concentration was investigated by injecting various concentrations of peptide solution (1, 2, 5.5,10, 25, 50, 100, and 200 µ*M*). Control experiments at each concentration were also performed. This included injecting peptide on a neutravidin-modified surface in the absence of TAR RNA.
6. For studies using neomycin and streptomycin bound to TAR, various concentrations of the drug (1, 5, 10, 20, 50, and 100 µ*M*) were flowed through after TAR RNA was immobilized onto the crystal surface. Control experiments were carried out by injecting neomycin or streptomycin after modifying the surface only with neutravidin ***(10)***.
7. The disruption of TAR-Tat binding by the antibiotics was investigated by injecting solutions of neomycin or streptomycin after Tat peptide was made to interact with TAR (*see* **Notes 14** and **15**).

3.4. Quantification of Immobilized RNA

1. Quantification was done by means of radiolabeling experiments.
2. The experimental setup was as described above except that no acoustic wave measurements were involved.
3. The RNA was labeled with ^{32}P at the 5' end. A mixture of the hot solution (20 µL, 35 pmol) and of cold TAR (480 µL, 465 pmol) in Tris buffer flowed through, following injection of neutravidin and the usual wash-off with buffer. TAR RNA was immobilized and the experiment performed as before.
4. The crystal was removed from the flow cell and placed in 5 mL of scintillant and shaken thoroughly (*see* **Note 16**).
5. The count for this solution was then measured and compared with the count for a solution taken before the experiment was performed. The amount of immobilized RNA was then calculated.

4. Notes

1. Once these vials are opened and set up on the synthesizer, several batches of the required sequences should be made because the shelf life decreases rapidly if the vials are left on the ports.
2. Ideally, buffer solutions should be made fresh at least weekly and should be aerated with a slow stream of nitrogen.
3. Streptomycin sulfate can be used without any further treatment.

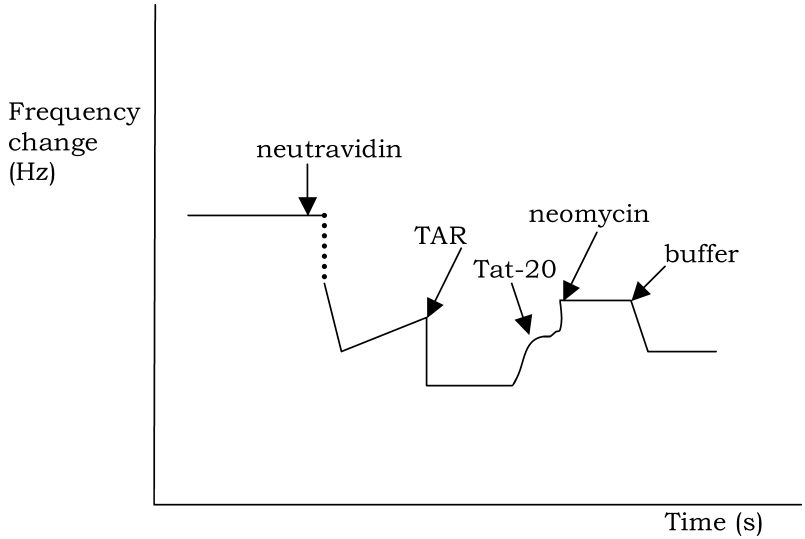

Fig. 6. A typical response plot for ternary TAR–peptide–neomycin complex.

4. The crystals are fragile and should be handled carefully. Additionally, they should be thoroughly cleaned by washing with ethanol, acetone, and water before drying with a stream of nitrogen gas. The cleaning process is critical to ensuring consistent results.
5. T4 polynucleotide kinase (PNK) catalyzes the transfer and exchange of P_i from the χ position of ATP to the 5'-hydroxyl terminus of polynucleotides. It is supplied in 50 m*M* KCl, 10 m*M* Tris-HCl (pH 7.4), 0.1 *M* EDTA, 1 m*M* dithiothreitol, 0.1 μ*M* ATP, and 50% glycerol.
6. The O-rings must fit tightly, otherwise leaking will occur, leading to the presence of unwanted air bubbles within the flow cell assembly. To avoid this, the O-rings on the cells should be replaced every 2–3 mo during continuous use or as required.
7. The flow of nitrogen has to be kept very low (about 6 mL/min) so that it does not cause noise associated with turbulent flow.
8. These syntheses may be carried out in-house if the synthesizer is available. However, commercial laboratories can provide these short sequences at a relatively low cost and negates the need for an academic laboratory to purchase the equipment.
9. Once stored at –20°C, these sequences can be used for up to 1 yr after production.
10. Each peptide contained the required basic region for binding, with longer sequences containing more amino acid residues from the carboxy terminal.
11. The sensor surface must be equilibrated with Tris-buffer before RNA can be immobilized. An ideal flow rate of 0.06 mL/min will lead to equilibration in about 15 min. However, there are occasions in which up to 30 min may be necessary.

12. The buffer wash requires about 30 min for the process to be complete and allow for stabilization of the series resonant frequency.
13. Stabilization will require approx 20–30 min.
14. A typical response plot for the formation of a ternary TAR–peptide–neomycin complex is shown in **Fig. 6**.
15. Binding affinity is directly linked with the inhibitory potency of neomycin or streptomycin.The acoustic wave-detection system shows that neomycin exhibits at least a 10-fold greater affinity for TAR RNA, and it is also a more potent inhibitor than streptomycin.
16. Liquid scintillation counters are used for detecting β decay. The sample is dissolved in a suitable solvent (scintillation cocktail). The radiation first interacts with the solvent, and the energy from this interaction is passed to a fluorescent chemical (fluorophore), which produces detectable light. The scintillations are measured by photomultiplier tubes, which turn the light pulses into electronic pulses, the magnitude of which is directly related to the energy of the original radioactive event.

Dedication

In memory of Dr. Kenneth Anil Deisingh (11th March 2007 —21st October 2005)

Tragically died on the morning of the 21st October 2005 in a car accident.

Left us far too soon. The courage you had was an inspiration to me and has helped me in ways I cannot express.

Always in our thoughts and sadly missed by all your family, friends and co-workers.

Sadie

References

1. Talanian, R. V., McKnight, C. J., and Kim, P. S. (1990) Sequence-specific DNA binding by a short peptide dimmer. *Science* **249 (4970),** 769–771.
2. Berger, C. and Jelesanv, I. (1996) Coupled folding and site-specific binding of the GCN4-bZIP transcription factor to the AP-1 and ATF/CREB DNA sites studied by microcalorimetry. *Biochemistry* **35(47),** 14984–14991.
3. Tassew, N. and Thompson, M. (2003) Kinetic characterization of the TAR RNA-Tat peptide and neomycin interactions by acoustic wave biosensor. *Biophys. Chem.* **106(3),** 241–252.
4. Glossary of terms for crystals (2000) http://www.ecliptek.com/crystals/glossary.html [Accessed 5 July 2005].
5. Thompson, M. and Stone, D. C. (1997) *Surface- Launched Acoustic Wave Sensors: Chemical Sensing and Thin-Film Characterization*, Wiley-Interscience, New York, pp. 10–20.
6. Deisingh, A. K. and Thompson, M. (2002) Detection of infectious and toxigenic bacteria. *Analyst* **127(5),** 567–581.

7. Kipling, A. L. and Thompson, M. (1990) Network analysis method applied to liquid-phase acoustic wave sensors. *Anal. Chem.* **62,** 1514–1519.
8. Tao, J., Chen, L., and Frankel, A. D. (1997) Dissection of the proposed base triple in human immunodeficiency virus TAR RNA indicates the importance of the Hoogsteen interaction. *Biochemistry* **36 (12),** 3491–3495.
9. Tassew, N. and Thompson, M. (2002) RNA-peptide binding and the effect of inhibitor and RNA mutation studied by on-line acoustic wave sensor. *Anal. Chem.* **74 (20),** 5313–5320.
10. Tassew, N. and Thompson, M. (2003) Binding affinity and inhibitory potency of neomycin and streptomycin on the Tat peptide interactions with HIV-1 TAR RNA detected by on-line acoustic wave sensor. *Org. Biomol. Chem.* **1,** 3268–3270.

16

Microchip-Based Electrochemical Enzyme Immunoassays

Madhu Prakash Chatrathi, Greg E. Collins, and Joseph Wang

Summary

In this chapter a microchip-based electrochemical enzyme immunoassay is developed and its performance is demonstrated for the determination of monoclonal mouse IgG as a model analyte. Such a direct homogeneous immunoassay requires the integration of electrokinetic mixing of alkaline phosphatase (ALP)-labeled anti-mouse IgG antibody (Ab-E) with the mouse IgG antigen (Ag) analyte in a precolumn reaction chamber, injection of immunochemical products into the separation channel, followed by rapid electrophoretic separation of enzyme-labeled free antibody and enzyme-labeled antibody–antigen complex. The separation is followed by a postcolumn reaction of enzyme tracer with *p*-aminophenyl phosphate (*p*-APP) substrate (S) and downstream amperometric detection of *p*-aminophenol (*p*-AP) product. Factors influencing the reaction, injection, separation, and detection processes are optimized. We have characterized the microchip-based immunoassay protocol.The resulting attractive analytical performance, along with distinct miniaturization and portability advantages of the electrochemical microsystem, offer considerable promise for designing self-contained and disposable chips for decentralized clinical diagnostics.

Key Words: Microchip; microfluidic; electrochemical detection; immunossay; antibody; amperometry; alkaline phosphatase.

1. Introduction

Micromachining technology offers considerable promise in developing microfluidic devices and analytical microsystems capable of performing clinically relevant assays ***(1)***. The advantages of such microsystems have been well documented, including their design flexibility, reagent economy, improved analytical performance, speed, and ability to handle nanoliter volumes ***(2–3)***. These features, along with the automation capability and highly selective antibody–antigen interactions, are particularly suitable for microchip-based immunoassay applications ***(4–9)***.

From: *Methods in Molecular Biology, Vol. 385: Microchip-Based Assay Systems: Methods and Applications*
Edited by: Pierre N. Floriano © Humana Press Inc., Totowa, NJ

Compared to optical detection schemes used in earlier microchip-based immunoassays ***(4–8)***, electrochemical detection (particularly amperometry) is an attractive choice because of the inherent miniaturization (of both the detector and control instrumentation), low cost and power requirements, and high compatibility with advanced micromachining/microfabrication technologies ***(10–13)***. Electrochemical detection is ideally suited for applications involving real samples because the analytical signal can be measured accurately even in colored and turbid samples.

The microchip platform used in this study allows complete integration of electrochemical immunoassays. The analytical steps consist of electrokinetic loading of the alkaline phosphatase-labeled anti-mouse antibody (Ab-E, reagent) and the mouse IgG antigen (Ag, analyte) into the precolumn reaction chamber (in which immunochemical reaction occurs), the injection of the products into the separation channel, a rapid electrophoretic separation of labeled free antibody and the labeled antibody–antigen complex, postcolumn addition of *p*-aminophenyl phosphate (*p*-APP), substrate, and its conversion to *p*-aminophenol (*p*-AP) through enzymatic reaction of the substrate with alkaline phosphatase enzyme (tagged to the antibody), and, finally, the electrochemical detection of the product (*p*-AP) using low potential applied to a screen-printed electrode.

2. Materials

1. Antibody and antigen buffer: 10 m*M* phosphate buffer, pH 7.4, 2.7 m*M* KCl, 120 m*M* NaCl, 0.1% (w/v) sodium azide (sodium azide is highly toxic, and care should be taken to avoid any exposure either by inhalation or through contact with skin). Store at room temperature (*see* **Note 1**).
2. The electrophoresis buffer: 50 m*M* Tris-base (*see* **Note 2**), pH 8.0 (*see* **Note 3**), 0.02% Tween 20 (*see* **Note 4**). Store at room temperature.
3. The postcolumn buffer: 50 m*M* Tris-base, pH 9.0, 0.02% Tween 20. Store at room temperature.
4. Mouse IgG (Sigma, St. Louis, MO) antigen solution is dissolved at 50 µg/mL in antigen buffer. Store in single-use aliquots of 50 µL at –20°C. Subsequent working standards are prepared from single-use aliquots by dilution in electrophoresis buffer.
5. Anti-mouse IgG (whole molecule, reagent grade) conjugated to alkaline phosphatase developed in goat (3 mg/mL stock solution; Sigma, St. Louis, MO) is diluted to 1 mg/mL in antibody buffer. Store in single-use aliquots of 50 µL at –20°C. Subsequent dilutions, prepared from single-use aliquots, are performed in electrophoresis buffer.
6. *p*-Aminophenyl phosphate salt (Universal Sensors, Ireland, UK) is light sensitive and therefore divided into several single-use aliquots (approx 5–10 mg), wrapped in aluminum foil, and stored in a desiccator. The substrate solution of 5 m*M* *p*-APP is prepared in postcolumn buffer (*see* **Note 5**) from a single-use aliquot.

The substrate solution prepared is stable for a period of just 2 h, and, hence, substrate solution must be prepared freshly before use (*see* **Note 6**).

3. Methods

The methods described below outline the following: (1) the microchip layout and steps involved in carrying out the immunoassay, (2) characterization of the homogeneous microchip immunoassay protocol, and (3) its analytical performance.

3.1. Microchip Layout

The microchip layout, as shown in **Fig. 1**, permits electrokinetic mixing of enzyme-labeled antibody and antigen, subsequent injection of the immunochemical products into the separation channel, separation of the free enzyme-labeled antibody from the enzyme-labeled antibody–antigen complex, post-column addition of substrate, and finally the end-column amperometric detection of the enzymatic product. The following steps are involved in performing electrochemical enzyme immunoassays on microfluidic chips:

1. The glass microchip used in this study (*see* **Note 7**) permits both precolumn and postcolumn reactions, and the integrated setup allows electrophoretic separation and electrochemical detection.
2. The glass microchip is washed with 0.1 *M* NaOH and water (20 and 10 min each, respectively) between a group of runs or after 2 h of continuous use to eliminate any changes in migration times (associated with protein adsorption).
3. The reagent (Ab-E) and analyte (Ag) reservoirs are filled with desired concentrations of ALP-tagged anti-mouse IgG and mouse IgG solutions.
4. The running buffer (RB) and buffer waste (BW) reservoirs are filled with electrophoresis buffer solution.
5. The substrate reservoir is filled with 5 m*M* *p*-APP dissolved in postcolumn buffer solution.
6. The screen-printed carbon (*see* **Note 8**) working electrode (WE), platinum counter electrode (CE), and Ag/AgCl wire reference electrode (RE) are placed in the detection reservoir, constituting an electrochemical cell (*see* **Note 9**).
7. The detection reservoir (DR) is filled with the electrophoresis buffer, and the screen-printed electrode is fixed perpendicularly against the separation channel outlet using a plastic screw (*see* **Note 10**).
8. Amperometric measurements are performed with an electrochemical analyzer 621A (CH Instruments, Austin, TX). The electropherograms are recorded with a time resolution of 0.1 s while applying the detection potential (usually, +0.7 V vs Ag/AgCl wire reference electrode) to the screen-printed carbon working electrode.
9. The electrochemical cell is turned on, and sample injections are performed after stabilization of electrochemical baseline noise.
10. Voltages necessary for electrokinetic injection, electrophoretic separation, and postcolumn reaction are applied using a home-made high-voltage power supply

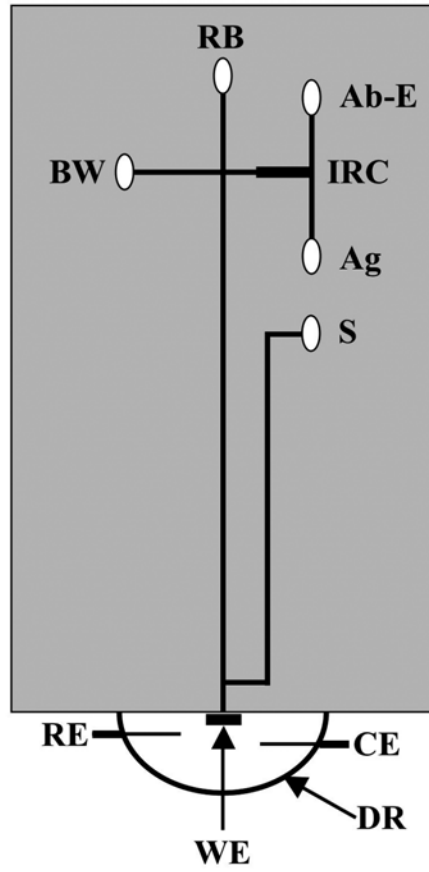

Fig. 1. Schematic of the immunochip used in this study. Key: RB, running buffer; Ab-E, enzyme-labeled antibody; Ag, antigen; S, substrate; IRC, immunoreaction chamber; DR, detection reservoir; RE, reference electrode; CE, counterelectrode; WE, working electrode; BW, buffer waste reservoir.

(*see* **Note 11**). The high-voltage power supply should be handled with extreme care to avoid electrical shock.

11. All injections/separations are performed by applying high voltages to the required reservoir with the detection reservoir grounded and other reservoirs floating.
12. Sample (Ab-E and Ag) injections are (unless otherwise noted) performed by applying a voltage of +250 V for 2 s to the analyte reservoir and subsequent application of +2000 V for 3 s to the reagent reservoir. During this step, the immunochemical reaction takes place in the precolumn reaction chamber (*see* **Note 12**) and the reacted immunochemical products (along with excess free ALP-labeled anti-mouse IgG) are introduced into the separation channel.

13. The free ALP-labeled antibody and ALP-labeled antibody–antigen are electrophoretically separated in the separation channel. The substrate (*p*-APP) solution is introduced through a postcolumn channel and reacts with alkaline phosphatase enzyme (tagged to the antibody), resulting in an electroactive product that is detected using an end-column amperometric detector.
14. Separations are usually performed by applying +2000 V (equivalent to a field strength of 256 V/cm) simultaneously to both the running buffer and substrate reservoirs. Maximal mixing leading to efficient enzymatic reaction is observed while using similar separation and postcolumn voltages (*see* **Note 13**).

3.2. Characterization of Immunoassay Protocol

The microchip system is characterized for its ability to carry out the immunoassay by recording electropherograms and identifying individual peaks (*see* **Fig. 2**). The individual steps leading to complete characterization are described here:

1. An injection of ALP-labeled antibody (7.5×10^{-6} g/mL) coupled to postcolumn addition of *p*-APP (5 m*M*) substrate resulted in a well-defined "free antibody" peak, with a migration time of 125 s, obtained through enzymatic reaction (*see* **Fig. 2A**).
2. A similar injection of the labeled antigen–antibody complex produced in an off-chip external incubation cell using a large excess of the antigen (*see* **Note 14**) resulted in a well-defined complex peak with a migration time of 345 s (*see* **Fig. 2B**). No response is observed for the free antibody, indicating the completeness of off-chip complexation because of the large excess of the antigen.
3. A similar saturation experiment conducted on-chip by employing precolumn mixing of the reagents (at the levels employed in the off-chip reaction) also yields a single complex peak (with lower sensitivity compared to off-chip complexation because of different reaction times leading to saturation) at a similar migration time (*see* **Fig. 2C**). This indicates effective mixing of antibody and antigen in the precolumn reaction chamber, allowing the immunoreaction to proceed to saturation.
4. Precolumn mixing of the antigen (1.56×10^{-15} g/mL) with the ALP-labeled antibody (7.5×10^{-6} g/mL) produced an electropherogram (*see* **Fig. 2D**) with two well-defined peaks at 125 and 340 s, corresponding to the migration of free labeled antibody and complex (*see* **Fig. 2D** vs **A** and **B**), respectively.

3.3. Analytical Performance

Success shown in the ability to mix the labeled antibody with the antigen, separate the labeled antibody from the labeled antibody–antigen complex, and conduct efficient on-chip immunochemical reactions as described in the section above prompted us to study the analytical utility of on-chip immunoassays. Described here is a procedure demonstrated for quantitative evaluation of the concentration dependence (*see* **Fig. 3**):

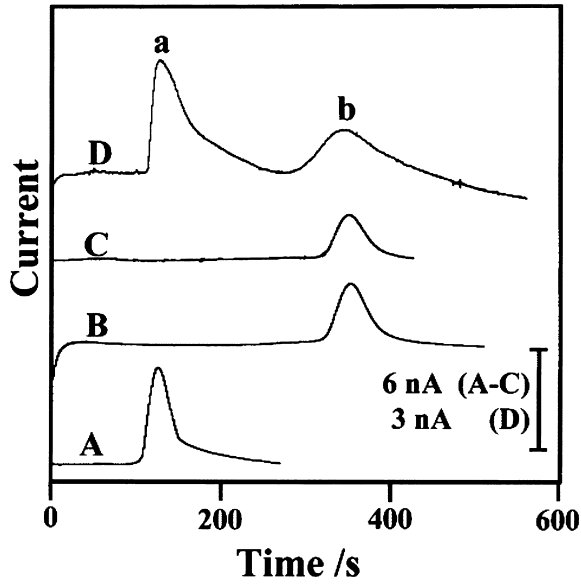

Fig. 2. Electropherograms resulting from the postcolumn addition of 5 m*M* *p*-APP substrate in connection with **(A)** enzyme-labeled free antibody alone, **(B)** off-chip complexation of the enzyme-labeled antibody with 2.5×10^{-3} g/mL antigen, **(C)** on-chip complexation of the enzyme-labeled antibody with 2.5×10^{-3} g/mL antigen, and **(D)** enzyme-labeled free antibody **(a)** and complex **(b)** using on-chip complexation with 1.56×10^{-15} g/mL antigen. Antibody concentration, 7.5×10^{-6}g/mL. The running buffer (pH 8.0) and postcolumn buffer (pH 9.0), 50 m*M* Tris with 0.02% v/v Tween 20. Separation and postcolumn voltages, 2000 V; injection voltage, (Ag) 250 V for 2 s and (Ab-E) 2000 V for 3 s. Screen-printed carbon electrode held at +0.7 V (vs Ag/AgCl wire reference electrode). (Reprinted with permission from Anal. Chem. 2001, 73, 5323–5327. Copyright 2001 American Chemical Society.)

1. The peak heights of the free antibody and the complex are measured at different antigen (IgG) concentrations from 0 to 3.9×10^{-15} g/mL in steps of 7.8×10^{-16} g/mL.
2. The complex signal increases in a nearly linear fashion up to 3.1×10^{-15} g/mL (sensitivity of 1.2×10^{-15} nA-mL/g; correlation coefficient of 0.997) and then slowly leading to saturation (*see* **Fig. 3B**).
3. Similarly, the free-antibody signal decreases with the addition of antigen in a linear fashion up to 2.4×10^{-15} g/mL (sensitivity of 3.5×10^{-15} nA-mL/g; correlation coefficient of 0.996), and levels off above 3.1×10^{-15} g/mL of antigen (*see* **Fig. 3A**).
4. The actual complex signal obtained for an antigen concentration of 3.0×10^{-16} g/mL is shown (*see* **Fig. 3**, inset), indicating a highly sensitive response with low noise levels. The low detection limit (*see* **Note 15**) obtained is comparable to a previously reported off-chip electrochemical immunoassay ***(14)***.

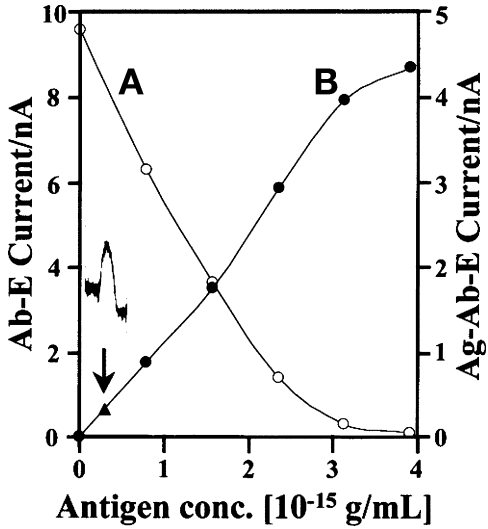

Fig. 3. Calibration plots: dependence of the free antibody (**A**, ○) and complex (**B**, ●) peak currents upon the concentration of the IgG antigen. Also shown (inset) is the portion of the electropherogram for 3.0×10^{-16} g/mL antigen concentration. Other conditions as in **Fig. 2D**. (Reprinted with permission from Anal. Chem. 2001, 73, 5323–5327. Copyright 2001 American Chemical Society.)

4. Notes

1. All the solutions should be prepared in high-purity water filtered through a Milli-Q water system (Millipore, Bedford, MA) that has a resistivity of 18 M -cm.
2. Tris buffer was proven to enhance the activity of the ALP enzyme tag. Alkaline phosphatase, a phosphomonoesterase, is a dimeric metalloprotein that has two Zn^{2+} ions and a M_g^{2+} ion in each active site, and these metal ions are believed to be responsible for the enzymatic activity. The enzyme activity is inhibited by, among other agents, metal ions in the solution, which form stable complexes with the enzyme. Tris buffer, however, because of the high stability constant of metal–Tris complexes, prevents the formation of alkaline phosphatase–metal complexes ***(15)***.
3. Hydrolysis of alkaline phosphatase is brought about by nucleophilic catalysis with phosphorylation of serine hydroxyl group, followed by hydrolysis of the serine phosphate ester and dissociation of inorganic phosphate. Tris is a good phosphoryl acceptor that causes a large increase in the maximal velocity of substrate turnover. This may be attributed to rapid dissociation of Tris phosphate so that the phosphoenzyme intermediate can react with Tris, thereby bypassing slow dissociation of inorganic phosphate from the enzyme–phosphate complex ***(16)***. A pH of 8.0 is used because the dissociation of the noncovalent complex of enzyme with bound inorganic phosphate is rate limiting at pH above 8.0 ***(17)***.

4. Adsorption of proteins leads to poor separations in capillary electrophoresis, and a neutral surfactant is needed to reduce the protein adsorption. Tween 20 is chosen because it is commonly used in immunological reagent preparations and does not negatively affect the reagents or immunoreaction ***(18)***.
5. The pH 9.0 of the postcolumn buffer is selected to meet the stability requirements of the *p*-APP substrate. This pH is found to result in generation of more stable enzymatic products and low electrochemical noise ***(17)***.
6. *p*-APP decomposes slowly in aqueous solution, and it is known that the substrate containing phosphate esters hydrolyzes slowly in aqueous solutions. Also, the enzymatic product *p*-AP decomposes readily, producing a brown solution as a result of oxidation by air (O_2) and light (UV). Wrapping the container in aluminum foil also helps by blocking light. Regardless, substrate solutions should be freshly prepared ***(17)*** after 2 h of use.
7. The glass microchip used in this study is custom-designed and fabricated by Micralyne (Alberta, Canada). The chip consisted of reagent (Ab-E) and analyte (Ag) reservoirs connected through 50-μm-wide channels to the immunoreaction chamber (IRC; 200 μm wide and 3.6 mm long) that leads to a four way injection cross. A running buffer (RB), sample waste reservoir (connected with a 5-mm-long channel), and a 78-mm-long separation channel are connected to the other side of the injection cross. A 77-mm postcolumn channel is joined 10 mm from the end of the separation channel to introduce *p*-APP substrate. All of the channels are 50 μm wide and 20 μm deep.
8. The screen-printed electrodes are fabricated with a semiautomatic printer (model TF 100; MPM, Franklin, MA). The Acheson carbon ink (cat. no. 49AB90, Acheson Colloids, Ontario, CA) is used for printing electrode strips ***(13)***. We have used extensively screen-printed electrodes because of their disposability and mass production. Similar performance can be obtained by using glassy carbon disc electrodes in laboratories not equipped with such a specialized and expensive screen-printer. However, the glassy carbon electrode must be polished periodically in order to obtain reproducible electrochemical responses.
9. The detection reservoir is fabricated in Plexiglas in which a platinum counter (CE) and Ag/AgCl reference (RE) electrodes are fixed. The cell contains a groove to house the screen-printed working electrode (WE), and the electrode is fixed perpendicularly to the separation channel outlet and held in place using a plastic screw. The detection reservoir contains an additional platinum wire, which serves as the cathode (ground electrode) for electrophoretic injection/separation steps.
10. A Plexiglas holder is fabricated to house the glass microchip (with reservoirs for sample, reagent, running buffer, and sample waste solutions) and detection reservoir. Platinum wires, inserted into the individual reservoirs, provided electrical contact from high-voltage leads to the solutions in the reservoirs ***(13)***.
11. A high-voltage power supply with an adjustable voltage (from 0 to +4000 V) is designed and made in-house. The power supply has multiple voltage terminals necessary to apply required voltages to injection/reaction, separation, and postcolumn reservoirs and to switch between injection and separation voltages.

12. The immunoreaction chamber (*see* **Fig. 1,** IRC) is designed to be wider (200 μm) than the separation channel (50 μm), to give a lower field strength in the reaction chamber. The resulting longer residence times for the reagents helps the immunoreaction to reach completion.
13. It is necessary to apply simultaneously both the separation and the postcolumn voltages in order to separate the products and to carry out postcolumn mixing in a controlled and efficient manner. The different mobilities of the reactants and products in the reaction zone result in increased band broadening. A balance must be sought in order to obtain maximal mixing without hindering separation efficiency. Since the lengths of the separation and postcolumn channels and the ionic strengths of the buffers used in these channels are very similar, maximal mixing (leading to efficient enzymatic reaction) is observed when the separation and postcolumn voltages are similar ***(9)***.
14. The off-chip immunoreaction used for comparison purposes is carried out by mixing the antigen and antibody solutions (with final concentrations of 2.5×10^{-3} g/mL and 7.5×10^{-6} g/mL, respectively). The mixing is carried out in a 1-mL cell at 25°C for an incubation time of 2 h.
15. The detection limit obtained in this assay (3.0×10^{-16} g/mL) is slightly lower than that (1.4×10^{-14} g/mL) reported for off-chip electrochemical enzyme immunoassay ***(14)***. This may be attributed to enzymatic amplification at ultra-small volumes and to the continuous supply of substrate (through postcolumn addition).

Acknowledgments

This publication was made possible by Grant AI056047 from the National Institute of Allergy and Infectious Diseases (NIAIO). Its contents are solely the responsibility of the authors and did not necessarily represent the official views of the National Institutes of Health (NIH).

References

1. Ahn, C. H., Choi, J.-W., Beaucage, G., et al. (2004) Disposable *smart* lab on a chip for point-of-care clinical diagnostics. *Proc. IEEE* **92,** 154–173.
2. Reyes, D. R., Iossifidis, D., Auroux, P. A., and Manz, A. (2002) Micro total analysis systems. 1. Introduction, theory, and technology. *Anal. Chem.* **74,** 2623–2626.
3. Auroux, P. A., Iossifidis, D., Reyes, D. R., and Manz, A. (2002) Micro total analysis systems. 2. Analytical standard operations and applications. *Anal. Chem.* **74,** 2637–2652.
4. Koutny, L. B., Schmalzing, D., Taylor, T. A., and Fuchs, M. (1996) Microchip electrophoretic immunoassay for serum cortisol. *Anal. Chem.* **68,** 18–22.
5. Chiem, N. and Harrison, D. J., (1997) Microchip-based capillary electrophoresis for immunoassays: analysis of monoclonal antibodies and theophylline. *Anal. Chem.* **69,** 373–378.
6. Linder, V., Sia, S. K., and Whitesides, G. M. (2005) Reagent-loaded cartridges for valveless and automated fluid delivery in microfluidic devices. *Anal. Chem.* **77,** 64–71.

7. Dodge, A., Fluri, K., Verpoorte, E., and de Rooij, N. F. (2001) Electrokinetically driven microfluidic chips with surface-modified chambers for heterogeneous immunoassays. *Anal. Chem.* **73,** 3400–3409.
8. Bromberg, A. and Mathies, R. A. (2003) Homogeneous immunoassay for detection of TNT and its analogues on a microfabricated capillary electrophoresis chip. *Anal. Chem.* **75,** 1188–1195.
9. Wang, J., Ibanez, A., Chatrathi, M. P., and Escarpa, A. (2001) Electrochemical enzyme immunoassays on microchip platforms. *Anal. Chem.* **73,** 5323–5327.
10. Woolley, A. T., Lao, K. Q., Glazer, A. N., and Mathies, R. A. (1998) Capillary electrophoresis chips with integrated electrochemical detection. *Anal. Chem.* **70,** 684–688.
11. Baldwin, R. P., Roussel, T. J., Crain, M. M., et al. (2002) Fully integrated on-chip electrochemical detection for capillary electrophoresis in a microfabricated device. *Anal. Chem.* **74,** 3690–3697.
12. Jackson, D. J., Naber, J. F., Roussel, T. J., et al. (2003) Portable high-voltage power supply and electrochemical detection circuits for microchip capillary electrophoresis. *Anal. Chem.* **75,** 3643–3649.
13. Wang, J., Tian, B. M., and Sahlin, E. (1999) Micromachined electrophoresis chips with thick-film electrochemical detectors. *Anal. Chem.* **71,** 5436–5440.
14. Jenkins, S. H., Halsal, H. B., and Heineman, W. R. (1988) Subattomole immunoassay with electrochemical detection. *Clin. Chem.* **34,** 1159–1159.
15. Plocke, D. J. and Vallee, B. L. (1962) Interaction of alkaline phosphatase of *E. coli* with metal ions and chelating agents. *Biochemistry* **1,** 1039–1043.
16. Simopoulos, T. T. and Jencks, W. P. (1994) Alkaline phosphatase is an almost perfect enzyme. *Biochemistry* **33,** 10375–10380.
17. Kreuzer, M. P., O'Sullivan, C. K., and Gilbault, G. G. (1999) Alkaline phosphatase as a label for immunoassay using amperometric detection with a variety of substrates and an optimal buffer system. *Anal. Chim. Acta* **393,** 95–102.
18. Engvall, E. and Perlmann, P. (1972) Enzyme-linked immunosorbent assay, ELISA. 3. Quantitation of specific antibodies by enzyme-labeled anti-immunoglobulin in antigen-coated tubes. *J. Immunol.* **109,** 129–135.

Index